Study of the role of the cyclin-dependent kinase inhibitor p21Waf1/Cip1 in cellular senescence

Irene Zapata Bodalo

▶ **To cite this version:**

Irene Zapata Bodalo. Study of the role of the cyclin-dependent kinase inhibitor p21Waf1/Cip1 in cellular senescence. Genetics. Université de Strasbourg, 2022. English. NNT : 2022STRAJ044 . tel-04013530

HAL Id: tel-04013530
https://theses.hal.science/tel-04013530

Submitted on 3 Mar 2023

HAL is a multi-disciplinary open access archive for the deposit and dissemination of scientific research documents, whether they are published or not. The documents may come from teaching and research institutions in France or abroad, or from public or private research centers.

L'archive ouverte pluridisciplinaire **HAL**, est destinée au dépôt et à la diffusion de documents scientifiques de niveau recherche, publiés ou non, émanant des établissements d'enseignement et de recherche français ou étrangers, des laboratoires publics ou privés.

UNIVERSITÉ DE STRASBOURG

ÉCOLE DOCTORALE 414 – Sciences de la vie et la santé

Institut de Génétique et de Biologie Moléculaire et Cellulaire

CNRS UMR 7104 – INSERM U 964

THÈSE présentée par :

Irene ZAPATA BODALO

soutenue le : 15 septembre 2022

pour obtenir le grade de : **Docteur de l'université de Strasbourg**

Discipline / Spécialité : Aspects moléculaires et cellulaires de la biologie

Study of the role of the cyclin-dependent kinase inhibitor $p21^{Waf1/Cip1}$ in cellular senescence

THÈSE dirigée par :

M KEYES Bill, PhD	Directeur de recherches, Institut de Génétique et de la Biologie Moléculaire et Cellulaire, Strasbourg

RAPPORTEURS :

Mme HAN Li, PhD	Directeur de recherches, Institut Pasteur, Paris
Mme MARTIN Nadine, PhD	Chargé de recherches, Centre de Recherche en Cancérologie de Lyon

AUTRES MEMBRES DU JURY :

M CHARVIN Gilles, PhD	Directeur de recherches, Génétique Moléculaire, Génomique et Microbiologie – GMGM, Strasbourg

[…] *"Quizá haya un lugar en el hombre desde donde pueda percibirse la realidad entera. Esta hipótesis parece delirante. Auguste Comte declaraba que jamás se conocería la composición química de una estrella. Al año siguiente, Bunsen inventaba el espectroscopio.*

……..

"El lenguaje, al igual que el pensamiento, procede del funcionamiento aritmético binario de nuestro cerebro. Clasificamos en sí y no, en positivo y negativo. (...) Lo único que prueba mi lenguaje es la lentitud de una visión del mundo limitada a lo binario. Esta insuficiencia del lenguaje es evidente, y se deplora vivamente. ¿Pero qué decir de la insuficiencia de la inteligencia binaria en sí misma? La existencia interna, la esencia de las cosas se le escapa. Puede descubrir que la luz es continua y discontinua a la vez, que la molécula de la bencina establece entre sus seis átomos relaciones dobles y que sin embargo se excluyen mutuamente; lo admite, pero no puede comprenderlo, no puede incorporar a su propia estructura la realidad de las estructuras profundas que examina. Para conseguirlo, debería cambiar de estado, sería necesario que otras máquinas que las usuales se pusieran a funcionar en el cerebro, que el razonamiento binario fuese sustituido por una conciencia analógica que asumiera las formas y asimilara los ritmos inconcebibles de esas estructuras profundas..."

Citando a Pauwels y Bergier (1960)
Rayuela, c. 86. Julio Cortázar

[…] *"Perhaps there is a place in man from where the whole of reality can be perceived. This hypothesis seems delirious. Auguste Comte declared that the chemical composition of a star would never be known. The following year Bunsen invented the spectroscope.*

……..

"Language, just like thought, proceeds from the binary arithmetical functioning of our brain. We classify by yes and no, by positive and negative. (…) The only thing that my language proves is the slowness of a world vision limited to the binary. This insufficiency of language is obvious, and is strongly deplored. But what about the insufficiency of binary intelligence itself? Internal existence, the essence of things, escapes it. It can discover that light is continuous and discontinuous at the same time, that a molecule of benzine establishes between its six atoms dual relationships which are nevertheless mutually exclusive; it accepts it, but it cannot understand it, it cannot incorporate into its own structure the reality of the profound structures it examines. In order to do that, it would have to change its state, machines other than the usual ones would have to start functioning in the brain, so that binary reasoning might be replaced with an analogical consciousness which would assume the shapes and assimilate the inconceivable rhythms of those profound structures…"

Citing Pauwels and Bergier (1960)
Hopscotch, ch. 86. Julio Cortázar

Acknowledgements

First, I thank Bill for giving me this opportunity, for his support, for always trying to help and for being willing to explain and debate. I am also grateful to my mid thesis committee (Dr. Sumara and Dr. Metzger) and thesis jury (Dr. Li, Dr. Martin and Dr. Charvin) for taking the time to evaluate and discuss my project.

Thanks a lot to all the present and former lab members of the lab for the great and enjoyable environment, and for all the help, advise and discussion (Matej, Tania, Birgit, Muriel, Jean-Luc, Daniel, Annabelle, Alba…). To Tania and Jean-Luc for making life easier. To Muriel for her trust. And to Matej for sharing so much scientific knowledge and advise, all kinds of help, squeezes and plenty unfortunate bad jokes and fun facts. I also appreciated working with the people from the IGBMC facilities (microscopy, cell culture, GenomEast, proteomics…), from security, reception, human resources and cleaning, and the administrative staff (IGBMC and the Doctoral School). Their kindness and recurrent help made everything nicer and easier on a daily basis.

I am so glad I met such great people during this time; for Mercè's nice and fun *tarannà*, Dan's loving enthusiasm, Bea's amazing energy and sensitivity, Arantxa's connection and company, and all good times and shared beers with Rocío, Birgit, Katka, Andrea, Alastair… Their company, understanding and help (inside and outside the IGBMC) made a huge difference in shaping this time as an incredible experience in so many ways.

Tones of thanks to Alba for the scientific, emotional and daily support. Thanks for teaching me so much wet and computer lab, for creating a great work environment, for the beers and parties, the mountain excursions and the climbing sessions, for the adventures, the omelettes, the company, for making like easier and funnier…and for reading and commenting all the drafts of this thesis on top of it!

Although it may seem far away, I am very thankful to Sara, Gemma and Saio for being such a cool, supportive team during university. I also feel really lucky to count with Tània's support, critical thinking and sense of humor.

Lastly, I am extremely grateful to my mother, who has enabled and always encouraged every goal I have been passionate about.

TABLE OF CONTENTS

Overview of the project(s) development

I started my PhD in Dr. Bill Keyes lab in December 2017, thanks to a fellowship co-funded by INSERM and the Region Grand-Est. My initial project was based on preliminary data from the lab that linked cellular senescence with cellular plasticity and reprogramming. Specifically, my original project was focused on studying the contribution of the senescence mediator $p19^{Arf}$ in these processes *in vitro*. To do so, I isolated primary mouse keratinocytes from the skin of wild type and p19-null mice, and induced them to senesce through oncogene infection or irradiation. I worked in this project for 1.5 years, but, due to many technical challenges and problems that could not be overcome, the project did not progress as expected. In addition, the project had started developing in a direction outside of the main interest and expertise of the lab. Therefore, after discussing with my Mid Thesis Committee members (Dr. Daniel Metzger and Dr. Izabela Sumara), it was decided that continuing the project was not the best avenue to proceed. Nonetheless, this experience allowed me to learn many of the techniques that I applied in my actual project, such as isolating and culturing primary cells derived from the skin of newborn mice, inducing and identifying senescence and techniques such as Western Blotting or immunofluorescence. Moreover, it also familiarized me with the experimental study of senescence and the current state of the literature in the field.

In summer 2019, we designed a new project based on studying the molecular role of p21 in cellular senescence, which is the core of the work presented in this thesis. I was able to start the validation of the mouse line at the end of September, when I first had access to a litter of the transgenic line in which all my experiments have been performed. Although the project was advancing well, it was critically delayed by the COVID pandemic, which was a significant setback because of both the quarantine time and the delay caused by the replacement of mice and stock. For instance, the possibility of performing *in vivo* experiments in aged mice to verify some of the hypotheses developed *in vitro* was compromised. I was able to properly finish the transcriptomic analysis that constitutes the main body of results of this thesis and to start exploring some of the hypotheses derived from it, as well as to develop some alternative experimental approaches to address the question of interest, thanks to a 4th year fellowship for 12 months which was awarded to me from Fondation ARC.

During my PhD, I also contributed to another project from the lab, which has been recently published in Plos Biology, titled ***"Aberrant induction of p19Arf-mediated cellular senescence contributes to neurodevelopmental defects***", by Dr. Muriel Rhinn et al.[1] (Annex

2). I am listed as a 2nd author of the manuscript. In this work, Dr. Rhinn characterized the induction of senescence in developing mouse embryos by maternal exposure to valproic acid (VPA), a widely prescribed drug for the treatment of several psychiatric conditions, but which has teratogenic effects in utero. The ectopic induction of senescence by VPA was associated with developmental malformations, such as exencephaly, microcephaly and spinal defects, and neurogenesis disruption. The detrimental effect of VPA-induced senescence was shown to be partially mediated by $p19^{Arf}$, since its ablation rescued the microcephalic phenotype. These findings demonstrated that aberrantly induced senescence disrupts embryonic development and causes developmental defects, and proposed this to be a potential mechanism by which VPA exposure exerts its detrimental teratogenic effects. My contribution to this project was the analysis of the data from a bulk RNA-seq performed on samples from brain tissue of wild type or $p19^{Arf}$-null mouse embryos untreated or exposed to VPA. At that time, there was no expertise in the lab for studying RNA-sequencing data, so I had to learn and apply the analysis independently, as I was doing for my own project in parallel. Specifically, I generated Fig. 6 and Supp. Fig. 12. The published article is attached in Annex 2.

Aims of the project

Although the role of p21 in mediating the proliferation arrest upon senescence initiation is well known, p21 has been shown to be involved in the regulation of many other cellular processes, and its exact contribution to the senescent phenotype besides growth arrest, once this has been irreversibly established, remains underexplored. Thus, the aim of this project was to investigate the role of p21 in senescence.

To tackle this question, we decided to downregulate p21 once senescence was fully established in cells in vitro. To do so, I took advantage of a commercial transgenic mouse line previously acquired by the lab. This line allowed the inducible downregulation of p21 through the administration of doxycycline. The functional effect of p21 loss in senescent cells would be inferred by analyzing the transcriptional changes that it caused. Primary cellular cultures from these mice were used to generate of RNA samples from proliferating and senescent cells with unperturbed or decreased p21 levels, and were analyzed by RNA-sequencing. The obtained data was used to determine and explore novel potential functions of p21 associated with its ability to influence gene transcription in senescent cells. Then, the potential interesting and novel roles of p21 in senescence revealed by this transcriptomic analysis were further explored through specific experiments. In parallel, I investigated the protein interactome of p21 in senescent cells by performing a co-immunoprecipitation for p21 and its binding proteins in senescent cells, through Mass Spectrometry. This result was aimed to be a complementary to the transcriptomic analysis, since it that was expected to provide insight into the molecular mechanism by which p21 regulates transcription in senescent cells.

In summary, the objectives of the project can be summarized in 4 points:

- **Model validation.** In vitro validation of senescence induction and efficient downregulation of p21 upon doxycycline administration in primary mouse dermal fibroblasts isolated from a newly acquired and commercially generated transgenic mouse line.
- **RNA-sequencing.** Identification and exploration of novel roles of p21 in senescence by assessing the transcriptional effect of its downregulation in senescent cells. Performed through pathway analysis and the study of the expression of candidate genes.

- **Exploration of hypotheses** generated from the analysis of the transcriptomic data with adequate experimental approaches.
- Identification of the **interactome of p21** in senescent cells. Performed though the co-immunoprecipitation of p21 and its binding proteins from protein extracts of senescent cells, and protein identification through mass spectrometry analysis.

Main abbreviations

ATM	Ataxia Telangiectasia Mutated protein
ATR	Ataxia Telangiectasia and Rad3-related protein
BrdU	5-Bromo-2'-deoxyuridine
BSA	Bovine Serum Albumin
Cat	Catalase
CCFs	Cytoplasmic Chromatin Fragments
CDK	Cyclin-Dependent Kinase
CDKi	CDK inhibitor
cDNA	Complementary DNA
Co-Ip	Co-Immunoprecipitation
DAPI	4',6-Diamidino-2-phenylindole
DDR	DNA Damage Response
DEA	Differential Expression Analysis
DEG	Differentially Expressed Genes
DMEM	Dulbecco's Modified Eagle Medium
DMSO	Dimethyl sulfoxide
DNA	Deoxyribonucleic Acid
Dox	Doxycycline
DREAM	Dimerization partner, Retinoblastoma-like, E2F And MuvB complex
ECM	Extracellular Matrix
EDTA	Ethylenediaminetetraacetic Acid
EdU	5-ethynyl-2'-deoxyuridine
ER	Endoplasmic Reticulum
Fwd	Forward (primer sequence)
HMGB2	High Mobility Group B2 protein
IGBMC	Institut de Génétique et de Biologie Moléculaire et Cellulaire
IgG	Immunoglobulin G
KD	Knock-down
KDa	Kilodalton (molecular mass unit)
KO	Knock-out
MDF	Mouse Dermal Fibroblasts
MMPs	Matrix metalloproteinases

mRNA	Messenger RNA
MS	Mass Spectrometry
NK	Natural Killer cells
PBS	Phosphate-buffered saline
PC	Proliferating control (RNA-seq analyzed conditions)
PCA	Principal Component Analysis
PCR	Polymerase Chain Reaction
PD	Proliferating, p21 knocked-down (RNA-seq analyzed conditions)
Pmp70	Peroxisomal Membrane Protein 1 (70kD). Official name: Abcd3
qPCR	Quantitative PCR (or real-time PCR)
Rb	Retinoblastoma protein(s)
RBP	RNA-binding protein
Rev	Reverse (primer sequence)
RNA	Ribonucleic Acid
rRNA	Ribosomal RNA
RT-qPCR	Reverse Transcription PCR
SA-β-gal	Senescence-Associated Beta-Galactosidase
SAHF	Senescence-Associated Heterochromatic Foci
SASP	Senescence-associated secretory phenotype
SC	Senescent control (RNA-seq analyzed conditions)
SD	Senescent, p21 knocked-down (RNA-seq analyzed conditions)
SD	Standard Deviation
SEM	Standard Error of the Mean
SERE	Simple Error Ratio Estimate (coefficient)
shRNA	Short hairpin RNA
siRNA	Small Interfering RNA
tRNA	Transfer RNA
Tub	α-Tubulin
UPR	Unfolded Protein Response
X-Gal	X-Galactosidase

INTRODUCTION

1. Cellular Senescence

1. 1 Definition and origin

The word senescence derives from the latin "senex" meaning "state of being old" or "process of becoming old". The idea that individual cells undergo an aging process dates from at least the last decade of 19th century (Maupas 1888-1889), when Maupas started describing a "*period of maturity followed by a period of decline or degeneration*" [2] in unicellular organisms (cited from Jennings 1944). Although the concept of "senescence" referring to this idea was already accepted in the study of protozoa[2,3], it was not applied to vertebrated cells until 1961, when Hayflick and Moorhead attribute to "cellular senescence" the "eventual degeneration" that primary human diploid fibroblasts experienced when cultured *in vitro*[4]. In their work, they demonstrated that the proliferative capacity of these cultures was intrinsically limited, and depended on the number of divisions. In 1965, Hayflick formally characterized senescence, associating it to the accumulation of damage at the cellular level and proposing it to be a common phenomenon of human diploid cells contributing to the aging of the organism[5]. Although these observations only reflected a specific case of senescence, Hayflick's work and interpretations settled the conceptual basis of the field of study of cellular senescence as we know it nowadays. While the essence of its definition has been maintained, the list of characteristics, causes and physiological functions of senescence have broadened over time.

Currently, cellular senescence is understood as a state of permanent proliferative arrest accompanied by a list of characteristic phenotypical changes, including a secretory activity[6,7]. It occurs in response to a variety of stimuli, mainly -but not exclusively- related to cellular damage[6,8]. The acquisition of senescence is characterized by a number of morphological, functional and expression markers often presented in diverse combinations. The heterogeneity of the senescent phenotype appears to be conditioned by the cause of its induction, the biological context and the cell type studied[8,9]. At the same time, the establishment of the senescent program is a dynamic and complex process driven by different but interconnected molecular pathways mediating modifications at all levels[7,10,11]. The presence of senescent cells *in vivo* has been described to contribute to an increasing number of biological processes, where they play important and sometimes contradictory roles[6,7,10,12].

1. 2 Hallmarks of senescence

The changes associated to the establishment of senescence affect cells at all levels. Although there is a general consensus of the overall characteristics of senescent cells in the field (Figure 1), a specific and universal (or model-specific) marker to identify them is still lacking[7,13,14]. This can be attributed to the high heterogeneity of the presentation of the senescent phenotype, which varies among different cell types, senescence inductors and other biological contexts[7,9]. Moreover, most of the characteristics associated to senescence are also present in other conditions[9]. For this reason, the assessment of senescence is normally achieved through the identification a combination of markers presented simultaneously[7,14]. A list of most of the commonly accepted and widely used markers of senescence are summarized next.

Proliferation arrest

The principal hallmark of senescence is the definitive proliferative arrest. By definition, and unlike in quiescence, senescent cells present a permanent arrest of the cell cycle, being unable to resume it regardless of pro-proliferative stimulation. The regulation of the cell cycle depends on the interaction of cyclins and the cyclin dependent kinases proteins (CDKs)[15]. When activated by interacting with the cyclins, the different CDKs phosphorylate and regulate multiple proteins involved in the cell cycle, controlling the action of the transcription factors required for each cell cycle stage. The activity of the CDKs can be inhibited by small proteins called CDK inhibitors (**CDKi**)[16]. There are 2 families of CDKi, the Ink4 proteins, which include $p15^{Ink4b}$, $p16^{Ink4a}$, $p18^{Ink4c}$ and $p19^{Ink4d}$ (not to be confused with $p19^{Arf}$), and the Cip/Kip family, composed by $p21^{Cip1/Waf1}$, $p27^{Kip1}$ and $p57^{Kip2}$. In senescence, cell cycle exit is mainly mediated by the activation of 2 interconnected tumor suppressor pathways: **$p19^{Arf}$/p53/$p21^{Waf1/Cip1}$** and **$p16^{Ink4a}$/pRB**[9]. In both cases, the inhibition of the action of the CDKs by the upregulation of CDKi, mainly p21 or p16, prevents the phosphorylation of the retinoblastoma family proteins (**RB**). When dephosphorylated, Rb proteins are able to bind E2F transcription factor, forming repressive complexes (**RB-E2F** and **DREAM**) that prevent the expression of the genes required for cell cycle progression[11,17]. Since p21 and p16 tend to accumulate in senescent cells and its expression is often sufficient to establish and maintain their proliferative arrest, their overexpression at the transcriptional and/or protein level is commonly used to identify senescent cells[14]. The absence of proliferation can also be identified through the lack of DNA replication measured by the incorporation of nucleotide

analogues (BrdU or EdU), immunostaining of proliferation markers (Ki67 or PCNA) or proliferative assays (cell counting or crystal violet staining of colony-formation)[9].

Despite being an essential feature of senescence, an arrest of proliferation is a shared characteristic of quiescence and terminal differentiation, so it is not sufficient to assess it and other markers need to be considered simultaneously[7,11]. Since post-mitotic and non-proliferating cells (quiescent or terminally differentiated) can develop features of senescence upon certain stimuli[14], a prompted arrest of the cell cycle is not an indispensable requirement for senescence establishment. Interestingly, it seems to exist a phenotypical -and maybe even mechanistic- overlap between senescence and differentiation. Several senescence markers (including the cell cycle inhibitors p21 and p16) are also indicators of terminal differentiation in different cell types, and it has been shown that, besides senescence, DNA damage can also promote differentiation[14]. This idea is beautifully developed in the 2021 review by Di Micco et al[14]. Moreover, under certain circumstances, cells classified as senescent may be able to restart proliferation, either due to genetic experimental manipulation[18] or spontaneously[19], especially in cancer related contexts[7].

They are alive: Apoptosis resistance

Together with senescence, apoptosis is the most important mechanism to prevent the expansion and eliminate irreparable damaged cells[8,20]. Senescence and apoptosis can be triggered by the same stressors, and they seem to be mutually exclusionary. Actually, senescent cells have been reported to be **resistant** to apoptosis upon diverse stimuli in different cell types[21]. This is suggested to be the result of the high expression of the antiapoptotic proteins from the **Bcl-2** family by senescent cells[9,22,23], as well as the epigenetic inhibition of the expression of proapoptotic gene Bax[9,24]. The mechanisms determining whether a cell undergoes senescence or apoptosis upon a damage signal are not fully understood [20,21]. While some cell types present a tendency for one or the other [21], the choice seems dependent on the extent and the duration of the insult[20]. In addition, both pathways are commonly regulated by **p53**, which has been proposed to be key in the decision[20,21,25].

This resistance to apoptosis has been successfully exploited in the development of **senolytics**, drugs that selectively eliminate senescent cells[14,22,26]. At the same time, the efforts directed to the identification of new senolytic targets have led to major contributions in our understanding on the key regulators and molecular pathways responsible for it[9,14,27,28].

Morphological changes

Senescent cells also undergo major and characteristic morphological changes. They typically exhibit an enlarged, flattened and irregular shape, often accompanied by multiple nuclei and extensive vacuolization (although these changes may depend on the senescence trigger)[9,18]. These changes are normally easily noticeable *in vitro* by bright-field or phase contrast microscopy[9]. Additionally, immunofluorescence staining of cytoskeletal, membrane or cytoplasmic proteins can also be useful to measure changes in cell shape[9] . Although they are more difficult to observe *in vivo,* some of them have been identified in recent studies[7,14].

The enlargement of the cell body has been proposed to be mediated by the activation of the **mTOR** pathway in senescent cells[9]. Interestingly, it has been recently reported that ATF6, one of the branches of the **unfolded protein response** (UPR), can control the cell shape of senescent cells, as well as influence other aspects of their phenotype[9,29].

In addition, these changes are also connected to a rearrangement of the **cytoskeleton** and the regulation of **adhesion**[9,30]. Some of the proteins contributing to regulating these processes in senescence include integrins, focal adhesion components (FAK, paxillin), the cytoskeletal proteins or its regulators (vimentin, Rac1, Cdc42 and Rock1) and the plasma membrane protein caveolin-1[30–32].

Senescent cells also exhibit morphological alterations concerning the nuclear structure and the chromatin organization[9,11]. For example, they often present enlarged and/or unshaped (lobulated, with invaginations, fragmented) nuclei[33]. In addition, they present a loss in nuclear integrity caused by the decrease in structural proteins of the nuclear lamina, such as LaminB1[9]. The downregulation of **LaminB1** is a common event of different senescence models and has been used as a marker of senescence[34,35]. It occurs at the transcriptional and translational level, as well as through autophagic degradation[9,14]. This can lead to chromatin remodeling, such as the loss of condensation of constitutive heterochromatin regions, or the release of chromatin fragments to the cytosol (CCFs for cytoplasmic chromatin fragments)[9,14]. The presence of **CCFs** (or other origin DNA fragments[11]) in the cytoplasm is sensed by the cGAS-STING pathway, activating the DNA damage response (DDR) and therefore contributing to a proinflammatory secretome[14,36–39].

Another important chromatin morphological feature occurring in senescence is the formation of nuclear senescence-associated heterochromatin foci (**SAHF**). They are spatially organized heterochromatic domains that can be visualized by DNA staining since they give a

darker, more intense DAPI signal[14]. These domains are enriched in repressive chromatin marks such as the tri-methylation of the histone H3 Lys9 (H3K9me3), the heterochromatin protein 1 (HP1), the histone variant macroH2A, the high mobility group protein A (HMGA) or the histone co-chaperone HIRA among others[11,40–42]. The formation of these highly compacted heterochromatic regions has been proposed to contribute to the silencing of proliferation-related genes and the irreversibility of the senescent arrest, as well as the control of the DDR[40,43]. Although SAHF are only present in some models of senescence induction and they are not apparent in mouse cells, they can serve as a senescent indicator[9,14].

Increased lysosomal content- SA-ß-galactosidase

Senescence cells present an enhanced lysosomal content[9]. Although many organelles are altered in senescence, lysosomes have the peculiarity of being the base for the most widely used assays to identify senescent cells: the **SA-ß-gal** staining. SA-ß-gal (or senescence-associated β-galactosidase) consists on a colorimetric reaction that gives a blue signal when catalyzed by lysosomal enzyme β-galactosidase[6]. The increase in lysosomal content is due to the increase in the number of lysosomes and their activity, but also to the accumulation of old residual lysosomal bodies called lipofuscins[44]. Alternative to SA-ß-gal, lysosomes can be detected by Sudan Black B (SBB) (or its biotin-labeled analog GL13), which selectively binds to **lipofuscins**[44,45]. However, a high lysosomal activity is not a necessary nor specific characteristic of senescence. While not all senescent cells stain positive with SA-ß-gal, none-senescent cells like macrophages can be false-positive[6,13]. Therefore, its use should be considered only in combination to other senescence markers.

Persistent DNA damage

DNA damage is a well-known inductor of cellular senescence. The presence of DNA damage activates a robust response known as DDR (DNA damage response). When the damage is irreparable, a **persistent DDR** causes cell cycle arrest, and the eventual induction -or reinforcement- of cellular senescence[9,11].

Upon the apparition of single or double-strand DNA breaks, multiple sensors of DNA damage can recruit the upstream regulators **ATM** and ATR to the site of the damage[11]. There, they phosphorylate the histone γ-H2Ax, facilitating the formation of repair complexes. In addition, the DDR signal is amplified, and the CHK1 and CHK2 kinases get activated. Among other substrates, they phosphorylate **p53**, increasing its levels by protecting it from degradation by the ubiquitin ligase MDM2[11]. Then, p53 upregulates the expression of the cyclin-

dependent kinase inhibitor **p21**$^{Waf1/Cip1}$ which arrests the cell cycle. In addition, ATM activation can also promote the expression of the senescent associated phenotype (**SASP**)[9,11].

Since most of the triggers of senescence cause some type of DNA damage, the activation of the DDR and the presence of permanent DNA damage foci (also known as DNA-SCARSs)[7] are a common feature of senescent cells[11]. Regardless of the mechanism causing damage, the DNA damage foci can be identified by the increased deposition of the histone **γ-H2Ax** or the enrichment of p53-binding protein 53BP1, detectable by immunofluorescent staining[11]. However, it cannot be considered a senescent marker since senescence can happen in the absence of DNA damage, and the DDR does not always lead to it[11,46,47].

Senescent secretome: the SASP

Senescence does not only alter the interior of the cells where it is induced but it also modifies their surroundings. Actually, the senescence program can be divided in 2 branches: an intrinsic and an extrinsic component[6]. Senescent cells remain metabolically active and develop a hypersecretory phenotype termed as the senescence-associated secretory phenotype or SASP. The SASP is formed by a broad plethora of soluble and insoluble factors including growth factors, chemokines and other cytokines, leukotrienes, reactive oxygen species (ROS), extracellular matrix components and remodelers[11,48–50] alarmins[51] (also called DAMPs: damage-associated molecular patterns), and exosomes[14]. SASP composition can be very **variable**, depending on the inducer of senescence, environment and cell type, and it can even vary over time[11,48]. Although senescent cells can develop a SASP in the absence of DNA damage[11,52], the DDR is known to be a potent activator [14]. Despite its variability, the SASP is considered an important hallmark of senescence[7] and continuous efforts are invested in developing its detailed understanding [11,53,54]. Our knowledge on SASP composition, effect and control is still evolving, and new regulators are still being described[55].

The SASP is regulated at multiple levels, including transcription, translation, mRNA stability, secretion and autocrine and paracrine feedback loops[46]. Multiple triggers and signaling pathways are involved in its regulation, such as the **DDR**[14,56], the **cGAS/STING** pathway[37–39] , **p38MAPK**[52], **JAK2/STAT3**[9,11,54] and the **inflammasome**[57], p53[58,59] or **Notch1**[60], among others[11,61]. Most of the cascades regulating the SASP converge in two main transcription factors: the pro-inflammatory nuclear factor-κB (**NF-κB**) and the CCAAT/enhancer-binding protein-β (**C/EBPβ**)[62,63]. They directly bind and activate the promoters of key regulators of inflammatory SASP genes such as **IL-1α, IL-6** and in human cells, **IL-8**. The expression of

these proteins constitutes an autocrine positive feed-back loop that amplifies the SASP[62,64]. The transcription factor **GATA4** can also upregulate the expression of pro-inflammatory genes following DDR activation by indirectly increasing the secretion of IL-1α [65].

The expression of SASP genes is also regulated epigenetically. Repressive marks are reduced at the promoters of specific cytokines due to the degradation of the methyltransferase **G9a**[66] and the downregulation of the histone deacetylase **SIRT1**[67]. On the other hand, the bromodomain-containing protein 4 (**BRD4**) binds to acetylated histones (H3K27) at super enhancer regions of SASP genes promoting their expression and preventing their repression by the Polycomb repressor complex 2 (**PRC2**), which methylates the same histone[14,68,69]. The presence of the histone variant **macroH2A1**, although depleted from SASP genes, is necessary to stablish a positive feed-back loop involving ER stress and the DDR that amplifies and maintains the SASP[70]. The deposition of histones variants **H2A.J**[71] and **γ-H2Ax**, this last mediated by **MLL1**(KMT2A)[72], also favors the transcription of SASP genes. Finally, high mobility group B2 **HMGB2** protein plays a key role on the chromatin remodeling that affects the expression of the SASP[73]. While its expression is reduced during the establishment of senescence, its presence at a basal level is necessary to allow SASP expression, since its interaction with chromatin at SASP loci prevents the spreading of heterochromatin silencing marks over them. More recently, the pro-inflammatory protein **HMGB1**, which was already known to be secreted in senescence[51], has also been proposed to affect the intrinsic SASP expression through influencing mRNA availability and chromatin remodeling[74].

In addition, at the posttranscriptional level, the mammalian target of rapamycin (**mTOR**) pathway also promotes SASP production by regulating the translation and stability of SASP mRNAs. Its activation causes an increase in the translation of IL-1a[75] and, through a different mechanism, the stability of a pro-inflammatory subset of SASP mRNA[76]. At the level of protein modification, the processing of some SASP factors involves the shedding of transmembrane proteins to allow its release in the extracellular space[77].

The composition of the SASP is also dynamically changing. For example, the composition of the SASP can switch over time due to the transmembrane receptor **NOTCH1**[60], which controls the transition between a more pro-inflammatory or immunosuppressive and TGF-β enriched SASP expression. NOTCH1 is also able to regulate SAHF formation affecting the of SASP regulation in a cell extrinsic manner[78].

The SASP is responsible for most of the biological effects attributed to senescence. The function of the SASP is highly dependent on its composition, as well as on the cellular environment that is exposed to it[11,48]. This could partly explain the pleiotropy of its beneficial and detrimental roles in different biological processes[6,12]. For example, the SASP can intrinsically reinforce or spread senescence to neighboring cells[49,58,64]. It also attracts and modulates the immune system, either activating or suppressing its action. In this way, the SASP can mediate the clearance of senescent cells by the immune system[79], or, when persistent, contribute to deleterious chronic inflammation or inflammaging[80]. It also plays a role in mediating developmental senescence[47,81], wound healing[82] and tissue repair[83] and plasticity induction[6,84]. On the other hand, the SASP can also promote tumorigenesis and metastasis[6,12,48,85]. All these functions are explained in more detail in further sections.

Other affected cellular components

The senescent program affects the cell at all levels. As a result, most organelles undergo senescence-associated modifications to adapt to the new transcriptional, proteic and metabolic requirements. The endoplasmic reticulum, mitochondria and the plasma membrane are some of the cellular compartments affected by senescence, but they are not the only ones.

Endoplasmic Reticulum (ER) stress

Endoplasmic reticulum (ER) stress has been observed in many models of senescence[86,87]. The ER is a membranous tubular network that plays a major role in calcium homeostasis, lipid, and protein biosynthesis and processing. ER stress occurs when unfolded or misfolded proteins accumulate and aggregate in the ER lumen and become toxic. This can be caused by multiple factors such as a shortage in chaperones, overproduction of proteins, oxidative stress or infections[86]. When facing ER stress, the ER **expands** and cells activate systems to detect and avoid the accumulation of unfolded or misfolded proteins[86]. On one hand, the **ERAD** pathway (ER-associated protein degradation) exports misfolded proteins from the ER to the cytosol where they are degraded. On the other, the unfolded protein response (**UPR**) attenuates protein synthesis and upregulates the transcription of chaperones, ERAD and autophagy factors[9,86]. Indeed, the UPR is often increased in senescence[86,87]. Most of the secreted proteins are synthesized and processed in the ER, as well as the factors allowing their secretion. Thus, UPR activation can occur in response to the increased protein synthesis of **SASP** components[88,89], among other reasons[9,90]. Moreover, the activation of the UPR has been shown to influence or regulate many hallmarks of senescence such as SASP

production[29,70,89,91] or **cell shape**[29] among others[29,90]. Altogether, it seems that the ER stress, and more specifically the UPR, is both consequence of and contributor to senescence[90].

Mitochondria

Senescence is associated to an accumulation of **dysfunctional mitochondria**[92]. Not only senescent cells show an increased mitochondria mass[93–95] but also their mitochondria present changes in morphology, function and dynamics. Their membrane potential is decreased, leading to the release of mitochondrial enzymes and intensified **ROS** production[93,95]. The accumulation of mitochondria is mainly explained by altered fusion and fission rates[96,97] and reduced mitophagy in senescence[98,99]. Mitophagy (selective autophagy of mitochondria) maintains mitochondrial turnover by targeting dysfunctional mitochondria for degradation. The increase in ROS production can cause lipid damage and accumulation, DDR activation and telomere shortening[95,100,101]. Interestingly, it has been shown that upon certain senescence-inducing damage stimuli, the accumulation of dysfunctional mitochondria establishes a positive feedback loop between ROS production and the DDR that is necessary for the establishment of senescence[93]. Actually, disrupting mitochondrial function can **trigger** senescence[94,101–103]. In addition, mitochondrial dysfunction is also implicated in **SASP** regulation[101,102,104]. Thus, mitochondria regulate different aspects of senescence by influencing ROS and energy production and controlling cellular metabolism.

Plasma membrane

The composition of the plasma membrane also presents specific alterations in senescent cells. For instance, and as previously mentioned, senescent cells upregulate **caveolin-1**, a component of caveolae (cholesterol-enriched microdomains of the membrane)[105]. In addition of altering the morphology[30,106], the expression of caveolin-1 is able to promote senescence[107–109]. Surface proteins specifically expressed in senescence can be used as **markers** to identify and isolate senescent cells[110]. This was the approach followed by the authors of the 2014 proteomic screening that identified 107 membrane proteins specific for senescence[111]. Another protein that is selectively enriched on the surface of senescent cells is **DPP4** (dipeptidyl peptidase 4) [112]. Interestingly, the expression of DPP4 can mediate the elimination of senescent cells by natural killers[112].

Metabolism and proteostasis

Senescence is associated to broad **metabolic** changes, including increased **glycolysis** and autophagy and altered **lipid** and **mitochondrial** metabolism (leading to increased **ROS** and

fatty acid accumulation)[113–116]. It has been proposed that metabolic reprograming is necessary for the acquisition of senescence in order to support its specific metabolic demands[103]. For example, the expression of the SASP requires an intensified ATP production by the mitochondria and increased glycolysis[88]. The intense production and secretion of SASP factors leads to proteotoxic stress that can be attenuated by autophagy[117]. Loss of **proteostasis** is also observed in senescence. Actually, the two major processes controlling proteostasis, protein degradation by **autophagy** and the **proteasome**, and protein **translation** are altered in senescence[76,118,119]. The main mediators of these processes are the p53, Rb and the mTOR pathway[101,114,118–122]. These changes in metabolism and proteostasis are not only a consequence of senescence but also contribute to its phenotype, controlling the establishment of senescence and **SASP** production[99,102,117,118,123].

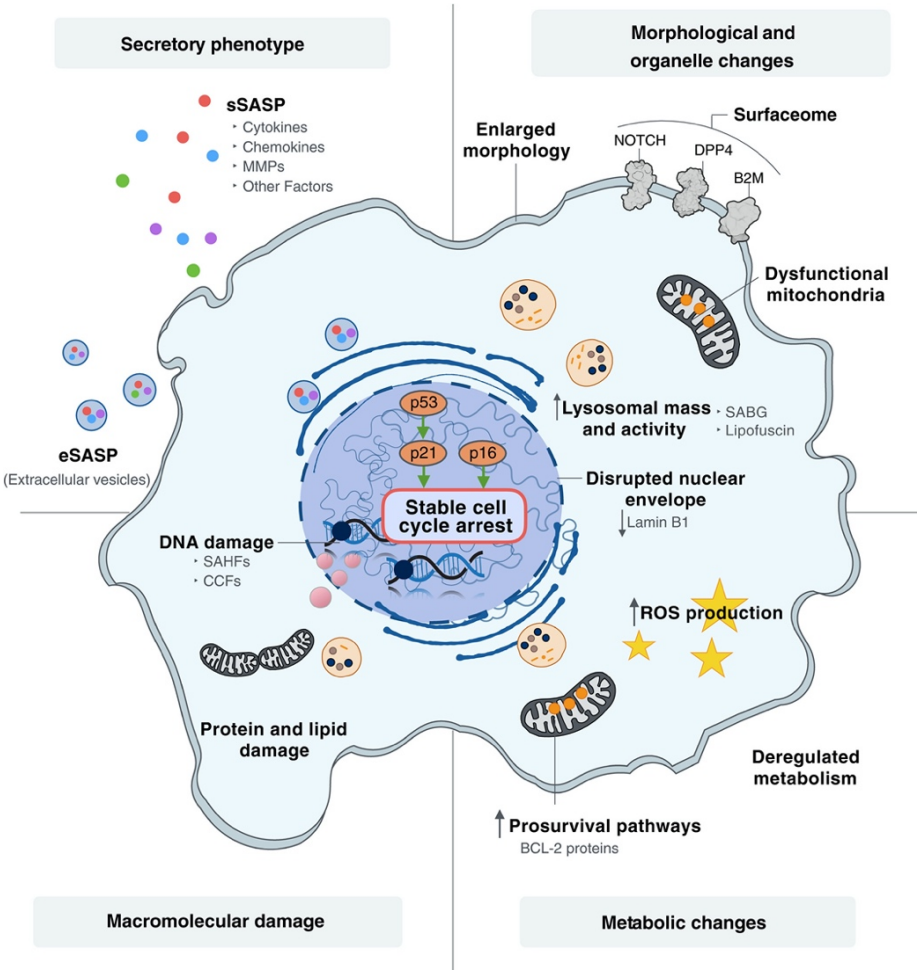

Figure 1. Hallmarks of cellular senescence. Senescent cells are typically characterized by an irreversible proliferative arrest, activation of prosurvival pathways and apoptosis resistance, characteristic morphological changes (enlarged size, disruption of the integrity of the nuclear envelope, remodeling of chromatin architecture), persistent DNA damage, increased lysosomal activity (detected via SA-ß-gal staining), secretome production (SASP), organelle adaptations (plasma membrane composition, mitochondrial number and activity, Endoplasmic Reticulum stress) and overall changes in metabolism and proteostasis. Figure from Ou et al. 2021

1. 3 Establishment of senescence

The establishment of senescence is a complex process. On top of being heterogenous, context dependent and caused by multiple factors, it involves the crosstalk and modification of many cellular processes and expression programs. Actually, most of the molecular markers and pathways used as markers of the senescent state are also important activators and mediators of its induction and maintenance. However, there is an agreement on which are the most important inductors, molecular axis and steps that more commonly mediate the acquisition of this irreversible state.

Triggers

The number of known stimuli able to induce senescence increase over time. Senescence is observed to arise in biological contexts in response to physiological cues, but it can also be intentionally triggered, either reproducing these physiological cues or through more artificial molecular interventions. The technical advances in cellular and molecular manipulation tools together with the development of more sensitive and precise markers to detect senescence *in vivo* is contributing to the unravelling of new mechanisms and situations that lead to the unravelling of the senescent program. Broadly, the inducers of senescence can be categorized in 3 groups: **damage or stress inductors**, that alter the integrity and presumed healthy functioning of cells and tissues, **developmental cues**, where senescence is induced in a programmed manner and in absence of evident damage, and "**contagious**" mechanisms, by which senescent cells amplify in number by "spreading" their phenotype via signaling to their neighboring cells. Most of the typical models to study senescence belong to the first category, which includes several subcategories and a wide variety of factors that challenge cellular function, from oncogenic activation to metabolic or DNA damaging agents[8].

Damage-induced-senescence

The first context where senescence was described was due to the limited proliferative potential of cells in culture and it was termed **replicative senescence**[4]. It is caused by the gradual shortening of **telomeres** in each replication cycle that ends up producing critically short telomeres[124]. Telomeres consists of repetitive sequences comprehending a single-strand over-hang of DNA that forms a t-loop protected by a complex of telomere-binding proteins called shelterin[125,126]. If this complex is disrupted and the integrity of telomere is compromised, these loops are sensed as DNA damage and the **DDR** is chronically activated, triggering the molecular cascade that leads to senescence[127,128]. The shortening of the

telomeres arises from the molecular mechanism of replication of linear chromosomes. The expression of the ribonucleoprotein enzyme Telomerase is able to prevent telomere shortening by restoring the repetitive telomeric sequences *de novo*[129]. However, telomerase is not generally expressed in human somatic cells, so progressive telomere shortening and replicative senescence are directly connected to the accumulation of proliferation cycles[130].

Besides telomere shortening, many other stressors have been identified as triggers of senescence. The chronic activation of the DDR is a general node of convergence of most of them, so insults generating direct or indirect DNA damage (**double strand breaks** or **oxidative stress**, respectively) DNA damage are general senescence triggers[131–133]. For instance, genotoxic agents (such as chemotherapeutic drugs), irradiation, mitochondrial disfunction, oncogene activation are reported causes of senescence[7,8,134,135].

Interestingly, senescence also arises upon maintained **mitogenic** signals. This is the case of oncogene activation[8,136]. **Oncogene-induced senescence** was first observed in 1997, when Serrano and colleagues showed that the overexpression of the Ras oncogene triggered a fast phase of hyperproliferation followed by senescence induction[137]. Similarly, loss of tumor suppressors can trigger the same response[138,139]. Persistent mitotic stimulation by interferon-B signaling have an analogous effect too[140]. In all these cases, senescence seems to be due to **hyperproliferation**, ROS accumulation and activation of the DDR[140–143].

Developmental senescence

Surprisingly, cells exhibiting senescent features were described during mouse embryonic development in 2013[47,81]. The presence of cells bearing senescence markers during development has been reported in several organisms: mouse, human, chicken, quail, *Xenopus*, axolotl, zebrafish and naked mole rat[47,81,144–149]. Some of the structures where senescence is observed include the apical ectodermal ridge of the limbs (AER), the neural tube, the hindbrain roofplate, the endolymphatic sac of the inner ear, the tip of the tail, the gut endoderm and the extra-embryonic placenta[6,12]. Senescent cells in the embryo appear transiently and in specific locations. Their presence is generally identified by **SA-ß-gal** staining, **absence of proliferation** and increased expression of SASP factors and the cell cycle inhibitors p21, p15 and p27. **Developmental senescence** seems to rely on the expression of the senescent mediator **p21**[47,81,149], while no increased expression of the common senescence markers p53, $p16^{Ink4a}$ or $p19^{Arf}$ or DNA damage is detected[6]. It is mainly induced through the **TGF-ß** /SMAD pathway[47,81,144,148], but the PI3K/Akt/FOXO[81,144] pathway and ERK[47,144] signaling also seem to be involved in its control. Actually, interference with the

senescence program by TGF-ß or ERK inhibition, and elimination or induction of ectopic senescence leads to patterning and developmental defects[1,47,81,144,148].

Secondary senescence

Interestingly, it has been shown that senescent cells can induce senescence in neighboring cells in a phenomenon called secondary senescence. While primary senescence normally arises in response of a damage signal (or a developmental cue), secondary senescence can occur by paracrine or juxtracrine signals from primary senescent cells. **Paracrine senescence** is mediated by secretion of SASP factors[64] Some of the factors that have been reported to spread senescence in a paracrine manner include TGF-ß, VEGF, CCL2, IL6, IL1-B, IP10 and IGFBP3[64,150–154]. On the other hand, **juxtacrine senescence** requires cell-to-cell contact. It has been reported that senescent cells can trigger senescence by sending ROS through gap junctions and generating oxidative stress and damage to neighbor cells[155]. NOTCH1 has also been reported to be a potent inductor of secondary senescence. Apart from regulating SASP composition and promoting paracrine senescence through TGF-ß secretion, NOTCH1 also mediates senescence induction via gap junctions[60]. Mechanistically, Notch signaling is activated in adjacent cells by the interaction of Notch receptors with its ligand JAG1, which is upregulated in senescence cells. In addition, NOTCH1 is able to regulate SAHF formation in SASP genes in a cell autonomous and non-autonomous way[78].

Main molecular drivers

Although senescence can be triggered by a variety of stimuli and in multiple contexts, the induction and establishment of the response is mainly dependent on two interconnected tumor suppressor pathways: p53/p21 and p16/pRb[137,156]. p53 and pRB are the key transcriptional regulators while p21 and p16 CDKis are able to arrest proliferation and activate pRB[13,18,157]. The chronic activation of these pathways can be sufficient to induce a senescent phenotype and their disruption facilitates its avoidance[18,158,159]. The activation of these paths leads to a deep change in gene expression mediated by an important remodeling of the epigenetic marks and chromatin estate of the senescent cell. As a result, the phenotype and functions of the cells become significantly altered in all levels in an, a priori, irreversible way.

The p53/p21 axis

The tumor suppressor **p53** is a master regulator of the senescence process. Its levels are mainly controlled by its degradation by MDM2[160]. In undamaged cells, p53 levels are low, and

it gets only stabilized, and then activated, upon damage or stress signal such as DNA damge (through the DDR) or oncogene activation[160]. p53 is a transcription factor able to recognize and bind to specific DNA sequences to promote its transcription, acting as a direct activator and indirect repressor of a variety of transcriptional programs[161]. Apart from senescence, p53 also controls a multitude of functions, such as genome integrity maintenance, DNA repair, apoptosis, cell cycle arrest, autophagy, metabolism, pluripotency and plasticity repression[162]. One of the most important mediators of p53 functions in senescence is its transcriptional target **p21**$^{Cip1/Waf1-}$ [163]. Although it is commonly accepted that an early induction of p21 is important for senescence initiation, and it is the main driver in developmental senescence[47,81], data from the end of the 90s showing that its levels do not persist over time[164–166] led to the idea that its importance in senescence may be limited to the onset of its establishment[13,46]. Upon p53 transactivation, the CDKi p21 inhibits the activity of cyclin-CDK complexes, especially affecting CDK2, preventing the phosphorylation of the retinoblastoma family proteins (RB1/pRB), p107/ RBL1, p130/RBL2). When unphosphorylated or hypophosphorylated, these proteins increase their affinity to the E2F transcription factors and are able to form the **RB-E2F** and **DREAM** repressive complexes, which repress the transcription of the genes necessary for the cell progression[17]. Moreover, Rb also interacts with different chromatin remodelers to modify the epigenome of senescent cells and mediate gene repression, such as the SWI/SNF complex or the histone methyltransferase Suv39h[167]. In this way, the activation of Rb is involved in SAHF formation[40] and controls other important senescent regulators[168].

The Cdkn2a locus – p16^{Ink4a} and p19^{Arf}

Astonishingly, the 2 main axis of senescence induction evolutionary converged in the *Cdkn2a* locus. The ***Cdkn2a*** locus encodes for two senescence mediators and tumor suppressor genes: *Ink4a* encoding for **p16^{Ink4a}**, and *Arf* for **p19^{Arf}** (p14^{ARF} in humans)[169,170]. On one hand, p19^{Arf} expression activates the p53 axis[171,172]. It does so by inhibiting the action of p53-degrading ubiquitin ligase MDM2 and therefore preventing p53 degradation[173]. Additionally, other p53-independent functions for p19^{Arf} have been described[174–177]. On the other hand, p16^{Ink4a} is a CDKi that selectively binds and inhibits CDK4 and CDK6. Although through the inhibition of different CDK complexes, its action converges with the p53-p21 axis on the hypophosphorylation of **Rb** and the consequent transcriptional repression of cell cycle[178]. The expression of p16 transcript and protein is repressed in most undamaged proliferating cells, it increases with age and it is induced in senescence[179–181]. This axis has been suggested to act as a second protective barrier against oncogenic transformation, being able to maintain

proliferative arrest in case of deactivation of the p53-p21 axis[159,164]. Although its expression is not completely restrained to senescent cells[13] and it is not necessarily induced in all of them[182], p16 has been commonly used as a specific marker for senescence, at both the transcriptional and protein level[14].

While it is assumed that the gene encoding $p16^{Ink4a}$ arose by tandem duplication of the proximal locus *Cdkn2b*, encoding the CDKi $p15^{Ink4b}$, *Arf* seems to have been originated from a later insertion of the sequence of the 1st exon of $p19^{Arf}$ [183]. Interestingly, *Arf* function seems to rely on this first unshared exon[183]. Although p16 and p19 share their last 2 exons genetic and transcriptionally, they have different promoters, and a shift in the reading frame gives rise to completely different protein sequences (hence the Arf name, from "alternative reading frame") with different molecular functions. Therefore, the transposition of the first exon of $p19^{Arf}$ into the *Cdkn2a* locus suggests the positive selection of a coordinated regulation[183]. Sespite the fact that both genes can be regulated independently, the entire locus is subjected to the control of some factors as a whole. Several pathways, transcription factors and epigenetic regulators have been reported to be involved in the regulation of the locus and its encoded genes, but the exact mechanisms involved it are not fully understood yet[9,46,183].

Epigenetic and chromatin regulators

The phenotypical modifications associated to the acquisition of senescence are significantly determined by striking changes in gene expression. This deep transcriptional shift is accompanied and mediated by global modifications of the epigenetic marks and the chromatin structure[184,185]. In consequence, an increasing list of factors implicated in the triggering, initiation and maintenance of the epigenetic modifications have been reported to act as critical mediators of the senescence process[7,55,184,186]. This includes DNA binding proteins, non-coding RNAs, histone variants and modifiers among others, and only a small selection of them are mentioned here.

A good example of the importance of epigenetic modifications in the control of the senescent phenotype is the regulation of the SASP genes. As previously described, many epigenetic modulators have been reported to control SASP expression[14]. Among them, we find the **HMGB2** protein, whose direct binding to SASP genes appears to stimulate their expression[73]. HMGB2 has been reported to localize to active genes encoding for senescent-related processes and to mediate chromatin reorganization in senescent cells[187]. Interestingly, although HMGB2 levels decrease at the upon senescence, and its ablation is enough to induce it, a remaining fraction of the protein is required to allow the expression of the SASP[73]. The

binding of HMGB2 to SASP loci during the establishment of senescence prevents the spreading of repressive marks in these regions. Thus, HMGB2 promotes the SASP by avoiding the silencing of the genes encoding it[73].

Another interesting group of chromatin regulators worth mentioning are the members of the Polycomb group, which participate into 2 different Polycomb Repressive Complex, **PRC1** and **PRC2**. Polycomb proteins maintain transcriptional repression of target sites in the genome by modifying the chromatin structure to control development, differentiation and proliferation[188]. Several members of these complexes are known to regulate senescence, and in fact, the disruption of some of its components can be sufficient to induce it[189,190]. This is primarily due to their ability to repress the *Cdkn2a/b*[183,190,191]. In proliferating cells, the PRC2 methyltransferase **EZH2**, together with other PRC1 members, maintains the repressive marks on the locus[190,192]. Upon senescence entry, these complexes are forced to dissociate from the *Cdkn2a/b* locus, which leads to its demethylation and allows the transcriptional of the senescence mediators that it encodes for[192]. Moreover, the loss of **EZH2** potentially favors the expression of the SASP, and additionally promotes senescence by triggering the DDR independently of its methyltransferase activity[69].

Perhaps the most prominent modification of the chromatin structure observed in senescence is the already mentioned formation of the **SAHF**, which is dependent on the activation of Rb proteins[40]. Other chromatin factors implicated in their formation are the histone chaperones of the **HIRA** complex (HIRA, UBN1, CABIN1 and ASF1a)[42,193,194], changes in the levels of the structural proteins HMGA and H1[195,196], the ubiquitin ligase adaptor SPOP[197] or an increased nuclear pore density[198]. However, SAHFs are not the only alteration of the chromatin that has been observed in senescent cells[199–203]. For instance, another chromatin feature associated to senescence is the unfolding of constitutive heterochromatin domains, such as the distension of pericentromeric satellite sequences[201]. Most of these structural modifications seem to be produced by alterations in the abundance of nuclear structural proteins, specifically to the loss of **LaminB1**[34,35,199,201,204]**.**

Senescence: a dynamic and heterogenous program of interconnected networks

Although senescence can be defined as an irreversible **state**, it can also be understood as a dynamic and multi-step **process**[97,205]. Typically, it would be initiated by a first -and reversible- arrest of the cell-cycle due to the activation of CDKi, mainly p21 and/or p16. Then,

the persistent activation of p53 and Rb would trigger a cascade of epigenetic modifications involving the downregulation of LaminB1 and the SAHFs formation[34,35,40,204]. These modifications cause a profound change in the transcriptome of the cell, altering its phenotype. Among the transcriptional programs, genes encoding for SASP factors will become upregulated. Positive feedbacks loops, especially among the SASP, DDR and ROS production by stressed mitochondria, would reinforce the senescence response[56,93,101,206,207]. Moreover, the epigenome and transcriptome of senescent cells can continue to evolve over time[60,61,208–211] (which may eventually lead to a more stabilized state[97]. This has led to the use of the terms "deep" and "**late**" senescence in contraposition to "**early senescence**" in order to refer to cells that have been in culture for long periods of time after senescence induction.

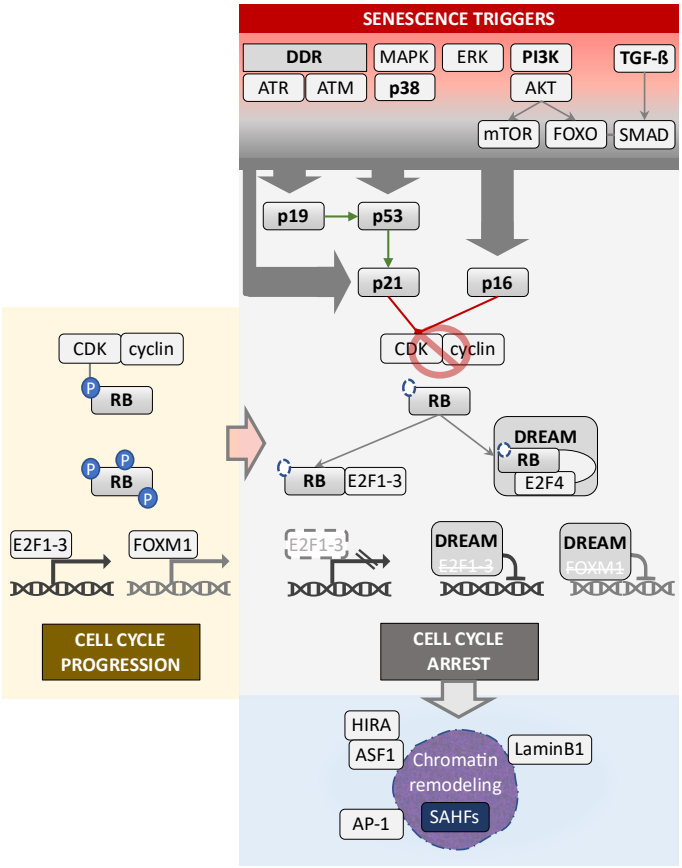

Figure 2. Main molecular drivers of senescence. Senescence-inducing stimuli trigger the upstream activation of different interconnected pathways (pink-grey panel) that converge on the induction of one or more senescence drivers: p19, p53, p21 and p16 (grey panel). In proliferative cells (yellow panel), the members of the retinoblastoma family (RB) are phosphorylated by active CDKs. The activation of the CDKi p21 and p16 prevent different CDKs from phosphorylating RB. When hypophosphorylated, RB proteins inhibit the transcription of cell-cycle related genes, causing a proliferative arrest. Further epigenetic modifications establish and stabilize the transcriptional programs regulating senescence (blue panel). Deep chromatin remodeling ensures the irreversibility of the phenotype.

Following this model, it is tempting to perceive the establishment of senescence as a linear program. However, this is likely to be an oversimplification. Although this sequence of events is often observed to occur as described, and recent data indeed suggests that the acquisition of senescence is governed hierarchically[55] , the establishment does not always develop in this straight ordered manner. A good example of this is the observation that senescence can be induced by the direct perturbation of most of the pathways known to be altered by it[7]. For instance, mitochondrial dysfunction[102], epigenetic signals[135], LaminB1 silencing[207,212] or even cell size manipulation can all be sufficient to trigger a senescence response[213]. This is likely to be the result of a strong **crosstalk** among all the networks implicated in the response. Therefore, senescence could be better defined as **dynamic** and **heterogeneous program** with multiple steps and highly interdependent regulatory pathways, whose development strongly depends on its biological context.

1. 4 Physiological impact of senescence

The activation of the senescence response and the presence of senescent cells can have an important impact on the tissue and organism harboring them. Despite it has been mostly viewed as a response to detrimental estates such as aging and oncogenic activation, senescence has been shown to play a role in many other pathological and physiological conditions. Nowadays, we known that the senescence program contributes to embryonic development, and controls wound healing and tissue repair, cancer development or aging, among others. Paradoxically, depending on the context, senescence can impact these processes in contradictory way. For this reason, senescent cells can be beneficial or detrimental in most of the scenarios where it develops.

Functions of senescent cells

In general, the functions associated to senescence can be classified in cell-intrinsic and cell-extrinsic effects. While the **intrinsic** effect of senescence refers to the functional changes developed by cells that enter senescence, the **extrinsic** effect is mainly attributed to the paracrine effect of the **SASP**. In this way, senescence cells can spread their phenotype mediating paracrine senescence, modify the extracellular matrix, signal and instruct neighboring cells and interact with the immune system. The cellular functions that are most importantly impacted by senescence are the control of proliferation and cell cycle,

acquirement of plasticity or reprogramming, remodeling of the extracellular matrix and tissue patterning and the recruitment and regulation of the immune system.

Growth arrest and proliferation

As discussed, one of the main characteristics of senescence is the irreversible arrest of the cell cycle. Considering that senescence often arises in response to oncogene activation and hyperproliferation, its intrinsic ability to suppress proliferation supports the idea that senescence acts as a **tumor suppressive** mechanism.

The presence of senescent cells can also determine the proliferative capacity of neighboring cells in a **paracrine** manner. On one side, senescent cells can induce secondary senescence in proximal cells through the SASP, therefore increasing the number of cell-arrested cells in a tissue[62,214]. On the other, the SASP has also been shown to promote cell proliferation through growth factors and matrix remodeling[48]. Paradoxically, when the SASP affects malignant or premalignant cells, the presence of senescent cells can contribute to cancer progression[85,215].

The other main processes involving growth arrest are the entry to quiescence and terminal **differentiation**. Despite the control of these processes rely on common pathways, there are important differences among them[7]. Although quiescent cells may eventually become senescent, upon pro-proliferative stimulation they typically re-enter the cell cycle. On the other hand, the boundary between differentiation and senescence is not that clear. In general, it is considered that in contrast to senescence, macromolecular damage is not necessarily observed nor a usual trigger of differentiation. However, it has been observed that the activation of the DDR has also been observed to promote differentiation in several cell types[14]. For this reason, it has been suggested that senescence could also act as a stress-induced differentiation program[14]. In addition, senescent cells can extrinsically promote myoblast differentiation, contributing to proper wound healing upon cutaneous injury[82].

Plasticity and reprogramming

The effect of senescence in cellular plasticity is also complex and paradoxical. Intrinsically, the activation of senescence acts as a **barrier** for cell platicity[6]. The expression of reprogramming factors causes the induction of senescence among a majority of cells, and only cells that avoid it undergo successful reprogramming[216,217]. Accordingly, the elimination of senescence mediators (p53, p16, p19 or p21) increases reprogramming efficiency[216–221].

Paradoxically, senescent cells can also **promote** plasticity. This is principally attributed to the secretion of SASP factors. The presence of senescent cells has shown to extrinsically promote the acquisition of plasticity in neighboring cells during reprogramming induction, aging and tissue damage[222–224]. This ability is one of the mechanisms by which senescent cells facilitate healing and regeneration in various tissues. However, in a tumorigenic context, the upregulation of stem-cell features associated to senescence can increase the potential of tumor initiation[225,226].

Tissue remodeling and patterning

The most important mechanism by which senescent cells alter their environment is likely to be via SASP secretion. The SASP is composed/constituted by many factors able to alter the tissue environment and signal the neighboring cells, such as cytokines, growth factors, extracellular matrix-associated proteins (CCNs), extracellular matrix components (collagens and glycoproteins), and remodeling enzymes (matrix metalloproteinases (MMPs), serine/cysteine proteinase inhibitors (SERPINs), tissue inhibitors of metalloproteinases (TIMPs)[48,58]. The release of these factors modifies the properties and architecture of the surrounding matrix, which can ultimately impact cell behavior. For instance, the **matrix remodeling** by senescent cells can promote proliferation[227] , invasiveness[58,228] or angiogenesis [229,230]. In this way, senescent cells can promote a pro-tumorigenic environment that favors cancer progression

A good example of how senescent cells can instruct remodeling of the surrounding tissue is found in **developmental senescence**. During embryonic development, the transient expression of senescent cells contributes to normal tissue patterning and embryonic development[6,47,81]. In fact, the ablation of these cells can result in patterning defects[47,81,144,148].

Another well studied effect of senescence on the modification of matrix composition is the control of fibrosis. During tissue repair, senescent cells can limit tissue **fibrosis**, thus promoting wound healing[82,231,232]. This effect is achieved by the secretion of matrix components and remodelers, mediators of paracrine senescence and activators of the immune system. On the contrary, the accumulation of senescent cells in the lung has been shown to impair lung function and contribute to idiopathic fibrosis[233].

Inflammation and immune recruitment

Senescent cells play an important role in the control of **the immune system**. An important part of the SASP component configure an inflammatory signature composed by immune-cell

attracting chemokines, activating cytokines, adhesion molecules, and other immune modulators[58,234]. The release of these factors is able to recruit and activate different immune cells, principally Natural Killers (**NK)**, monocytes/**macrophages** and **T cells**[235]. In addition, senescent cells often upregulate the expression of specific surface proteins that mediate their recognition and clearance by immune cells[79,231,236]. By activating an immune response, senescence cells can extrinsically **suppress tumor progression**[79,236] and resolve fibrosis[231] to promote **tissue repair** and homeostasis maintenance.

On the contrary, the SASP from oncogene-induced senescent cells can also exert an **immunosuppressive** effect, accelerating cancer development[237,238]. Besides, senescent cells can escape the immune clearance, resulting in their accumulation and contributing to detrimental effects[239]. If oncogene-induced senescent cells are not properly removed, they can progress into cancer formation[236]. Moreover, the chronic release of inflammatory signals by the accumulation of non-removed senescent cells is thought to contribute to chronic inflammation or "**inflammaging**", which has been strongly associated with the development of virtually all age-related diseases[80]. In accordance, the removal of senescent cells has been shown to reduce the presence of inflammatory cytokines and improve associated pathologies[240].

Beneficial or detrimental?

By altering these processes, senescence can contribute to organism health and disease, being beneficial or detrimental depending on the context. Ultimately, this depends on the recipient cells (type of tissue, cell type, tumorigenic state…), the composition of their SASP and their dose in terms of quantity and time in a tissue. In general, it seems that when senescent cells are **transiently** present, they have a beneficial effect, while when they become **chronic** and accumulate, they favor detrimental outcomes. In physiological situations, when senescent cells are expressed transiently, they contribute to maintain -and restore- tissue balance, and then they are removed by the immune system. This is what is observed during development, tissue healing or in cancer suppression. However, when they are not eliminated, senescent cells accumulate and disrupt the homeostasis of the tissue, impairing organism function and contributing to tumor progression, scarring, inflammaging and the progression and onset of numerous pathologies[157,205,241].

The reason for this could be both an excessive number of senescent cells and, as a result, their maintained secretion. This is explained by the time-dose effect of the SASP on recipient cells,

well exemplified by the 2017 article published in our lab by Ritschka et al.[224]. Although SASP can promote the plasticity of neighboring cells, its exact effect seems to depend on the length of its exposure. Transient exposure of primary mouse keratinocytes to SASP induced their functional dedifferentiation to skin stem cells, while a prolonged treatment caused them to senesce in a paracrine manner. As a result, stem cell functions were hindered intrinsically by senescence despite an increased transcriptional expression of stem cell markers. Besides the detrimental effect of the chronic release of pro-inflammatory molecules, senescence may spread through paracrine senescence. Thus, if the removal of senescent cells is not efficient, it could create an amplification feed-back leading to disproportionate number (and signaling) of senescence cells. This imbalance can compromise organs and tissues function[157,205].

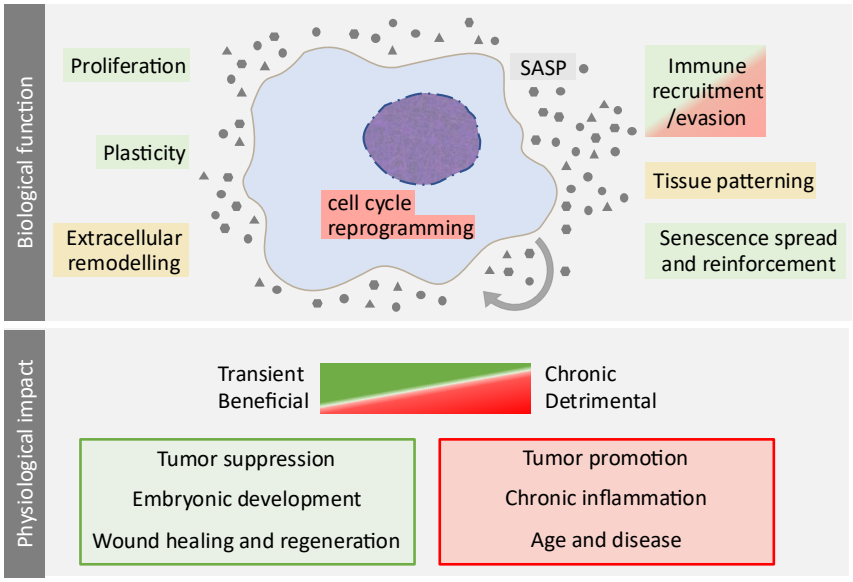

Figure 3. Senescence-related processes. **Top)** Biological functions affected by senescence. Senescence contributes (yellow), inhibits (red) or promotes (green) different biological functions both cell intrinsic and extrinsically by altering their environment through the SASP. **Bottom)** Physiological impact of senescent cells. Beneficial (green) or detrimental (red) contribution of senescence to organism health is associated their transient or chronic presence respectively.

During **aging**, senescent cells accumulate[242]. The reason for this is not clear yet[205]. It has been hypothesized that over the lifetime, the immune system may become increasingly more inefficient in detecting and clearing senescent cells. However, it can also be due to an amplification of the senescent cells that somehow develop molecular mechanisms to escape their removal. Moreover, the presence of senescence-inducing stimuli could increase with age, favoring the apparition and accumulation of senescencent cells over time[205]. Regardless of its cause, the accumulation of senescent cells in aged organisms seems to contribute importantly to the onset and progression of many diseases such as osteoarthritis,

atherosclerosis, glaucoma, type 2 diabetes, and neurodegenerative diseases (Alzheimer's and Parkinson's disease), among many others[8,26]. The selective elimination of senescent cells has been repeatedly shown to lengthen the lifespan and healthspan of mice[240,242,243]. Accordingly, the use of drugs that either selectively eliminate senescent cells, known as "**senolytics**", or modulate/supress the SASP, "**senomorphics**", has demonstrated to be beneficial to delay or reduce the severity of many of these conditions[14,26]. These are promising strategies that are currently being explored in order to improve aging and health, highlighting the importance of understanding the molecular mechanisms behind the detrimental effects of senescence in the first place.

2. p21 - *Cdkn1a*

2. 1 Description and history

p21, also known as **Waf1** or **Cip1**, (and, historically but less often nowadays, as **CAP20, SDI1, MDA6, CDKN1** and **PIC1**), is a potent cell cycle inhibitor protein encoded by the *Cdkn1a* gene (for Cyclin-dependent kinase inhibitor 1A). It was the first described member of the **Cip/Kip** (Cdk Interacting Protein/Kinase Inhibitory Protein) family of CDK-cyclin inhibitors (CDKi). Apart from p21, this family includes $p27^{Kip1}$ and $p57^{Kip2}$, encoded by *Cdkn1b* and *Cdkn1c* respectively. These 3 proteins share their CDK-cyclin complex binding domains, but the rest of their sequence is more divergent, suggesting differences in function and mechanisms of regulation for each of them[244].

The **cell cycle** progression is controlled by CDKs. By forming complexes with cyclins, the levels of which are tightly regulated and fluctuate during the cell cycle, the different CDKs become active. By phosphorylating their target proteins, they control key transcription factors necessary to progress through the phases of the cell cycle[15,245]. CDKi interact and inhibit the action of CDKs, and therefore, control cell cycle progression. CDKi are grouped in 2 classes, the Ink4 family (which includes $p15^{Ink4b}$, $p16^{Ink4a}$, $p18^{Ink4c}$ and $p19^{Ink4d}$) and the **Cip/Kip family**[16]. In contrast with Ink4 proteins, the Cip/Kip family are **promiscuous** proteins able to interact with different CDK-cyclin complexes, being able to interfere with the cell cycle at different phases. Moreover, these proteins have acquired extra functions by becoming transcription regulators that modulate other functions than the cell cycle[245,246]. They can act as modulators of differentiation, apoptosis and cytoskeletal dynamics.

p21 was **independently described** by several groups in parallel at the beginning of the 90s, explaining the different names given to it[163,247–249]. Initially, p21 was shown to interact with different CDK-cyclin complexes[248,250,251], and with PCNA[249,252], and to block the cell cycle through inhibiting the action of CDKs[247,248,251] and the synthesis of DNA[249]. At the same time, p21 was proposed to be a target of p53[163,247,253] , mediating its tumor suppressor activity[163] and contributing to the induction of senescence[249]. Over time, the role of p21 has been shown to involve much more than cell cycle inhibition, senescence or tumor suppression. Nowadays, p21 is known to be an important regulator of apoptosis, differentiation, reprogramming, DNA repair and genome stability, migration and cytoskeletal dynamics, and transcriptional regulation, among others[254]. Moreover, its transcription can be induced dependent and

independently of p53, and its expression, stability and localization are regulated at different levels by a plethora of factors[255,256]. For this reason, novel functions and implications of p21 activity are still being investigated at the moment.

2. 2 Gene and protein structure

p21 is a protein of 159 amino acids (164 in humans) and about 18KDa of molecular weight. It is encoded by the 2nd and 3rd exon of the *Cdkn1a* **gene**, located at chromosome 17 (chromosome 6 in humans). In mice, this gene can generate two **transcript variants**[257] (and multiple variants have also been observed in human cells[258–261]. Despite encoding for the same polypeptide, these variants are transcribed from different promoters and contain distinct parts of its first exon, suggesting specific regulatory mechanisms for each of them. In fact, and despite the lack of information about the separate regulation of these variants,

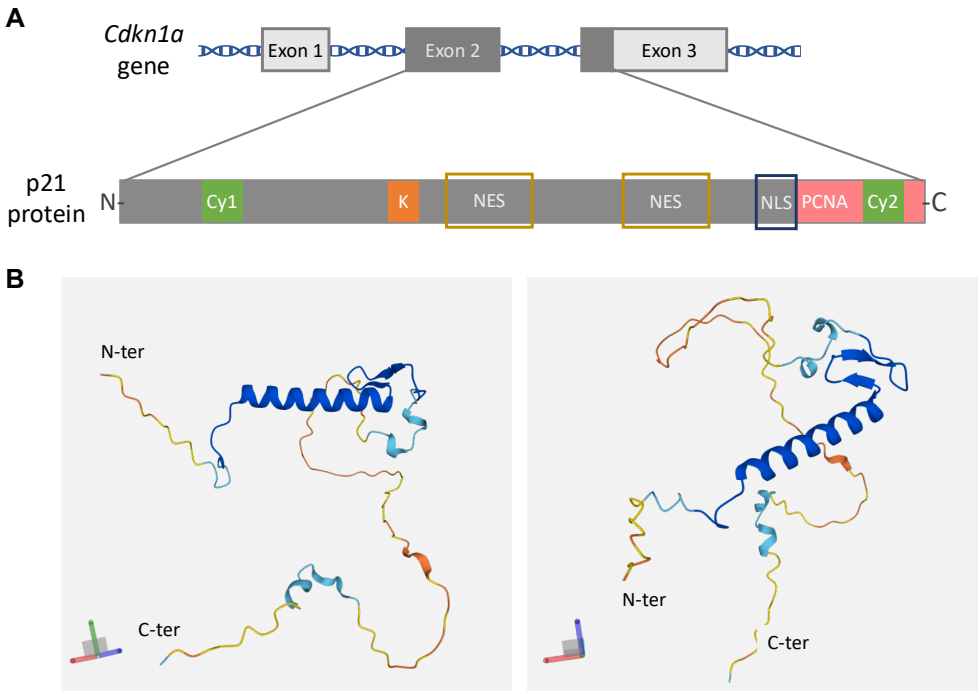

Figure 4. *Cdkn1a* gene and p21 protein structure. A) Schematic representation of *Cdkn1a* locus and p21 protein structure. Top: Mouse *Cdkn1a* gene encoding p21 protein in its 2nd and 3rd exon. Protein coding sequence in darker grey. Bottom: p21 protein structure. Cyclin binding domains (Cy1 and Cy2) in green, CDK binding domain (K) in orange, PCNA binding domain in pink. Nuclear export signals (NES) and nuclear localization sequence (NLS) marked by orange and blue boxes respectively. Amino terminal domain (N-) and carboxyl terminal domain (-C) indicated. **B)** 3D structural model of p21 protein. 2 representations from different orientations (axis position depicted at bottom-left of each image). In dark blue, helix structure between Cy1 and K binding domains conferring structural flexibility between them. Colors, indicating the confidence of the structural model, ranging from very high (dark blue) to very low (orange), are conserved for visualization purposes only. Images obtained at P39689 entry of UniProtKB webpage (from AlphaFold Protein Structure Database).

differences in their transcriptional and translational regulation have already been reported[262,263].

Several functional **domains** have been described in the protein sequence of p21[264] (Figure 4). The three Cip/Kip proteins (p21, p27 and p57) present high homology at their amino terminal region (N-ter), which contains the domains of interaction with **cyclins** and **Cdks**. The carboxy terminal (C-ter) region of p21also contains a second cyclin binding domain, a domain of interaction with **PCNA** (proliferating cell nuclear antigen), a **nuclear localization** signal (NLS) and two **nuclear export** signals (NES), as well as different degradation motifs and a putative **zinc finger** region[264,265]. When in solution, p21 lacks a tertiary stable structure: it is considered an "**intrinsically disordered protein**"[266]. This enables promiscuous protein-to-protein interactions. Thanks to this feature, p21 is able to bind to several CDK-Cyclin complexes through structural adaptation[267]. In fact, disordered proteins are able to promiscuously interact with many other proteins, and for this reason, they are often able to perform multiple functions by associating with **different partners**.

2. 3 Molecular regulation

P21 was initially discovered as a transcriptional target of p53 that was activated in response to DNA damage[163,247,249]. Besides DNA damage, p21 is induced by other stress-related triggers: oncogene activation, hyperproliferation, ROS accumulation, cytotoxics or physiological stimuli (tissue development, terminal differentiation) [264,268]. Since its discovery, numerous mechanisms for p21 regulation have been reported, showing that p21 expression is regulated at multiple levels: at gene transcription, by post-transcriptional factors, and through post-translational modifications. To illustrate it, only the most relevant p21 regulators, mostly discovered in human cells, have been included in this section.

Transcription

Although *Cdkn1a* transcription is mainly promoted by p53, several other transcription factors can directly bind this locus to induce or block its expression. In addition, other upstream proteins can modulate p21 expression by activating or repressing its direct regulators.

P53-dependent transcription

A major transcriptional activator of p21 is the tumor suppressor **p53**[163] (El-Deiry 1993). Also known as "the guardian of the genome", p53 coordinates the cellular response to stress signals (DNA damage, oncogenic activation, oxidative stress…) by controlling the activation of different programs, such as apoptosis, DNA repair or senescence[269]. It does so through the transcriptional regulation of target genes, including p21. p53 upregulates p21 transcription by directly binding to its promoter. Curiously, other members of the p53 family (p63 and p73) are also able to induce p21 transcription by binding to the same sequence element[270].

Many factors activate and stabilize p53 through protein modification, therefore enhancing p21 expression[255,256,261,271,272]. One example is **p300/CBP**, which stabilizes p53 after being recruited by another tumor suppressor involved in DNA damage repair, BRCA1[273]. In fact, upon **DNA damage**, the principal mediators of the DDR (ATM-CHK2 and ATR-CHK1) and other induced proteins (PIN1, GADD34, MOZ, CDA1) also act upon p53 through different mechanisms to promote the transcription of p21[255,261]. **Oncogenic signals** such as the loss of tumor suppressors or the activation of oncogenes (Ras, c-Myc, E2F-1…), also upregulate p53, usually by activating ARF (**p19^{Arf}**), the senescence mediator[274]. Moreover, RAS activation induces the expression of the proapoptotic tumor suppressor NORE1A, which promotes the nuclear localization of p53[275]. Another interesting regulator of the p53-dependent transcription of p21 is **KLF4**, one of the 4 Yamanaka factors used to induce pluripotency in somatic cells and mediator of epithelial differentiation[276,277]. In response to DNA damage, KLF4 can cooperate with p53 to activate p21[278,279]. Paradoxically, it can also act as an oncogene by suppressing the expression of p53 upon RAS activation[277]. Its contradictory function in promoting or preventing tumorigenesis seems to be mostly dependent on p21 induction[280]. Additionally, p21 expression is also favored by p53 thanks to the recruitment of the transcriptionally permissive histone H2A.Z to p21 promotor, facilitating its expression[281].

P53-independent transcription

p21 expression can also be **induced independently of p53**[256,271]. Some of the transcription factors that directly bind to p21 to induce its expression are SP1 and SP3, SMAD2/3/4, AP2, BRCA1, GAX, HOXA10, E2A, vitamin D receptor (VDR), retinoic acid receptor (RAR), E2F1 and E2F3, C/EBPα, C/EBPß, STAT1, STAT5 and STAT3[272,282]. In consequence, the inhibition, activation or competition with these factors by other molecules can also impact p21 expression. For instance, the transcriptional coactivator **p300/CBP** has been shown to cooperate with SP1, BETA2, MyoD or KLF6 to promote p21 expression in response to

progesterone, calcium or nerve growth factor (NGF)[272,282]. **TGF-ß**-dependent Smad activation stimulates p21 expression[283,284]. Importantly, the cooperation of TGF-B/SMAD and the PI3K/FOXO constitutes the molecular mechanism directing p21-mediated **developmental senescence**[81].

On the other hand, the direct binding to p21 locus can also prevent its transcription. Some of the known direct **repressors** of p21 are SMAD6, SMAD7, AP4, ZNF76, CUT, HIC1, TBX2 and possibly RUNX1 and RUNX2[256,261,271]. **C-MYC** can repress p21 transcription by interfering with its activators (SP1, SP3, MIZ-1), inducing its repressor AP4 or recruiting the silencing methyltransferase DNMT3A to its promoter[261,285,286]. Indeed, p21 transcription is dependent on **epigenetic** marks, and preventing its methylation or deacetylation with DNA methyltransferase or histone deacetylase inhibitors (HDACi) can favor its expression[271,287–289].

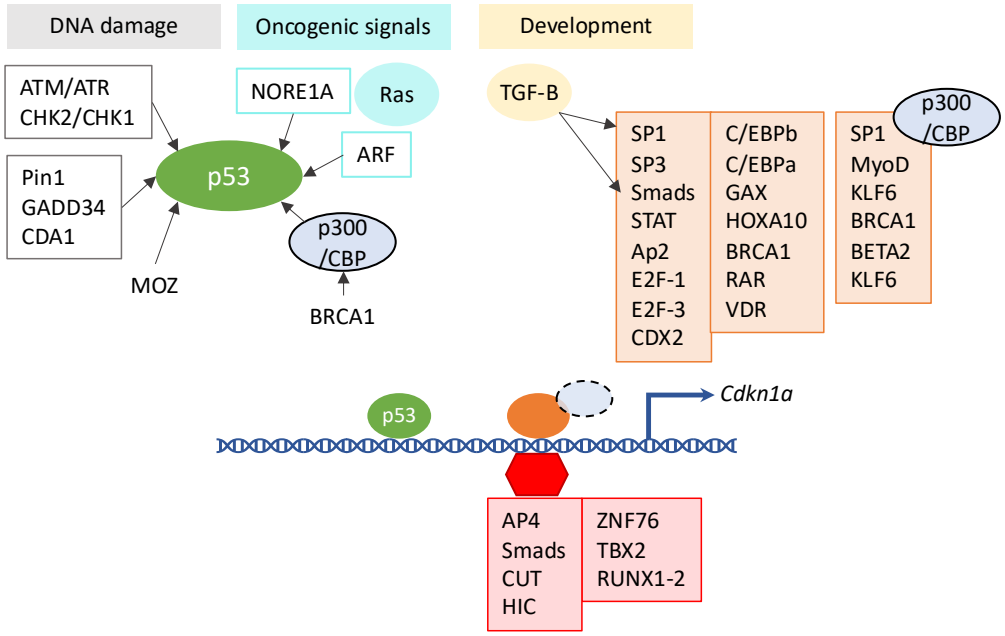

Figure 5. Transcriptional regulation of *Cdkn1a*. Different signals, such as DNA damage or oncogenic activation, activate p53 (green), the main transcriptional regulator of *Cdkn1a*. The p21 locus can be transcribed independently of p53, for instance (but not exclusively), in response to developmental cues (yellow). Aditional transcriptional factors are able to induce (orange) or repress (red) *Cdkn1a* expression. Some of Cdkn1a inducers act in cooperation with the transcriptional co-activator p300/CBP (blue). (Adapted from 2019 Al Bitar et al. review on p21)

Post-transcriptional regulation: *Cdkn1a* mRNA

The expression of p21 is also regulated post-transcriptionally at the **mRNA** level. Different factors (miRNAs, RNA binding proteins and translation factors) interact with *Cdkn1a*

transcript to control its degradation, **stability** and **translation** efficiency[261,289]. **MicroRNAs** (miRNAs) are short RNA sequences thought to regulate the expression of approximately 30% of mammalian genes[290]. They control mRNA stability and translation through binding to complementary sequences of target transcripts. Several mi-RNAs have been shown to downregulate p21 expression either via direct mRNA binding (miR-17, miR-20a, miR-20b, miR-93, miR-106a, miR-106b) or indirectly through p53 direct repression (miR-125a, miR-125) or by other mechanisms (let-7a, miR-29 family)[261].

The stability of *Cdkn1a* transcript is also controlled by different kinds of **RNA-binding proteins**. While HuD, HuR, Rbm38 (or RNPC1), Rbm42, Rbm24, CUGBP1, PCBP1(hnRNP E1), PCBP2 (hnRNP E2), NF90 (spliceosome component), TAX (non-canonical RNA-binding protein) and ZONAB (transcription factor) stabilize *Cdkn1a* transcript and enhance its translation, MSI-1, Calreticulin (CALR), hnRNP K, AUF1 (hnRNP D), FXR1 and DDX41 exert the opposite role[261,291–294]. **Methylation** of *Cdkn1a* mRNA by NSUN2 and METTL3/METTL4 also enhances its translation[295]. In addition, a specific p21 transcript is favored by the phosphorylated **translation factor** eIF2α-P (α subunit of eukaryotic initiation factor 2)[260]. Upon cellular stress (UVB, UVC), the GCN2 kinase phosphorylates eIF2α (eIF2α-P), which then decreases general protein synthesis and promotes the translation of mRNAs involved in stress adaptation response, including p21's [262].

Post-translational modifications

The stability, activity and cellular localization of p21 is regulated post-transcriptionally. Several phosphorylation sites for p21 have been described. More recently, methylation and acetylation have also been reported. Ubiquitin marks promote p21 degradation although it can also occur independently of ubiquitination via direct interaction with the proteasome.

Phosphorylation, methylation and acetylation

The function and abundance of p21 is controlled by different post-translational modifications. **Phosphorylation** of different serine (Ser) and threonine (Thr) residues by diverse kinases determine its binding affinity, cellular localization, stability and degradation[246,254]. At least 8 phosphorylation sites have been described to impact p21 level and activity: Thr-57, Ser-98, Ser-114, Ser-130, Thr-145, Ser-146, Ser-152 and Ser-160 (human nomenclature). Phosphorylation at Thr-145 by Akt1[PKB], PKA, PKC and Pim-1 prevent the **nuclear translocation** of p21 and favors its cytoplasmic accumulation. This modification can also disrupt p21 **binding** with PCNA. Phosphorylation of Ser-153 by Dyrk1 or PKC can

also promote cytoplasmic translocation. Akt1, Pim-1, NDR and PKC can also phosphorylate Ser-146. When this residue is phosphorylated by Akt1 or PKCδ, it promotes p21 **stability**, but this modification has the opposite effect when performed by PDK1-activated PKCζ. Similarly, phosphorylation at Ser-130 by JNK1 and p38 also promote p21 stability but it results in its ubiquitin-dependent **degradation** (through SCF^{Skp2}) if mediated by the CDK2-Cyclin E (CDK2-CycE) complex. Interestingly, CDK6-Cyclin D (CDK6-CycD) phosphorylation of Ser-130 disrupts the **association** of p21 with CDK2, thus preventing cell cycle arrest. GSKß phosphorylation at Thr-57 also promotes p21 degradation. In addition, methylation and acetylation of p21 have also been reported. **Methylation** of Arginine 156 by PRMT6 favors the phosphorylation at Thr-145, promoting cytoplasmic localization and mediating cytotoxicity resistance[296]. The **acetylation** of p21 by Tip60 also counteracts its ubiquitination and degradation, **stabilizing** it upon DNA damage[297]. Accordingly, p21 deacetylation by Sirt1 enables its degradation and improves cardiac regeneration by promoting cardiomyocyte proliferation[298].

Ubiquitin-dependent and independent degradation

P21 is an unstable protein with a short half-life of around 30 minuts[299]. Its **degradation** can occur dependent or independently of ubiquitination. The ubiquitin-proteasome proteolytic pathway is the main mechanism of intracellular protein degradation, impacting most of the molecular pathways of the cell. It is a multistep hierarchic system where E3 ligases are responsible for the specific targeting of the proteins that are degraded in the proteasome complex[300]. **Ubiquitin-dependent** proteasomal degradation controls p21 levels through the cell cycle[301,302]. Different cell cycle-related ubiquitin E3 ligases such as SCF^{Skp2}, $CRL4^{CDT2}$ and APC/C^{CDC20} target p21 at different stages of the cell cycle. Another E3 ligase, $CRL2^{LRR1}$, controls cytoskeletal dynamics motility by specific degradation of cytoplasmic p21[302,303]. PARK2, a protective factor in the development of Parkinson's disease, promotes neurogenesis and neural differentiation through binding and ubiquitination of p21 in neural stem cells[304]. Other reported E3 ubiquitin ligases of p21 are MKRN1, RNF126, FBXO22, UBR5 and PSMD2[289,305,306]. The **ubiquitin-independent** proteolysis of p21 can occur via direct binding to the proteasome complex (26S, the C8α subunit and the activator $PA28\gamma^{REG\gamma}$)[302]. Moreover, MDM2 and MDMX can promote p21 degradation independent of their ubiquitin E3 ligase activity[302]. On the other hand, and in addition to phosphorylation, p21 can be stabilized and **protected** from degradation by interacting with different factors such as Hsp90[307] (recruited by WISp39), cyclin D1[308] (promoted by Ras) or NPM^{B23} [Ref. 309], TSG101[310] or C/EBP- α [311].

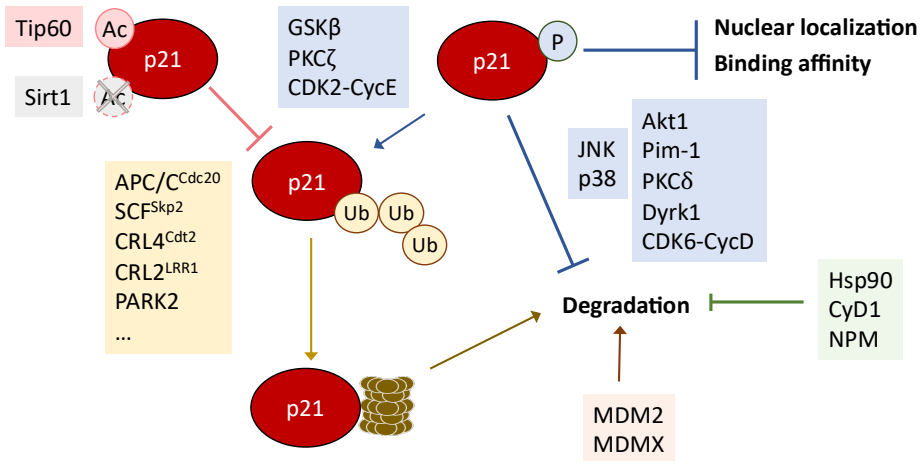

Figure 6. Post-translational modifications of p21. Post-translational marks regulate p21 activity, localization and stability and its protein effectors. Principal kinases that phosphorylate (P) p21 and phosphorylation related processes regulated by it in blue. Ubiquitin-ligases and ubiquitin marks (Ub) in yellow. Acetylation (Ac) and acetylase represented in pink, deacetylase in grey. Brown cylinder representing the proteasome. Ubiquitin-independent degradation promoted by proteins in orange box. Factors preventing p21 degradation in green. "Cyc" as *Cyclin* abbreviation. (Adapted from 2019 Al Bitar et al. review on p21)

2. 4 Cellular functions regulated by p21

Multiple molecular processes and cellular programs are impacted by p21 activity, mainly because of its numerous interactors. The expression of p21 has been shown to control cell cycle progression, survival or cell death, DNA repair, genome stability, cytoskeletal dynamics (which influence cell adhesion and migration) and transcription. The ultimate contribution of p21 to these processes is dependent on the cellular context, levels, activity, cellular localization and importantly, its binding partners.

Cell cycle

The cell cycle is a multistep process that leads to the division of one cell into two daughter cells with the same genetic material. This process is developed by the coordinated sequence of phases: G1, S, G2 and M. These 3 first states are part of the interphase, where cells grow, duplicate its genetic material (S phase stands for "DNA synthesis") and prepare for division. During mitosis, or M phase, is when the cell actually undergoes division. Additionally, cells can enter in G0, a resting state where they leave the cell cycle generally from G1, either transiently (quiescence) or definitively (differentiation). The transition through the different phases of the cycle is regulated by different CDK-cyclin complexes. While the expression of CDKs does not vary much, the levels of different cyclins are the limiting factor for phase

transition. When in complex with cyclins, CDKs phosphorylate and inactivate the proteins of the retinoblastoma family (pRB^{RB1}, p130^{RBL2} and p107^{RBL1}), which act as transcriptional repressors of the cell cycle. When phosphorylated, they become inactive, allowing the progression through the different phases[15,17]. By interacting with different CDK-cyclin complexes, CDK inhibitors (CDKi) like p21 or p16 prevent them from phosphorylating their targets, activating RB proteins and causing the block of the cell cycle.

When **RB** proteins are hypophosphorylated, they are able to bind to key transcriptional activators of the cell cycle. RB1 binds and inhibits the transcription factors E2F1-3 (forming the **RB-E2F** repressive complex), blocking the G1/S transition. On the other hand, p130 and p107 can bind to proteins from the MuvB complex, forming the **DREAM** complex and disrupting the transcription of genes necessary for G1/S and G2/M by MuvB containing complexes (MMB for B-MYB-MuvB and FOXM1-MuvB respectively)[17]. Since p21 is able to interact with different CDK-cyclin complexes through its N-ter domain, it can arrest the cell cycle at different phases, although it preferentially arrests cells in G1 phase[246,248,312]. In addition, the structural similarity between p21 and CDK regulators also enables it to control their activation by competing with their regulators[312]. For example, p21 can disrupt the interaction between CDC25A and CDK2 by competitive antagonism[313]. **CDC25** proteins are phosphatases that can interact with and activate CDKs. By disrupting this interaction, p21 prevents CDK2 from activation, arresting the cell cycle. In addition, p21 can block proliferation by another CDK-independent path. Through its C-terminal PCNA-binding domain, p21 interacts with **PCNA**, preventing its binding with the DNA synthesis machinery and inhibiting DNA synthesis[314,315]. Finally, p21 can also control the expression of cell cycle genes via **transcriptional repression** via direct interaction with cell cycle related transcription factors (explained below).

Paradoxically, p21 has also been reported to **promote cell cycle** progression by mediating the assembly of cyclin D with CDK4 and CDK6 [246,316,317]. The sequestration of p21 in cyclin D/CDK4-6 complexes can prevent it from interacting and inhibiting the action of CDK2 complexes[246]. In addition, when hyperphosphorylated by CDK2, p21 can activate CDK1 and promote G2/M transition[318].

Cell death

P21 is also a regulator of cell death pathways, controlling processes like apoptosis, necrosis and autophagy[319]. Its role in these processes seems to depend on its **localization** and

phosphorylation state. The cytoplasmic expression of p21 upon DNA damage has been reported to have an **anti-apoptotic** effect[320]. The inhibition of apoptosis can be related with different events[321]. On one side, the activation of CDKs and the evolution of the cell cycle is a necessary step for apoptosis. Therefore, p21 can protect cells from apoptosis via CDK inhibition. In addition, p21 is able to interact with several apoptotic mediators in the cytoplasm, inhibiting their action. Among others, p21 has been shown to interact with pro-caspase 3 [322], ASK1[323] and SAPK[324]. Additionally, p21 could prevent apoptosis via transcriptional regulation. In fact, the induction of p21 was reported to upregulate the expression of an anti-apoptotic paracrine secretome[325]. Paradoxically, a **pro-apoptotic** role for p21 has been reported in different contexts[326]. For example, p21 favors apoptosis and prevents autophagic death in mouse embryonic fibroblasts stressed with ceramide[327]. On the other hand, p21 can also activate **autophagy** in cancer cells[328,329]. In a different context, the activation of myocardial autophagy by cytoplasmic p21 improved cardiac hypertrophy by preventing oxidative damage[330]. In addition, p21 has also been reported to mediate **necrosis**, another mechanism of cell death[331].

DNA repair and genome stability

Although controversial, p21 may play a role in the **DNA repair** process. Depending on the experimental conditions and the cell models studied, p21 has shown to inhibit, promote or not affect DNA repair, mostly due to its ability to interact with PCNA [312,332]. Increasing evidence is showing that p21 **contributes** to different mechanisms of DNA repair [333–338]. It is likely that the role of p21 in DNA repair may depend on the extent of the genotoxic damage and the pathways affected by it. It has been proposed that upon low levels of DNA damage, p21 induces cell cycle arrest, inhibits apoptosis and promotes DNA repair. However, after intense damage, p21 is degraded, resulting in apoptosis induction[312]. Rapidly after damage, p21 is recruited to DNA damage regions, colocalizing with DNA repair factors[339]. This is preceded by and dependent on the recruitment of PCNA to the sites of the damage. By regulating the interaction of different repair factors, mainly with **PCNA**, p21 modulates the DNA repair process, generally increasing its efficiency [333–337]. Moreover, p21 expression promotes genome stability by favoring "error-free" reparation pathways upon double-strand breaks of the DNA[338]. Actually, base levels of p21, in association with PCNA, are necessary to maintain **genomic stability** even in unstressed cells[340]. However, the role of p21 in DNA is complex, and many studies have presented opposite results[312,341]. For instance, maintained levels of p21 through forced stabilization (after UV irradiation or in p53 null cell lines)

promoted DNA damage and increased genomic instability[342,343]. In any case, the contradictory data on the role of p21 in DNA repair and genome stability should not be overlooked.

Cellular migration and cytoskeleton dynamics

The three members of the Cip/Kip family proteins have been implicated in the regulation of cytoskeleton dynamics and cell motility. Specifically, p21 has been shown to promote **cytoskeleton remodeling** and increase cell motility[254,303,344–347]. Mechanistically, cytoplasmic p21 binds and inhibits ROCK, preventing the activation of the Rho/ROCK/LIMK cascade that suppresses cofilin expression[344,345]. Increased cofilin activity favors cytoskeleton remodeling, reduces actin stress fibers and enhances cell motility. Additionally, p21 has also been reported to regulate microtubule dynamics through ROCK-independent mechanisms, promoting microtubule stabilization, cell spreading and focal adhesion formation[348]. Moreover, p21 can also promote cell migration and invasion through its co-**transcriptional** activity. For instance, in human breast cancer cells, p21 mediates the TGF-β-mediated upregulation of pro-metastatic genes by interacting with Smad3 and p/CAF [349]. Altogether, p21 seems to favor cell migration and invasion, mainly via cytoskeleton remodeling when localizing in the cytoplasm, although it also impacts it in the nucleus via transcriptional regulation. In contrast, when p53 is ectopically expressed in the cytoplasm together with p21, they cooperate to **suppress** cell invasion[350], exemplifying once again its complex contribution to any given cellular process.

Transcription regulation

Several cellular processes are controlled by p21 thanks to its ability to regulate transcription, mostly acting as a transcriptional co-repressor. Actually, p21 mediates the transcriptional activity of p53, especially in transcriptional repression[161,351]. By influencing transcription, p21 impacts many pathways, including cell cycle and cell division, apoptosis, differentiation, DNA damage, oxidative stress, inflammatory response, senescence and aging[255,264].

There are different mechanisms by which p21 regulates transcription due to its ability to promiscuously interact with a wide variety of factors. On one side, p21 indirectly controls the activity of different transcription factors through its action as a **CDK inhibitor**. For instance, p21 interaction with CDK-cyclin complexes prevents the phosphorylation of Rb proteins, allowing the formation of the RB-E2F and DREAM repressive complexes that silence the expression of E2F1-3 and FOXM1 targets[161,352–354]. Some targets of these complexes include genes involved in cell cycle, DNA repair or apoptosis[354]. Moreover, p21 has been reported to

directly interact with different transcription factors, such as E2F[355], c-Myc[356], STAT3[357], Nrf2[358], estrogen receptor alfa (ER-α)[359]. Consequently, p21 can influence the cellular programs under their control, including cell cycle progression, DNA synthesis and oxidative stress response. In addition, p21 can interact with the co-transcriptional activator and activators p300 and CBP and regulate them[255,360]. Through the **modulation of p300/CBP activity**, p21 can influence processes like NF-κB activity[361], keratinocyte differentiation[362] or DNA methylation[363]. The overall transcriptional effect of p21 in some these processes may not be straight forward, depending on its interactors and cellular context. For instance, p21 has been shown to either repress or enable inflammation in different models[364,365]. In any case, it is clear that p21 is a multifaceted protein with complex and broad effects on the transcription regulation of multiple pathways.

2. 5 Biological processes impacted by p21

Because of its involvement on important molecular mechanisms controlling cellular behavior, identity and survival, p21 has been reported to play a role in several physiological and pathological states at the cellular, tissular and organism level. Depending on the biological context, p21 regulation has been shown to have major effects on processes like cancer development, cellular differentiation, regeneration and wound healing, and senescence.

Differentiation, stem cell renewal and reprogramming

The physiological expression of p21 has been shown to be implicated in the **differentiation** of different cell types, independently from p53 activation[254,264,366]. Among others, p21 increase correlates with or promotes differentiation in erythroid progenitors, oligodendrocytes, neurons, peripheral blood monocytes, chondrocytes, megakaryocytes, and skeletal muscle cells[254]. The mechanisms by which p21 contributes to the differentiation process are not only related to its ability to establish a cell cycle arrest, necessary to terminally differentiated cells, but also through the regulation of other cellular processes [367,368], such as cytoskeleton remodeling[344] or apoptosis inhibition[323]. Although p21 positively correlates with differentiation in most scenarios, it can have the opposite effect in other cell types, such as granulocytes or osteoblasts[369,370]. In other cases, its role is more contradictory or ambiguous[254]. For example, p21 expression increases at the onset of differentiation but decreases in terminally differentiated keratinocytes[367,371]. On the other hand, p21 is also

necessary for maintaining the **stem cell renewal** of some populations, such as keratinocytes[372], hematopoietic[373], neural[374] or leukemia[375] cells, preventing their exhaustion. However, p21 is also important for restricting stem cell renewal in hematopoietic cells and keratinocytes by promoting differentiation[372,373] and its ablation can lead to increased stem cell potential and carcinogenetic susceptibility[372]. In addition, p21 expression is a barrier for the **reprogramming** of induced pluripotent stem cells (iPS), and silencing it improves the efficiency of the process[376,377]. One of the mechanisms by which p21 may favor differentiation over pluripotency maintenance is by repressing the transcription of the reprogramming factor Sox2[378].

Regeneration and wound healing

Low p21 expression in the MRL "healer" mouse was linked to the exceptional ability of this strain to achieve **complete regeneration** of ear hole puncture wounds[379]. In fact, lack of p21 was shown to be sufficient to recapitulate this phenotype in normal mice. Interestingly, low levels of p21 have also been reported in Egyptian spiny mouse (*Acomys cahirinus*), another "healer" rodent able to close ear hole wounds in a similar manner[380]. Indeed, p21 expression has been shown to **impair** the regeneration of multiple organs, such as liver[381–385], bone[386], cartilage[387,388], skin[389], and lung[390]. Interestingly, some of these studies suggest that the negative impact of p21 induction on tissue repair seems to depend on the dynamics of its regulation and the state of the tissue previous to the lesion; impaired regeneration and delayed wound healing related to p21 expression specifically affected previously damaged or aged tissues, which tended to retain increased p21 levels for prolonged periods of time after injury[384,385,389–391]. The mechanisms by which p21 ablation enhances regeneration may be related to its impact on multiple molecular processes, including increased proliferation, reduction of TGF-β signaling and scar formation, limited senescence and preservation of stem/progenitor cells and enhanced cellular plasticity[392]. On the contrary, in some contexts, p21 expression may be **required** for proper regeneration. After muscular injury, regeneration was delayed in p21-null mice due to hindered expression of muscular synthesis genes and inhibited muscle differentiation[393]. In a model of dorsal thoracic hemisection of spinal cord in rats, local delivery of cytoplasmic p21 at the injury site promoted axonal regeneration in neurons and functional recovery by modulating cytoskeletal dynamics and the activity of the immune system[394].

Cancer and disease

Although *Cdkn1a* is normally considered a tumor suppressor gene, p21 can have a **dual role** in cancer[254,272]. This is explained by its contradictory effect on many of the processes that constitute hallmarks of cancer development, such as apoptosis, proliferation, genomic instability or migration. On the anti-tumorigenic side, p21 is an important mediator of the **tumor suppressive** activity of p53[163,395,396]. Contrary to initial observations[397], ablation of p21 in mice leads to increased tumor formation at around 16 months of age[398]. Because of the relatively late onset of tumors in comparison with models deficient for other tumor suppressor genes and the low frequency of loss-of-function mutations observed in human cancers, it has been proposed that p21 may not act as a classical tumor suppressor[254,272]. This idea is nicely explained in the 2009 review by Abbas and Dutta, where they suggest that p21 actually prevents cancer development by synergizing with tumor suppressors and antagonizing oncogenes. Upon exposure to mutagenic agents, p21 was shown to delay tumor formation and metastasis[372,399]. In fact, lack of p21 has been observed to promote tumor formation, aggressiveness and chromosome instability, especially when accompanied by co-expression of oncogenes or loss of other tumor suppression genes[272,395,400–404] .

On the contrary, in some contexts, p21 depletion has been shown to delay the onset and reduce the incidence of tumor formation, even upon DNA damage or in combination with oncogenic induction (c-Myc) or inactivation of tumor suppressors (p53-null mice)[254,398,405,406]. Actually, p21 overexpression is observed in several human cancers, often correlating with aggressiveness, invasiveness and treatment resistance[254,272,407,408]. The **pro-tumorigenic** activity of p21 has been associated to its cytoplasmic localization, which confers apoptosis resistance[254,409,410]. Interestingly, acquisition of a senescent phenotype in contraposition to cell death can promote tumor development, invasiveness and relapse[407,411–413]. In addition, nuclear p21 can also support tumor development by favoring cell cycle progression via stabilizing cyclin-CDK complexes[272,414]. Even when acting as a cell cycle inhibitor, p21 can potentiate leukemia development, by restricting DNA damage and maintaining self-renewal of cancer stem cells[375]. Taken together, the overall contribution of p21 to cancer development depends on its impact on the cellular processes driving tumorigenesis[254]. Differences in its molecular context, cancer type, cellular localization and damage induction can determine its role as either an oncogenic protein or a tumor suppressor.

Apart from cancer, p21 activity has been associated with other pathologies. In the immune system, p21 is a repressor of **autoimmunity**, and its deficiency has been shown to propitiate the development of lupus-like autoimmunity[415], endotoxic shock[365,416] and arthritis[417–419]. In contrast, p21 can also mediate pathological inflammation[364]. Actually, induction of p21 expression has been shown to enhance the transcription of genes associated to atherosclerosis, osteoarthritis and rheumatoid arthritis[325]. In the same study, transcripts associated with the development of Alzheimer's disease were also positively regulated by p21.

Senescence

p21 is an important **mediator** of cellular senescence. In some contexts, induction of p21 is able to promote senescence[158,420–422], while its ablation delays or abolishes its establishment[397,423–426]. In fact, p21 was originally described as an overexpressed gene in senescent fibroblasts[249], and it is currently used as a **marker** of cellular senescence. Together with p15, p21 is one of the few senescence mediators conserved in **developmental** senescent cells, where other common markers of damage-induced senescence (p53, $p16^{Ink4a}$, $p19^{Arf}$) are not expressed[47,81]. However, and despite being an undeniable contributor to the senescent program, its expression is not strictly necessary for its establishment[47,81,424,427–429].

The importance of p21's role in senescence has been mostly associated to the **onset** of the response. Its increase mediates cell cycle withdraw at the beginning of the establishment of senescence[425]. However, at later timepoints and at least in some contexts, the proliferative arrest relies on other senescence mediators[159,166,430]. This idea is further supported by the observation of a drop in p21 levels in several models of fully senescent populations[164–166,328].

The contribution of p21 to the senescence phenotype involves other mechanisms besides mediating the **cell cycle arrest**. For instance, it has been recently proposed that the p21 level at the moment of chemotherapy treatment determines the commitment to senescence in a human epithelial cancer cell line[431]. Moreover, p21 maintains **cell viability** by restraining DNA damage in DNA-damage induced senescent cells[432]. Although p21 plays an **antioxidant** protective role under low levels of oxidative stress by interacting with Nrf2, a master regulator of the antioxidant response[358,433], its activation can also lead to increased levels of reactive oxygen species (ROS), as observed in senescent cells[422]. Maintained activation of p21 is actually required for ROS accumulation, which causes DNA damage and activates the DDR, creating a feedback loop that is necessary and sufficient for establishing senescence[93,422]. In

fact, the extent of **ROS accumulation** in response to p21 is a critical determinant of the activation of apoptosis in senescent cells[434].

Finally, increasing data supports the idea that p21 contributes to remodeling the **transcriptional program** characteristic of senescent cells. Overexpression of p21 was shown to induce the expression of a senescence-associated gene signature[325]. HMGB2, a key regulator of the chromatin remodeling that enables **SASP** expression and whose expression decreases upon senescence induction[73], is transcriptionally repressed by p21 upon senescence induction[435]. Last year, Sturmlechner et al. described that in response to stress, p21 regulates the transcriptional activity of Rb to induce the expression of SASP factors that mediate the immune-clearance of senescent cells[436].

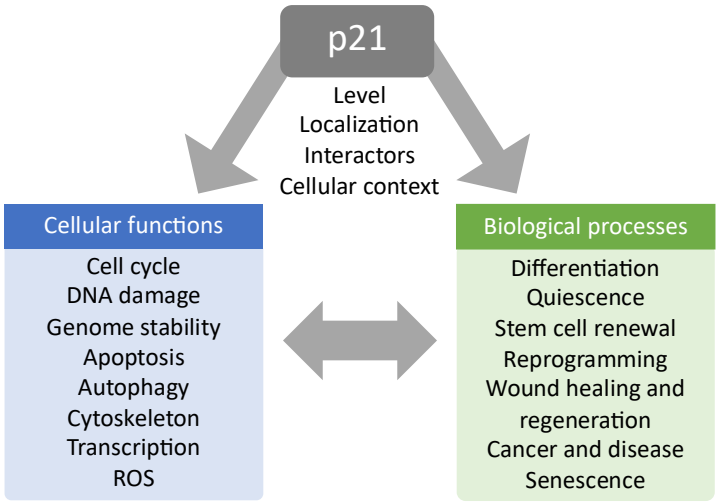

Figure 7. Cellular functions and biological processes controlled by p21. Due to its ability to regulate important cellular functions (blue), such as cell cycle progression, DNA repair, cellular survival, cytoskeleton dynamics, transcription or ROS accumulation, p21 contributes to different biological processes (green), from a cellular (differentiation, senescence) to a tissular and systemic level (wound healing, cancer). The role of p21 in these processes is often dual and contradictory, and its specific impact depends on its levels, cellular localization, molecular interactors and biological context analyzed.

RESULTS

1. Model Validation

1. 1 Model description and validation

Mouse model: p21 inducible knock-down by doxycycline inducible *shCdkn1a*

In order to investigate the role of p21 in senescence, we took advantage of a new mouse model acquired in the lab: a p21 inducible knock-down mouse line. It was generated by the company *Mirimus, Inc.* (https://www.mirimus.com), who is specialized in using interference RNA and CRISPR-Cas9 technologies to generate genetically modified animal models for scientific research. In this model, the administration of doxycycline, an analogue of the antibiotic, induces the expression of a short hairpin RNA (shRNA) specifically targeting *Cdkn1a* mRNA, leading to its degradation and the consequent reduction in p21 (mRNA and protein). In addition, the transcription of the shRNA is coupled with a GFP signal that can be used as an expression reporter of the system.

Briefly, the conditional knock-down model was generated by a Tet-ON system (activated, "ON", in the presence of tetracycline or its derivatives)[437]. This is achieved by a bitransgenic modification of the organism (Fig. 15A)[438,439]. The transcription of the GFP-shRNA is driven by a TRE promoter (tetracycline response element), downstream of the *Col1a1* gene. The activation of this promoter requires the action of a reverse tetracycline transactivator (M2-rtTA), which in this case is expressed from the *Rosa26* promoter. M2-rtTA requires the presence of its ligand, doxycycline, to transactivate the TRE promoter. Therefore, it is only in the presence of doxycycline that the shRNA is synthesized. Then, in the cytosol, it is processed into a small interference RNA (siRNA) duplexes, which binds to the target mRNA, in this case *Cdkn1a*, and is incorporated into the RISC complex for target-specific mRNA degradation, impeding its translation and decreasing the overall levels of the encoded protein[440].

To generate a usable colony, the commercially acquired mice were mated together with a Rosa26-M2-rtTA mice, to generate a double homozygous line prior to my incorporation in the laboratory.

In vitro model: primary mouse dermal fibroblasts

We decided to test the potential of this model *in vitro* by using cells directly extracted from the mice of this double homozygous line. The use of primary cells was found appropriate due

to their ability to develop a senescence response when exposed to known inducers of senescence. We decided to use primary mouse dermal fibroblasts to test our model, as these are frequently used to study senescence, and they are relatively straight-forward to generate. The protocol used to isolate and culture these cells can be found in the material and methods section of this thesis. In brief, fibroblasts were isolated using mechanical and enzymatic dissociation of the dermis of 0-2-day old mice pups, whose skin was mechanically detached after their euthanasia. After their dissociation, dermal cells were plated in plastic dishes and fed with fibroblast culture media. When the culture was close to confluency, fibroblasts were frozen in working aliquots and kept in liquid nitrogen. To prevent the development of replicative senescence in our cultures, fibroblasts were thawed and kept at low passage to perform each experiment.

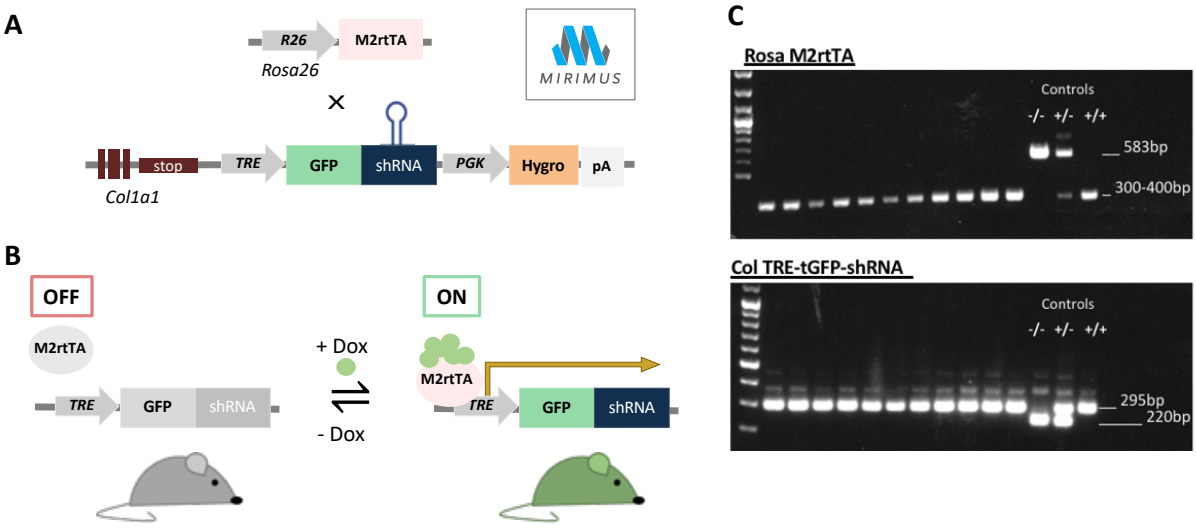

Figure 8. Description of the bitransgenic Tet-ON system of the model. A) Schematic representation of the R26-rtTA and TRE-shRNA cassettes generating the inducible knock-down of p21. Tetracycline reverse transactivator (M2rtTA) was expressed from the *Rosa26* (*R26*) promoter. A construct containing the green fluorescent protein (GFP) and the shRNA sequence targeting *Cdkn1a* mRNA under the tetracycline responsive element (TRE) promoter was insserted downstream of the collagen 1a1 locus (*Col1a1)*. It also encoded for hygromycin (Hygro) resistance, used for its generation process. PGK: strong housekeeping promoter phosphoglycerine kinase, pA: poly-A tail. **B)** Simplified schema of the Tet-ON system. The expression of the shRNA-GFP containing construct is dependent on the activation of M2rtTA in the presence of doxycycline (Dox). **C)** Genotyping of the mice by Tania Knauer-Meyer. To validate the presence of the described constructs in the strain, mice were genotyped according to company recommendations. The insertion of both constructs was validated by 2 PCR reactions, one per construct. The gels of these reactions confirmed the double homozygosis constructs in the mouse strain. Figures adapted from and Dow et. al 2012 and Mirimus webpage.

Induced p21 knock-down validation

The first part of the project consisted in the *in vitro* establishment of our p21 inducible knock-down model. I examined whether, upon addition of doxycycline into the cell culture media of primary mouse dermal fibroblasts, p21 was reduced at the mRNA and protein levels, and GFP expression was induced. This was validated in different contexts. First, I examined the effectiveness of the system in proliferating cells, where I also observed that the downregulation of p21 was reversible when doxycycline was removed. Then, after verifying the induction of senescence by irradiation, I tested it in irradiation-induced senescent cells. Finally, I optimized the conditions to produce proliferating and senescent cells with unaltered or reduced p21 levels, from which I collected mRNA samples that were used to perform bulk RNA-seq analysis. I discuss each of these steps in detail below.

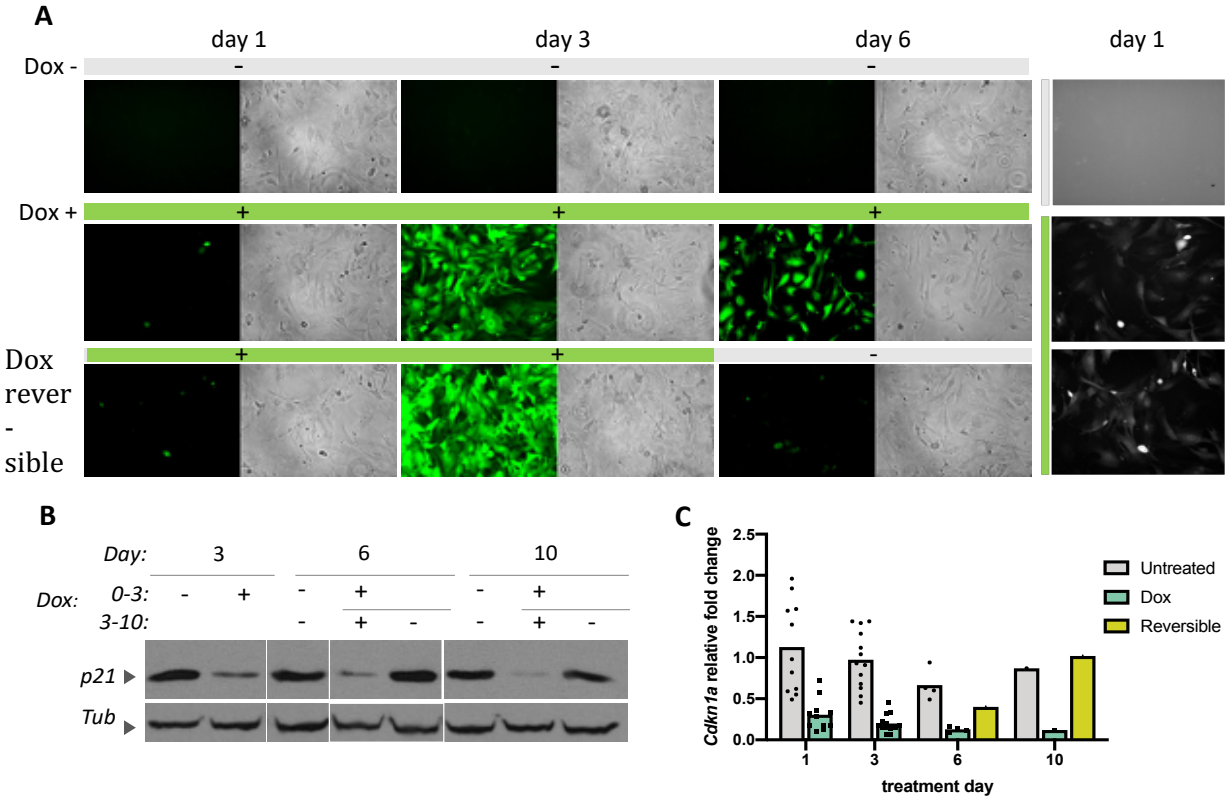

Figure 9. Doxycycline induced knock-down of p21. A) GFP signal of doxycycline treated cell. Fluorescence (odds) and phase contrast (even columns) 20x magnification images of cells exposed to doxycycline at different times. Day 1 fluorescence image is depicted again in last column with different parameters. Control untreated cells in top row, cells in permanent presence of doxycycline in mid row. Cells from bottom row were exposed for 3 days and then treatment was removed until the end of the experiment. **B)** Representative Western Blot of p21 (~18KDa) at different timepoints. α-Tubulin (~55KDa) was used as loading control. n=2. The original image of the film was cropped to invert the order of lanes 5 and 6 to facilitate the interpretation of the figure. **C)** Relative quantification of *Cdkn1a* mRNA. All samples were normalized to the average expression of control untreated cells at day 1. The ribosomal *Rplp0* transcript was used as housekeeping to normalize the differences in cDNA loading across samples. n=1-11.

Effective and reversible induction of p21 knock-down in proliferating cells

To examine whether the inducible model worked, doxycycline was added to the media of low passage proliferating mouse dermal fibroblasts derived from the skin of new-born transgenic rtTA-shRNA mice at a concentration of 2ug/mL. To validate the expression and function of the shRNA containing construct, the expression of the GFP reporter signal was checked via

microcope and RNA and protein samples were analyzed by RT-qPCR and Western Blot to monitor p21 levels at different timepoints.

GFP expression upon doxycycline induction of the silencing construct

The expression of the GFP reporter was assessed by fluorescence microscopy. Fluorescent signal was rapidly induced upon doxycycline administration. After 24h, treated cells presented a weak signal that was clearly distinct from the untreated controls (Fig. 9A, last column), which remained negative over time. GFP expression increased over time following induction, and all doxycycline-treated cells showed a strong fluorescent signal after 3 days of treatment (Fig. 9A). After 3 days, cells in treated and untreated plates were counted and split. Interestingly, there were almost twice as many cells in treated plates as in the untreated (fold change of 1.96, n=2). Due to the known function of p21 as a cell cycle inhibitor, an increased proliferation rate following its decrease would be expected. Thus, the higher cell number in doxycycline treated cultures hinted that the knock-down of p21 was occurring.

To test the reversibility of the construct expression half of the treated cells were then switched to doxycycline-free media at the moment of splitting, while the other half continued to be cultured with it. I observed that the GFP signal was progressively lost when doxycycline was removed, becoming virtually undetectable 4 days after the media switch. On the other hand, cells that were uninterruptedly exposed to doxycycline kept expressing a strong GFP signal over time, and untreated controls remained negative during the entire experiment (Fig. 9A).

Effective repression of p21 mRNA and protein

Next, and in parallel I collected RNA and protein samples from the same cells that I used to assess the GFP expression. The level of p21 protein was measured by Western Blot at 3, 6 and 10 days of the experiment was assessed by Western Blot (Fig. 9B). After 3 days with doxycycline, p21 protein was efficiently reduced. After 3 days with doxycycline, p21 levels were efficiently reduced (Fig. 9B, lane 2). After 6 days, p21 expression was almost totally abrogated (Fig. 9B, lane 4), and it was almost undetectable after 10 days (lane 7). When

doxycycline was removed from the media of treated cells after 3 days, p21 expression rapidly returned, and after 3 days, 6th day of the experiment, its protein level was comparable to the untreated controls (Fig. 9B, lane 5 and 8). Meanwhile, the expression of p21 in control untreated cells remained relatively stable (Fig. 9B, lane 1, 3 and 6).

In addition, I measured p21 mRNA at day 1, 3, 6 and 10 of the experiment. Isolated RNA from these samples was retrotranscribed (RT) to cDNA, and p21 mRNA was quantified by qPCR using specific primers for *Cdkn1a* (Fig. 9C). This result showed that the downregulation of p21 could be detected by qPCR. *Cdkn1a* levels were strongly reduced after 24h with doxycycline, and they reached a minimal expression after 3 days. This reduction in *Cdkn1a* mRNA persisted over time. The withdraw of doxycycline after 3 days of treatment also caused an increase in p21 at the mRNA level, which after 7 days of doxycycline removal, was the same as in untreated cells. Although this reversion effect was only verified once by RT-qPCR, it was consistent with the protein dynamics observed by Western Blot and the loss of GFP signal.

Induced knock-down of p21 in senescent cells

Irradiation induces senescence in mouse dermal fibroblast

Since our goal was to explore the role of p21 in senescence, I characterized the induction of senescence, establishing an irradiation protocol to induce it, as has previously been used[441,442]. Fibroblast cultures were exposed to a 10Gy irradiation, passaged once, and maintained in culture. The proliferative arrest of the culture was noticed around 3 days after irradiation. 6 days after irradiation, cells had adopted the expected senescent phenotype, consisting on a characteristic flat, enlarged morphology (Fig. 10B). Senescence state at this timepoint was confirmed by SA-ß-gal staining (Fig. 10A, D), EdU incorporation (Fig. 10C,E), and transcriptional measurement of the senescence-associated markers p21, $p16^{Ink4a}$, $p19^{Arf}$, Ki67 and Hmgb2 by RT-qPCR (Fig. 10F).

The quantification of the SA-ß-gal staining in proliferating and irradiated cultures showed a strong clear increase of positive cells at day 6 after irradiation: from 5.4% in proliferating to 88.2% in irradiated cells, on average (Fig. 10D, n=4). To measure the proliferative arrest consistently observed in irradiated cultures, I exposed the cells to a pulse of EdU. EdU incorporation was detected by click reaction and quantified (Fig. C, E). This showed a marked reduction of the number of nuclei that had incorporated EdU in irradiated cells, which was mainly attributed to a decrease in DNA replication previous to division. On average, EdU

incorporation in irradiated cells was reduced by 72.6% when compared to proliferating cultures (Fig. 10E, 9.5% in irradiated vs 35.7% in proliferating, n=3).

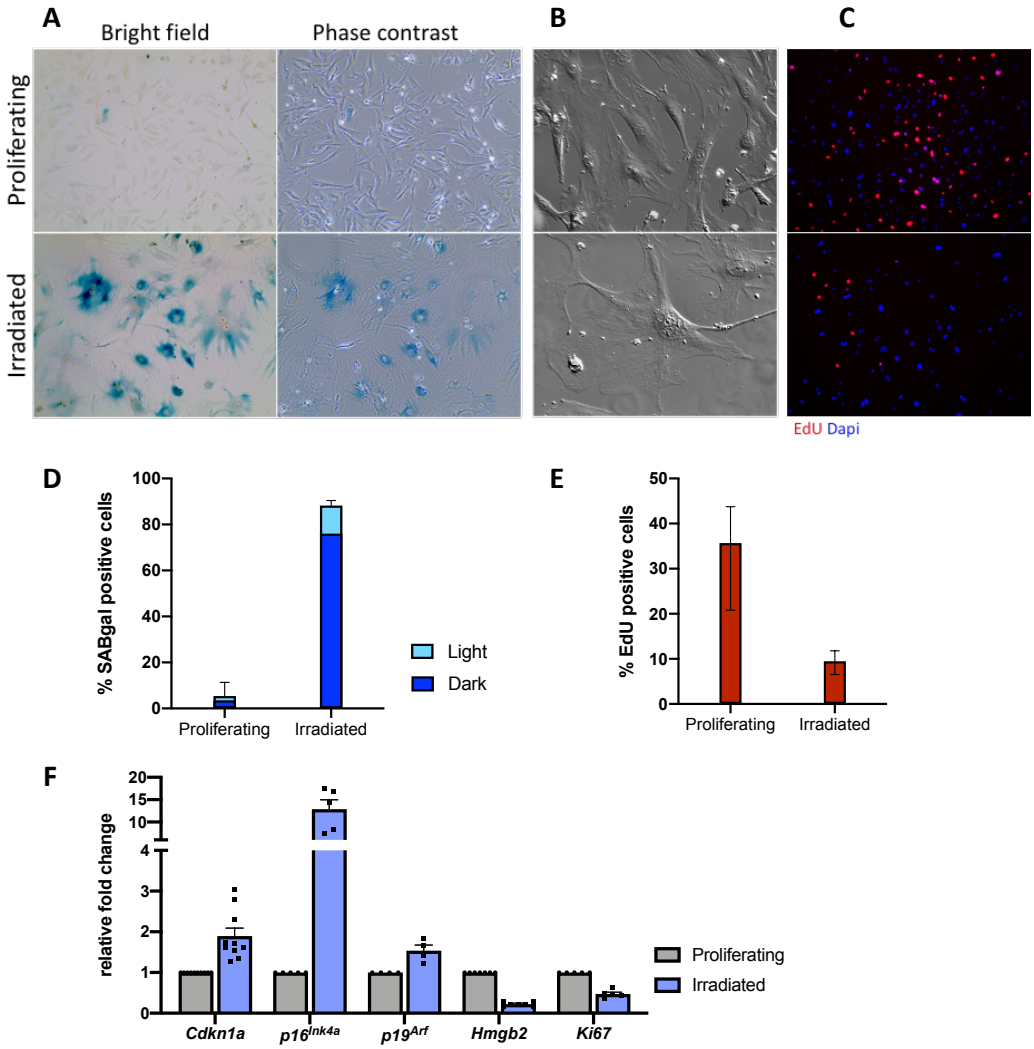

Figure 10. Irradiation induced senescence characterization. Cells were irradiated and senescence was assessed after 6 days. **A-C)** Images of proliferating (top) and irradiated senescent cultures (bottom row). **A)** Bright field (left) and phase contrast (right) at 20x magnification images of SA-ß-gal staining. **B)** Differential interference contrast (DIC) microscopy images at 40x magnification (left). **C)** Fluorescent microscopy images of Dapi (blue) and EdU (red) at 10x magnification (right). **D)** Average quantification of SA-ß-gal staining. Positive cells divided according to signal intensity (light or dark). Error bars for the standard error of the total mean (SEM), n=4. **E)** Average quantification of nuclei containing EdU signal. Error bars for SEM, n=3 (EdU pulse: 16h n=2, 3h n=1). **F)** Relative fold change of the selected transcripts quantified by RT-qPCR. *Rplp0* was used as housekeeping. Average expression, error bars for SEM, n= 4-10.

Senescence-associated transcriptional changes were measured by RT-qPCR (Fig. 10F). As expected, I observed an increase in the mRNA encoding the senescence mediators p21 (*Cdkn1a*), p16 (*Cdkn2a/Ink4a*) and p19 (*Cdkn2a/Arf*). I also confirmed the expected reduction of *Hmgb2*, a key senescence gene involved in controlling the epigenetic remodeling

leading to the SASP expression, in irradiated cells. Moreover, the decline in proliferation and cell cycle was also reflected by a downregulation of *Ki67* transcript.

Effective induction of p21 knock-down in senescent cells

Once I confirmed that I was able to induce senescence in mouse primary fibroblasts, I then tested the efficiency of p21 knock-down in senescent cells. Doxycycline was added to the media of senescent fibroblasts at day 6 after irradiation. The expression of the construct was confirmed by the detection of GFP expression by florescence microscopy (Fig. 11A). RNA and protein samples were collected at different timepoints, and quantified by RT-qPCR and Western Blot to validate the knock-down of p21 (Fig. 11B,C).

GFP expression upon doxycycline induction of the silencing construct

Similar to what happened in proliferating cells, the addition of doxycycline in the media culture induced the expression of GFP in senescent cultures, which was detected by fluorescence microscopy (Fig. 11A). This signal started shortly after doxycycline administration, and it was clear after 3 days. After 6 days, virtually all cells expressed high levels of GFP, which were maintained indefinitely in all the experiments performed.

In addition to the fluorescent microscopy images included here to demonstrate the GFP expression, I also recorded timelapse videos of untreated and doxycycline exposed cells at different timepoints in order to assess the fate of individual cells when the expression of the shRNA against p21 was activated (not shown). The images taken at the onset of the treatment showed that the GFP signal appeared during the first hours after doxycycline administration. Notably, I did not observe an increase in cell death or any major phenotypical change associated to p21 knock-down in the timelapse videos, which were recorded for 18h at day 0, 1, 2 and 3 after doxycycline addition to the media. Indeed, GFP expressing cells remained viable after 3 days, indicating that p21 was not required for the short-term survival of the cell culture at this timepoints.

Effective repression of p21 mRNA and protein in senescent cells

Next, I examined if the activation of the construct by the addition of doxycycline also lead to the effective knock-down of p21 in senescent cells. Senescent cultures were exposed to doxycycline the 6th day after irradiation, and protein samples were collected after 3 and 6 days, corresponding to day 9 and 12 after irradiation. After 3 days with doxycycline, the level of p21 was strongly reduced, and after 6 days p21 protein was practically undetectable by Western Blot (Fig. 11B). Additionally, RNA samples were collected from days 0 to 4 after the

start of the treatment, corresponding to day 6 to 10 after irradiation. RNA was isolated and retrotranscribed to cDNA, which was used to quantify *Cdkn1a* transcript by qPCR (Fig. 11C). This confirmed that the construct could be induced, and the knock-down of p21 was effective, as could be detected by qPCR in senescent cells. The mRNA of p21 tended to decrease over time from the first day of doxycycline treatment in all samples analyzed. After 3 days, *Cdkn1a* reached minimal levels, which were maintained in later timepoints in all samples analyzed (including data not shown in Fig. 11C).

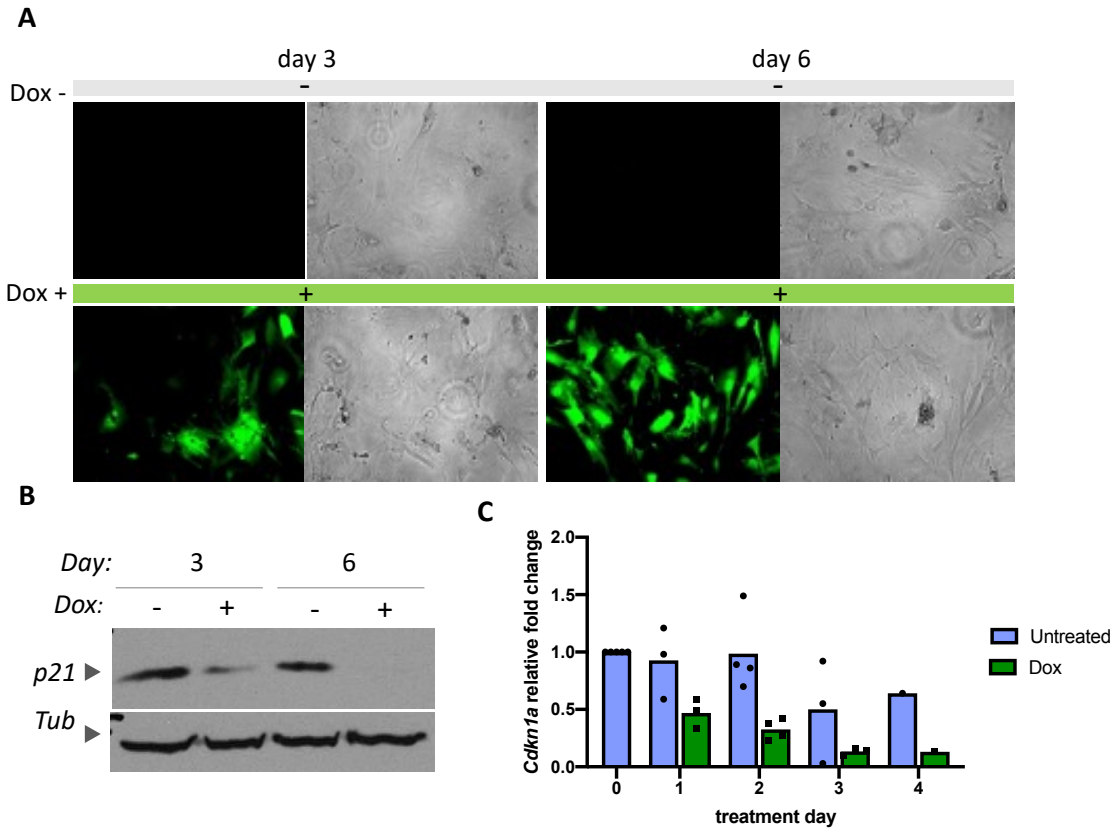

Figure 11. Doxycycline induced knock-down of p21 in senescent cells. Senescent cells 6 days after irradiation were treated with doxycycline to induce the knock-down of p21. **A)** GFP signal of doxycycline treated cells for 3 and 6 days, corresponding to irradiation day 9 and 12. Fluorescence (odds) and phase contrast (even columns) 20x magnification images of senescent untreated cells (top row) and doxycycline exposed cells (bottom row). **B)** Representative Western Blot of p21 (~18KDa) after 3 and 6 days of doxycycline treatment. α-Tubulin (~55KDa) was used as loading control. n=3. **C)** Relative quantification of *Cdkn1a* mRNA. All samples were normalized to the average expression of control untreated cells before the treatment, at irradiation day 6. The ribosomal *Rplp0* transcript was used as housekeeping to normalize the differences in cDNA loading across samples. In this graph, n >=3 for days 0-3 and n=1 for day 10.

1. 2 Model optimization for bulk RNA-seq analysis

Once the p21 knock-down upon doxycycline treatment was validated in proliferating and senescent cells, we wanted to use the model to explore the role of p21 in cells that have already achieved a senescent state. p21 was previously described to regulate transcription through its interaction with multiple transcription factors (see *Introduction: p21-Cdkn1a: Cellular functions regulated by p21: Transcription regulation*). Therefore, we were interested to investigate the possible effect of p21 depletion on transcription in senescent cells. We wanted to perform a bulk RNA-seq analysis of senescent cells with unaltered or reduced levels of p21. In order to prepare the samples for RNA-sequencing, I first needed to optimize the knock-down further, selecting the proper timepoint following knock-down induction, and the optimal dose of doxycycline to use.

Treatment timepoint

First, I validated the time-window to start the doxycycline treatment in senescent cells. I wanted to start decreasing p21 expression under 2 conditions: first, cells should be senescent, and second, p21 levels should be increased in comparison to proliferating cells. To assess the proper timepoint to start the knock-down, I collected protein samples at different timepoints after irradiation and p21 protein levels were assessed by Western Blot (Fig. 12). Although p21 levels showed some variability among experiments, they consistently increased during the first days after irradiation, and they stayed high until around day 9. I noticed that p21 signal tended to decrease at later timepoints, which will be discussed later in this thesis. Until this moment, I had validated the knock-down of p21 in senescent cells starting the administration of doxycycline at day 6 after irradiation, when cells presented senescent phenotype. The results of the Western Blot confirmed the upregulation of p21 at this moment. Therefore, I validated day 6 after irradiation as a good timepoint to start the induction of p21 down-regulation in senescent cells.

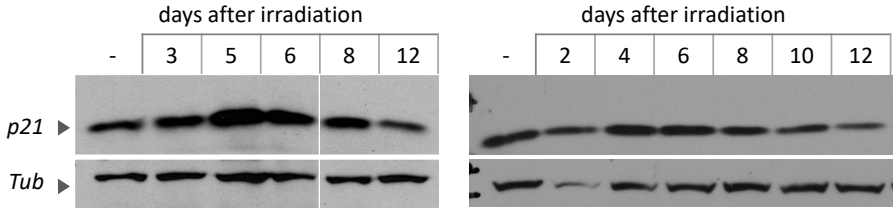

Figure 12. p21 time-course after irradiation. Time-course expression of p21 after irradiation. Representative Western Blots from 2 independent experiments. Top panels for p21 signal (~18 KDa) and bottom for α-Tubulin (Tub) at ~55 KDa, used as loading control. Left image was cropped to exclude uninformative sample. Notice the lesser loading of the second lane at the right gel corresponding to day 2 after irradiation.

Collection timepoint and doxycycline dose

Once the appropriate timepoint to induce the knock-down of p21 was confirmed, I optimized the dose of doxycycline to be used. Specifically, 2 different doses of doxycycline and several timepoints were evaluated on senescent cells.

To choose the time of doxycycline treatment to use for my samples, I focused on the first days after knock-down induction because we were interested in the early transcriptional changes that might result from p21-knock-down. I tested the effect of doubling the dose of doxycycline previously used on the efficiency of the knock-down. It was rationalized that this might increase the rate of knock-down, which might lower the chances of a compensatory adaptation. Thus, I treated senescent cells at the 6th day after irradiation with the standard doxycycline dose used until that moment and twice this concentration (2ug/mL vs 4ug/mL). Then, I collected RNA samples every day up to day 4 after the induction of the silencing construct, which corresponded to day 7 to 10 after irradiation.

The RT-qPCR analysis on p21 transcripts showed a statistically significant drop in treated cells after 1 and 2 days with doxycycline, which corresponded to post-irradiation days 7 and 8 (Fig. 13A). When analyzing the samples treated with the standard (1x Dox) dose of doxycycline, the difference with controls was only significant after 2 days of treatment, at post-irradiation day 8. The downregulation was not statistically significant at any other timepoint analyzed, with either 1x or 2x dose of doxycycline.

In addition, I assessed the functional effect of p21 reduction by measuring the expression of *Hmgb2*, since it has been described that its transcription is negatively regulated by p21[435]. I observed the expected increase in *Hmgb2* mRNA correlating to downregulation of p21 upon doxycycline addition (Fig. 13B). Its expression levels were found to be very similar between the 2 doses of doxycycline evaluated.

Although the number of samples used to produce this result was low (5 experiments in total, n=1-2 for each specific timepoints, Fig. 13 for details), all experiments gave similar results, suggesting a level of robustness that allowed me to extract preliminary conclusions. Taking these results into account, we decided to narrow the selection of the samples to day 1 and 2 of doxycycline treatment, corresponding to day 7 and 8 after irradiation; and given that there was no significant difference between the two tested doses, to use the standard dose (1x),

which already corresponded to an higher dose than the standard recommendation in the literature[438,439,443].

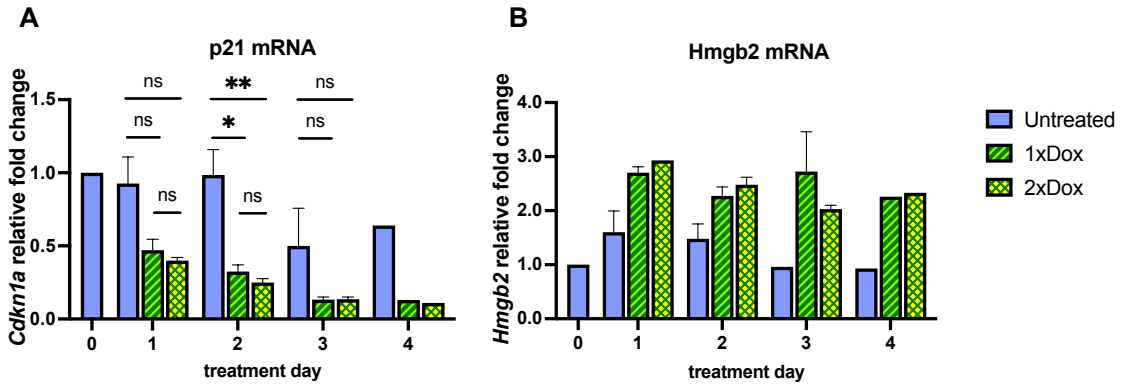

Figure 13. Optimization of dose and time of doxycycline treatment. The efficiency of p21 knock-down was assessed by RT-qPCR quantification of p21 (A) and Hmgb2 (B) transcripts. Two doses of doxycycline (Dox) were used and 4 timepoints were evaluated. **A)** p21transcript (*Cdkn1a*) relative fold change. Multiple unpaired t-test, two asterisks for p-value <0.01, one for p-value <0.05. n=3-5 for days 0 to 3 (except n=2 for 2xDox day 3), n=1 for day 4. **B)** *Hmgb2* transcript quantification. N=2-5 for days 0 to 3 for all bars with error, n=1 for the rest. No statistic test was performed. Mean and SEM. All experiments were normalized to day 0 untreated (n=5). Dose of doxycycline corresponding to 2ug/mL (1x) and 4ug/mL (2x). Cells were treated for 24h 6 days after irradiation, corresponding to day 0 in the figure. n=1-5.

Sample selection

After narrowing down the window of optimal conditions to induce the knock-down of p21 in proliferating and senescent cells, I decided to evaluate them in more detail to definitely select the best samples to use for RNA-sequencing. Based on the results from the previous section, we chose to use 1 or 2 days of doxycycline treatment in senescent cells. To assess the most comparable timepoint to use for the proliferating control, I collected samples from 1 to 3 days after treatment (Fig. 14B).

I evaluated samples from 7 biological replicates since the cells used corresponded to 7 mice, coming from 3 different litters. The replicates were handled in 3 experimental batches respecting these litters of origin (Fig. 14A). A total of 12 samples representing different conditions (proliferative/senescent, treated/untreated, 0 to 3 days of treatment) were produced and analyzed per experiment (Fig. 14B). The mRNA samples of all 7 replicates were analyzed by RT-qPCR (Fig. 15). I quantified p16 levels to verify the senescent state of each sample (Fig. 15C). This confirmed the induction of senescence in irradiated samples, regardless of the p21 knock-down condition. Again, I used Hmgb2 expression to validate the functional effect of p21 knock-down (Fig. 15B, E and H). The increase in Hmgb2 levels clearly correlated with the decrease of p21 mRNA (Fig. 15A, D and G) in all samples.

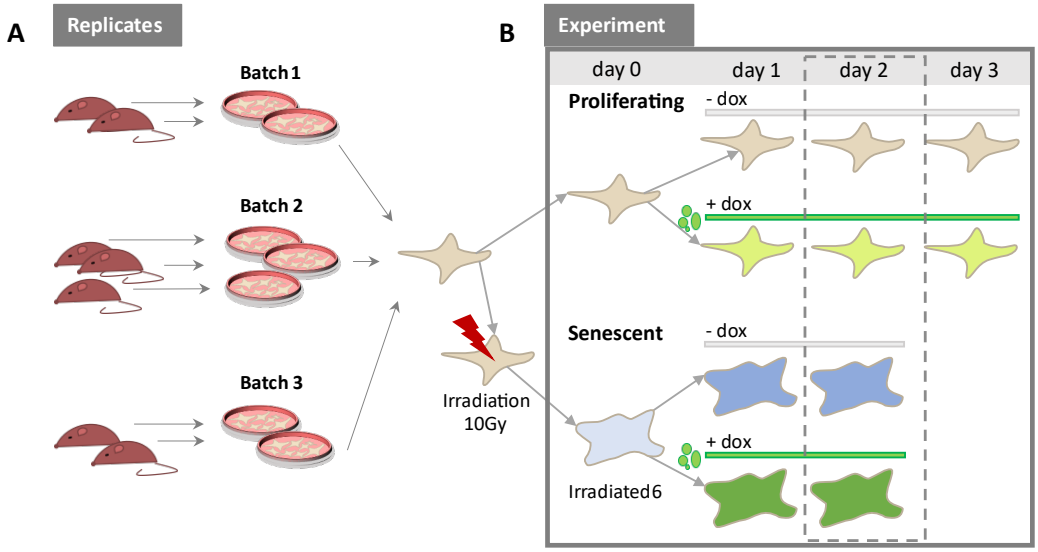

Figure 14. Experimental procedure to generate RNA-seq candidate samples. A total of 84 RNA samples representing 12 different conditions and produced in 7 biological replicates were generated. **A)** Dermal fibroblasts were extracted from 7 mice and used as biological replicates in 3 experimental batches corresponding to the 3 litters of origin **B)** A total of 12 samples representing different conditions were produced and analyzed per experiment. 7 of them belonged to proliferating cells, 4 untreated and 3 treated with doxycycline for 0 to 3 days. 5 more samples were generated in senescent cultures, 3 untreated and 2 treated with doxycycline for 0 to 2 days, starting from day 6 after irradiation. Dashed box indicating the final conditions selected to perform the bulk RNA-seq analysis.

To select the replicates to analyze by RNA-seq analysis, I focused on the efficiency of the knock-down of p21 in senescent cells (Fig. 15F). This efficiency was estimated by calculating the proportion of p21 transcript present in doxycycline treated cells in comparison to their corresponding untreated sample (Fig. 15F and I). In senescent cells, the decrease of p21 mRNA after 2 days of doxycycline treatment was 18.86% greater than after 1 day (Fig. 15F) (p-value <0.005 in a paired t-test, average fold change of 0.58 and 0.39 for day 1 and 2 of knock-down respectively). Considering this, the selected timepoint for the senescent samples corresponded to day 8 after irradiation, when the samples where p21 was knocked-down had been exposed to doxycycline for 2 days, and the level of p21 transcript was reduced by more than 60% on average. Focusing on this parameter, the 4 replicates that presented the strongest reduction in p21 mRNA (in red, Fig. 15F), with an average decrease of 76.5% (fold change of 0.335 ± 0.045), were selected for the subsequent RNA-sequencing analysis. Moreover, these replicates belonged to only 2 experimental batches, which could conveniently help reduce the technical variability created by a batch effect among experiments.

To decide which treatment length was the most equivalent in proliferating samples, I also evaluated the efficiency of the knock-down at different timepoints (Fig. 15I). Firstly, I noticed

that the decline of p21 mRNA occurred faster in proliferating cells. A similar reduction level to 2 days treatment in senescent cells was reached between day1 and 2 of treatment in proliferating cultures (fold change of 0.382 ± 0.167 after 1 and 0.287 ± 0.117 after 2 days). When deciding which timepoint produced the most comparable samples to the senescent condition, it was presumed that the dynamic of the molecular changes due to p21 loss that

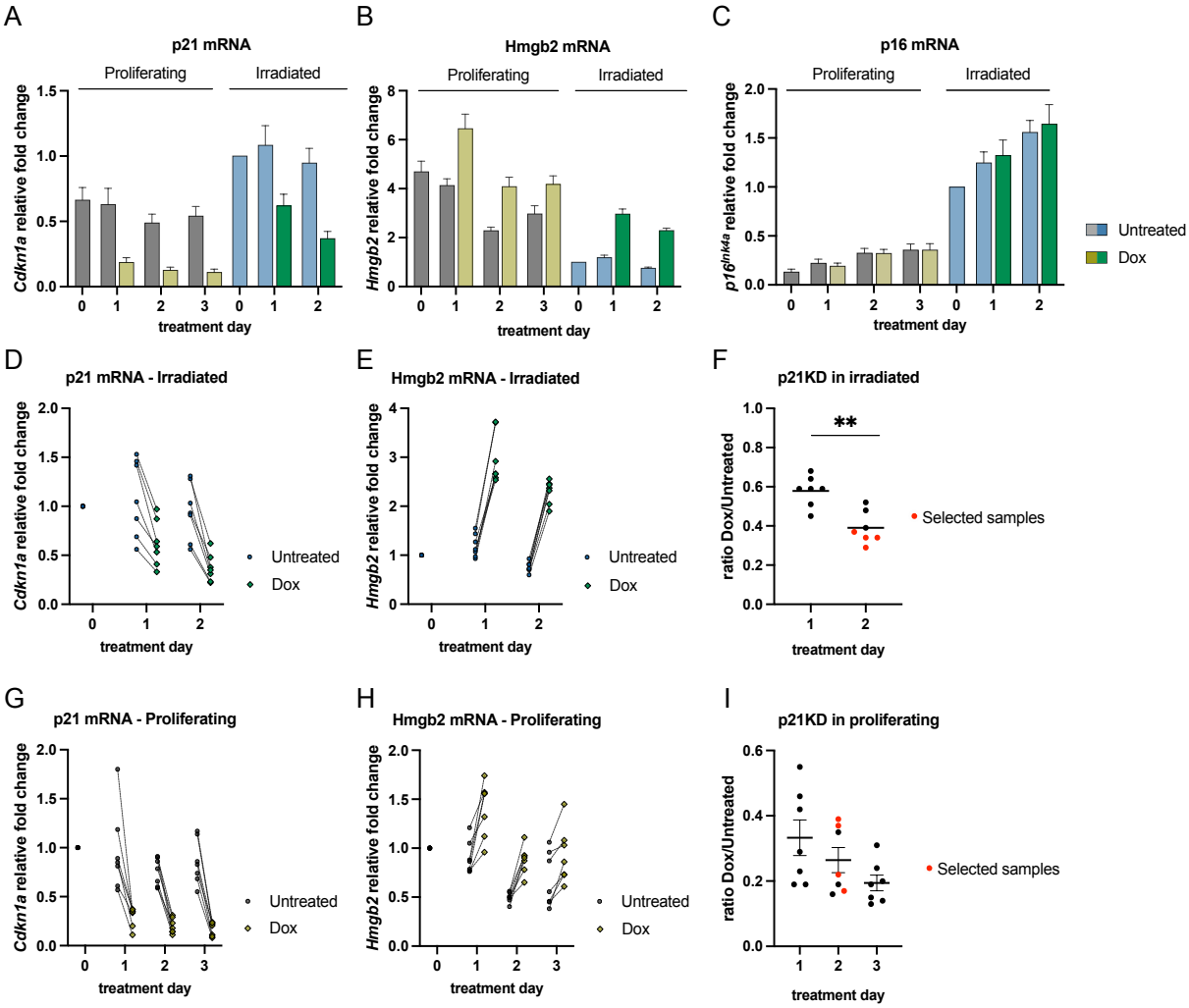

Figure 15. Sample evaluation by RT-qPCR analysis. RNA from 84 samples of 7 replicates from 12 different conditions was extracted and the retrotranscribed cDNA of specific mRNAs were quantified by RT-qPCR. **A-C)** Mean relative fold change and SEM of *Cdkn1a* (A), *Hmgb2* (B) and *p16^{Ink4a}* (C) across all replicates. Each experiment was normalized to senescent cells day 0 (before starting the induction of p21 knock-down by doxycycline (Dox) treatment). Proliferative samples in grey (untreated) and yellow (Dox treated) and senescent in blue (untreated) and green (Dox treated). **D-E and G-H)** Relative fold change of *Cdkn1a* (D,G) and *Hmgb2* (E,H) of individual samples (dots) connected by experiment (lines). Senescent (D,E) and proliferative (E,H) samples were analyzed separately. Each experiment was normalized to untreated sample before the start of the treatment. **F and I)** Relative abundance of p21 mRNA (*Cdkn1a*) in doxycycline treated compared to untreated samples of the corresponding condition (same timepoint, proliferating or senescent). Expressed as a ratio of the value of untreated vs treated samples. Individual samples in dots, mean and SEM indicated. Finally selected samples for the RNA-seq in red. (F) Paired t-test comparing the ratio between 1 and 2 days of treatment in senescent cells with p-value <0.005.

could lead to transcriptional changes may be influenced by time. The length of the treatment was considered to be the most critical factor to take into account, and the best was to use the same for proliferating and senescent samples. Therefore, proliferating samples treated with doxycycline for 2 days were chosen (in red, Fig. 15I).

In summary, to evaluate the transcriptional changes that p21 loss produced in senescent cells, I selected samples belonging to 4 experimental conditions derived from the combination of 2 factors: proliferating or senescent (8 days after irradiation), and untreated or 2-days treated with doxycycline to induce p21 knock-down (Fig. 14B). The final samples were selected based on the decrease in fold change in p21 mRNA in doxycycline treated vs untreated senescent cells among 7 replicates. These samples belonged to the 4 replicates presenting the strongest downregulation in this condition, and they were produced in 2 experimental batches. In total, 16 samples of extracted RNA belonging to 4 experimental conditions were sent to the GenomeEast platform to perform a bulk RNA-sequencing analysis.

2. RNA-seq Analysis

2. 1 Data description

A total of 16 extracted RNA samples were sent for sequencing by GenomEast sequencing platform. They were categorized in 4 different conditions from the combination of 2 factors: proliferating or senescent, and untreated or treated with doxycycline to induce the knock-down of p21 (Fig. 16, left). To simplify the nomenclature, untreated cells were considered "controls" and doxycycline treated cells belonged to the "p21 knock-down" group. To facilitate the nomenclature, an abbreviation of 2 letters was assigned to each condition: *P* or *S* for "**p**roliferating" or "**s**enescent", and *C* or *D* for "**c**ontrol" or "p21 knock-**d**own" (Fig. 16, right). Samples were named using these abbreviations, and a number from 1 to 4 was assigned to determine the biological replicate. The four biological replicates were generated in 2 experimental batches, 1-2, and 3-4 being obtained in the same experimental batch.

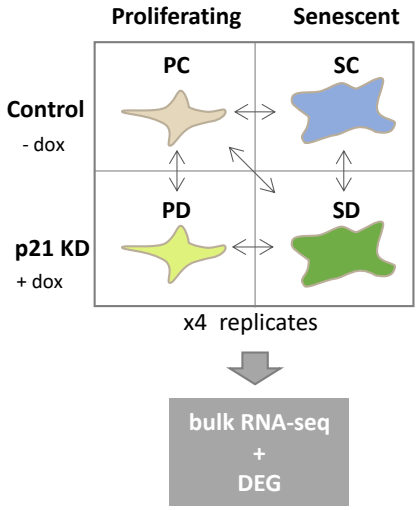

Sample	Batch	Condition	
PC1	A	PC	Proliferating Control
PC2	A	PC	
PC3	B	PC	
PC4	B	PC	
PD1	A	PD	Proliferating p21 knock down
PD2	A	PD	
PD3	B	PD	
PD4	B	PD	
SC1	A	SC	Senescent Control
SC2	A	SC	
SC3	B	SC	
SC4	B	SC	
SD1	A	SD	Senescent p21 knock down
SD2	A	SD	
SD3	B	SD	
SD4	B	SD	

Figure 16. Classification of RNA-seq analyzed samples. A total of 16 RNA samples corresponding to 4 replicates of 4 conditions were analyzed by RNA-seq. Each condition was assigned a name based on the 2 variables studied: senescent state (proliferating or senescence) and level of p21 (unaltered or knocked-down). In consequence, each group could be distinguished by a 2 letters abbreviation which corresponded to these 2 factors: P for proliferating, S for senescent, C for "control" untreated and D for doxycycline (dox) induced p21 knock-down. A number was assigned to each replicate. Individual samples were named based on their condition and replicate (left table). Replicates 1-2 and 3-4 were generated in parallel in the same experimental batch (left table).

These samples were sequenced by the GenomEast platform, who also performed their standard analysis, including the mapping of the reads, normalizations, quality control and a differential gene expression analysis (DEG) comparing different conditions. In this analysis, the batch of origin of each sample was taken into account. They provided us with a detailed report -done by Matthieu Jung- containing the pipeline used for the sequencing, descriptive data of the quality of the samples, and an overview of the DEA results.

Data exploration

The provided report included a descriptive analysis of the samples, including the measure of the distance between samples, estimated by the Simple Error Ratio Estimate (SERE) coefficient and represented in a heatmap, and the principal component analysis (PCA), among others. These analyses are discussed next.

Simple Error Ratio Estimate coefficient heatmap - SERE

The *Simple Error Ratio Estimate* (SERE), was represented in a heatmap (Fig. 17). It quantifies global sample-to-sample differences. The SERE coefficient indicates the similarity between 2

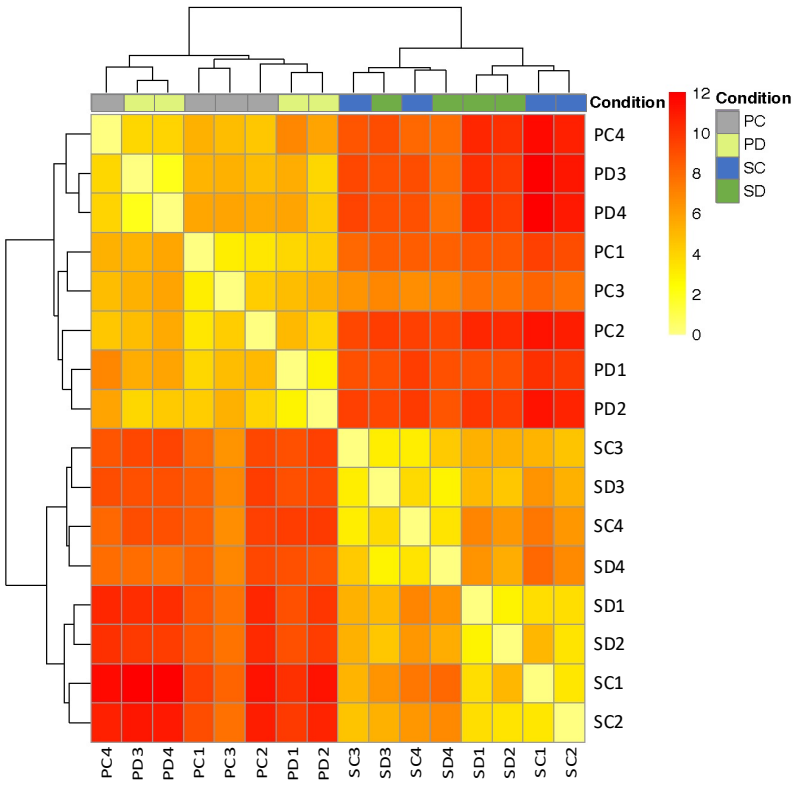

Figure 17. Heatmap of sample-to-sample distances (SERE coefficient). Figure generated by the GenomEast platform and adapted from their report. Heatmap representing the distance between samples corresponding to the SERE coefficient. Samples were hierarchically clustered by similarity.

samples. Citing the report, a coefficient of 0 indicated data duplication, a score of 1 corresponds to faithful replication, and this coefficient is greater than 1 if samples are truly different. The more different the samples are, the higher the SERE coefficient is (quoted from the report). Thus, the interpretation of this heatmap (Fig. 17) indicated that proliferating and senescent samples formed two groups, and the 8 samples of each group clustered together. The knock-down of p21 did not have such a strong effect as to cause samples to separate in groups depending on their p21 level. This indicated that the senescence state, proliferating or senescent, was the predominant factor explaining the transcriptional differences among samples. In other words: senescent samples remained "senescent" independently of the knock-down of p21, while proliferating samples could be considered proliferative regardless of p21 levels. This conclusion was also reflected in the *Principal Component Analysis* (PCA) graph (Fig. 18).

Principal Component Analysis - PCA

The Principal Component Analysis is a technique to reduce the dimensionality of the data to show the main sources of variance and detect batch effects. The analysis computes a few

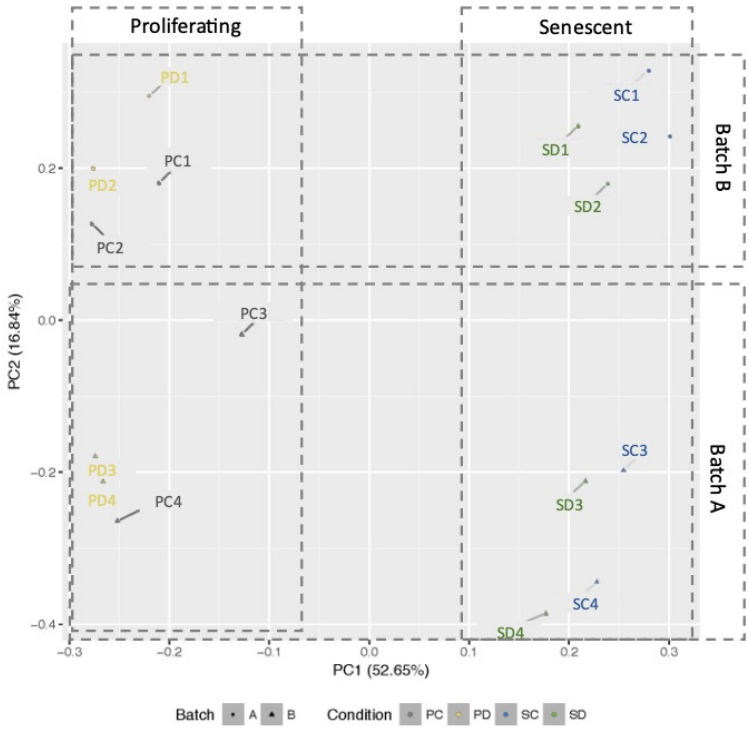

Figure 18. Principal Component Analysis. Figure generated by the GenomEast platform and adapted from their report. Axes representing the principal components (PC) that explained the variation among samples the most. In brackets in each axis, percentage of variance explained by each axis: horizontal x axis a 52.65% and vertical y axis a 16.84%. The distance between samples and their relative position indicates the variation between them explained by these components. Dotted rectangular boxes grouping samples depending on their senescence state (top labels) or their experimental batch (right labels).

principal components, which are linear combinations of the variables (genes) that explain the maximum variability between the samples. In the graph of figure 18, each sample was positioned in a 2-axis plot representing the first two principal components, and their relative position showed the variance between samples. Interestingly, proliferating and senescent samples clearly clustered at opposite sides of the x axis, which explained 52.65% of the variance, showing again that there were major global differences between these groups. On the other side, we observed that each experimental batch positioned at different sides of the y axis (Fig. 18). This axis, which corresponded to the second principal component and explained 16.84% of the variance, was clearly defined by the batch origin of the samples. This was taken into account, and a batch effect correction was performed during the Differential Gene Expression analysis (DEA).

Differential gene expression analysis - DEA

To explore the transcriptional differences between conditions, a differential gene expression analysis (DEA) was performed. It provides a quantification of the differences in expression of each gene between 2 comparisons, and estimates its statistical significance. The result of the DEA was delivered in a table format through a TSV file (tab-separated values), which can be opened in spreadsheet software like *Microsoft Excel*. It contained a table assigning a row per gene, and provided different columns indicating their raw and normalized read counts as well as descriptive data of the locus and the encoded transcript and associated protein. The result of the differential expression analysis comparing different pairs of conditions was provided in 3 additional columns per comparison, which contained the fold change in the expression of each gene expressed as log2 fold change, the significance of this change in p-value, and an

Name of the comparison (A vs B)	Number of over-expressed genes (A > B)	Number of under-expressed genes (A < B)	Number of significantly differentially expressed genes
SC vs PC	3939 | 884	3763 | 422	7702 | 1306
SD vs SC	885 | 248	269 | 2	1154 | 250
PD vs PC	1097 | 21	734 | 7	1831 | 28
SD vs PD	4090 | 1105	3862 | 208	7952 | 1313
SD vs PC	3821 | 1066	3575 | 198	7396 | 264

Table 1. Differentially expressed genes in all the performed comparisons. A total of 5 comparisons were performed (first column). The number of significantly differentially expressed genes in each comparison is specified in columns from 2 to 4. Statistical significance was determined by an adjusted p-value <0.05. Total number of genes in last column, only upregulated genes in 2nd column (log2 fold change > 0) and only downregulated genes in 3rd column (log2 fold change < 0). A more stringent filter of an absolute log2 fold change ≥ 1 (≥ 1 or ≤ -1, corresponding to a fold change ≥ 2 or ≤ 0.5) was applied to obtain the second number of each column (after the vertical line).

adjusted p-value correcting for the multiple testing performed. 5 out of the 6 possible comparisons between conditions were requested, the ones that were estimated to be the most useful to determine the transcriptional changes associated to all the physiological states reflected in our samples (Table 1, first column). The results of this analysis were used to explore the RNA-seq data.

2. 2 Model exploration – Single comparisons

The aim of the RNA-seq was to explore the role of p21 in regulating gene expression in senescent cells. To do so, I wanted to determine which transcriptional changes were associated to the senescence response, as well as to the knock-down of p21 in proliferating and in senescent cells. I focused on studying the 3 main comparisons related to these processes (Fig. 19), which were analyzed separately.

To describe the specific transcriptional changes associated to the acquisition of senescence in our model and validate the results of the RNA-seq analysis, I used the comparison of control senescent to proliferating cells (SC. vs. PC). Since we were interested in the role of p21 specifically in senescence, we wanted to determine which transcriptional changes caused by its loss were specific to the senescent state. Therefore, I was first interested in characterizing and confronting the effect of p21 decrease in proliferation. For this, I studied the changes that proliferating cultures underwent when p21 expression was abrogated when compared to unmanipulated proliferating cells. Finally, the comparison that more directly described the effect of p21 loss in senescence came from comparing senescent cells with decreased levels of p21 to unmanipulated senescent cells (SD. vs. SC). After a descriptive analysis of the genes whose transcription was affected in each comparison, the functions associated to these changes were explored by pathway analysis.

The results from the analysis of each of the comparisons were structured in the same way. First, the number of differentially expressed genes was described and graphed in a Volcano plot and summarized in a table format. I then used Enrichr webside tool[444–446] to perform pathway analysis on these genes to uncover the biological effect that these changes in expression may cause. This analysis was done using 3 gene sets each time: a list of all the differentially expressed genes, only the genes that were upregulated, and only the downregulated ones. The results were represented as dotplot figures, which shows the enrichment of the top terms found in the 3 gene lists of each comparison.

Several other databases were then consulted, and I used the ones that better summarize the observed results to create the figures. In order to present the conclusions in a summarized and unbiased manner, 2 dotplots were generated. The first contained a totally unbiased list combining the 5 most enriched pathways of the KEGG database in each of the 3 gene sets. The second dotplot presented a selection of term belonging to the combination of the 3 Gene Ontology databases: Biological Process, Molecular Function and Cellular Component. This selection aimed to summarize the general results observed. To do so, they were selected from an unbiased list of the 5 most significantly enriched terms in each geneset. The enrichment was assessed based on its adjusted p-value, and the threshold of significance was established at ≤0.25.

Comparison	Associated process
SC vs PC	Senescence acquisition
PD vs PC	p21 knock-down in proliferation
SD vs SC	p21 knock-down in senescence

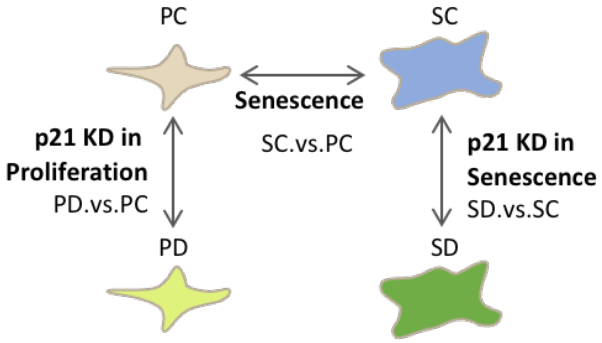

Figure 19. Schematic representation of the analyzed comparisons. To unravel the role of p21 in senescence, 3 comparisons reflecting the transcriptional changes associated to 3 processes were explored (top table).

Senescence acquisition (SC.vs.PC) - Senescence-Control vs Proliferating-Control

The first comparison analyzed was Senescent-Control vs Proliferating-Control (SC.vs.PC). This comparison described the transcriptional changes associated to the senescence response. We expected to find an increase in the expression of known genes associated to the senescent phenotype, as well as a decrease in those related to the proliferative capacity.

DEG in SC.vs.PC

The acquisition of senescence affected the expression of a total of 7702 genes (adjusted p-value <0.05), from which 3939 were upregulated and 3763 downregulated in senescent cells in comparison to proliferating ones (Fig. 20A). Although the number of genes presenting an increased and decreased expression was similar, the extent of the change, in terms of expression level, was greater among upregulated. This was reflected by filtering the DEG by log2 fold change (log2FC). Using a cut-off of |log2FC|>1, the number of upregulated genes doubled the downregulated ones (844 vs 422, Fig. 20B).

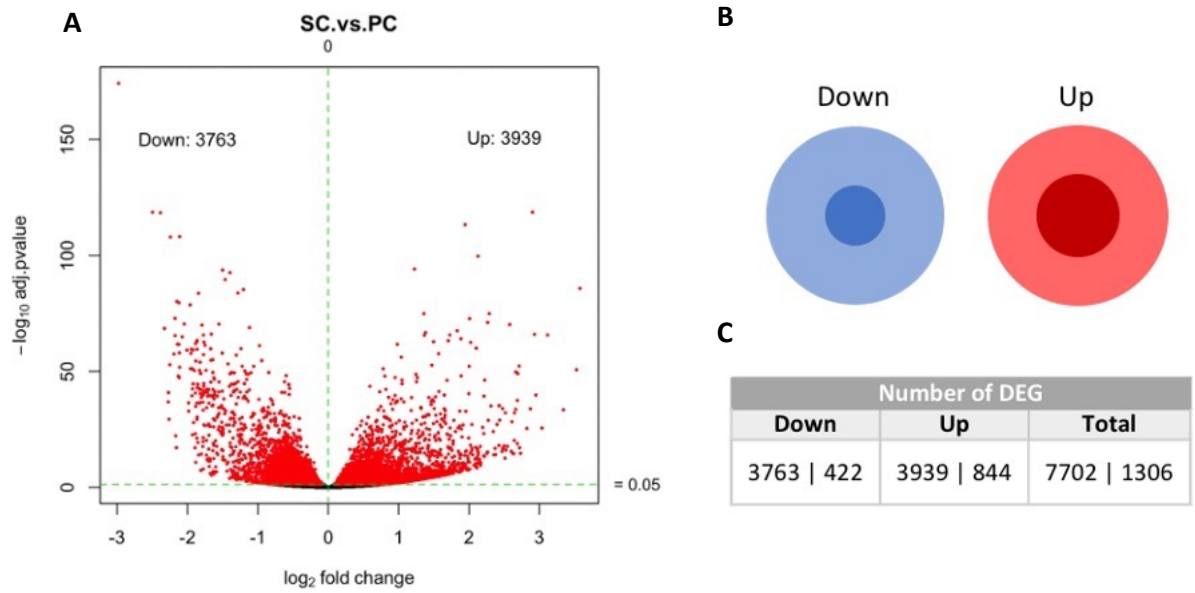

Figure 20. DEG in the SC. vs. PC comparison. In all cases a threshold of an adjusted p-value <0.05 was applied to assess significance. **A**) Volcano plot representing the results of the comparison. Vertical axis representing the adjusted p-value (as -log10), and horizontal axis the log2 fold change (log2FC). Significant genes marked in red. Green lines indicating the significance threshold applied (no filtering for log2FC). **B)** Visual representation of the number of downregulated (blue) and upregulated genes (red), size relative to each value. Lighter circle corresponding to no filtering for fold change, dark circle to filtering by |log2FC|>1. **C)** Number of DEG in the comparison. For the second number, a filter of |log2FC|>1 was applied.

Pathway analysis SC.vs.PC

In order to define which phenotypical functions altered in senescence were reflected by the differences in gene expression between proliferating and senescent cells, I graphed the most enriched pathways associated to the transcriptional signature of this comparison (Fig. 21). I noticed that the enrichment of most of the pathways associated to the totality of genes varying their expression in senescent cells was mainly explained by the downregulated genes. Meanwhile, I detected weaker enrichment values among the upregulated genes, and with terms that were more ambiguous and difficult to interpret, which may suggest a greater

variability among the functions regulated by them. This could be understood that less defined processes are associated to the genes that are upregulated in senescence.

Figure 21. Most enriched terms in the SC.vs.PC comparison. Pathway analysis was performed on 3 gene lists: all DEGs (purple), downregulated genes (blue) and upregulated genes (red). Only significant terms were colored, the rest are shown in grey. Size of the dots corresponding to the fraction of genes belonging to the term that is present in each input gene list (OverlapNum). **A)** KEGG 2021 Human. Unbiased term selection, with the exception of the addition of "Cellular Senescence". **B)** Gene Ontology 2021. Representative selection of the most enriched terms in each sublist from Gene Ontology databases (Biological Process, Cellular Component, Molecular Function).

As expected, the most enriched terms among all the genes affected in senescence were related to proliferation, such as *Cell Cycle* or *DNA replication*, due to the downregulation of these signatures (Fig. 21A). Terms related to DNA repair (*Mismatch repair*) were also downregulated. Additionally, gene expression and RNA-related pathways were also clearly downregulated in senescence cells (Fig. 21, *Spliceosome*, *Ribosome*, *RNA transport*, *RNA binding*, *Gene expression* among others). Interestingly, genes related to adhesion were also present in all gene lists. Most of them were only significant by the downregulated genes (*focal adhesion, cell-substrate junction, cadherin* binding), with the exception of *extracellular matrix organization*, which was significant in genes increasing their expression. In this last list, I also noticed pathways related to vacuoles, cytokine production and lysosomes. This was in agreement with the increase in vacuoles, the number and function of lysosomes, and SASP production, which has been reported in in senescent cells. The *p53 pathway* appeared to be affected in 2 of the used databases. Although it was altered in all the submitted lists, in KEGG it was only significant among the upregulated genes. Additionally, I added *"Cellular senescence"* into the list of terms of Fig. 21A, which ranked the 16th most enriched pathways in the complete list of DEG in KEGG database. Most of the genes associated to this pathway decreased their expression upon senescence induction.

In conclusion, the expected enrichment of functions associated to the phenotypical changes associated to senescent cells was validated through pathway analysis. For example, cell cycle and proliferation function were reduced, and genes related to lysosomes and cytokine production increased their expression. This demonstrated that the acquisition of a senescent transcriptional signature was detectable in our RNA-seq data when comparing senescent to proliferating cells (SC.vs.PC).

P21 Knock-Down in Proliferating Cells (PD.vs.PC) - Proliferating-Knock-Down vs Proliferating-Control

By comparing proliferating cells with p21 knock down (PD) to control proliferating cells (PC), I wanted to better determine the role of p21 outside of senescence. I expected this result to reflect the basal function of the p21 in normal undamaged proliferating cells. This would serve as a control to allow me to distinguish which function were transcriptionally affected by p21 loss specifically in proliferating or senescence cells, and which ones were commonly disturbed in both contexts.

DEG in PD.vs.PC

Knocking-down p21 in proliferating cells affected the expression of 1831 genes, from which 1097 were upregulated and 734 were downregulated (adjusted p-value <0.05, Fig. 22). However, the change in expression was proportionally smaller than in other comparisons. When a filter of log2 fold change (log2FC) of |log2FC|>1 was applied, only 21 and 7 genes were upregulated and downregulated respectively.

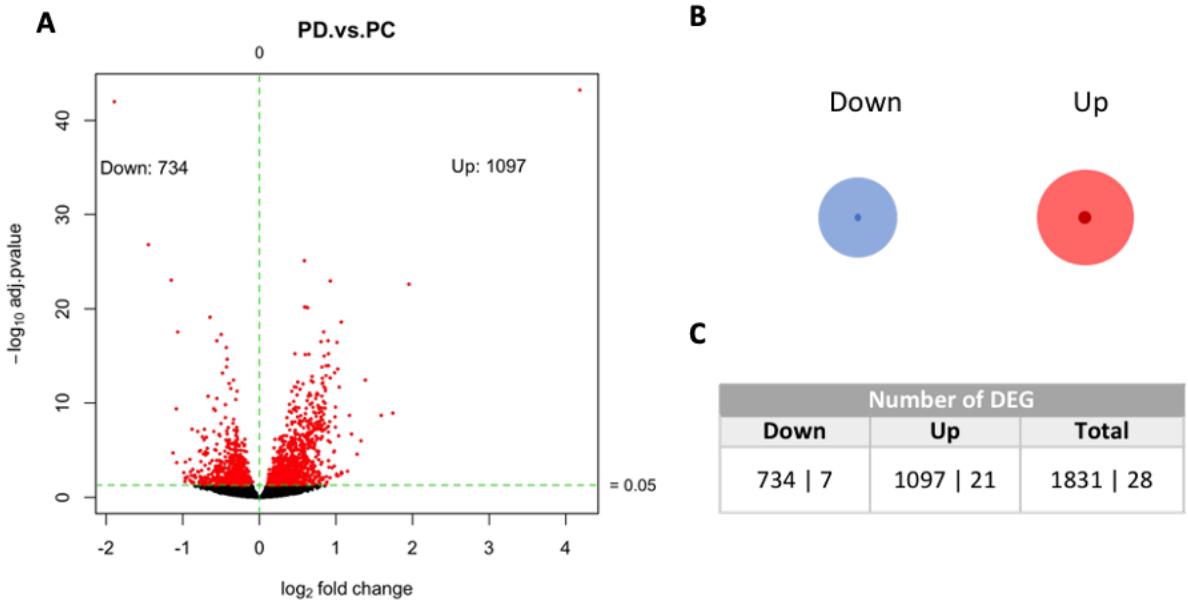

Number of DEG		
Down	Up	Total
734 | 7	1097 | 21	1831 | 28

Figure 22. DEG in the PD. vs. PC comparison. In all cases a threshold of an adjusted p-value <0.05 was applied to assess significance. **A**) Volcano plot representing the results of the comparison. Vertical axis representing the adjusted p-value (as -log10), and horizontal axis the log2 fold change (log2FC). Significant genes marked in red. Green lines indicating the significance threshold applied (no filtering for log2FC). **B)** Visual representation of the number of downregulated (blue) and upregulated genes (red), size relative to each value. Lighter circle corresponding to no filtering for fold change, dark circle to filtering by |log2FC|>1. **C)** Number of DEG in the comparison. For the second number, a filter of |log2FC|>1 was applied.

Pathway analysis in PD vs PC

In agreement to p21's role as a cell cycle inhibitor, most of the top pathways enriched among the upregulated genes were associated to proliferation, such as *Cell cycle* or *DNA replication* (Fig. 23). The upregulated genes were also associated to the cytoskeleton, including terms like *microtubule cytoskeleton* and *tubulin binding.* Similarly to the result of the SC.vs.PC comparison, *Focal adhesion* and *Translation* were enriched in the list of downregulated genes in PD.vs.PC. On the other hand, *Lysosome* or *Extracellular matrix organization* also appeared enriched in the downregulation list, in contraposition to their transcriptional change in

senescence. *Cellular senescence* and *p53 pathway* were significantly enriched among upregulated and downregulated genes in this comparison.

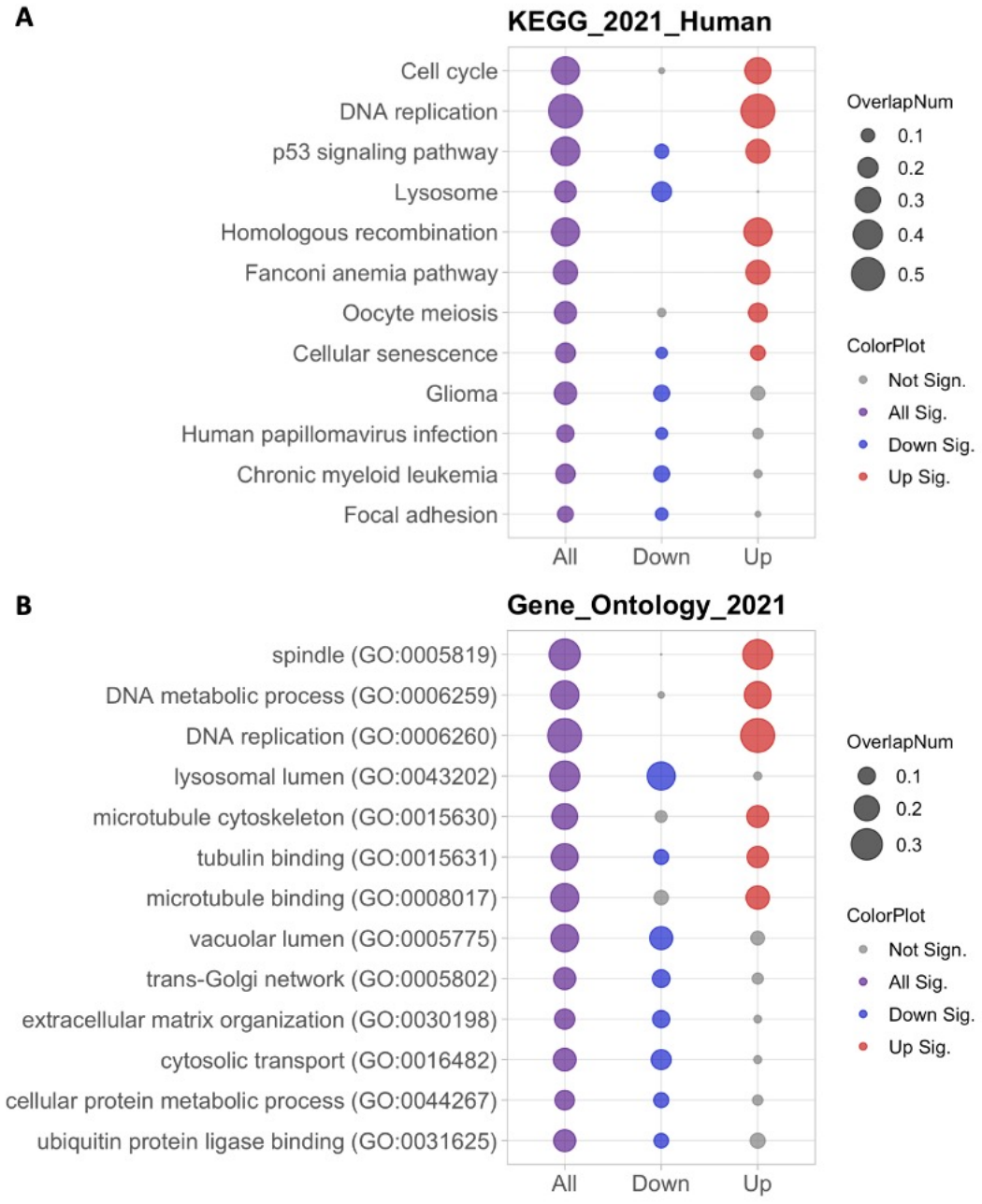

Figure 23. Most enriched terms in the PD.vs.PC comparison. Pathway analysis was performed on 3 gene lists: all DEGs (purple), downregulated genes (blue) and upregulated genes (red). Only significant terms were colored, the rest are shown in grey. Size of the dots corresponding to the fraction of genes belonging to the term that is present in each input gene list (OverlapNum). **A)** KEGG 2021 Human. Unbiased term selection, with the exception of the addition of "Cellular Senescence". **B)** Gene Ontology 2021. Representative selection of the most enriched terms in each sublist from Gene Ontology databases (Biological Process, Cellular Component, Molecular Function).

P21 Knock-Down in Senescence (SD.vs.SC) - Senescence-Knock-Down vs Senescence-Control

To study the role of p21 in senescent cells, I focused on the comparison of senescent cells with p21 knock-down (SD) to control senescent cells (SC). Since the only controlled variable between these groups is the levels of p21, the transcriptional changes between them were expected to reflect p21 function in senescent cells.

DEG in SD.vs.SC

The knock-down of p21 in senescent cells was associated to a transcriptional change of 1154 genes (adjusted p-value <0.05, Fig. 24). Most of them were upregulated (885 genes vs 269 downregulated), which is in agreement with the known repressive role of p21 in transcription. This was even more evident when a more stringent filter was applied to consider only genes with a log2 fold change (log2FC) of |log2FC|>1. In this case, only 2 genes were considered downregulated, one of them being p21 (*Cdkn1a*), while 248 were upregulated. This result suggested that p21 expression is mostly associated with gene repression in senescent cells.

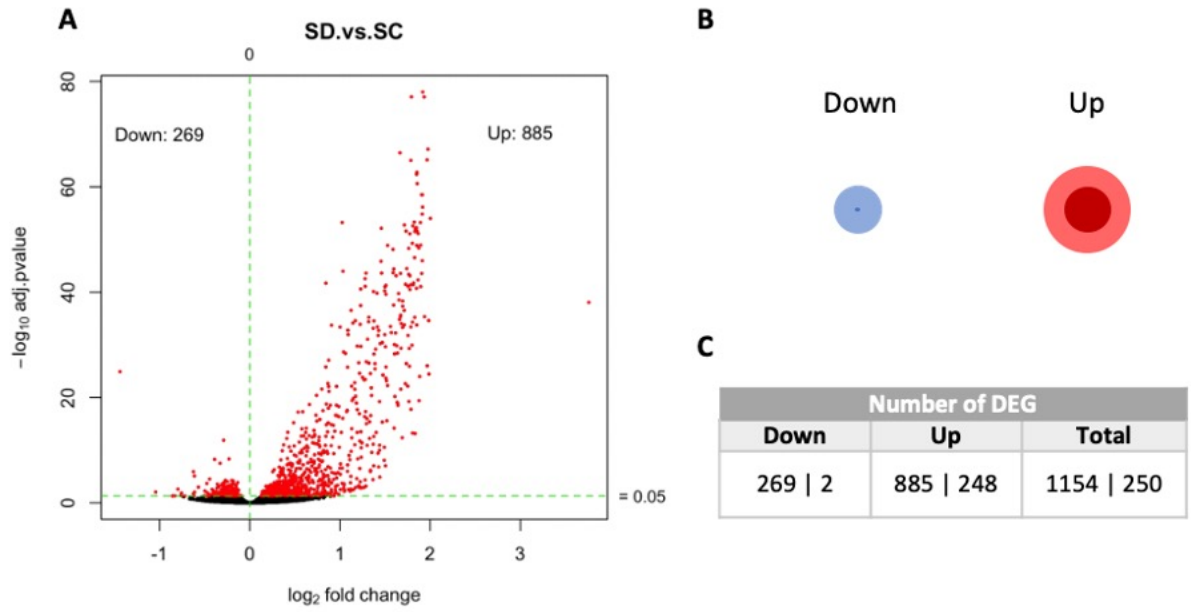

Figure 24. DEG in the SD. vs. SC comparison. In all cases a threshold of an adjusted p-value <0.05 was applied to assess significance. **A**) Volcano plot representing the results of the comparison. Vertical axis representing the adjusted p-value (as -log10), and horizontal axis the log2 fold change (log2FC). Significant genes marked in red. Green lines indicating the significance threshold applied (no filtering for log2FC). **B)** Visual representation of the number of downregulated (blue) and upregulated genes (red), size relative to each value. Lighter circle corresponding to no filtering for fold change, dark circle to filtering by |log2FC|>1. **C)** Number of DEG in the comparison. For the second number, a filter of |log2FC|>1 was applied.

Pathway analysis in SD vs SC

Lastly, I performed pathway analysis on the genes changing upon p21 knock-down in senescence (Fig. 25). The result strongly resembled that obtained in the last comparison, p21 knock-down in proliferating cells (PD.vs.PC). The most significantly altered signature among the DEG was due to the upregulated genes, and it was associated to cell cycle and proliferation (*Cell cycle, DNA replication, microtubule cytoskeleton organization involved in mitosis*). Another upregulated signature was DNA damage (*DNA repair, Mismatch repair).* Among the pathways related to the downregulated genes, *Focal adhesion* and *ECM-receptor interaction*

Figure 25. Most enriched terms in of the SD.vs.SC comparison. Pathway analysis was performed on 3 gene lists: all DEGs (purple), downregulated genes (blue) and upregulated genes (red). Only significant terms were colored, the rest are shown in grey. Size of the dots corresponding to the fraction of genes belonging to the term that is present in each input gene list (OverlapNum). **A)** KEGG 2021 Human. Unbiased term selection, with the exception of the addition of "Cellular Senescence". **B)** Gene Ontology 2021. Representative selection of the most enriched terms in each sublist from Gene Ontology databases (Biological Process, Cellular Component, Molecular Function).

were found. In this comparison *Cellular senescence* was significantly enriched in the list of upregulated genes.

Overall, pathway analysis revealed that the transcriptional signature associated to p21-knock-down in senescence was very similar to the changes related to its loss in proliferating cells, and in many cases it followed an opposite trend to that observed by the acquisition of senescence (SC.vs.PC).

Conclusion – Model exploration, single comparisons

This first analysis consisted of an unbiased exploration of the most affected pathways in each comparison. It allowed me to confirm expected results regarding the acquisition of senescence and the effect of p21 downregulation. I summarize the observations obtained in this section in figure 26.

Several pathways associated to the senescent phenotype were enriched among the differentially expressed genes between senescent and proliferating samples (Fig. 26). For example, the most enriched signature in this comparison was due to the decrease in the expression of cell cycle associated genes. Several other signatures associated to the acquisition of senescence were altered by p21 loss, mainly in the opposite direction. Since p21 is a known mediator of the senescence response, it made sense that its decrease caused a reversion in the expression of genes altered in senescence. Additionally, the transcriptional change associated to p21 knock-down in both proliferating and senescent cells was similar. As expected, the strongest enrichment detected in these comparisons corresponded to an increase in proliferation. This corresponded to the principal function of p21: the inhibition of cell cycle. This suggested that genes strongly regulated by p21 were defining the main pathways associated to p21 loss. In consequence, it was not surprising that the top terms affected by p21 loss in senescence and proliferation were consistent.

Although the obtained results were a further validation of the model, most of the pathways detected were changing in a predictable pattern. Therefore, a deeper exploration of the data was necessary in order to unravel novel functions regulated by p21 in senescent cells.

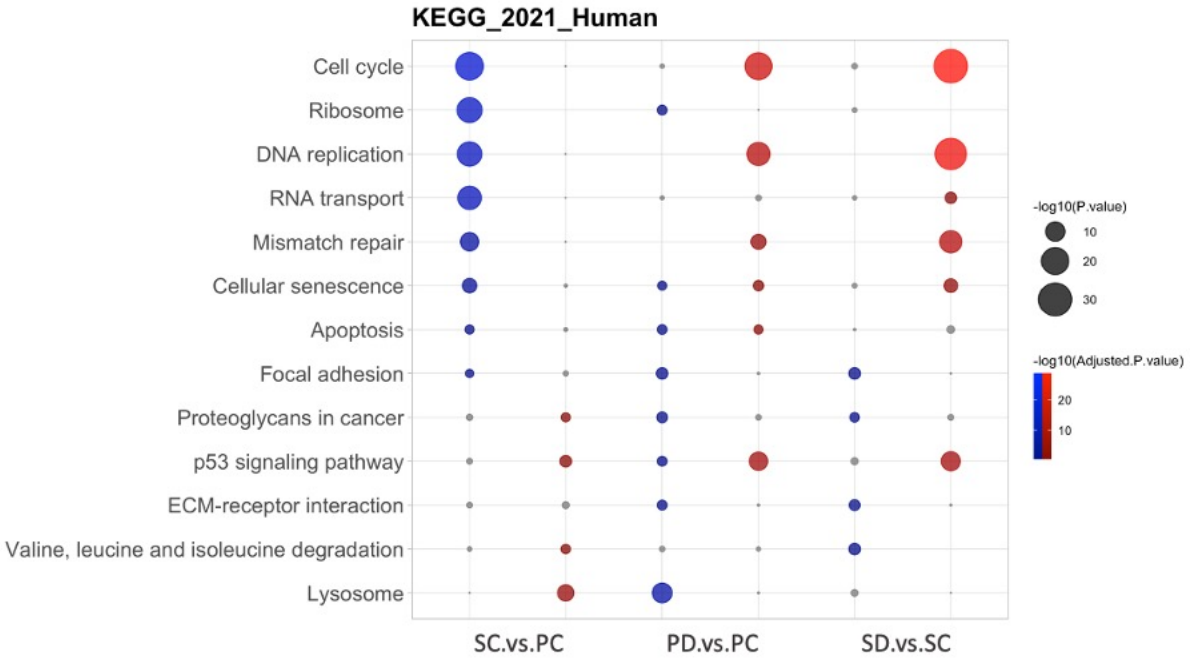

Figure 26. Representative enriched terms among comparisons. The enrichment of a selection of pathways from KEGG Human 2021 database, among the upregulated and downregulated genes of each comparison was represented in a dotplot. Comparisons were: SC.vs.PC (senescence), PD.vs.PC (p21 knock-down in proliferation) and SD.vs.SC (p21 knock-down in senescence). Size of the dot corresponding to the p-value, and its color, to the adjusted p-value, both expressed in -log10. Blue and red dots for enrichments among downregulated and upregulated gene lists, respectively. Grey dots for not significant enrichments (adjusted p-value >0.25).

2. 3 Comparison of comparisons

After the first exploration of the DEG in the different main comparisons, I realized that the strong enrichment of some transcriptional signatures was probably preventing the detection of other potentially interesting functions. This is the case of the clear upregulation of proliferation related genes when p21 is lost in senescent cells (SD.vs.SC). Although this was a relevant result in line with the literature, it could be hiding other enhanced phenotypes yet to be discovered. Therefore, I concluded that this level of analysis was not sufficient to unravel novel functions controlled by p21 in senescent cells.

Since a deeper understanding of our data was required, I decided to dissect the transcriptional changes of the differentially expressed genes after p21 knock-down in senescent cells over the different conditions. It was reasoned that genes associated to the same functions would tend to behave similarly[447]. This isolation of functionally related genes would then allow the identification of functions masked when diluted among more enriched

signatures. Moreover, the clustering of transcriptional signatures could help me to better describe how phenotypes were changing in different conditions.

Therefore, I subdivided the up and down-regulated genes in SD.vs.SC in groups according to their behavior in the other main comparisons. First, I analyzed their expression when p21 was knocked-down in proliferating cells (PD.vs.PC), and secondly, during the acquisition of senescence acquisition (SC.vs.PC). In this way, I would be able to obtain subsets of genes following the same transcriptional tendency. These sublists were used to perform pathway analysis, which allowed me to explore functions associated to each geneset. To represent which functions were associated to each sublist of genes, the enrichment of a representative selection of terms from each of the subsets of upregulated or downregulated genes in the SD.vs.SC comparison was represented in a dotplot. These terms were selected from different databases aiming for the best representation of the general result observed across all of them. In order to reduce the bias of selection, they were chosen from an unbiased sublist including only the 10 most enriched pathways detected in each sublist, ordered by adjusted p-value.

p21 Knock-Down in Senescence vs Proliferation (SD.vs.SC vs PD.vs.PC)

In order to explore the role of p21 specifically in senescence, I compared the transcriptional changes associated to p21decrease in senescent (SD.vs.SC) and proliferating cells (PD.vs.PC) (Fig. 27). The effect of p21 loss in both situations was compared, and this was used to group the differentially expressed genes in SD.vs.SC. In order to define which functional programs were controlled by p21 specifically in senescent cells, I performed pathway analysis on each of these lists, and the most enriched terms in each list were analyzed.

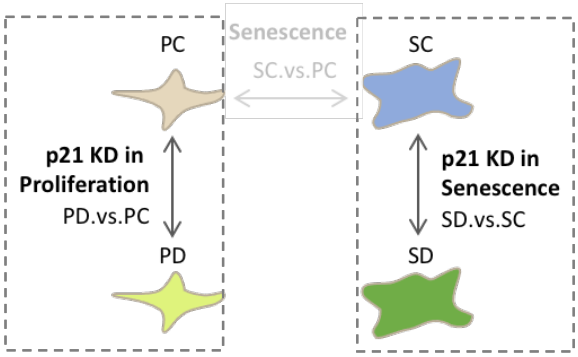

Figure 27. Comparison of comparisons: p21 knock-down in proliferation or senescence. Comparison of the transcriptional changes associated to p21 loss in proliferating and senescent cells.

Gene classification: SD.vs.SC DEG in PD.vs.PC

To illustrate the comparison of these comparisons, figure 28A shows the transcriptional change of each gene in each of these comparisons on a 2-axis scatter plot (Fig. 28A and Supp. Fig.1). The position of a gene in the space of a gene contains information about how p21 loss is affecting its transcription in both senescence and proliferating cells, and differentially expressed genes were colored.

DEG in SD.vs.SC were subdivided into 4 different subgroups: upregulated genes were separated into the ones that were either also upregulated or not significantly changing in PD.vs.PC, and same criteria was applied for downregulated genes (Fig. 28). It is worth noticing the absence of genes whose transcription was affected by p21 in opposite directions. I could also appreciate a difference in the distribution of commonly affected genes, since most of them belonged to the upregulated signature. While only half of the downregulated genes in SD.vs.SC were also downregulated in the proliferating comparison (135/269), around 60%

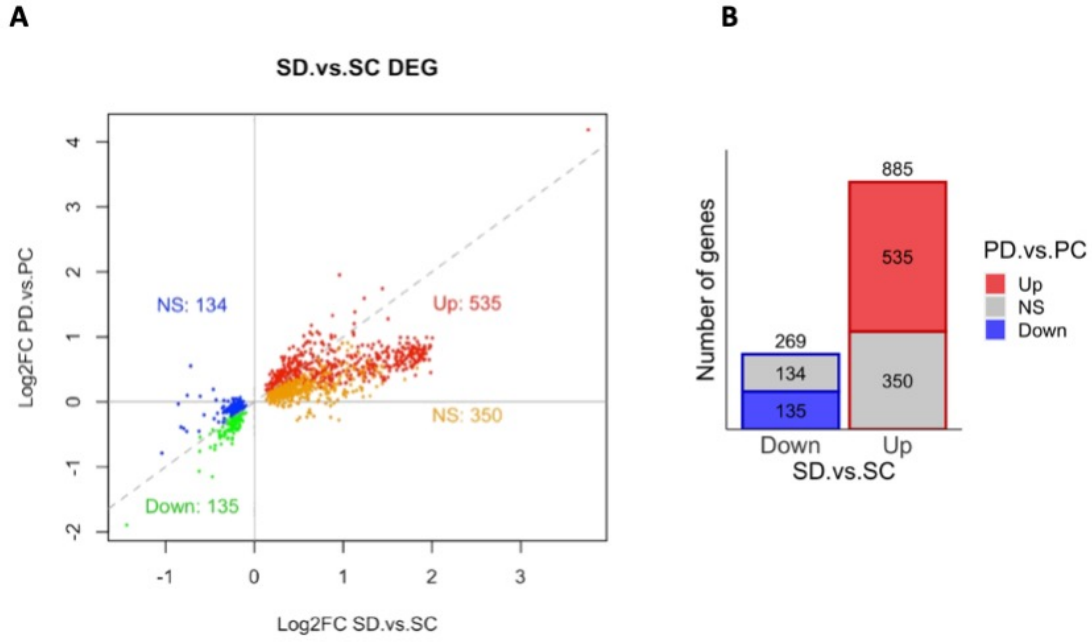

Figure 28. DEG in SD.vs.SC in the PD.vs.PC comparison. All the DEG in the SD.vs.SC comparison were subdivided depending on their expression behavior in the PD.vs.PC comparison. **A)** Scatter plot of expression change in both comparisons. All DEG in the SD.vs.SC comparison in a 2d scatter plot. Each gene was represented by a dot, its location being determined by the expression change in both comparisons expressed as log2 fold change. The x axis corresponding to the SD.vs.SC comparison, and the y axis to PD.vs.PC. A color code was used to identify the significance and direction of transcriptional change, label indicating behavior in both comparisons (NS: not significant). A diagonal dashed line of slope=1 was plotted to depict the position of same expression change in both comparisons. **B)** Bargraph quantifying the number of genes in each subgroup. Left bar with blue border for downregulated, and right bar with red border for upregulated genes in SD.vs.SC comparison. Fill color of the bar corresponding to the PD.vs.PC comparison (upregulated in red, downregulated in blue, NS: not significant in grey).

of the upregulated genes were also affected in both comparisons PD.vs.PC (535/885). In addition, I observed a group of genes at the top-right quadrant deviating to the right from the diagonal line (Fig. 28A). Although many of them were significantly changing in both comparisons, their position clearly indicated that the loss of p21 is causing a stronger increase in their expression in senescent cells.

Pathway analysis: SD.vs.SC DEG in PD.vs.PC

To define which programs were controlled by p21 specifically in senescence, I performed pathway analysis on each of these 4 lists. To visualize the obtained results, I generated dotplots representing the enrichment of the most enriched pathways in each sublists (Fig. 29). In order to synthetize the results, I compiled a selection of the most enriched terms in each sublist. Different databases were consulted, and the chosen terms were selected from the combination of databases that allowed the best representation of the observed results in each case. The results of all the sublists of upregulated (in red) and downregulated (in blue) genes in the SD.vs.SC were compared (Fig. 29).

As expected, pathways related to proliferation, such as *Cell Cycle* and *DNA replication*, were significantly enriched in all the subsets of genes upregulated in SD.vs.SC. *DNA repair* showed the same behaviour (Fig. 29A). This enrichment was stronger among the commonly upregulated list, which showed a lower adjusted-pvalue and bigger overlap. In addition, these were the enriched terms detected among the cluster of genes that presented a stronger increase in SD.vs.SC than PD.vs.PC, positioned at the right of diagonal line in Fig. 28A (pathway enrichment not shown).

When I analysed the list of genes specifically upregulated in SD.vs.SC (not significantly changing in PD.vs.PC), I could find some new pathways among the top enriched list: terms related to RNA binding or processing, like *RNA transport*, *adherens junctions* and also the polycomb 2 complex (*ESC/E(Z) complex*). However, the stronger signature was still related to proliferation and DNA damage repair (*Cell Cycle, DNA replication, DNA repair)*.

The strongest enrichment among the lists of downregulated genes (Fig. 29B) after p21 loss belonged to terms associated to adhesion (*Cell-substrate junction, Focal adhesion, extracellular structure organization)*. The vast majority of genes associated to these pathways were found to be downregulated in both comparisons. Interestingly, a decrease in *protein transport* and *secretion* related genes was also detected. Although these signatures were detected among the commonly decreased genes, the biggest overlap was found among the

senescence-specific downregulated list. Additionally, genes related to protein degradation seemed specifically downregulated in senescent cells (*ERAD pathway).* On the other hand, I found that most of the genes associated with a lysosomal signature decreasing in senescence were also downregulated in proliferating cells since the "*lysosome*" signature was only enriched in the commonly downregulated list.

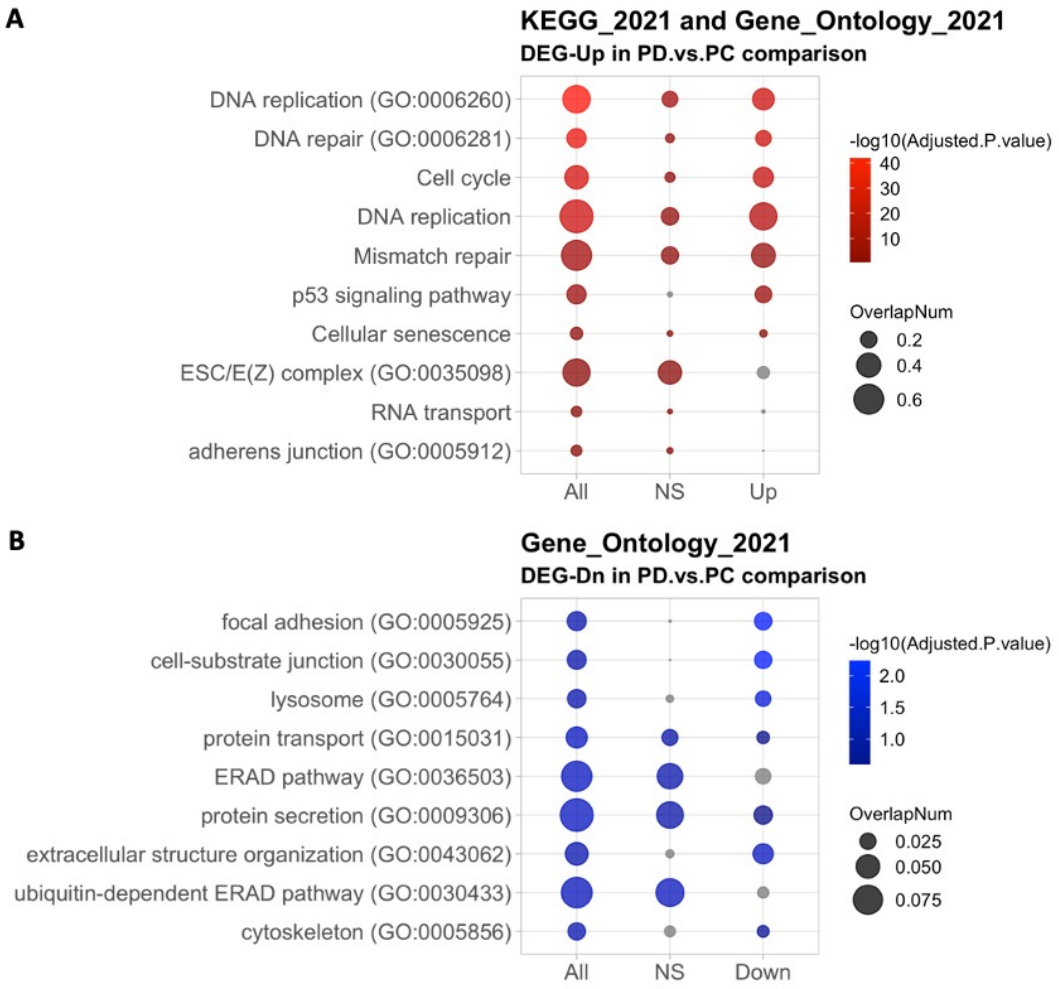

Figure 29. Representative enriched pathways across sublists derived by SD.vs.SC and PD.vs.PC comparisons. Size of the dots corresponding to the fraction of genes of the list overlapping to the term. Color according to adjusted p-value expressed in -log10, from darker to lighter showing increasing statistic significance increases, grey for not significant enrichment (adjusted p-value >0.25). **A)** Selection of top pathways among upregulated genes in SD.vs.SC. From KEGG Human 2021and Gene Ontology 2021 databases. **B)** Selection of top pathways among downregulated genes in SD.vs.SC. From Gene Ontology 2021 databases. (Gene Ontology including Biological Process, Molecular Function and Cellular Component).

Conclusion. SD.vs.SC DEG in PD.vs.PC

Overall, most of the transcriptional changes caused by the knock-down of p21 were shared among both comparisons. In agreement with the literature, p21 loss was associated to an increase in the expression of genes related to proliferation, independently of the context. In

a similar way, the genes downregulated in both comparisons were mainly related to the cellular adhesion to the extracellular matrix[325]. Actually, most of the top enriched terms in the genes affected by p21 loss only in senescence were also significant in the common list.

Notably, the baseline gene expression in the 2 comparisons was very different. Taking this into consideration, the same fold change in expression of a gene in both comparisons could have relatively different weight in each cellular context. This explained the relatively higher increase in proliferation related genes in SD.vs.SC, where many of these genes had been actually repressed during the acquisition of the senescence state. Information about the magnitude of the expression change in each comparison was not proportionally comparable and did not necessarily reflect the actual expression level among all 4 conditions. This was a clear limitation and the interpretation of these results needed to be done with caution. In other words: the specific role of p21 in senescence could not be understood without taking into account the transcriptional context specific to senescent cells.

p21 Knock-Down AND Senescence (SD.vs.SC vs SC.vs.PC)

After gaining insight of how the transcriptional programs affected by p21 loss in senescence were altered in proliferating cells, I realized that in order to understand which functions are controlled by p21 specifically in senescent cells, I needed to understand how these functions were altered in senescence (Fig. 30).

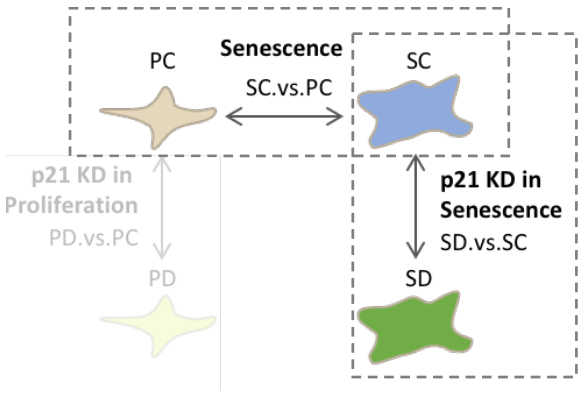

Figure 30. Comparison of comparisons: p21 knock-down in senescence and senescence acquisition. Comparison of the transcriptional changes associated to p21 loss in senescent cells (SD.vs.SC) and those due to the induction of senescence (SC.vs.PC).

Gene classification: SD.vs.SC DEG in SC.vs.PC

To picture how the genes altered by p21 downregulation in senescence were affected by the acquisition of senescence, I plotted the transcriptional changes suffered by each gene in the

acquisition of senescence in the y axis (SC.vs.PC) and upon p21 knock-down in senescent cells in the x axis (SD.vs.SC) (Fig. 31A and Supp. Fig. 2).

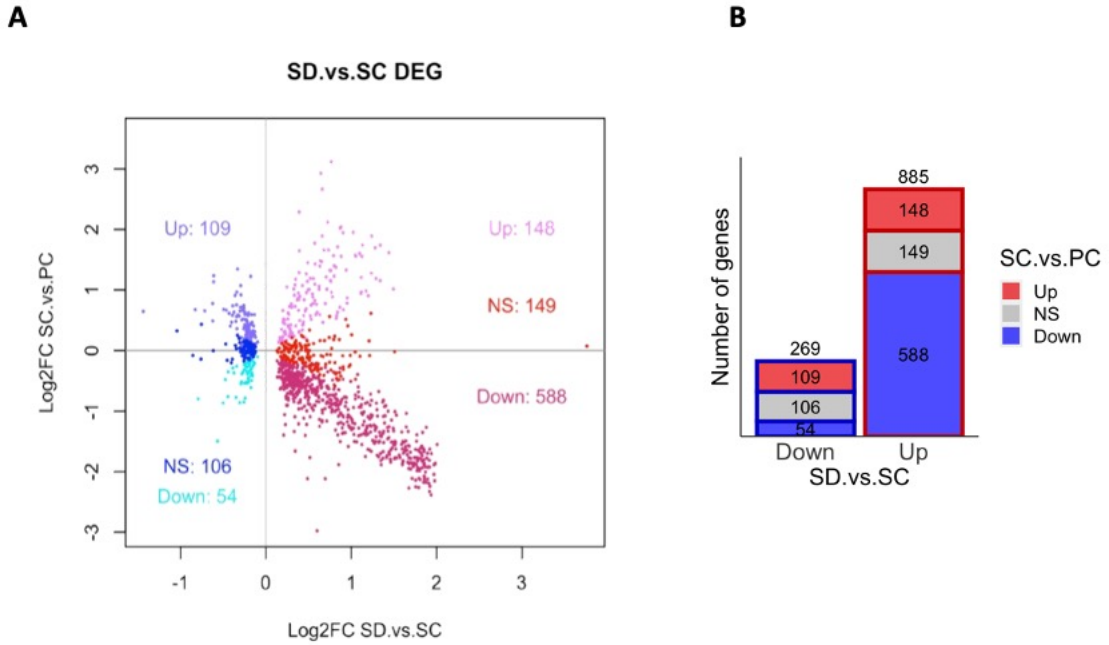

Figure 31. DEG in SD.vs.SC in the SC.vs.PC comparison. All the DEG in the SD.vs.SC comparison were subdivided depending on their expression behavior in the SC.vs.PC comparison. **A)** Scatter plot of expression change in both comparisons. All DEG in the SD.vs.SC comparison in a 2-d scatter plot. Each gene was represented by a dot, its location being determined by the expression change in both comparisons expressed as log2 fold change. The x axis corresponding to the SD.vs.SC comparison, and the y axis to SC.vs.PC. A color code was used to identify the significance and direction of transcriptional change, label indicating behavior in the SC.vs.PC comparison (NS: not significant). **B)** Bargraph quantifying the number of genes in each subgroup. Left bar with blue border for downregulated, and right bar with red border for upregulated genes in SD.vs.SC comparison. Fill color of the bar corresponding to the SC.vs.PC comparison (upregulated in red, downregulated in blue, NS: not significant in grey).

The classification of the DEG in the SD.vs.SC according to their behavior in the *senescence* comparison (SC.vs.PC) suggested that the loss of p21 in senescent cells caused a transcriptional reversion of the senescent signature: more than 66% (588/885) of upregulated genes in SD.vs.SC were downregulated in senescent cells, and more than 40% (109/269) of downregulated genes in SD.vs.SC increased in senescent cells (Fig. 31B). Since p21 is an important inductor and mediator of senescence this was not totally unexpected. In fact, we anticipated that the analysis of these genes would reveal the senescence-associated phenotypes the acquisition of which was directly mediated by p21 expression (Fig. 32 and 33). On the other hand, I found 445 differentially expressed genes whose transcription upon p21 downregulation (SD.vs.SC) did not show a reversed tendency to that presented due to the acquisition of senescence (SC.vs.PC). 255 of them were significantly changed by p21 loss in senescence (SD.vs.SC) (106 down and 149 upregulated) but were not changed significantly

upon senescence establishment (SC.vs.PC). Interestingly, the remaining 202 were following the same direction in both comparisons, with 54 genes decreasing and 148 increasing by both, senescence establishment and p21 knock-down in senescent cells. This suggested that the loss of p21 in senescence cells could be reinforcing some of the transcriptional changes associated to the senescence response.

Pathway analysis: SD.vs.SC DEG in SC.vs.PC

To understand the contribution of each of these groups of genes to the transcriptional programs controlled by p21 in senescence I performed pathway analysis on the 6 lists just described. Then, I compared the enrichment of different pathways among all the lists containing the genes upregulated or downregulated after p21 decrease separately. This result was summarized in Fig. 32, where the most representative terms were selected using different databases.

First, I analyzed the pathways associated to the genes downregulated upon p21 knock-down (Fig. 32A). When all downregulated genes were analyzed together, cell adhesion was the most consistent signature found among all databases. Although related genes were present in the 3 lists, pathways associated to cell adhesion were specifically enriched among the genes whose expression was also decreasing upon the induction of senescence (SC.vs.PC). In this list, I also found an enrichment of ribosome encoding genes. In line with this, many terms related to proteins, such as *Protein secretion*, *Protein transport* and *ERAD pathway* (Endoplasmic-reticulum-associated protein degradation), were observed. This suggested that p21 loss may affect the level and localization of proteins in senescent cells. Interestingly, I observed that the term *Peroxisome* was enriched among the genes upregulated by the induction of senescence. Peroxisomal function had been described to be altered in aged cells, but the contribution to peroxisomal defects to the senescence response remained underexplored

Then, I focused on the analysis of the pathways associated to the transcriptional increase upon p21 loss (Fig. 32B). As expected, the detection of the top enriched pathways was explained by its enrichment in the cluster of genes that were downregulated by the induction of senescence. Among these pathways, many terms related to proliferation were found, such as *Cell cycle* an *DNA replication*, but also related to DNA damage, like *Mismatch repair*. Actually, a deep contrast among the lists was observed. While many pathways were strongly enriched in the list of genes downregulated in senescence, very few terms showed a significant enrichment in the other lists, and even these ones presented obvious higher

adjusted p-values (and smaller overlaps). This was a clear indication of the loss of statistical power caused by the compartmentalization of genes in small groups. However, I still detected some interesting pathways enriched in the list of genes that were also upregulated in senescence. Specifically, terms related to Notch signaling and Interferon response caught my attention (*Signaling by NOTCH2*, *Type I interferon pathway,* BioPlanet database). Finally, p21 loss caused an increase in the expression of genes associated to *p53 signaling* in all lists, which was significant in most of them. This was not unexpected, since p21 is a known to mediate the action of p53-dependent repressing complexes[353,354,448,449].

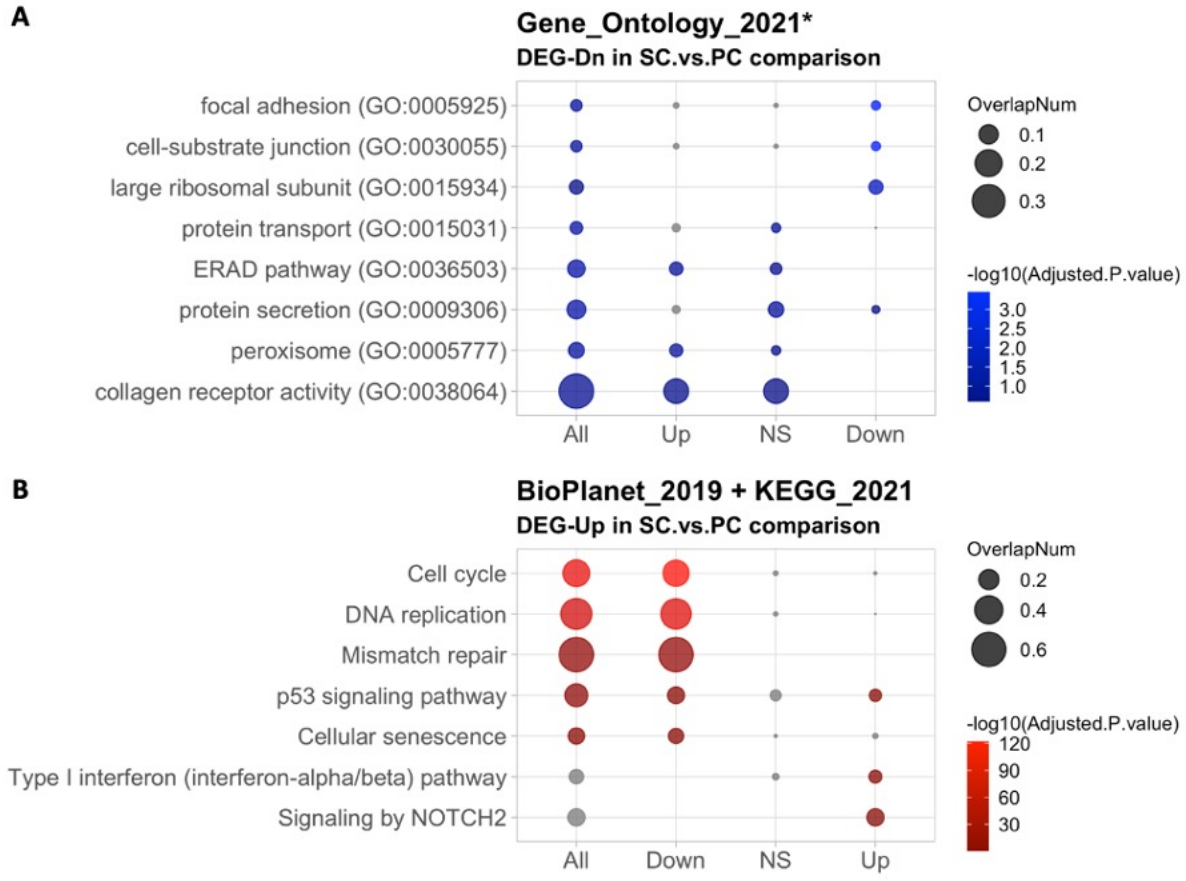

Figure 32. Representative enriched pathways across sublists derived by SD.vs.SC and SC.vs.PC comparisons. Size of the dots corresponding to the fraction of genes of the list overlapping to the term. Color according to adjusted p-value expressed in -log10, from darker to lighter showing increasing statistic significance increases, grey for not significant enrichment (adjusted p-value >0.25). **A)** Selection of top pathways among downregulated genes in SD.vs.SC. From Gene Ontology databases. (Gene Ontology 2021 including Biological Process, Molecular Function and Cellular Component, and "peroxisme" from Cellular Component 2018 version). **B)** Selection of top pathways among upregulated genes in SD.vs.SC. From BioPlanet 2019 and KEGG Human 2021 databases.

Pathway exploration: p21 loss and senescence reversion

The comparison of the enrichment of the top terms detected in the sublists of the differentially expressed genes upon p21 knock-down in senescence was used to provide an unbiased description of the transcriptional programs associated to specific genes. The terms depicted in Fig. 32A and 32B intended to be a fair representation of the signatures observed across all the databases analyzed. Thus, they were selected from the 10 most significantly enriched in each list, and they belonged to the minimum number of databases that allowed the best exemplification. However, I wondered if a deeper exploration of the results could help me unravel less obvious functions controlled by p21 in senescence.

p21-mediated senescence response: transcriptional reversion

First, I focused on the part of the senescent transcriptional signature reversed by p21 loss (Fig. 33). Most of the genes whose expression was affected by p21 downregulation in senescent cells (SD.vs.SC) seemed to revert the transcriptional changes produced by the acquisition of senescence (SC.vs.PC). A deeper analysis of the functions associated to these genes could reveal novel functions directly controlled by the increased levels of p21 during the induction of senescence.

In Fig. 33A I portrayed the main functions related to a transcriptional increase in senescence and downregulated after p21 knock down. I found very few pathways significantly enriched in most of the databases analyzed (not shown), and the adjusted p-value of the ones detected was relatively high. Although the interpretation of these terms was not obvious, they seemed to be mainly related to the processing of misfolded proteins, lysosomes and lytic functions and microtubule binding. It is worth noticing that, as previously mentioned, the term *peroxisome* was significantly enriched (Gene Ontology 2018 version, Cellular Component).

Figure 33B showed some of the significantly enriched terms from the genes upregulated in SD.vs.SC and downregulated in senescence (SC.vs.PC). As already described, a proliferative signature could be inferred by the presence of terms related to cell cycle and DNA metabolism, bult also by changes in the cytoskeleton related to cytokinesis and chromosome segregation. Terms related to DNA damage response often appeared, such as *DNA repair* and *damaged DNA binding*. I also detected many terms affecting gene expression, like histone and DNA modifications, nuclear transport and RNA processing and transport. Interestingly, I noticed some pathways related to immune cells that, although having a high adjusted p-value, were significantly enriched (*natural killer cell mediated cytotoxicity*, *natural killer cell lectin-*

like receptor binding. Not in Fig. 33B: *natural killer cell mediated immunity* and *granulocyte differentiation*, adjusted p-value ranging from 0.098 to 0.154).

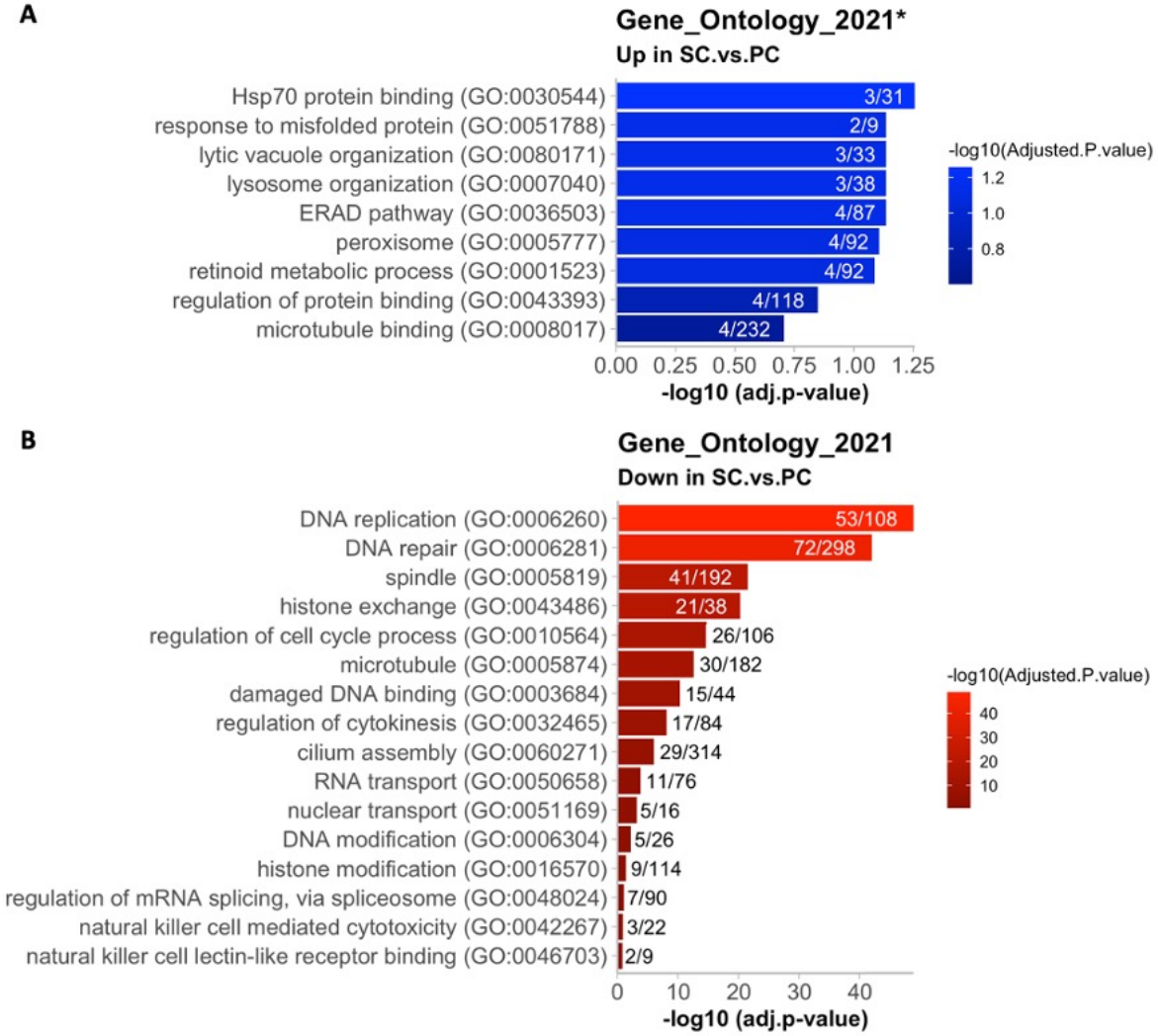

Figure 33. Pathways of senescence reversal by p21 knock-down. Selection of the most representative and interesting terms significantly enriched in each list. Enrichment represented by adjusted p-value, expressed as -log10, determining bar length and color (the lightest the more significant, not significant in grey). Overlap of genes in the term present in the list depicted as a fraction in each bar. Significancy threshold: adjusted p-value <0.25. **A)** Terms associated to downregulated (blue) genes in SD.vs.SC and upregulated in SC.vs.PC. From Gene Ontology databases (2021 version of Biological Process, Molecular Function and Cellular Component, and 2019 version of Cellular Component 2019 for "peroxisome"). **B)** Terms associated to upregulated (red) genes in SD.vs.SC and downregulated in SC.vs.PC. From Gene Ontology 2021 databases (Biological Process, Molecular Function and Cellular Component).

Alternative role of p21-mediated senescence response: not transcriptional reversion

The fact that some genes affected by p21 loss in senescence seemed not to revert the transcriptional changes induced by senescence acquisition suggested that p21 may have an effect on senescent cells different from the mediation of the acquisition of a senescent phenotype. Therefore, I was interested in which functions could be related to the

differentially expressed genes in SD.vs.SC that were not portraying a reversion of how they changed in senescence, so I performed pathway analysis on them (Fig. 34). Once again, upregulated and downregulated genes were analyzed separately.

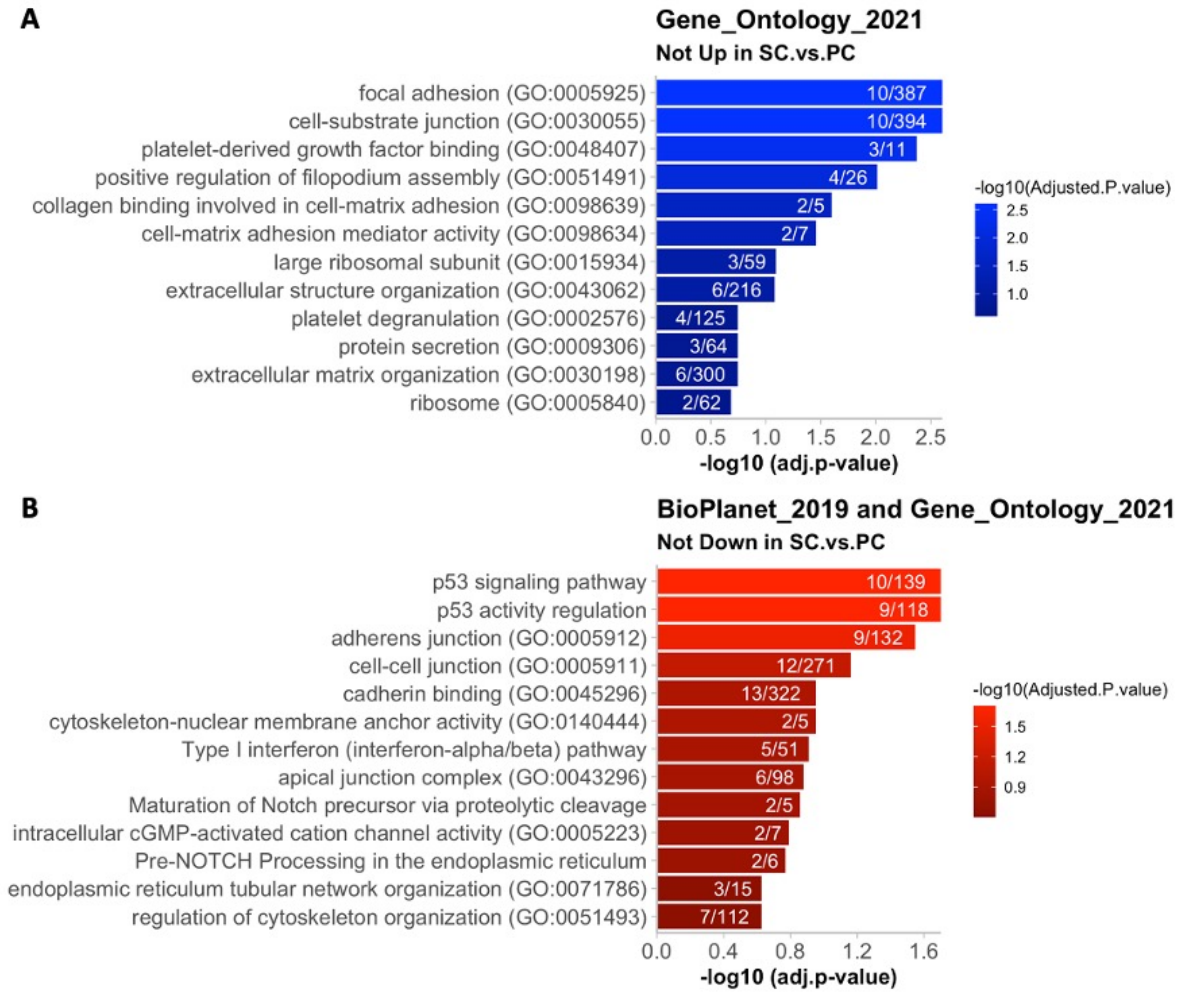

Figure 34. Pathways not reversing senescence affected by p21 knock-down. Selection of the most representative and interesting terms significantly enriched in each list. Enrichment represented by adjusted p-value, expressed as -log10, determining bar length and color (the lighter the more significant, not significant in grey). Overlap of genes in the term present in the list depicted as a fraction in each bar. Significance threshold: adjusted p-value <0.25. **A)** Terms associated to downregulated (blue) genes in SD.vs.SC that were not upregulated in SC.vs.PC. From Gene Ontology 2021 databases. **B)** Terms associated to upregulated (red) genes in SD.vs.SC that were not downregulated in SC.vs.PC. From BioPlanet 2019 and Gene Ontology 2021 databases (Gene Ontology including Biological Process, Molecular Function and Cellular Component).

Since the splitting of the genes in small groups caused the loss of statistical power, I decided to combine the lists of differentially expressed genes in SD.vs.SC that were either not affected or changing in the same direction upon senescence establishment (SC.vs.PC). Even so, there was a small number of genes overlapping with their corresponding significantly enriched

term. A combination of the most representative and interesting terms significantly enriched in each comparison was displayed in Fig. 34A and Fig. 34B.

The downregulated genes upon p21 loss in senescence (SD.vs.SC) which were not upregulated in senescence (SC.vs.PC) (Fig. 34A) showed a clear enrichment of pathways related to cell adhesion (*focal adhesion* and *cell-substrate junction*) and extracellular matrix organization. Again, the result suggested that p21 loss could decrease the expression of genes involved in protein metabolism, since terms like *protein secretion* and *ribosome* were detected.

On the other hand, several databases showed *p53 signaling* as the most enriched pathways in the upregulated in SD.vs.SC that were not downregulated on SC.vs.PC (Fig. 34B). Apart from this one, the only other transcriptional signature that appeared to be consistent among all the significant pathways was related to the upregulation of molecules involved in cell binding, as terms like *adherens junction*, *cell-cell junction*, *cadherin binding* and *apical junction complex* suggested. In addition, the cytoskeleton and Notch processing also seemed to be affected. Interestingly, the term *Type I interferon (interferon alpha/beta) pathway* was significantly enriched in the BioPlanet database, suggesting that p21 loss could increase the expression of the interferon response.

Conclusion: SD.vs.SC DEG in SC.vs.PC

By using this approach, I was able to distinguish the role of p21 in mediating the establishment of senescence from other ways in which its loss affected senescent cells. The increase of p21 upon the induction of senescence was associated to a transcriptional repression, mainly of genes mainly related to proliferation. Actually, this was the main contribution of p21 to senescence described in the literature[351,353,448,450]. In addition, I also observed other interesting functions potentially repressed by p21, like the transport and processing of RNA or the expression of natural killers related genes. Interestingly, p21 also seemed to promote the transcription of peroxisomal genes in senescence, whose expression was decreased after the knock-down.

I also explored transcriptional signatures controlled by p21 that were not directly associated to the acquisition of the senescent phenotype. For example, many genes related to cellular adhesion were downregulated when p21 was lost, despite not being upregulated when p21 expression increased in senescence. On the other hand, the interpretation of the pathways enriched by genes upregulated upon p21 knock-down that were not repressed by senescence

was less obvious. In this context, *p53 signaling* was the term that most consistently appeared across all databases. Some pathways related to Notch processing and the interferon response caught my attention too. I found them interesting due to their connection to SASP production and interaction with the immune system, key hallmarks of senescence[60]. Also linked to immunity, Natural Killer related pathways were found significantly enriched among the genes potentially repressed by p21 in senescence (up in SD.vs.SC, down in SC.vs.PC).

Finally, it was interesting to notice that several terms related to cell binding were enriched in lists generated from genes changing in both directions; although most of them were significant among downregulated genes, others like *adherens junctions* or *cadherin binding* were upregulated. This suggested that p21 expression could play a role in remodeling the environment of senescent cells, probably affecting the membrane proteins exposed and secreted, and even the extracellular matrix.

Conclusion - Comparison of comparisons

By separating the DEG in SD.vs.SC in different groups depending on their transcriptional behavior in the other comparisons, I aimed to isolate the predominant pathways masking less enriched signatures. This approach allowed the exploration of other functions controlled by p21 in senescent cells. It revealed the potential effect of p21 in adhesion, protein processing, translation, peroxisomes and the immune system among other functions. However, it was clear that the compartmentalization of genes in subgroups was accompanied by the loss of statistical power. Relatively high adjusted p-values and low overlaps in the significantly enriched terms of these sublists were a clear indication. It was concluded that this analysis was not sufficient to unravel novel functions controlled by p21 in senescent cells.

2. 4 Role of p21 in senescence: Physiological interpretation

My previous analysis suggested novel pathways potentially affected by p21 in senescent cells. However, the dissection of genes in different subsets in the comparison of comparisons caused a loss of statistical power and introduced biases related to the fragmentation of functionally related genes in different groups artificially.

I realized that, although we could describe functions controlled by p21, I was not able to understand how these changes affected senescent cells. In order to explore this, I classified genes in 18 groups based on the transcription changes experienced in 3 comparisons: senescence (SC.vs.PC), p21 knock-down in senescence (SD.vs.SC) and p21-defficient senescence (SD.vs.PC) (Fig. 35). The addition of this last comparison gave me information on the differences between p21-defficient senescent and proliferating cells. Afterall, in a physiological situation, the relevance of p21 should be measured by its impact on the phenotypes expressed by senescent cells when compared to healthy proliferating ones.

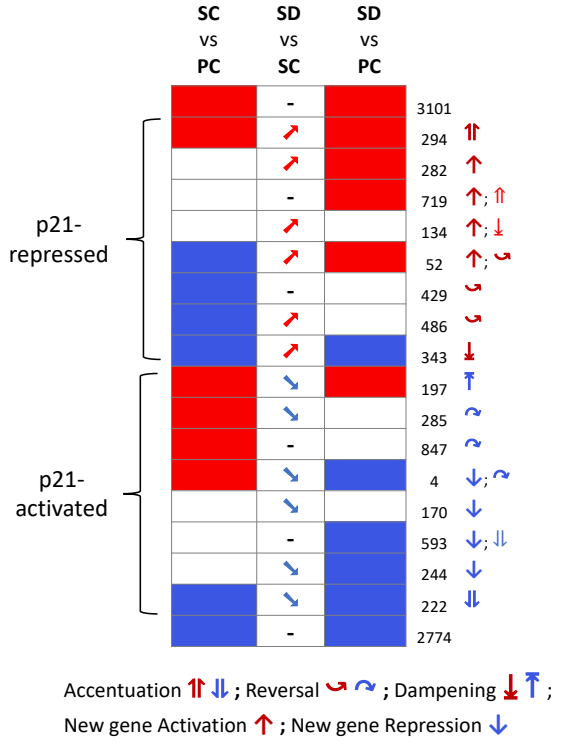

Figure 35. Gene classification based in the effect of p21 knock-down in the senescent signature. Genes were grouped in different categories depending on their transcriptional change in the 3comparisons evaluated. In this order: SC.vs.PC (senescence), SD.vs.SC (p21 KD in senescence) and SD.vs.PC (p21-deficient senescent compared to proliferating cells). While side columns are represented as colored cells, arrows were used to picture changes in the middle comparison (SD.sc.SC). Only significantly changing genes were colored; upregulated in red, downregulated in blue (p-value <0.05). Next to each row: number of genes of each category, sign of the transcriptional effect of p21 loss relative to the changes associated to the senescence response (bottom legend).

In general, genes could be categorized in 2 groups: activated or repressed by p21 in senescent cells (Fig. 35, left-side labels). The activated genes showed a decrease in expression linked to p21 loss, while repressed genes were upregulated. This tendency could be directly observed in the SD.vs.SC comparison, or inferred by the difference in expression between control and p21-deficient senescent cells in comparison to proliferating (SC.vs.PC and SD.vs.PC).

Regarding the contribution of p21 to senescence, I observed that the knock-down of p21 in senescent cells had different effects on the senescent response. Although for some genes the loss of p21 reversed or dampened the transcriptional changes linked to the induction of senescence, in other cases it actually accentuated them. However, other genes were not affected by senescence but only by p21 decrease. The categories *New activation* and *New repression* were assigned to the groups of genes whose expression was up or downregulated by p21 loss but were insensitive to senescence acquisition, highlighting other roles of p21 in senescent cells besides the mediation of the senescent response.

Looking at the different effects that p21 had over the transcriptional signature of senescent cells, I wondered which of these categories were meaningful for us. To understand what was really happening to senescent cells when p21 was downregulated, a physiological interpretation of our data was required. The function of p21 mediating the canonical features of senescence had been already vastly explored in the field, so I decided to focus on its contribution to other aspects of the senescent phenotype. This analysis aimed to unravel the functions controlled by p21 that relevantly affect the phenotype of senescent cells.

Methodological reasoning: physiologically relevant effect of p21 loss in senescence

To determine the transcriptional changes due to p21 loss in senescence that could have a physiological relevance on the phenotype of senescent cells, I was interested in the genes that were significantly affected in p21-deficient senescent cells in comparison to control proliferating cultures whose transcriptional change was determined by the knock-down of p21 in senescence. For this, three comparisons were evaluated (Tab. 2, Fig. 36A and 38A.). First, I was interested on the phenotype of senescent cells lacking p21 when compared to normal, proliferating controls, reflected by the SD.vs.PC comparison. The specific impact of p21 loss had in senescence was revealed by the comparison SD.vs.SC. To be sure that the contribution of p21 was specifically relevant in the context of senescence, senescent and proliferating cells lacking p21 were compared (SD.vs.PD). Only differentially expressed genes

whose change was determined by p21 downregulation in senescence (SD.vs.SC, changing in the same direction in both comparisons) were included. In this way, genes whose expression change was primarily determined by the knock-down of p21 (and that were equally affected by it in senescent and proliferating cells) should be discarded. Transcriptional changes in each comparison were considered relevant based on p-value, with the significance threshold at p-value < 0.05. To be strict in order to perform pathway analysis, I decided to filter significant genes by the adjusted p-value of the most meaningful comparison, SD.vs.PC. Then, the activated and repressed genes by p21 in senescence were analyzed by pathway analysis, and a selection of the most representative and interesting associated functions from different databases was represented in form of bar graphs.

Comparison	Meaning
SD vs PC	Physiological impact of p21 loss in senescence: phenotype of senescent cells lacking p21 when compared to normal proliferating controls.
SD vs SC	Genes affected by p21-loss in senescence. The knock-down of p21 determines the changes in the comparison above (SD.vs.PC).
SD vs PD	Different expression only if expression level was not solely determined by p21-loss. Comparison is determined by the expression changes due to the knock-down of p21 in senescence (SD.vs.SC).

Table 2. Transcriptional impact of p21-knock-down in the senescent phenotype. The expression changes in three different comparisons were analyze to define the transcriptional effect of p21 loss in senescence that reflected its physiological impact on the senescent phenotype. Each comparison provided different information on p21's control of transcription (Meaning). Only genes that were significantly affected in the same direction (up or downregulated) in the three comparisons were considered. Significancy was evaluated by p-value (<0.05), and additionally filter by adjusted p-value (<0.05) in the main comparison, SD.vs.PC. Abbreviations: SC: senescent control; SD: p21-knock-down in senescence; PC: proliferating control; PD: p21-knock-down in proliferating cells.

Activated by p21 in senescence

The genes potentially activated by p21 specifically in senescence were selected based on their transcriptional tendency in all the comparisons considered. Since it was assumed that p21 expression was directly or indirectly contributing to their expression in senescent cells, they were downregulated upon p21 knock-down (SD.vs.SC). This decrease contributed to the observed downregulation of the genes that senescent cells lacking p21 presented when compared to proliferating controls (SD.vs.PC). Moreover, the role of p21 was especially relevant in senescent cells, since these genes were also less expressed in senescent than in proliferating cells where p21 expression had been dampened (SD.vs.PD) (Fig. 36A). These criteria were fulfilled by a total of 286 genes (Fig. 36B). A representation of their expression in all samples is depicted in the heatmap of Fig. 36C.

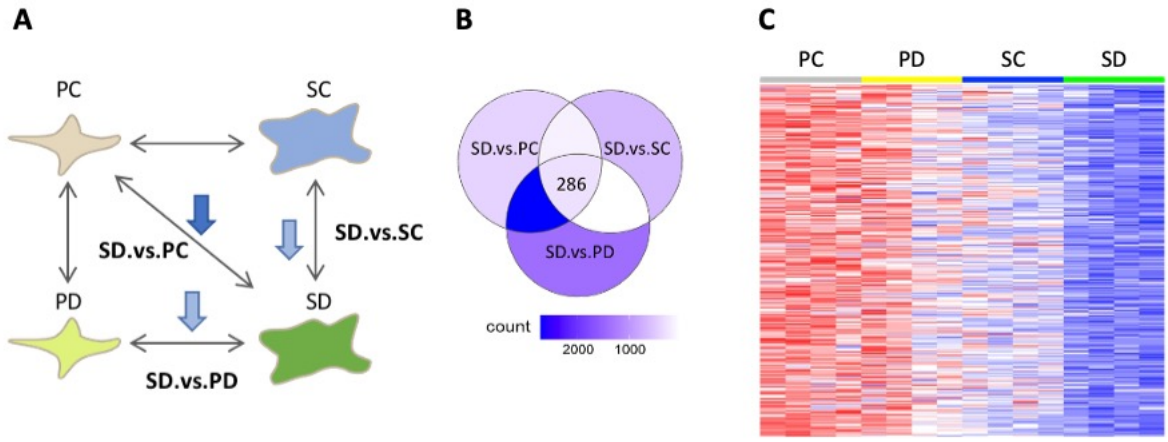

Figure 36. Genes activated by p21 in senescence. A) Transcriptional tendency of each gene in the 3 evaluated comparisons. Genes whose expression was downregulated in SD.vs.SC, SD.vs.PD (p-value <0.05) and SD.vs.PC (adjusted p-value <0.05) were selected. **B)** Venn diagram of activated genes resulting from the overlap of the 3 conditions evaluated. The intensity of the color of each overlap corresponds to the number of genes included. **C)** Heatmap of the expression (normalized reads) of the 286 genes activated by p21 in senescence. 16 columns corresponding to individual samples, grouped by condition. One row per gene. Color range was scaled per row, from low in blue to high expression in red.

The pathway analysis of the genes whose transcription was favored by p21 in senescence cells was used to identify the phenotypical changes that p21 loss may cause in senescent cells. To illustrate them, the enrichment of selected terms from different databases were represented as a bar graph in Fig. 37. In this case, term reiteration was avoided. The most consistent signature downregulated by p21 knock-down in senescence affected protein level and function, including translation and protein localization, degradation and modification related terms. Other affected functions were cell adhesion and autophagy, as well as mitochondrial coding genes.

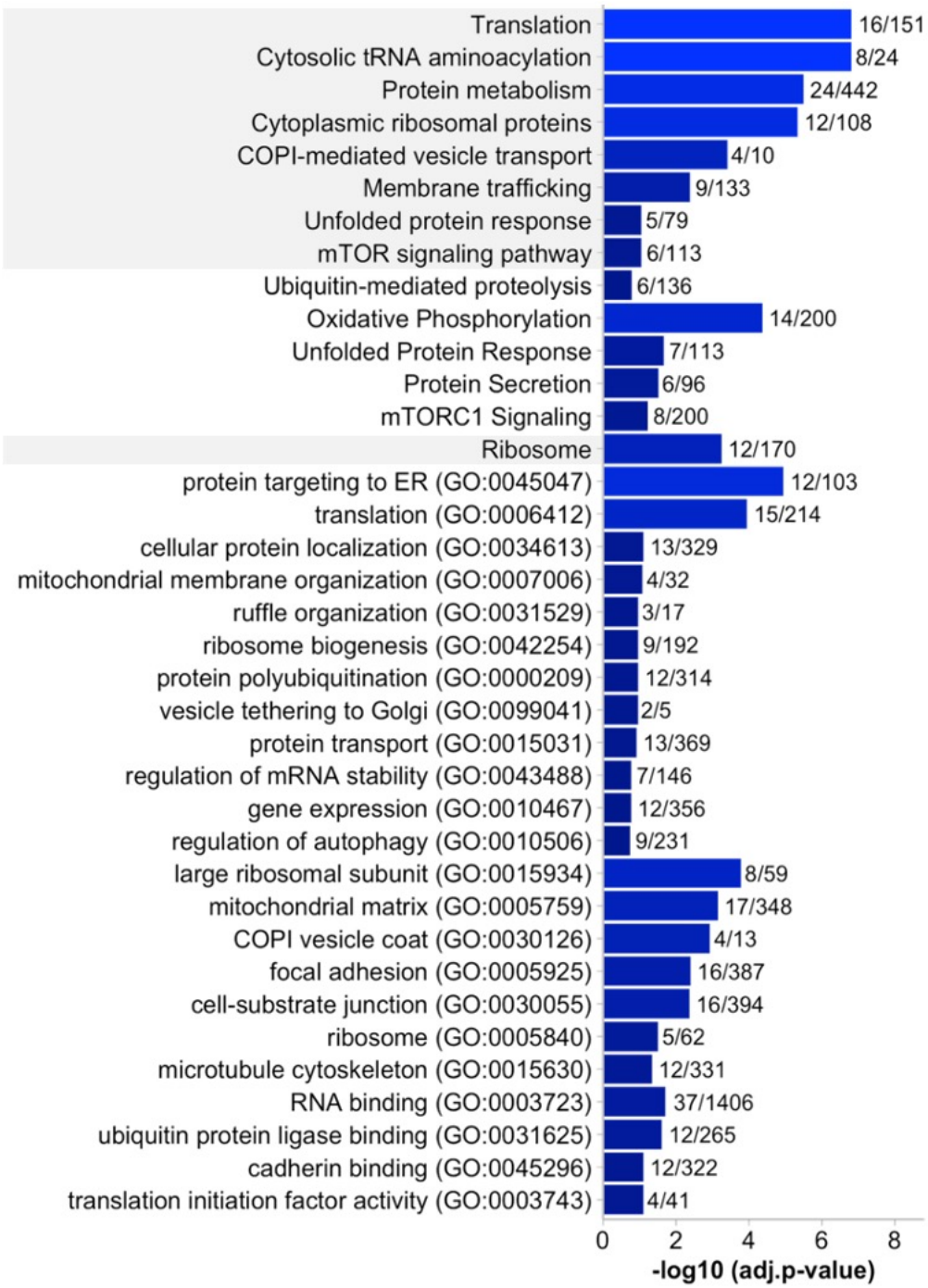

Figure 37. Pathway analysis of genes activated by p21 in senescence. Selected terms grouped by database; groups defined by background color of the pathway name. Databases by order: BioPlanet 2019, Hallmark 2020, KEGG Mouse 2019, and Gene Ontology 2021 (Biological Process, Cellular Component and Molecular Function). Term reiteration from different databases was avoided. Significancy: adjusted p-value < 0.25. Length and color of the bars corresponding to the adjusted p-value, the more significant the lighter. Overlap between list and term showed as a fraction of the number of genes in the list divided by the total genes of the term.

Repressed by p21 in senescence

As in the last comparison, the genes potentially repressed by p21 specifically in senescence were identified by their transcriptional tendency in the same comparisons. In this case, p21 acted as a repressor; these genes were upregulated when p21 was reduced in senescent cells (SD.vs.SC). This upregulation was contributing to the increase in expression that they presented in senescent cells lacking p21 when compared to proliferating controls (SD.vs.PC). Additionally, the role of p21 was especially relevant in senescent cells: the lack of p21 caused a significantly stronger expression of these genes in the senescence context compared to a proliferative situation (SD.vs.PD) Fig. 38A. A total of 388 genes followed these criteria Fig. 38B. A representation of their expression in all samples is depicted in the heatmap of Fig. 38C.

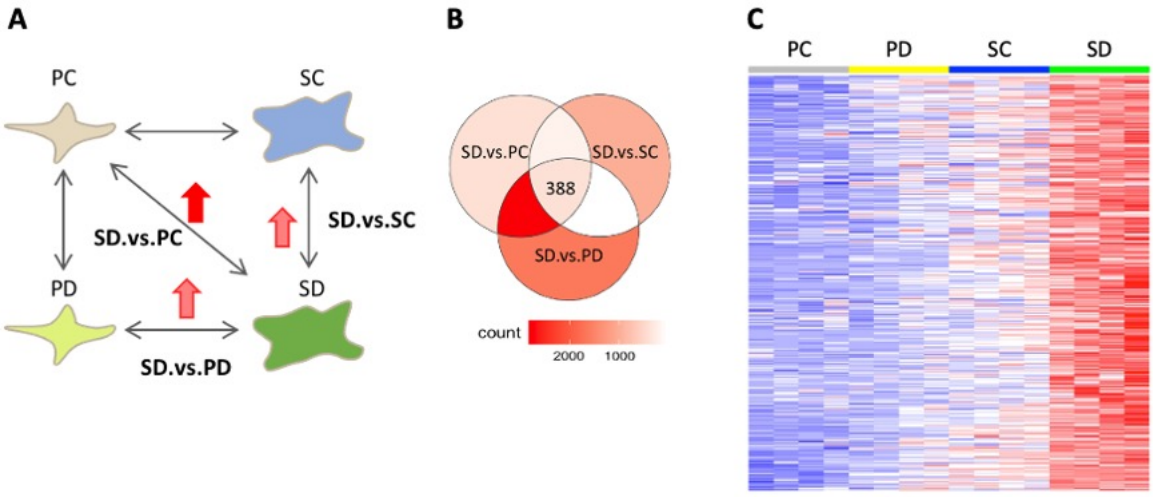

Figure 38. Genes repressed by p21 in senescence. **A)** Transcriptional tendency of each gene in the 3 evaluated comparisons. Genes whose expression increased in SD.vs.SC, SD.vs.PD (p-value <0.05) and SD.vs.PC (adjusted p-value <0.05) were selected. **B)** Venn diagram of repressed genes resulting from the overlap of the 3 conditions evaluated. The intensity of the color of each overlap corresponds to the number of genes included. **C)** Heatmap of the expression (normalized reads) of the 388 genes repressed by p21 in senescence. 16 columns corresponding to individual samples, grouped by condition. One row per gene. Color range was scaled per row, from low in blue to high expression in red.

The signatures enriched in the pathway analysis of the genes repressed by p21 specifically in senescence corresponded to the functions upregulated by the lack of p21 in senescent cells (Fig. 39). I detected very few terms significantly enriched across all the evaluated databases, so the reiteration of terms was favored when selecting the interesting terms to represent in Fig. 39. Interestingly, most of these terms consistently matched to the same signatures. Apart from p53 signaling, there was a clear enrichment in TNF-alpha, Interferon response, Inflammation and other immune related functions, like specific and general cytokine production. I decided to include terms related to natural killers and T-cells that were present,

although its enrichment was not significant. Similarly, many pathways related to cell adhesion, cytoskeletal reorganization and cell junctions depicted were close to significance.

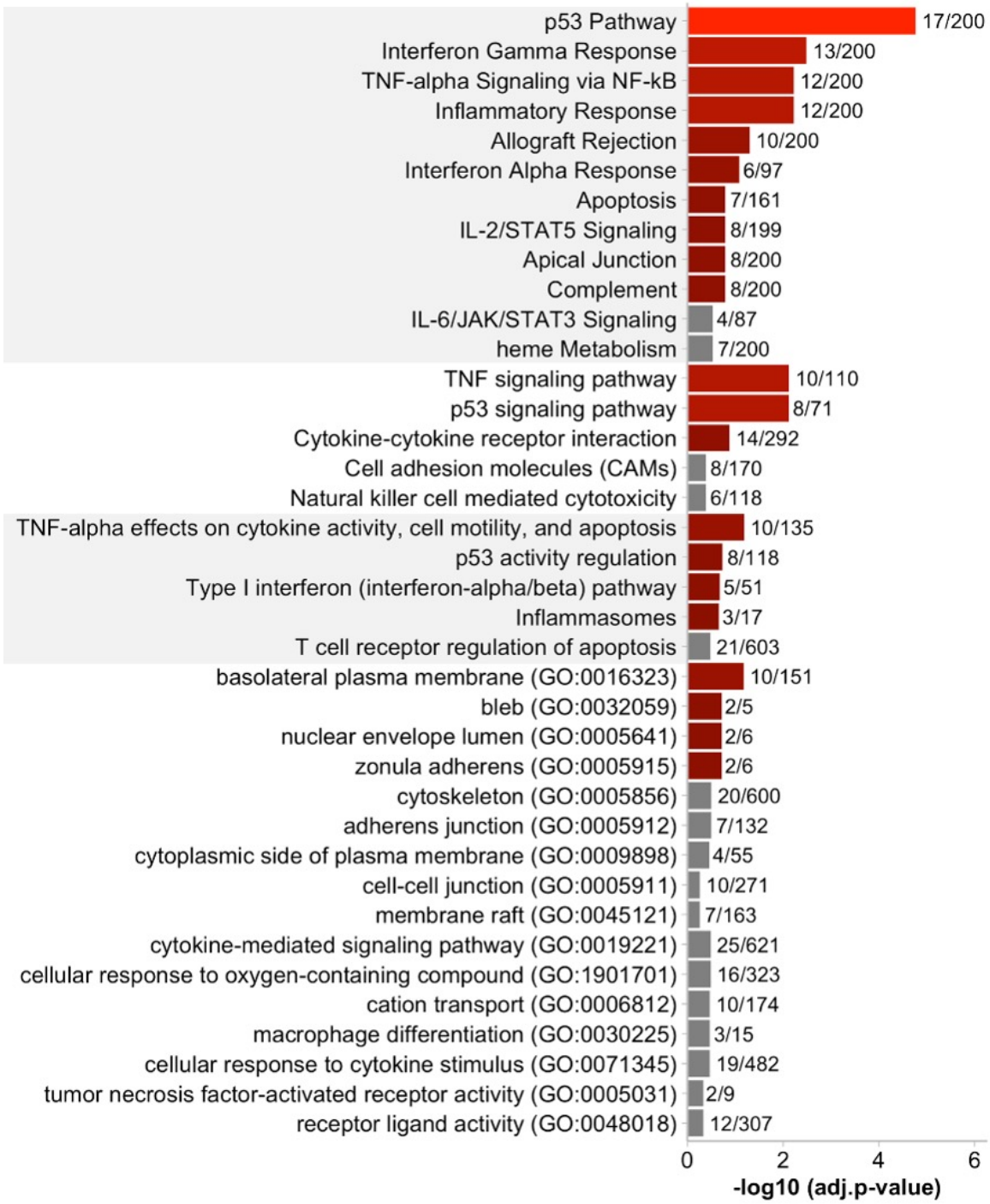

Figure 39. Pathway analysis of genes repressed by p21 in senescence. Selected terms grouped by database; groups defined by background color of the pathway name. Databases by order: Hallmark 2020, KEGG Mouse 2019, BioPlanet 2019 and Gene Ontology 2021 (Biological Process, Cellular Component and Molecular Function). Very few significant terms per database, term reiteration from different databases was favored. Significance: adjusted p-value < 0.25. Length and color of the bars corresponding to the adjusted p-value, the more significant the lighter. Overlap between list and term showed as a fraction of the number of genes in the list divided by the total genes of the term.

These terms often appear in Gene Ontology databases, which comprised especially low adjusted p-values in general for this comparison.

2. 5 Specific functions regulated by p21 in senescence - Heatmaps

The previous analysis gave us insight on the impact of p21 loss in senescence suggesting many transcriptional programs to be regulated by p21. To proceed with my analysis, I decided to take a closer look at the ones that seemed most interesting and relevant to us.

To see how the genes related to specific processes were regulated in senescence and how p21 loss affected them, I represented their expression in heatmaps. This kind of graph served to visualize the expression level of each gene in our samples and their fold change (in log2 fold change) across the different comparisons considered in previous analysis: senescence (SC.vs.PC), p21 knock-down in senescence (SD.vsSC), senescent cells without p21 in comparison to control proliferating cells (SD.vs.PC) and p21 knock-down in proliferation (PD.vs.PC). Genes were considered to be affected by p21 in senescence following the criteria of Fig. 35: when their expression was significantly changing in the SD.vs.SC comparison, or when their significance or the direction of their expression change was different in SC.vs.PC and in SD.vs.PC (significant: p-value <0.05). Taken together, these comparisons helped in the understanding of how different sets of genes related to specific functions were regulated by p21 in senescent cultures.

p53 induced transcriptional repression: the DREAM complex

Pathway analysis on several lists of genes showing an increased expression upon p21 loss in senescence revealed that many of them were known p53 targets (Fig. 26, 29, 32, 39). As described in the introduction, p21 is both a target of p53 and a mediator of its transcription repression function. Most of the p53-repressed targets are silenced by repressor complexes. One of the most important of these complexes is DREAM. As detailed in the introduction (see *Introduction::p21-Cdkn1a::Cellular functions regulated by p21:: Cell cycle*) , p21 expression favors the formation of the DREAM complex[353,354]. In senescence, the formation of the DREAM complex is responsible for the silencing of many genes necessary for cell cycle progression and proliferation. Therefore, it was expected that the p21 down-regulation would reduce the formation of this complex, consequently leading to an increased expression of its targets.

To validate that this was the case in our model, that an important part of the transcriptional signature upregulated upon p21 loss was controlled by the DREAM complex, I explored the behavior of these genes in our data. I selected a set of 1008 human genes that were reported to be targets of DREAM by Fischer et al. in 2016[449]. From the list of 991 mouse orthologs that

I created, 959 could be found in our RNA-seq data. Their expression was represented in the heatmaps of Fig. 40.

As predicted, 643 out of the 959 DREAM targets present in our RNA-seq showed a significant downregulation upon the induction of senescence (SC.vs.PC). This seemed highly dependent on p21 levels, since its reduction led to the de-repression of 446 of them (SD.vs.SC), and only 313 showed a significant reduction in SD.vs.PC. Although p21 loss upregulated a similar number of DREAM targets in proliferating and senescent cells (420 in PD.vs.PC, 484 in SD.vs.SC), many of which were altered in both conditions (359), the magnitude of the increase was, in general, higher in the senescent context.

This confirmation of the role of p21 in the damage induced p53-p21-DREAM repressive axis further validated the effective reduction of p21 protein at the functional level in the p21 knock-down condition. Moreover, it was described that most of DREAM targets are cell cycle related genes. The mediation of DREAM action by p21 provided the mechanistic explanation of the strong proliferative transcriptional signature detected among the upregulated genes upon p21 knock-down (SD.vs.SC and PD.vs.PC).

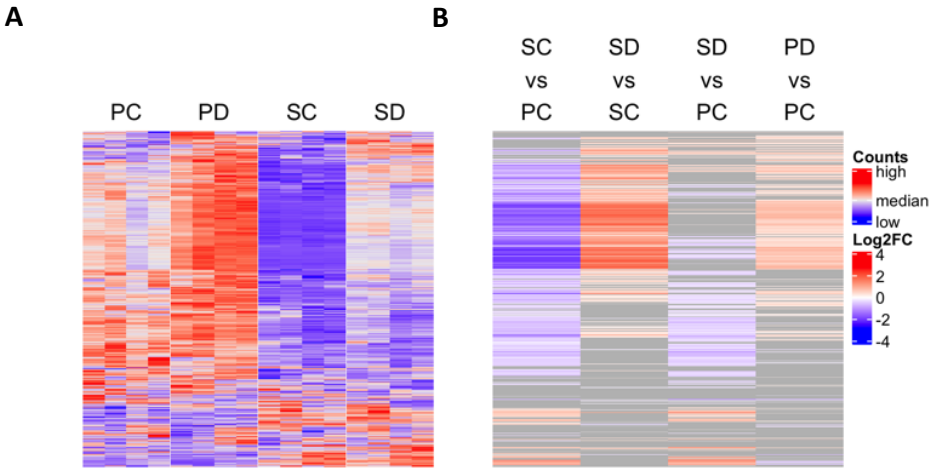

Figure 40. Heatmap of DREAM target genes. 959 DREAM reported targets were detected in our RNA-seq. Each row was representing one gene. The order of rows in A and B was maintained. **A)** Normalized counts, scaled per row, of the 16 individual samples grouped per condition respecting the biological replicate order. **B)** Log2 fold change values in different comparisons. Not significant changes were depicted in grey (p-value ≥ 0.05).

Immune related pathways

Although most of the genes whose expression was increased upon p21 loss in senescence were related to the cell cycle, I had noticed several immune related pathways enriched among them (Fig. 32-34 and 39). Most of these terms were related to the interferon response, TNF-

α, cytokine signaling and Natural Killers pathways. The complex crosstalk between senescent cells and the immune system is key in the understanding of many biological situations, from the clearance of the senescent population to the development of "inflammaging"[80,234]. Therefore, I was interested in knowing if p21 could actually play a role in regulating some of these processes.

SASP

The expression and secretion of the SASP is a key hallmark of senescent cells. One of the main effects of the SASP is the recruitment and activation of an immune response (see *Introduction: Cellular senescence: Physiological impact of senescence: Functions of senescent cells: Inflammation and immune recruitment*). This mediates the clearance of senescent cells preventing their accumulation, which has been largely associated to the detrimental effects of senescent cells (see *Introduction: Cellular senescence: Physiological impact of senescence: Beneficial or detrimental?*). This is the reason why I was very interested in assessing the effect of p21 decrease in senescence in the regulation of the SASP.

The composition of the SASP is heterogeneous and varies depending on many factors, such as the damage induction stimuli, cell type or biological context[11]. In order to explore the expression of a representative signature of the SASP, I selected a list of SASP factors proposed to be "representative" based on the literature[53]. Among the 24 SASP factors commonly upregulated in senescent cells described in Schafer et al. 2020, 8 were affected by p21 loss in senescent cells. Moreover, they proposed a list of 7 "most representative SASP factors", 2 of which were among the 8 genes affected by p21 (Gdf15 and Il15) (Fig. 41). All the 8 of them showed an increased transcription following p21 decrease. While Mmp9, Il7, Ccl5/Rantes, Il15, Icam1, Serpinb2 and Gdf15 were significantly upregulated in the SD.vs.SC comparison (p-value <0.05), Ccl2 increase was only significant in the SD.vs.PC comparison, presumably due to the cumulative increase related to the induction of senescence (SC.vs.PC) and the dampening of p21 (SD.vs.SC). Similarly, the other 7 factors were also significantly upregulated by the induction of senescence, SC.vs.PC. Therefore, the effect of p21 knock-down appeared to be the intensification of the transcriptional induction of SASP related to senescence, which occurred independently of the forced reduction in p21 levels of our model. In addition, I noticed other cytokines that were upregulated upon p21 loss in senescence: Cxcl10, Ccl25, Cxcl2, Cxcl3. On the opposite side, only Cxcl5 showed the opposite tendency, with its downregulation being significant in SD.vs.PC but not in SC.vs.PC comparison.

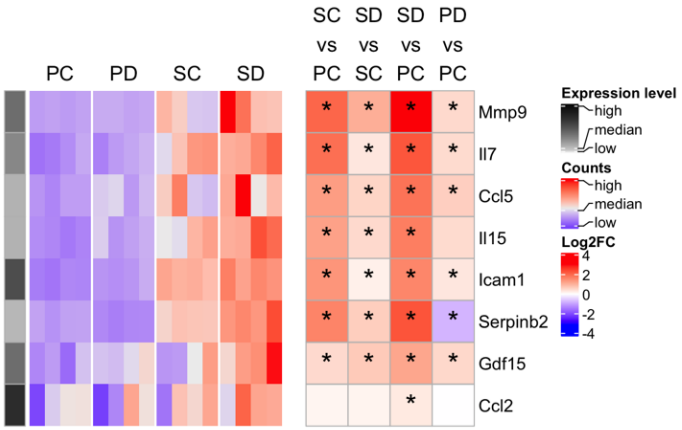

Figure 41. Heatmap of SASP genes. Expression of SASP factors from Schafer et al. 2020. significantly affected by p21 loss in senescence. From the 24 SASP factors, 8 were affected by p21 loss in senescence (either significant in SD.vs.SC or not significant in SC.vs.PC but significant in SD.vs.PC). 2 of them were part of the « representative » list: Gdf15 and Il15. Figure including 3 heatmaps. Left: relative expression level of the gene in comparison to the rest of transcripts in proliferating cells. Middle: expression in the 16 individual samples, grouped by condition and scaled by row. Right: expression fold change in log2 in the 4 analyzed comparisons. Significant change marked by an asterisk (p-value <0.05).

This analysis suggested that knock-down of p21 in senescent cells correlated with an increase in the transcription of several key SASP factors, and this was the major tendency among most of the genes that were investigated.

Chemokine and cytokine secretion

In order to gather more information on the effect of p21 on the secretion or production of recruiting factors of the immune system, I selected terms associated to chemokine (Fig. 42A) and cytokine secretion (Fig. 42B) from Gene Ontology databases. I created heatmaps showing the behavior of the genes significantly affected by p21 in senescence belonging to these terms. I could observe that most of the genes controlled by p21 in senescence related to the secretion of chemokines and cytokines showed an increased expression upon p21 downregulation in senescence. This result was not explored further, and it was clear that its accurate interpretation would require a deeper understanding of the function of these genes in the senescent context. However, I found interesting to notice that these global screenings of immune recruiting molecules all pointed to at an apparent suppressive role of p21 on the immune response in senescence.

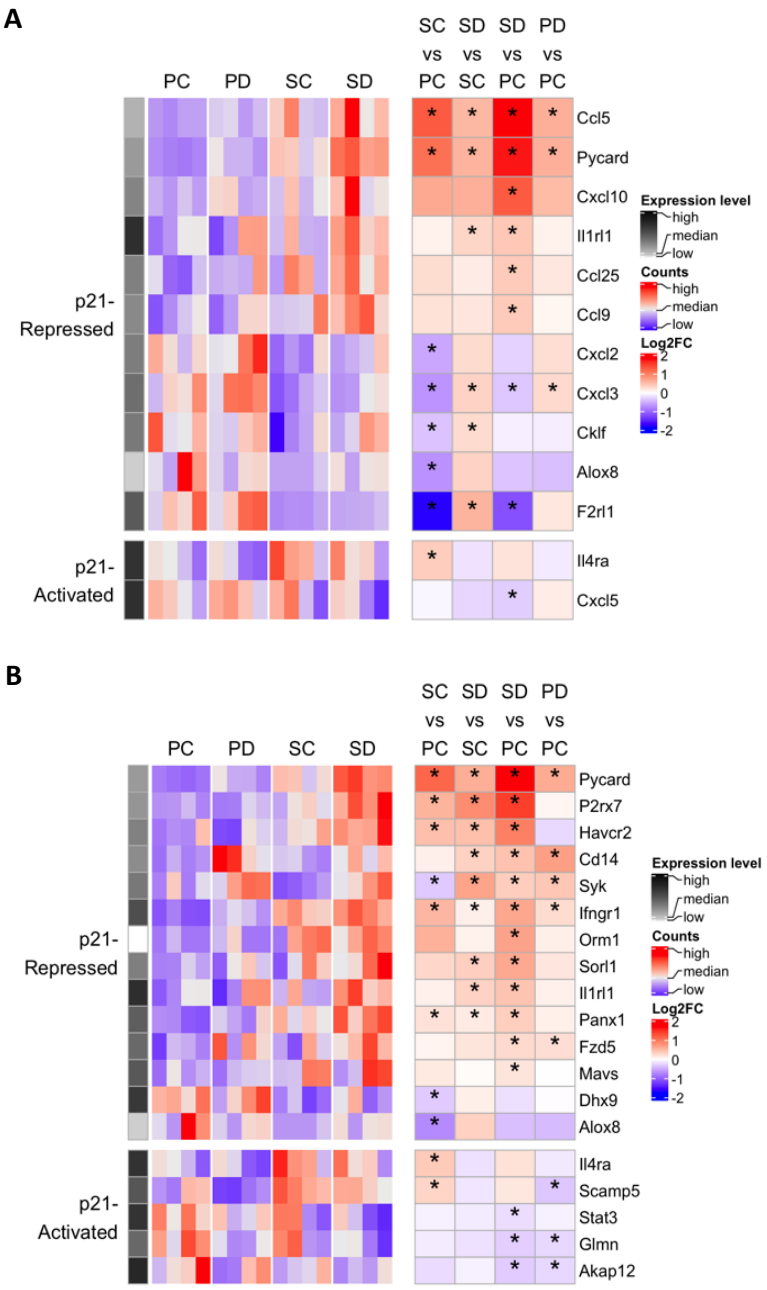

Figure 42. Heatmap of Chemokine and Cytokine production genes affected by p21 decrease in senescence. Genes were divided by Repressed (top) and Activated (bottom) by p21 (left label). Each figure including 3 heatmaps. Left: relative expression level of the gene in comparison to the rest of transcripts in proliferating cells. Middle: expression in the 16 individual samples, grouped by condition and scaled by row. Right: expression fold change in log2 in the 4 analyzed comparisons. Significant change marked by an asterisk (p-value <0.05). **A)** Chemokine production. Gene Ontology combination of terms. Biological Function: positive regulation of chemokine production (GO:0032722; before GO:0090197) and chemokine production (GO:0032602; before: GO:0090195). Molecular Function: chemokine activity (GO:0008009) **B)** Cytokine secretion. Gene Ontology Biological Process term: Positive regulation of cytokine production (GO:0001819).

Natural killer mediated clearance

The potential upregulation of the SASP by the loss of p21 in senescence suggested that p21 decrease could actually have an effect on the immune mediated clearance of senescent cells in physiological conditions. As mentioned, terms supporting this hypothesis were already observed in the pathway analysis of the genes upregulated by p21 knock down in senescence (Fig. 39), specifically among the genes that were downregulated upon the induction of senescence (Fig. 33). Specifically, terms related to natural killers caught my attention.

It had been reported that the expression of NKG2D ligands by senescent cells mediates their own clearance by natural killers[79,231,235]. Therefore, I examined the expression of the murine NKG2D ligands[451]. From the 9 described ligands, 5 of them were present in our RNA-seq data (Fig. 43). The expression of 4 of them, Raet1d, Raet1e, H60b and Ulbp1/Mult1, was significantly increased a upon p21 knock-down (SD.vs.SC) while H60c showed a very low expression. Interestingly, their expression seemed to decrease by the induction of senescence; in the case of Raet1e and Ulbp1 this was significant. In addition, Icam1 and Il15, critical mediators of NK activation and recognition[79,235] also presented an increased expression upon senescence induction (SC.vs.PC), which was also accentuated by p21 knock-down (SD.vs.SC).

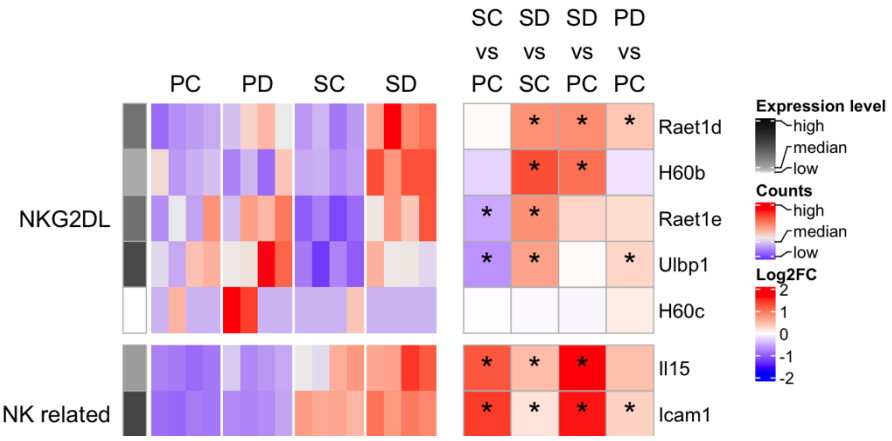

Figure 43. Heatmap of Natural Killer related genes. NK (Natural Killer) related genes divided in NKG2D ligands (top) and other genes modulating NK function (NK related bottom, left labels). Figure including 3 heatmaps. Left: relative expression level of the gene in comparison to the rest of transcripts in proliferating cells. Middle: expression in the 16 individual samples, grouped by condition and scaled by row. Right: expression fold change in log2 in the 4 analyzed comparisons. Significant change marked by an asterisk (p-value <0.05).

Together, these results showed that p21 loss in senescence was associated to an increased expression of key molecules known to mediate the recognition and clearance of senescent cells by natural killers.

TNF-α signaling: molecular mechanism regulating inflammation

The idea that p21 loss may sustain and increase the transcription of a pro-inflammatory signature in senescent cells led me to questioning the mechanism by which this effect may be achieved. The results of the pathway analysis of the genes potentially repressed by p21 in senescence presented some interesting answers to this that I decided to explore further. Among the 388 genes potentially repressed by p21 in senescent cells, I had observed an enrichment of terms related to inflammation and cytokines, TNF-α and interferon signaling in different databases (Fig. 39). When I looked into the literature to better understand the role of TNF-α pathway in senescence, a 2017 article by Kandhaya-Pillai et al. in *Aging* described similar observations[54]. This article proposed a molecular mechanism by which "*TNFα-senescence initiates a STAT-dependent positive feedback loop, leading to a sustained interferon signature, DNA damage, and cytokine secretion"*. I actually observed an enrichment in DNA damage and repair signatures in different sublists of genes upregulated by p21 knock-down in senescence (Fig. 29, 32 and 33), and one analysis showed that these genes could also be enriched in STAT signaling (Fig. 39).

The cited article described 78 human genes whose transcription was significantly upregulated by the induction of TNF-α. 86 murine orthologs corresponding to these genes were found, all of them present in our RNA-seq data. In agreement with the article, 60 of the transcripts were differentially expressed in senescence (SC.vs.PC, p-value <0.05), and most of them, 51, were upregulated (log2 fold change >0). In order to know if the loss of p21 in senescent cells was affecting the transcription of the TNF-α induced genes described, I selected the genes affected by p21 in senescent cells and I represented their expression and transcriptional change in different comparisons in the heatmaps of figure 44. From the 15 genes affected by p21 knock -down in senescence, 12 of them showed an increase in transcription.

This effect was also observed when I performed the same analysis on the genes from the term "TNF via NF-kB" of the Hallmark 2020 database, which showed a strong enrichment among the potentially repressed genes by p21 in senescence (Supp. Fig. 3). In this case, 56 genes belonging to the term were found to be affected by p21 decrease in senescence, 44 of them being repressed by its expression (excluding *Cdkn1a*).

These observations made me consider the activation of TNF-α signaling as one plausible mechanism by which p21 loss could potentiate the inflammatory phenotype in senescent cells, increasing the expression of DNA damage, interferon signature and cytokine secretion.

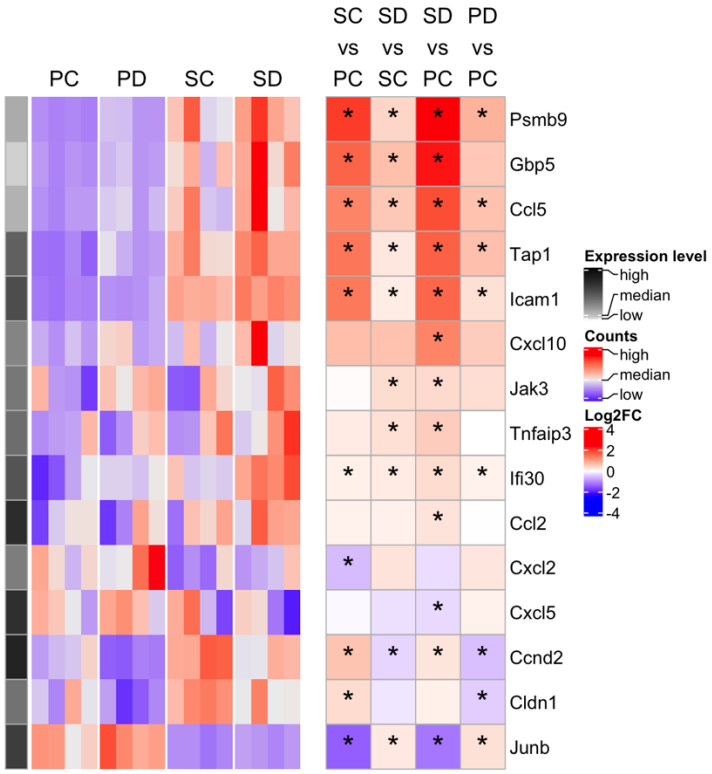

Figure 44. Heatmap of TNF-α in senescence. Affected genes by p21 in senescence from Kandhaya-Pillai et al. Aging 2017: TNFα-senescence initiates a STAT-dependent positive feedback loop, leading to a sustained interferon signature, DNA damage, and cytokine secretion. Figure including 3 heatmaps. Left: relative expression level of the gene in comparison to the rest of transcripts in proliferating cells. Middle: expression in the 16 individual samples, grouped by condition and scaled by row. Right: expression fold change in log2 in the 4 analyzed comparisons. Significant change marked by an asterisk (p-value <0.05).

Conclusion – p21 and the immune response

In conclusion, these results implied a potential role for p21 in the recognition and clearance of senescent cells by the immune system. Although the functional effect of the transcriptional changes associated to p21 loss remain unexplored, it led me to speculate on the novel idea that p21 downregulation in senescent cells could favor the production of at least some of the SASP factors that favor the recruitment of the immune system and allowing the recognition of senescent cells by immune cells such as natural killers, and it could even affect the mechanism of their removal. In addition, I suggested a molecular mechanism that could contribute to explain this effect, the induction of the TNF-α signaling pathway, which seemed to be favored by p21 loss in senescent cells.

Translation

Furthermore, pathway analysis revealed that p21 seemed to play an important role in sustaining the expression of genes involved in protein translation (Fig. 37). To get an overview on this, I created a heatmap of the genes affected by p21 knock-down in senescence belonging to "translation" term on the Gene Ontology: Biological Process database (Fig. 45). This confirmed that many genes involved in translation reduced their expression due to p21 loss in senescence. Remarkably, I noticed that the ribosome coding gene *Rplp0* was one of these hits. Rplp0 was one of the housekeeping genes often used to normalize the RT-qPCR values. The implications of this were considered in the *Discussion* part of this thesis (*Discussion:: Role of p21 in senescence: Hypothesis examination:: Translation and ribosome biogenesis*).

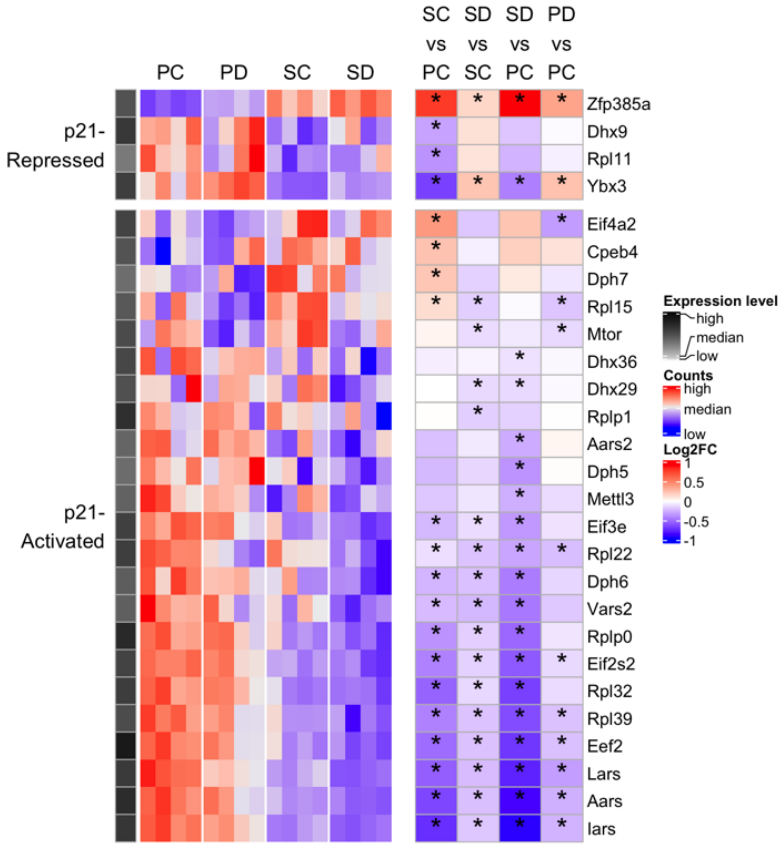

Figure 45. Heatmap of Translation genes. Genes affected by p21 in senescence related to translation. Genes were divided in "Repressed" (top) and "Activated" (bottom, left label) by p21 in senescence. From a combination of terms: Gene Ontology Biological Process: Cytoplasmic translation (GO:2000766), aminoacyl-tRNA metabolism involved in translational fidelity (GO:0106074). This second term contributed with only 4 genes of the p21-activated genes in the heatmap. Figure including 3 heatmaps. Left: relative expression level of the gene in comparison to the rest of transcripts in proliferating cells. Middle: expression in the 16 individual samples, grouped by condition and scaled by row. Right: expression fold change in log2 in the 4 analyzed comparisons. Significant change marked by an asterisk (p-value <0.05).

Peroxisomes

Lastly, we were especially interested in one particular hit on the pathway analysis of the genes induced in senescence (SC.vs.PC) whose expression was reduced by p21 inactivation (SD.vs.SC). The term *peroxisome* (GO: 0005777) was enriched in Gene Ontology Cellular Component 2017 version database. Peroxisomes are single membrane organelles that are critical for regulation of fatty acid metabolism and the production of reactive oxygen species (ROS)[452,453]. Their activity importantly impacts the energetic metabolism of the cell, membrane composition, redox homeostasis and the expression of an inflammasome and the immune activation[453–455]. Although these functions are usually deeply altered in senescence cells, and it had been reported that peroxisomal alterations occur in many senescence contexts[454,456], the role of peroxisomes and senescence remained greatly underexplored. Actually, I found only one 2002 article strictly and directly addressing this connection[457] (Legakis et al., 2002). This is why we decided to explore the effect of senescence, and the expression of p21, on peroxisomes in our data.

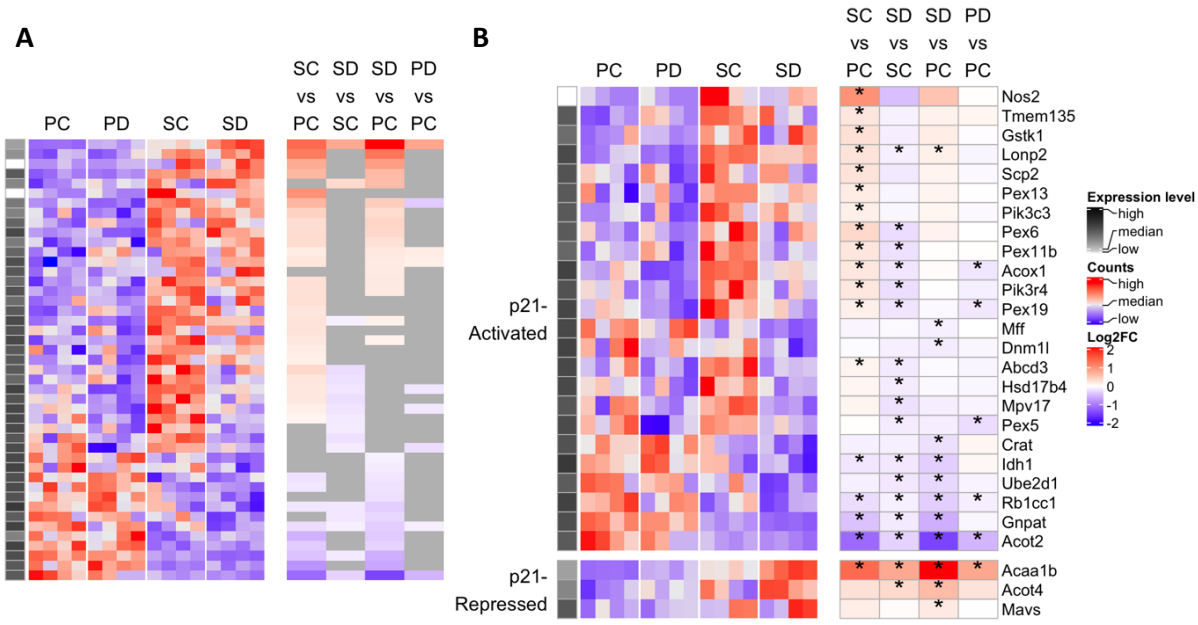

Figure 46. Heatmap of peroxisomal genes affected in senescence. Expression of peroxisomal genes in different comparisons. **A)** Expression of 45 peroxisomal genes significantly changing in at least one of the three comparisons evaluated (SC.vs.PC, SD.vs.SC or SD.vs.PC). Only significant log2 fold changes were colored. **B)** 27 peroxisomal genes significantly affected by p21 knock-down in senescence. Significant Log2 fold changes are marked with an asterisk**.** One gene per row. Each figure containing 3 graphs: Grey column expressing the average expression level of in proliferating control samples in comparison to the rest of the RNA-seq transcripts. Heatmap of the expression level of each individual sample, grouped by condition, scaled per row. Heatmap of log2 fold change of each gene in the comparisons of interest. Peroxisomal genes belonged to Gene Ontology terms related to peroxisomes (GO: 0005777, GO:0030242, GO:0015919, GO:0043574, GO:0016559, GO:0007031, GO:0016558, GO: 0045046), most of the genes being included in the term *peroxisome organization* GO:0007031.

I extracted a list of 90 peroxisomal genes from combining a set of peroxisome related terms from the Gene Ontology database. From these, there were 45 genes significantly changing in at least one of my comparisons of interest: SC.vs.PC, SD.vs.SC and SD.vs.PC (Fig. 46). I observed a general upregulation in the expression of peroxisomal genes upon the induction of senescence (SC.vs.PC), while p21 loss seemed to dampen their expression. Specifically, 36 genes were differentially expressed in senescent cells (SC.vs.PC): 27 increasing their expression and 9 decreasing. From the 27 upregulated genes, 13 were downregulated by p21 knock-down, and only 1 was increased. On the other hand, 4 of the downregulated genes in senescence (SC.vs.PC) further reduced their expression due to p21 loss, and none of them was significantly induced upon p21 knock-down in senescence (Fig. 46A, legend table of Fig. 47). On the other hand, if I focus specifically on the effect of p21, 27 genes were found to be affected by p21 decrease in senescence, 24 of them decreasing their expression upon p21 loss (Fig. 46 B, legend table of Fig. 47).

To gain insight on the function of the peroxisomal genes with an altered expression by either the establishment of senescence or the decrease of p21in this context, I took advantage of the tools available in the KEGG database webpage (Fig. 47). By coloring the genes contained in the *peroxisome* pathway according to their transcriptional behavior, I could observe that senescence, and p21 expression, seemed to affect the expression of many metabolic enzymes, as well as proteins involved in peroxisomal biogenesis (Fig. 47).

Taken together, these observations contributed to a link between senescence and peroxisomes. This data indicates that the establishment of senescence correlates with an increased transcription of peroxisomal genes, which would potentially lead to an amplified presence and/or function of peroxisomes in senescence. In this context, p21 would mediate or facilitate these transcriptional changes, and its loss seemed associated to the downregulation of the expression of peroxisomal genes.

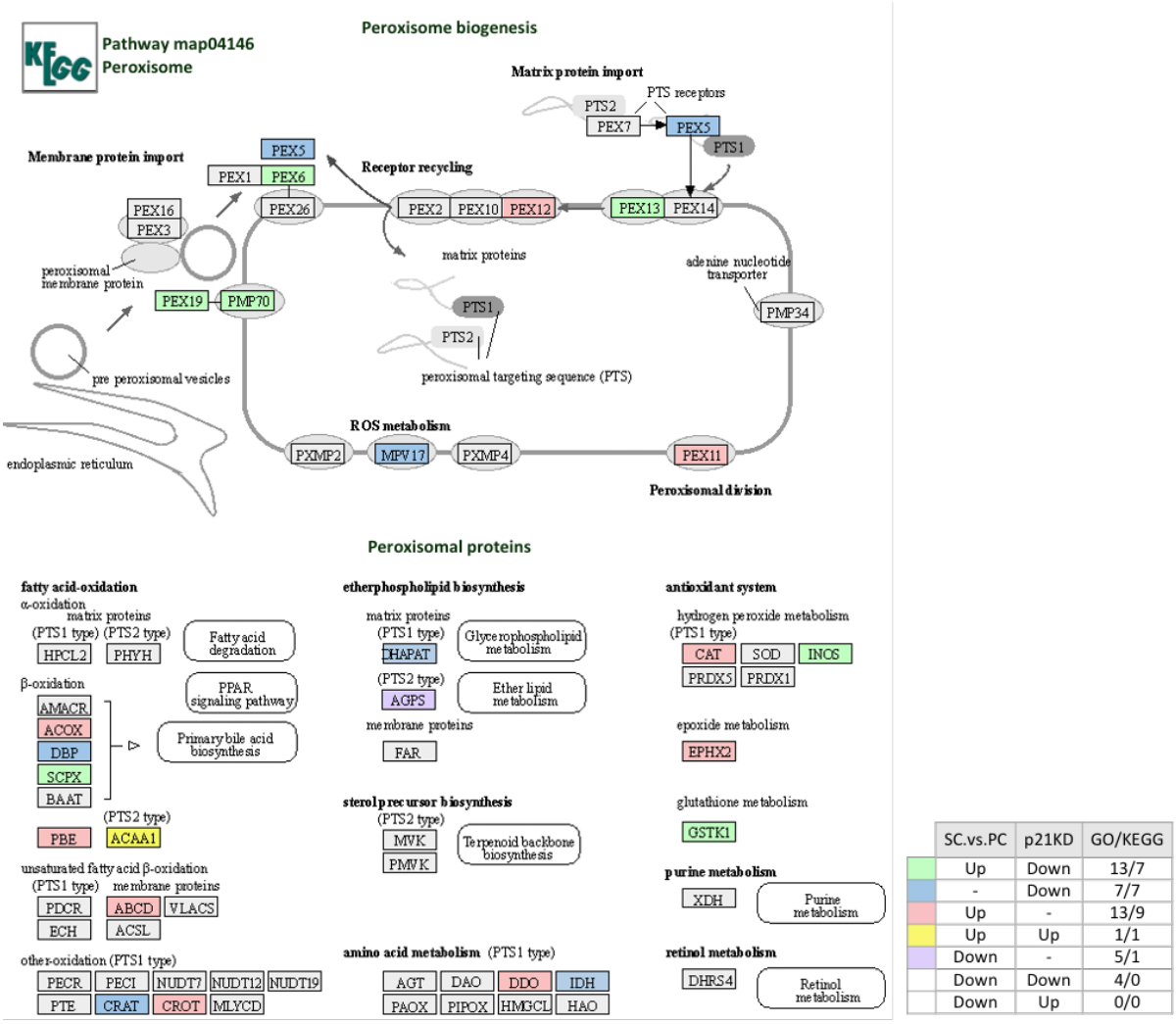

Figure 47. Peroxisome KEGG pathway. Pathway map04146:Peroxisome of KEGG database. Peroxisomal genes were colored to indicate their transcriptional behavior in the acquisition of senescence (SC.vs.PC) and upon p21 knock-down in senescence using the RNA-seq data (legend as a table, bottom right corner). Last column of legend specifying the number of genes in each group detected in Gene Ontology terms (Fig. 46) and in this KEGG map separated by a slash.

3. Hypothesis Exploration

3. 1 Model considerations

Permanent proliferative arrest

The analysis of the pathways upregulated by p21 loss in senescent cells a showed a striking enrichment in proliferation and cell cycle related pathways. Although this was an expected result which could be explained by the inability of the DREAM complex to form in the absence of p21, an increase in proliferating cells in our cultures due to the induction of the knock-down could not be discarded.

Although the acquisition of the senescent state 6 days after irradiation had been assessed, certain level of heterogeneity in our cellular cultures was to be expected, and a minimal presence of non-senescent cells could not be totally excluded. The ability of p21 to block the cell cycle by directly interacting with cyclins and PCNA is one of the first barriers of proliferation during the establishment of senescence (see *Introduction: p21: Cellular functions regulated by p21: Cell cycle*). Therefore, if cells that were not fully senescent were still present in our plates by the time of exposure to doxycycline, they would experience a boost in proliferation due the reduction of p21 levels. In this case, even if the fraction of proliferating cells in the culture was very small, the transcriptional signature of a proliferative population could be consistent enough to be strongly enriched in samples with an overrepresentation of this group of cells. With all this in mind, I realized that I could not discard that the upregulation of proliferation-related pathways upon p21 knock-down was not due to a real increase in proliferation in our samples attributed to the presence of residual non-senescent cells.

To test if the knock-down of p21 could be favoring the emergence of non-senescent populations in irradiated cultures, I kept and observed untreated and doxycycline treated irradiated plates over time. Although most of the irradiated plates stayed arrested over time, small patches of proliferating cells started to be visible around day 9-10 after irradiation when p21 was downregulated (3-4 days after the induction of the knock-down), but they only became clearly obvious around day 12 after irradiation (after 6 days in doxycycline). Although their frequency was variable among experiments, proliferating clusters of fibroblasts were observed in the vast majority of the p21 knock-down irradiated cultures at

late timepoints (from day 12 on). Even in plates where p21 levels were not manipulated, isolated patches of growing cells were often perceptible around 12-15 days after irradiation, although their detection was less obvious and their growth much slower than in the presence of doxycycline.

To visualize the presence of emerging proliferating populations, irradiated plates with and without doxycycline were fixed at different timepoints and stained with crystal violet (Fig. 48A). A visual evaluation suggested that although the size of proliferating regions enlarged over time, they did not seem to increase in number. To better analyze this, crystal violet proliferation assays were performed: irradiated pre-senescent cells were plated at exponentially decreasing concentrations in duplicates, fixed 2-3 weeks after irradiation, and stained with crystal violet (Fig. 48B, top panels). The number of dividing clusters in the absence of doxycycline was variable and difficult to estimate, since their slow growth made them difficult to detect when plated at low concentrations (Fig. 48B, top-left). Patches of proliferating cells emerged in most of the experiments when p21 expression was abrogated, although their frequency was variable across replicates (n=5). Their presence only seemed to be avoided when cells were plated extremely sparsely (~5000 cells in a 9.5cm^2 well), which compromised cell viability. While some clusters grew isolated in a defined round shape, others were more irregular, and it was often not possible to determine the boundaries between them, so their quantification seemed unreliable.

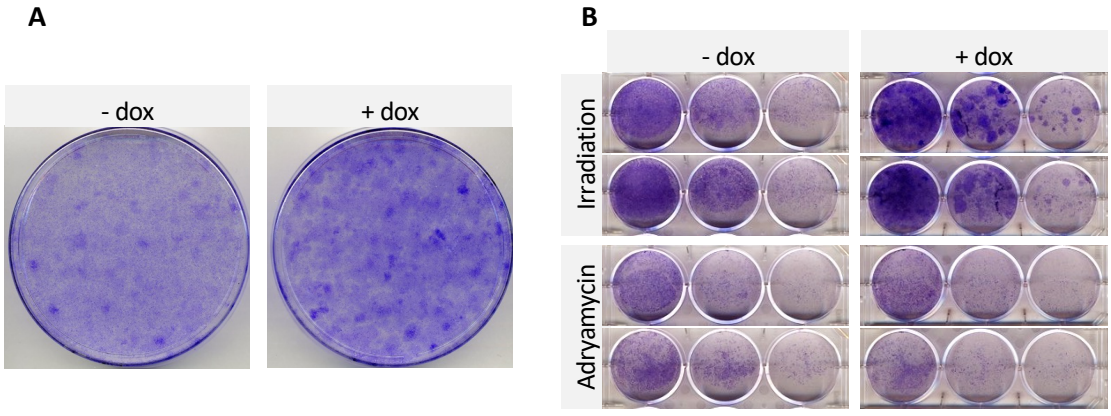

Figure 48. Crystal violet staining of late senescent cultures. A) Irradiated plates with emerging proliferation clusters. Crystal violet staining on untreated (left) or doxycycline treated plates (right) fixed 21 days after irradiation, 15 days in doxycycline. **B)** Crystal violet proliferation assay. Irradiated (top) and adriamycin treated (bottom) cells with unaltered (left) or dampen levels of p21 (right) were fixed 22 days after damage induction, 16 days in doxycycline. Irradiated and adriamycin treated cells were plated 4 days after damage in decreasing concentrations (columns from left to right: 47.5, 23.75 and 11.875 x 10^3 cells in each 9.5cm^2 well). Crystal violet staining in irradiated cells was performed in different cell concentration plates fixed in a range of 15-30 days after irradiation a total of 5 times, and 2 times in adriamycin treated cultures.

In summary, I found that the existence of non-senescent cells in irradiated plates was recurrent, and their growth was favored by the downregulation of p21. Although their presence may have contributed to the enrichment of the proliferation related signature detected in our pathway analysis, their number at the timepoint when the cells were collected for the RNA-seq was estimated to be very low. Still, even when irradiation could be a useful model to study senescence in fibroblasts at early timepoints, the presence of proliferating cells may impact the results generated in this system. Therefore, the validation of the obtained conclusions in other models of senescence would strengthen our results.

Alternative model: adriamycin induced senescence

Based on the results of the previous section, I decided to look for a senescence model that avoided the presence of non-senescent cells in the culture. Adriamycin is the commercial name of doxorubicin, a topoisomerase inhibitor that, due to its ability to cause DNA damage and induce apoptosis, has been widely used as a chemotherapeutic drug for treating a variety of cancers[458–460]. It acts by triggering the DNA damage response, mainly through the generation of DNA double-strand breaks. Additionally, this compound had been reported to promote senescence in a variety of cell lines[459,461,462]. Therefore, I decided to test if it could be used as an alternative model of damage-induced senescence in mouse dermal fibroblasts.

I used adriamycin to induce senescence following a similar protocol to the irradiation one used previously. Instead of irradiating proliferating fibroblasts, I exposed them acutely to the drug[462]. After adding the adriamycin into their culture media for 24h, the compound was removed, and the cells were kept in culture in the same way that was done with irradiated plates. As expected, adriamycin caused a rapid and potent induction of apoptosis, which was manifested by an increased cell death observed in treated plates. The remaining cells had arrested proliferation, and started developing a senescence phenotype. 6 days after their exposure to adriamycin, cells had acquired the characteristic senescent morphology. It was at this timepoint when we decided to administer doxycycline to induce the knock-down of p21 in the same way I did with irradiated plates. To verify the establishment of senescence and the induction of p21 knock-down in adriamycin treated cells, I collected RNA samples from proliferating and senescent cells 8 days after adriamycin exposure, either with unmanipulated levels of p21 or exposed to doxycycline for 2 days (the same way that RNA-seq samples were produced). The transcriptional expression of senescence markers was analyzed by RT-qPCR (Fig. 49E). This first test confirmed that, 8 days after being exposed to adriamycin, dermal fibroblasts presented the expected morphological (Fig. 49C-D) and

transcriptional changes associated to senescence (Fig. 49E). The senescence mediators p21 (*Cdkn1a*) and p16 (*Ink4a*) were upregulated, and *Hmgb2* and *Ki67* transcripts were repressed (Fig. 49E, purple). In addition, doxycycline effectively downregulated p21 expression, which was indicated by the increase in *Hmgb2* transcription and the downregulation of *Cdkn1a* in this model (Fig. 49E, cyan).

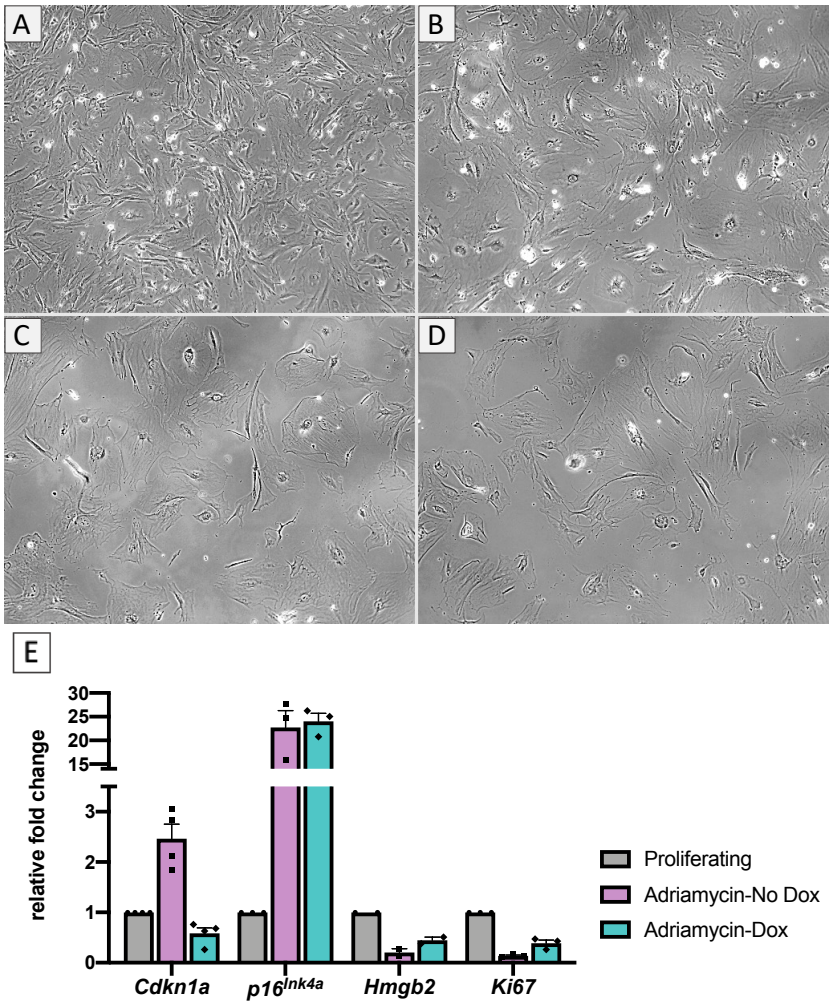

Figure 49. Adriamycin induced senescence. A-D) Senescent morphology in adriamycin treated cells. Representative images of proliferating (A) and senescent cells (B-D) 8 days after senescence induction via irradiation (B) or acute adriamycin treatment (C-D). 6 days after adriamycin exposure, cells were culture with doxycycline for 2 days to induce p21 knock-down (D). All 4 conditions were produced in parallel from the same original culture, fixed and imaged by phase contrast at 10x magnification. **E)** Transcriptional expression of senescence markers**.** The mRNA expression of the senescence markers $p21^{Cdkn1a}$, $p16^{Ink4a}$, Hmgb2 and Ki67 was quantified by RT-qPCR in proliferating (grey) and adriamycin induced senescent samples (purple and cyan). Senescent cells untreated (purple) or treated for 2 days with doxycycline to induce p21 knock-down (cyan) were collected after 8 days of adriamycin exposure (n=2-4).

In order to detect the emergence of proliferating cells in this model, I performed crystal violet proliferation assays (n=2). To compare both models, senescence was induced either by

irradiation or adriamycin in parallel using the same original cells. The higher lethality of adriamycin was evident since far fewer cells were observed over time in comparison to irradiated plates. At 22 days following damage induction, and 16 days in doxycycline, cells were fixed and stained with crystal violet (Fig. 48B). Even though the same number of cells were seeded at day 3 to 5, there were noticeably fewer cells in plates treated with adriamycin at the end of the experiment, which suggested that the negative impact in cell viability of this treatment may persist beyond the first days.

Interestingly, and unlike with irradiated cultures, I never detected the emergence of growing populations in adriamycin treated plates in any of the experiments performed (n=6), even when the p21 expression was abrogated (Fig. 48B). Consequently, I considered that adriamycin-induced senescence was a potential model to use for validating the results obtained in irradiated cells in order to control for the bias that the marginal presence of proliferating cells could cause.

3. 2 Exploration of RNA-seq derived hypothesis

The results of the RNA-Seq pathway analysis suggested some novel or under explored functions controlled by p21 in senescent cells. Some of these hypotheses were particularly interesting to us, either because of their novelty or their potential implications, so we decided to further explore them further. In particular, I investigated the effect of p21 on peroxisomes and cytokine secretion, and the fate of p21 in later timepoints of senescence.

Peroxisomes

Pathway analysis revealed an enrichment of peroxisomal genes in the transcriptional signature upregulated in senescence that decreased upon knock down of p21. Peroxisomes (initially named microbodies) are ubiquitous eukaryotic multifunctional organelles that interact physically and functionally with other subcellular compartments[452,453,456,463]. They are formed by a single membrane, do not contain DNA, and have a diameter typically ranging from 0.1 to 1um. They are heterogeneous and highly dynamic: their number, size, and even proteome can greatly vary among cell types, tissues and in response to changes in metabolic requirements[452,453]. Among their functions, they play a key role of catabolic (oxidation fatty acid oxidation) and anabolic (lipid biosynthesis) lipid metabolism, as well as contributing to the detoxification via metabolization of free radical species, especially hydrogen peroxide[453]. Their activity impacts a number of physiological processes, such as nervous system

development and function or inflammation modulation[453,455]. In fact, alterations of peroxisome function, enzymes (such as catalase) and regulators (like PPAR-activators) have been associated to a number of age-related pathologies, such as inflammatory and neurodegenerative diseases, diabetes, obesity and cancer[452,453,456,463,464]. Due to the significant overlap of biological functions and pathways regulated by peroxisomes and altered in senescent cells (especially ROS level regulation)[454], and the lack of information on the role of peroxisomes in senescence, the relation between senescence, p21 and peroxisomes was a potentially relevant and interesting result for us to explore.

Peroxisomal *aggregates*

A first exploration of the biological function of the peroxisomal genes that were potentially affected by p21 and senescence, revealed several membrane proteins (see Fig. 40). Among the proteins that seemed to be upregulated in senescence through p21 (increasing in

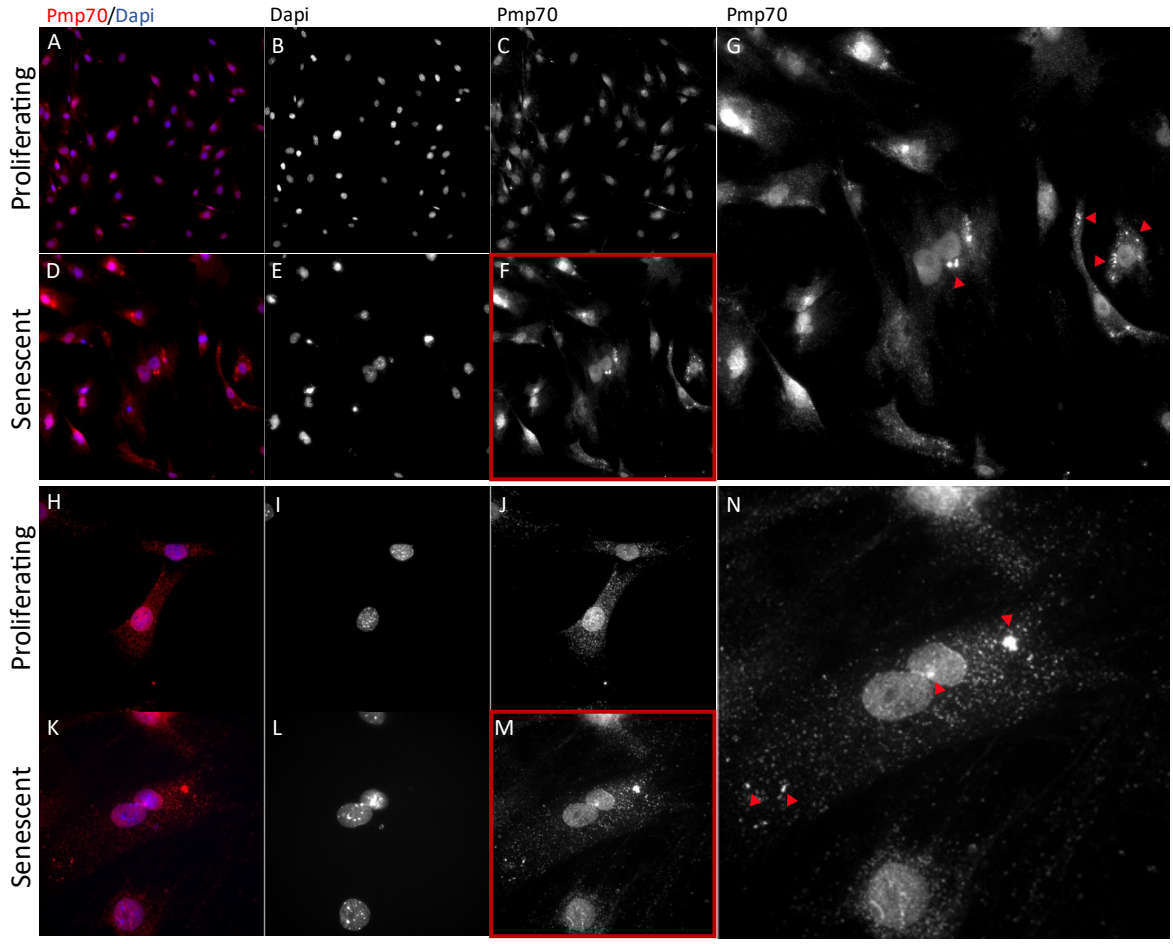

Figure 50. Identification of peroxisomal "aggregates". Immunofluorescent staining of peroxisomal marker Pmp70 (red) and Dapi (blue). Proliferating (A-C and H-J) and senescent cells (D-G and K-N) Widefield fluorescence images at 20x (A-G) and 63x (H-N) magnification. Pmp70 signal in F and M enlarged in G and N, red arrows indicating peroxisomal aggregates.

senescent cells and decreasing by p21 knock-down), there was the transporter Pmp70, also known as Abcd3, which mediates the uptake of metabolites. To explore the differences in peroxisomes in senescence that could be attributed to p21, I took advantage of this peroxisomal membrane marker.

I performed immunofluorescence against Pmp70 protein in order to visualize peroxisomes in proliferating and senescent cells 8 days after irradiation (Fig. 50). As expected, peroxisomal staining presented a punctuated cytoplasmic pattern. Strangely, we noticed the presence "patches" of peroxisomal signal often occurring in the staining (Fig. 50 G). This pattern resembled an aggregation of peroxisomes, so we referred to the phenotype as peroxisomal "aggregates". Interestingly, these aggregates were mostly observed in senescent cells. The increased presence of aggregates in senescent cultures was confirmed through the quantification of aggregate containing cells in proliferating and irradiation and adriamycin induced senescent cultures, as detailed in following sections (Fig. 54).

Preliminary characterization

We decided to gather information on the characteristics and nature of the perceived peroxisomal aggregates. I observed their morphology and cellular localization through more detailed imagining by using different magnifications, confocal microscopy and cytoskeletal staining. The impact of aggregates in peroxisomal activity was screened by immunostaining of a peroxisome functional marker, catalase. In addition, I tested if autophagy, a process associated to similar visual peroxisomal phenotypes, could be responsible for their appearance by immunostaining of the autophagy marker p62.

Phenotypical description

To gain insight on the phenotypical characteristics of peroxisomal aggregates detected by widefield immunofluorescence, I imaged them at different magnifications using spinning disk confocal microscopy (Fig. 51). In addition, phalloidin staining was performed in order to visualize the actin cytoskeleton of cells and assess the cellular localization of aggregates. In this way, I was able to identify a variety of events that could be perceived as peroxisomal aggregates when visualized at low magnifications in a widefield microscope.

Some cells presented several aggregates spread through the cytoplasm without any identified pattern (Fig. 51A, E). Aggregates were frequently located in specific and defined regions of high concentration of signal, possible due to an uneven distribution of peroxisomes (Fig. 51B-D). Interestingly, dense regions were often localized around the nucleus (Fig. 51D, F bottom-

right), or even between nuclear structures in multinucleated cells (Fig. 51E, F top-right). The detection of strong peroxisomal signal in cells with small cytoplasm (Fig. 51D top) and cellular protrusions (not shown) suggested that strong peroxisomal signals might arise through dynamic morphological reorganization of cell shape: it was feasible to imagine that the shrinkage of a cellular area would present intense peroxisomal signal due to the gathering of peroxisomes that otherwise would be sparsely distributed. Although I observed curious alterations on the actin cytoskeleton in some cells, I was unable to notice any connection between actin cytoskeleton abnormalities and aggregates.

After these observations, I realized that the peroxisomal aggregates detected by widefield imaging were probably a combination of different phenomena. Signal from large peroxisomes, clusters of peroxisomes in contact (or close proximity), and regions with uneven and high accumulation of peroxisomes would all probably be perceived as aggregates, and maybe even indistinguishable, in our low magnification widefield images. Although the presence of aggregates was obvious in many cases, the variability of their size and shape

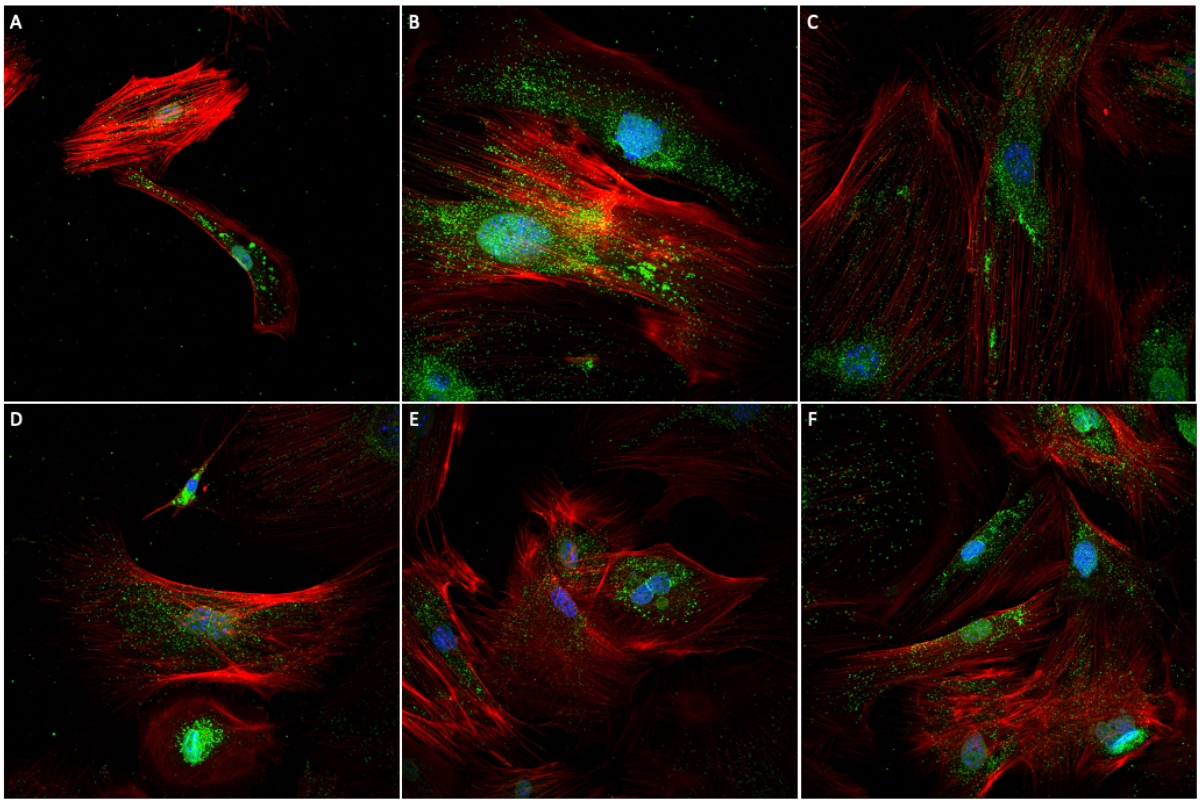

Figure 51. Examples of peroxisomal aggregates observed in senescent cells. Immunofluorescent staining of senescent cells 8 days after senescence induction (irradiation or adriamycin treatment). Composite images showing nuclear Dapi staining (blue), Pmp70 peroxisomal marker immunostaining (green) and phalloidin staining of actin cytoskeleton (red). Maximum intensity Z-projection of spinning disk confocal microscopy images at 40x magnification.

made it difficult to set a threshold allowing their objective identification. Altogether, aggregates were considered to be an umbrella category for all these different situations.

Functionality: Catalase or "ghost" peroxisomes

We wondered if impaired peroxisomal function may be related to the formation of aggregates. One of the most important enzymes of peroxisomes is catalase. Catalase is an antioxidant enzyme predominantly located inside peroxisomes, that can decompose hydrogen peroxide and reduce ROS levels[465]. Its deficiency has been correlated with senescence and age-related diseases, among other pathologies[454,457,466,467]. In fact, catalase has been used as a marker to discriminate functional peroxisomes from non-functional peroxisomal "ghosts", which are "empty" peroxisomal membranes unable to import the matrix proteins necessary for their activity. Since peroxisomal function can be compromised by catalase absence, we decided to assess catalase localization in peroxisomes in senescent cells in order to infer problems in their activity.

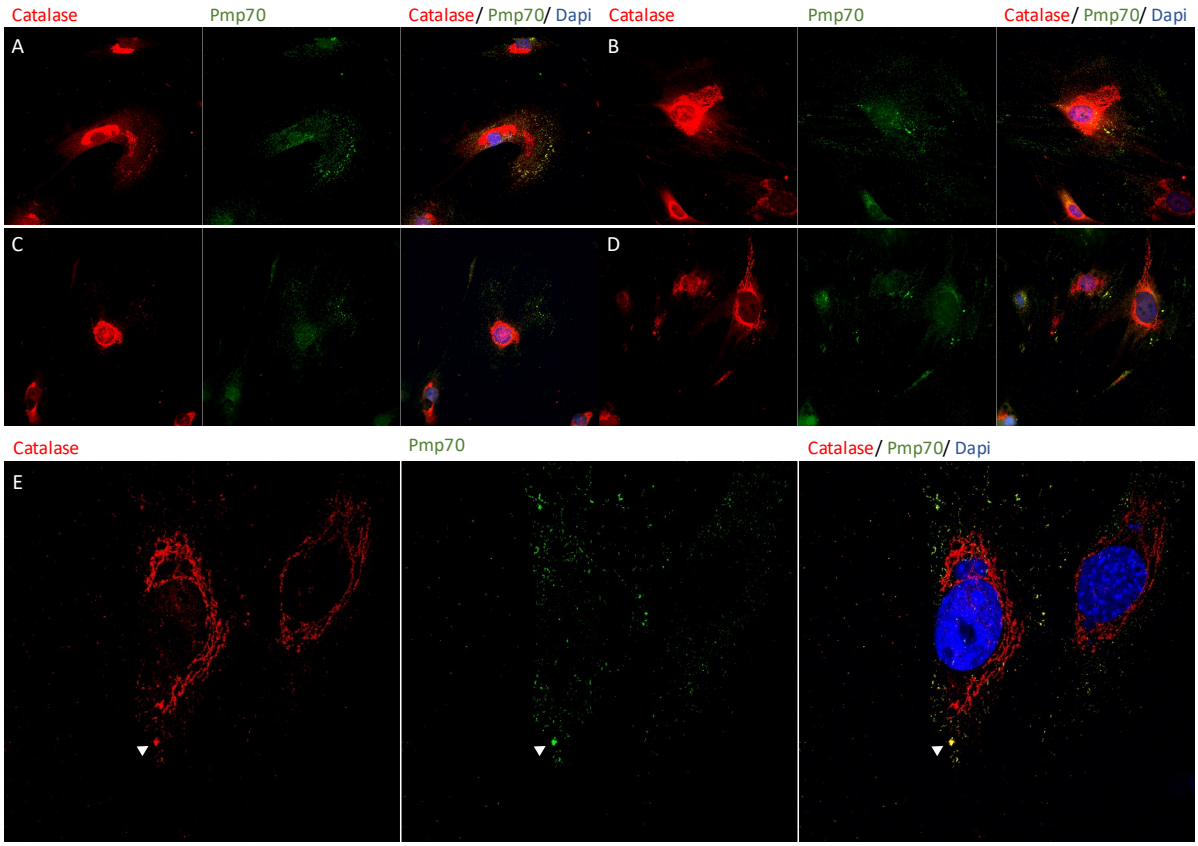

Figure 52. Catalase presence in aggregates in senescent cells. Immunofluorescence staining of peroxisomal markers in senescent cells. Each panel shows Catalase (red), Pmp70 (green) and their composite image including Dapi (blue). **A-D)** Widefield fluorescent microscopy at 40x magnification. **E)** Representative aggregate signaled by white arrow. Maximal Z-projection of spinning disk confocal microscopy image at 100xmagnification. *Notice unexpected and potentially unspecific signal resembling ER or Golgi structure in the catalase staining.

I performed immunostaining against Pmp70 (peroxisomal membrane) and catalase in proliferating and senescent cells 8 days after senescence induction, either by irradiation or acute adriamycin treatment (n=2). Cells were imaged by widefield and confocal fluorescent microscopy at different magnifications (Fig. 52). Although no co-localization measurements were performed, the visual analysis of the images confirmed the presence of catalase in the vast majority of aggregates identified by Pmp70 staining. No noticeable differences were observed between senescent cells induced via irradiation and adriamycin treatment. Although the presence of catalase alone was not an indicative of correct peroxisomal activity, after this staining, the hypothesis of defective peroxisomal function in aggregates remained unsupported. The pattern of catalase signal did not infer any impairment of the peroxisomal import machinery or function of peroxisomes in aggregates. Thys hypothesis was not further explored due to time restrictions and the complexity of assessing functional defects in the multiple activities of peroxisomes.

Pexophagy

A search across the literature revealed a couple of studies that included immunofluorescence images of peroxisomal structures resembling the phenotype observed by us, which were referred to as "aggregates" or "clusters" of peroxisomes by the authors [468,469] (Fig. 2 of Deosaran 2013, Fig. S1 in Defourny 2019). In both cases, the authors of the articles related these structures to the process of pexophagy. Pexophagy is a form of selective autophagy by which most peroxisomes (~75%) are degraded when damaged or excessive in number[470].

The ubiquitin receptor p62 is involved in the recognition of ubiquitinated peroxisomal proteins and their delivery to autophagosomes for lysosomal degradation, and has been used as a pexophagy marker[468,470]. In order to know whether aggregates were derived from peroxisomes undergoing pexophagy, I decided to perform immunofluorescence against p62 in proliferating and senescent cells 8 days after senescence induction by irradiation and adriamycin treatment (n=2). Close examination by widefield and confocal fluorescent microscopy at different magnifications (20x-100x) showed the expected pattern of p62 in our samples. Despite no co-localization measurements were performed, a visual screening of at least 40 cells per condition suggested that p62 signal did not show an obvious correspondence with the localization of aggregates, identified by Pmp70 staining (Fig. 53).

Although no association between pexophagy and aggregates was observed, the interpretation of this result was inconclusive. My experimental analysis was far from thorough: no quantification was performed and only one pexophagy marker was used. In

addition, the significance of a lack of co-localization between p62 and aggregates was not obvious. Based on the data from Deosaran et al. (2012 publication), p62 signal was expected to co-localize with pexophagic structures, and therefore its absence could suggest that aggregates were not undergoing pexophagy[468]. However, and even though a less detailed analysis was performed in this case, Defourny et al. (2019 paper) attributed the formation of peroxisomal clusters to an impairment in peroxisomal autophagy[469]. In light of these contradictory hypothesis, and with the limited amount of data generated at the moment, I could not properly understand the implications of p62 absence in aggregates in our model.

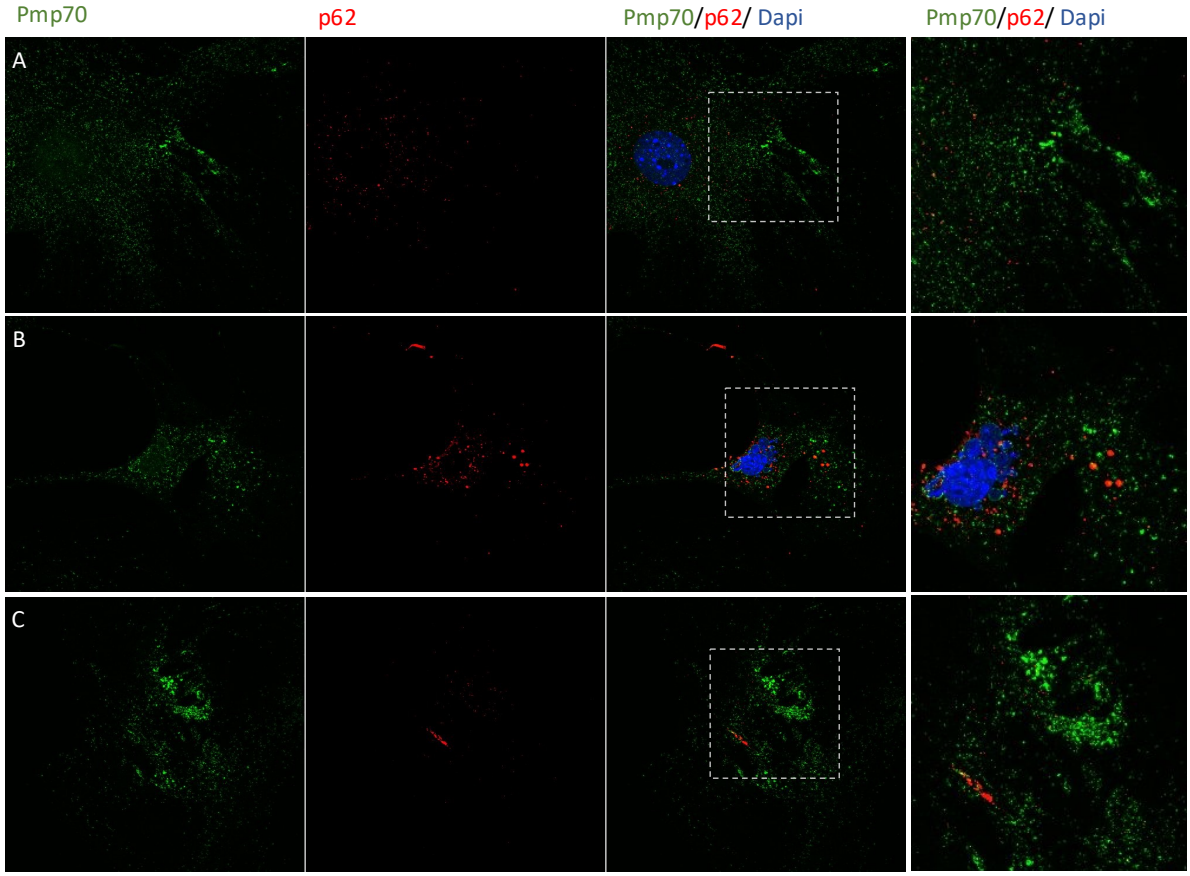

Figure 53. Pexophagy marker p62 does not localize to aggregates. Representative images of visual screening for p62 and aggregate co-localization. Senescent cells 8 days after irradiation or adriamycin treatment were immunostained for peroxisome marker Pmp70 (green), autophagy marker p62 (red) and Dapi (blue). **A-C)** Composite image of Pmp70, p62 and Dapi at the 3rd column of each panel. Last column corresponding to a close-up image of white square field indicated in the composite. Maximum Z-projection of spinning disk confocal microscopy images at 63x magnification are displayed.

Incidence of aggregates: association with senescence and p21

To validate the association between senescence and the observed peroxisomal aggregates, I quantified the number of cells containing aggregates in senescent and proliferating cells (Fig.54) using 2 models of senescence induction in parallel: irradiation and adriamycin. This confirmed that senescent cells presented significantly more aggregates than proliferating cells (Fig. 54 orange bars). The percentage of cells with aggregates was similar between irradiated and adriamycin-treated cultures (18,73% and 18,05% respectively), suggesting that this phenotype was associated to senescence in at least 2 different models.

Next, we decided to assess the role of p21 in peroxisomal aggregation. On one hand, I quantified the percentage of cells containing aggregates in cells with either unaltered or decreased p21 levels in both models of senescence, irradiation and adriamycin. To induce the knock-down of p21, day 6 senescent cells were treated with doxycycline for 2 days, while senescent controls remained in doxycycline-free media until day 8 after senescence induction, when they were fixed. This was the same as the samples used in the RNA-seq analysis that uncovered this association. This quantification showed no significant difference in the number of cells containing aggregates in senescent cells upon p21 down-regulation (Fig. 54, green bars for p21 knock-down). The same result was observed when later timepoints were analyzed (irradiated and adriamycin-treated senescent cells 12 days after

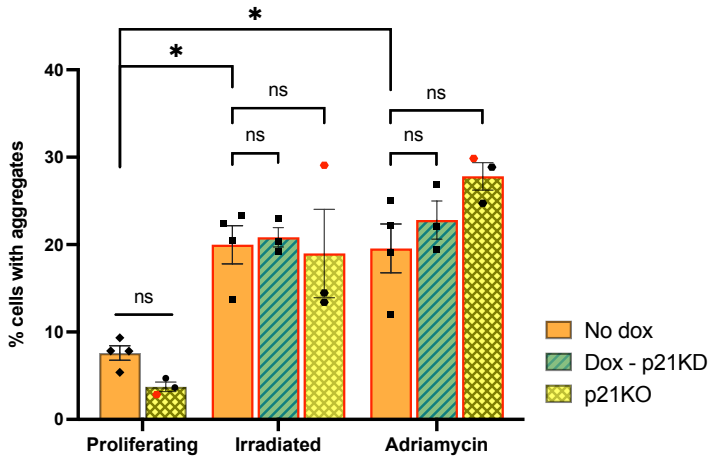

Figure 54. Aggregate presence in senescent cells. Percentage of cells containing aggregates in proliferating and senescent cells cultures. Senescence was induced 8 days after irradiation or adriamycin treatment. A 2 days doxycycline treatment was used to induce the knock-down of p21 in senescent cells 6 days after damage induction (green bars). Orange bars corresponding to proliferating and senescent cells with unaltered p21 levels. In yellow, p21 deficient cells (red dots for p21 "pseudo-knock out" cells, explained in the text). Aggregates were identified manually based on the visualization of the peroxisomal marker Pmp70 imaged by immunofluorescent microscopy. Significancy assess by p-value <0.05 by Wilcox test.

damage, untreated or after 6 days with doxycycline to induce p21 knock-down, n=1, data not shown).

On the other hand, we also decided to quantify peroxisomal aggregation in the complete absence of p21. It was hypothesized that the induction of p21 during senescence could be necessary for the appearance of the phenotype, even if its decrease during 2 days did not have an evident effect. For this purpose, I extracted dermal fibroblasts from the skin of pups from a mouse line deficient for p21 (p21KO), (Fig. 54, yellow). Cell cultures lacking p21 were treated as previously described for p21-inducible knock-down cells. 8 days after senescence induction via irradiation or adriamycin, they were fixed and stained against Pmp70. In addition, and because of time restrictions and small number of samples available, data from an experiment performed with a "p21 pseudo-knock-out" cells was included in the analysis of this condition (indicated by red dots, Fig. 54, yellow columns). The "p21 pseudo-knock-out" was produced using p21-inducible knock-down cells, but where the expression of p21 had been previously inhibited by continuous presence of doxycycline in the culture media before and during the experiment to induce and maintain p21 knock-down. At the moment of senescence induction by irradiation or adriamycin treatment, cells had been pre-treated with doxycycline for 7 days.

The number of cells which containing aggregates seemed reduced in proliferating cells in the absence of p21 (Fig. 54, yellow bars). While this trend was similarly observed in senescent irradiated cultures, the opposite happened in adriamycin-induced senescent cells (Fig. 54, yellow bars). However, none of these changes were statistically significant. Although I could not find any obvious effect associated with the lack of p21 in the number of senescent cells containing aggregates, these results were clearly inconclusive. The contradictory tendencies observed between both senescence models, the small number of samples, and the questionable inclusion of the "pseudo-knock-out" experiment, caused the interpretation of these results to be rather unreliable. Due to time constraints and the lack of an evident and noticeable effect on peroxisomal aggregates by p21 deficiency in senescent cells, we decided not to pursue this line of work. At the moment, the question of the requirement of p21 for aggregate formation in senescent cells remains unaddressed.

Conclusion on peroxisomes, senescence and p21

Pathway analysis of the RNA-seq results revealed a possible connection between senescence and peroxisomes, with a potential role for p21 in its regulation. Using immunofluorescence to visualize peroxisomes, an interesting phenotype resembling peroxisomal aggregates was

found to be enriched in senescent cells in 2 models of senescence induction. These aggregates contained catalase, an antioxidant enzyme key in peroxisomal function whose absence is commonly associated to defects in peroxisomal activity. Although based on the literature aggregates resembled clusters of peroxisomes undergoing pexophagy, our results did not support or refute this hypothesis. Preliminary observations of p62 staining suggested no co-localization between aggregates and this pexophagy marker, but the interpretation of this result was inconclusive. Finally, preliminary results suggested that p21 reduction in senescent cells, either via reduction in already senescent cultures by 2 days of knock-down, or in cells constitutively deficient in p21, did not significantly alter the incidence of aggregates in senescent cells. However, the number of replicates analyzed in these experiments was low, and the accuracy of the extrapolated conclusions in most of the cases is unclear. Although this line of work potentially was considered to be potentially interesting, it remains underexplored, and the obtained results should be interpreted with caution.

Immune recruitment: Cytokine secretion

When performing pathway analysis on the genes upregulated by p21 loss in senescence, I observed an enrichment of several terms related to the immune system. While p21 downregulation seemed to increase the expression of membrane proteins involved in the recognition of senescent cells by the immune system, (see Fig. 43), several classic SASP factors and cytokines were also upregulated (see Figs. 41 and 42). However, it was difficult to infer the extent of the impact that these transcriptional changes had on protein expression, end even less on cellular function.

To know if the observed increased expression of immune-related transcripts was reflected at the protein level, we decided to test if p21 loss could affect the secretome of senescent cells. By using cytokine arrays, the level of multiple secreted cytokines can be easily assessed in my samples. These arrays provide membranes with discrete dots containing bounded antibodies against a selection of cytokines. Upon sample incubation (and the addition of the required reagents), each dot produces a chemiluminescent signal proportional to the presence of a cytokine. In this way, the relative abundance of a panel of cytokines can be screened without the need of performing separate immunoassays requiring specific antibodies. Different samples can be compared by using different membranes in parallel.

To detect the changes in cytokine levels associated to p21 loss in senescence, I collected the conditioned media from senescent cells with unmanipulated or decreased levels of p21, and

I analyze them using a commercial cytokine array. I induced senescence by irradiation in proliferating fibroblasts, and 6 days later, half of the plates were treated with doxycycline to decrease p21 expression. At day 8 after irradiation, coinciding with the timepoint of the samples analyzed by RNA-seq, fresh media was supplied to the culture and collect it after 24 hours (Fig. 55A) This procedure was repeated twice, and a total of 4 supernatants were incubated with 4 membranes from a commercial cytokine array comprising a panel of 40 mouse cytokines and chemokines. This assay allowed the determination of the relative levels of the selected cytokines. The signal of each cytokine at different exposures was quantified according to the provided indications.

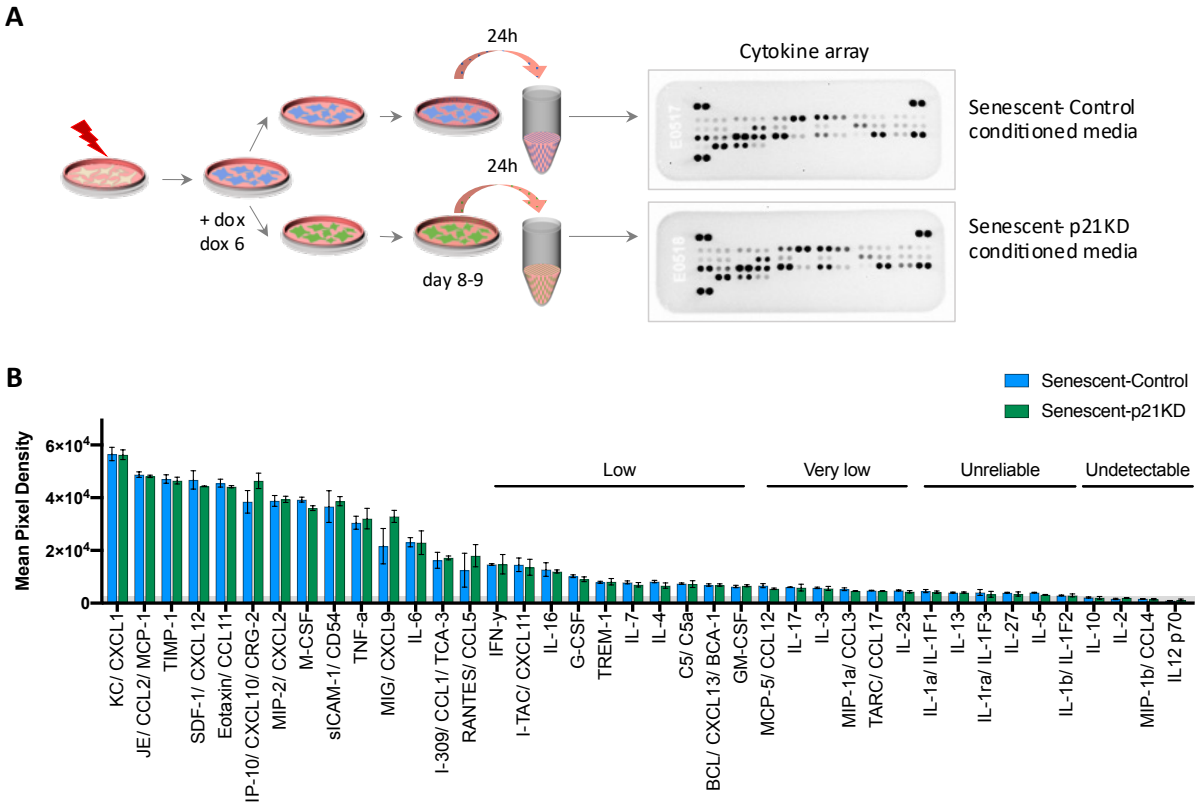

Figure 55. Cytokine array of senescent conditioned media. A) Schematic representation of the experiments. Cells were irradiated to induce senescence. After 6 days, half of the cells remained in doxycycline free media (control) and p21 knock-down was induced in the other half by the addition of doxycycline. At day 8 after irradiation, fresh media was supplied to the cultures, and 24 hours later, conditioned media was collected. After volume correction by the number of cells from each sample, the collected media was analyzed by cytokine array (real membranes from the experiment shown). The experiment was repeated twice (n=2). **B)** Mean pixel density of each cytokine. Quantification of cytokine signals from a representative exposition representing their relative abundance. Cytokines were ordered by average relative abundance from left to right. They were categorized as highly expressed (left, unspecified), low, very low, unreliable and undetectable. Bars of the mean expression of media from senescent control (blue) and p21 knocked-down senescent cells (green), error bar of the range (2 values per condition, n=2 experiments analyzed).

The signal between the assayed cytokines was very variable and I categorized them as *highly expressed*, *low*, *very low*, *unreliable* and *undetectable* (Fig. 55B, representative exposition). The signal of 27.5% of the cytokines was too weak for their expression to be contemplated (11/40, Fig. post1B, left side), being undetectable in 4% of them (4/40, Fig. post1B, *undetectable*). After discarding the cytokines with a very low signal (6/40, 15%. Fig. post1B, *very low*), only 24 cytokines (60%) were considered to display a strong enough signal to be reliable.

I calculated the relative fold change of these 24 cytokines upon p21 loss by comparing their level in media from senescent cells with decreased p21 expression to control senescent cells from the same experiment. Most of the cytokines showed a relatively small change upon p21 loss. From these 24, only 15 cytokines presented and average relative fold change in abundance of more than 10% (>1.1 or <0.90) when p21 was reduced (Fig. 56). The levels of only 8 cytokines displayed a fold change of more than 15% on average (>1.15 or <0.85): Cxcl12, Il-4 and Timp-1 decreased and Cxcl9, Cxcl10, Ccl5, Tnf-α and sIcam1 were upregulated by p21 loss in senescent cells.

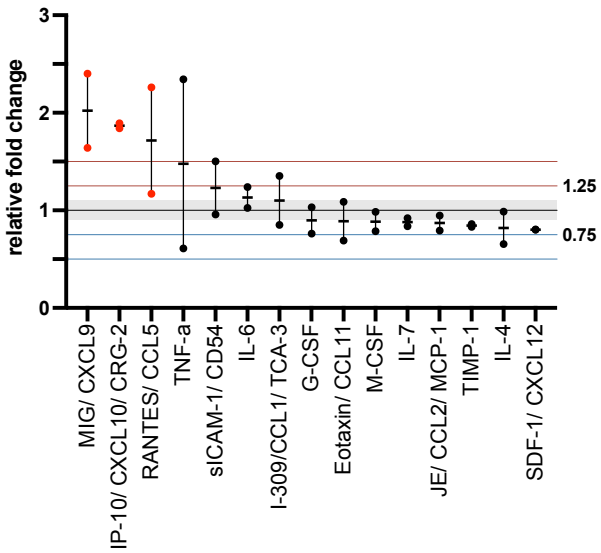

Figure 56. Relative fold change of selected cytokines in upon p21 loss in senescence. The abundance of each protein was assessed using the most representative exposure time for each cytokine. Cytokine abundance in the conditioned media of p21 knocked-down senescent cells was normalized to its correspondent senescent control. Represented cytokines were among the 24/40 most expressed proteins detected by cytokine array (Fig. 55B) and presented an average fold change of more than 10% (>1.1 or <0.9, grey zone). Dots depicting relative fold change in cytokine abundance in both experiments (n=2), horizontal line for the mean. Reliably altered cytokines by p21 loss in senescence in red (fold change >25%). Horizontal grids at fold change of 25% and 50% (0.75, 1, 1.25 and 0.5).

In order to confidently consider that the levels of a cytokine were altered by p21 loss, 2 criteria were established: they should present an average fold change of abundance greater than 25% (>1.25 or < 0.75), and its expression had to vary in the same direction in both experiments. Only 3 cytokines met these conditions: Cxcl9, Cxcl10 and Ccl5 (in red in Fig. 56). Interestingly, their secretion strongly increased in the absence of p21 in senescent cells, more than 70% (fold change of 2.02 for Cxcl9, 1.87 for Cxcl10 and 1.72 for Ccl5). Their transcription was also significantly increased in senescent cells without p21 when compared to proliferating cells (SD.vs.PC) in the RNA-seq analysis. Only Cxcl10 and Ccl5 transcripts were significantly increased by p21 knock-down in senescence (see Figs. 41, 42A), and they both were potential targets of Tnf-α (Fig. 44)[54,471,472].

This experiment supported the results obtained in the RNA-seq analysis, which suggested that the loss of p21 in senescent cells increased the expression of some SASP components related to the recruitment of the immune system.

p21 level in late senescence

Another interesting observation from the RNA-seq analysis was the fact that p21 loss seemed to potentiate some of the transcriptional changes associated to senescence cells. In some way, senescent cells with decreased p21 levels had acquired a "more senescent" phenotype. A possible interpretation for this would be that the decrease of p21 in later timepoints of senescence may be actually part of this physiological response, at least in some senescence contexts. In line of this idea, I had observed a that p21 protein levels tended to decrease from around days 7-9 after irradiation on when I characterized the time-course expression of p21 by Western Blot (see Fig. 12). Thus, I hypothesized that the forced downregulation of p21 in our model could have prompted a deeper, more advanced stage of senescence, where senescence-associated transcriptional changes would have been accentuated.

In order to explore this hypothesis, I tested p21 protein levels at later senescence timepoints by Western Blot (Fig. 57). I collected protein samples from senescent cultures at different days from day 6 after irradiation (Fig. 57A). Additionally, samples from previous experiments were also included in the analysis (Fig. 9,12,13). Since I had observed that irradiated mouse dermal fibroblast cultures could eventually resume proliferation in my hands (Fig. 48), protein samples were also collected from adriamycin induced senescent cells, which did not present this limitation (Fig. 57B).

The protein level of p21 was variable among experiments (Fig. 57). Some of this variability could be attributed to technical inaccuracies, such as an inexact protein quantification and uneven loading of some samples revealed by the tubulin signal, or slight differences in sample handling and methodology linked to the time distance between experiments. However, p21 signal was consistently lower at day 12 than at day 6 (or the closest earlier timepoint available) after the induction of senescence (Fig. 57). This tendency was observed in all experiments analyzed (no contradictory results were intentionally excluded), in both irradiated (Fig. 57A, n=7) and adriamycin-treated senescent cells (Fig. 57B, n=2). Indeed, p21 protein seemed to drop around day 8-9 after the induction of senescence, or even earlier in some cases (Fig. 57A1, A4, A7 and B1).

Importantly, more replicates would be needed in order to confirm these observations, especially from senescence models other than irradiation where the total and permanent proliferative arrest of the culture could not be guaranteed (Fig. 48). In addition, it is important to highlight that, although we observed a decrease in p21 protein in late senescent

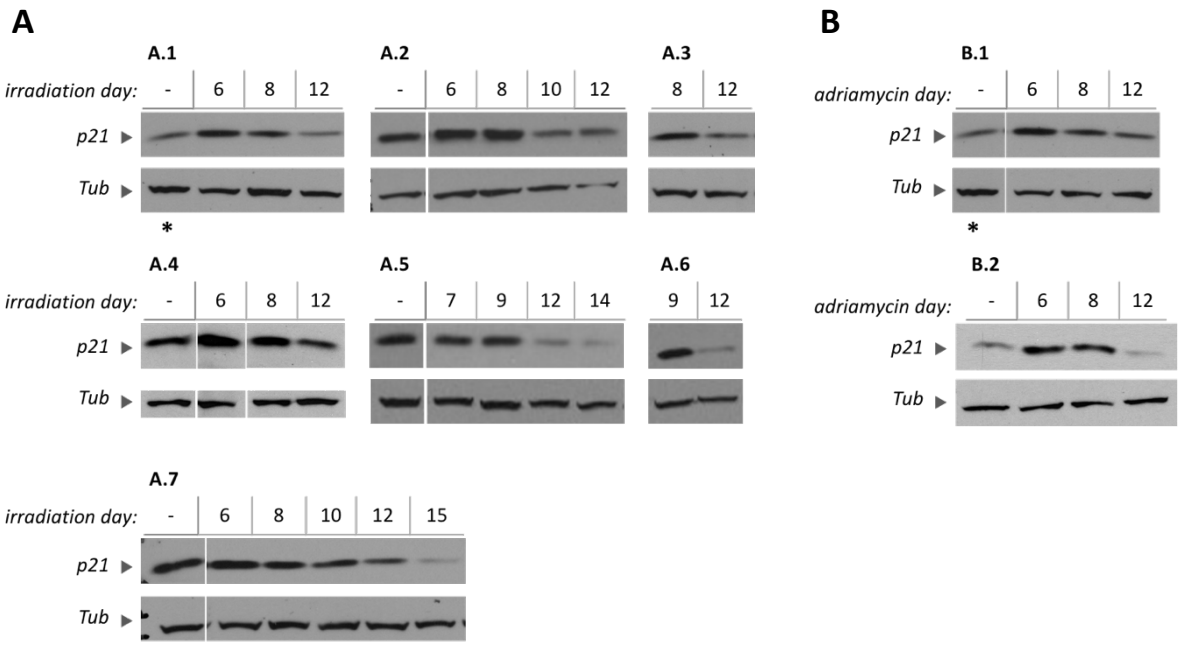

Figure 57. Protein level of p21 in late senescence. The level of p21 protein was assessed by Western Blot in late senescent cells, ranging from day 6 to 15 after the induction of senescence. **A)** Irradiation-induced senescence. A total of 7 experiments were analyzed. 2 of the images were already presented in figure 5 of this thesis (A4 and A7). **B)** Adriamycin-induced senescence. Protein samples from 2 experiments**.** Top panels for p21 signal (~18 KDa), bottom for α-Tubulin (~55 KDa), which was used as a loading control. Samples were collected at day indicated after senescence induction by irradiation (A) or adriamycin treatment (B), dash to indicate non-treated samples. Some images were cropped to exclude non relevant samples. Experiment A1 and B1 were done in parallel and they shared the same unirradiated control sample. This sample was only blotted once, and its image has been duplicated (marked by an asterisk).

cells in 2 different models, this may occur in other senescence contexts, such as with different senescence inductors, in other cell types, or *in vivo*. However, and after considering these limitations, my Western Blot results strongly supported the hypothesis that, while p21 increases in senescent cells during the first days after senescence induction, its protein level decreases at later timepoints.

Although this idea has already been proposed in the literature (see *Introduction: p21: Biological processes impacted by p21: senescence*), to our knowledge there is no clear consensus about the dynamics of p21 protein in late senescent cells. Therefore, the confirmation of this result would be a significant contribution to our understanding of the dynamics of p21 in senescence, entailing potential implications on its function in senescent cells.

4. Alternative approach: p21 interactome

4. 1 Protein interactors of p21 in senescence

The main research line developed to explore the role of p21 in senescence was focused on gene expression changes associated to p21 loss in senescent cells. However, parallel to these experiments, we also considered other experimental approaches to untangle this question. Specifically, we were curious to know more about the interactome of p21 in the senescent context. We presumed that discovering of novel interactors could uncover new functions potentially regulated by p21 in senescence. In addition, getting insight on the proteins interacting with p21 in senescent cells could shed light on the molecular mechanism behind the transcriptional changes observed in our RNA-seq.

p21 co-immunoprecipitation (Co-Ip)

In order to study the interactome of p21 in senescent cells, we decided to perform a co-immunoprecipitation of p21 and its interactors (Co-Ip), and to analyze it by mass spectrometry (MS). This would allow me to identify the interactome of p21 in senescent cells, and hopefully infer the cellular functions and molecular mechanism impacted by p21. To perform the Co-Ip, I used commercial Protein Sepharose G beads (Fig. 58B). The beads were bound to a specific antibody against p21 which, upon incubation with the protein extract from irradiated senescent cells (Fig. 58A), bound to p21 protein. The elution of the proteins captured by the beads contained both p21 and its interacting partners (Fig. 58B). As a control, I used an antibody against mouse IgG, which provided us a list of unspecific bindings. This experiment was repeated twice, and a total of 4 samples from 2 independent experiments were sent to the Proteomic Facility of the IGBMC, where it was analyzed by MS.

The effective and specific capturing of p21 by the beads was validated by Western Blot (Fig. 59). I loaded a total of 5 samples: the input (In), which was the protein lysate from senescent cells after its pre-clearing by incubation with beads without antibody, the supernatants (SN) -or flow-through-, containing the proteins that were not retained after incubation with the beads, and the elution (El), with the target protein and its interactors. Since the concentrations of the different samples were not measured, the amount of protein of each

sample was only estimated, and it was observed by Ponceau staining of the membrane (Fig. 59B).

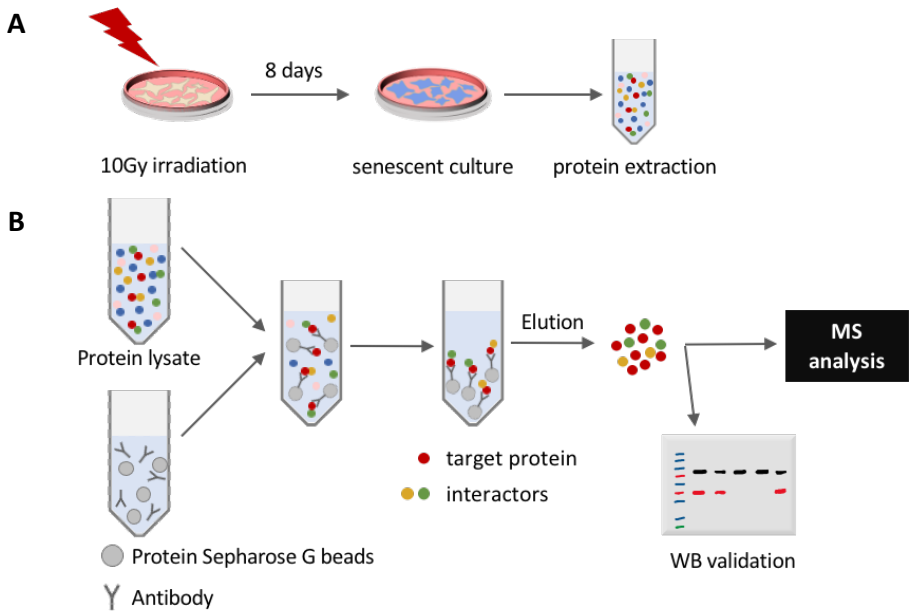

Figure 58. Co-Immunoprecipitation process. Scheme of the experiment. **A)** Protein samples were collected from senescent cells 8 days after irradiation. Co-immunoprecipitation was performed on these protein lysates. **B)** Protein lysates were incubated with beads associated with antibody against target protein. After pre-clearing steps, half of the protein lysate (input) was incubated with protein beads containing an antibody against p21 to detect specific interactors. As a control, the other half was incubated with beads associated to an anti-immunoglobulin G (IgG) antibody to detect unspecific binding. The presence or absence of p21 in the eluted fraction was validated by Western Blot (WB) before sending the samples to the IGBMC proteomic facility for mass spectrometry analysis (MS). The experiment was performed twice and a total of 4 samples were analyzed (n=2).

As expected, he presence of p21 by immunoblotting at ~18KDa was detected in the input (In), supernatants (SN) and the elution from p21-bound beads (El-p21) (Fig. 59A). Additionally, an unspecific band around 125 KDa in the input sample was observed, as well as a band corresponding to the heavy chain of the immunoglobulin antibodies (~55KDa) in the rest of lanes. Importantly, p21 was strongly enriched in the elution from beads incubated with the specific antibody against it (El-p21) in comparison to the elution from control beads incubated with unspecific antibody against IgG (El-IgG) (Fig. 59A, lanes 5 and 4). At the same time, the presence of p21 in the supernatant (the flow-through of proteins that were not collected by the beads) from beads capturing p21 (SN-p21) was lower than in beads holding IgG (SN-IgG), confirming that p21 was being selectively retained (Fig. 59A, lanes 3 and 2). Lastly, the relative abundance of p21 was clearly reduced in the supernatant (SN-p21) and

increased in the eluted (El-p21) fraction from beads bound to its specific antibody, further supporting the efficient capturing of p21 by the beads (Fig. 59A, lanes 3 and 5).

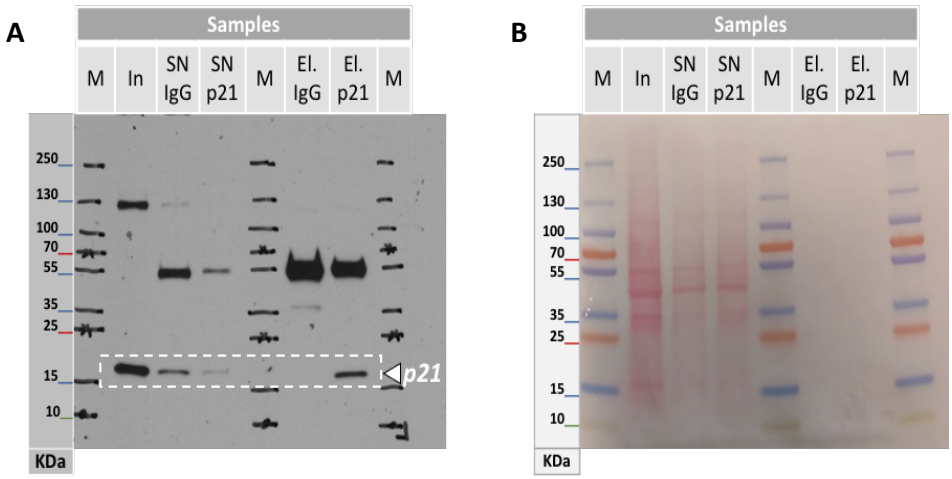

Figure 59. Co-Immunoprecipitation validation. p21 and its interactors were co-immunoprecipitated using protein G agarose beads with an antibody against p21. In parallel, an antibody against mouse IgG was used as a control for unspecific binding. **A)** Western Blot against p21 (~18KDa) of different fractions in the co-immunoprecipitation (Co-Ip) process. Heavy IgG chains(~55KDa) and unspecific bands (~130KDa) were also detected. The experiment was performed twice and a total of 4 samples, 2 p21 Co-Ip and 2 controls IgG Co-Ip, were sent for MS analysis (n=2). **B)** Ponceau staining of the membrane to show amount of loaded protein in each lane**.** Samples: M: marker, protein ladder; In: input, pre-cleared sample by incubation with beads; SN: supernatant, flow-through after incubation with beads and antibody; El.: elution; IgG: control antibody anti-mouse immunoglobulin G (IgG); p21: antibody anti-p21. Loading: In. 1% of the total input, 11.5uL; SN 1%, 5uL; El. 6.7%, 8uL. MS: mass spectrometry.

p21 localization in senescent cells

In order to correctly interpret the results from the MS, I decided to determine the major cellular localization of p21 in senescent cells. This information should provide the necessary context for the understanding of the potential functional meaning of p21 interactions revealed by the proteins detected though MS Co-Ip analysis. I performed immunofluorescence staining of p21 in senescent cells 8 days after irradiation, just in the same conditions that were used to obtain the Co-IP-MS samples. The imaging of p21 staining by spinning disk microscopy revealed a heterogenous intensity signal strongly and consistently enriched among the nuclei senescent cells (Fig. 60). Thus, it could be presumed that a significant number of p21 interactions would have a nuclear localization.

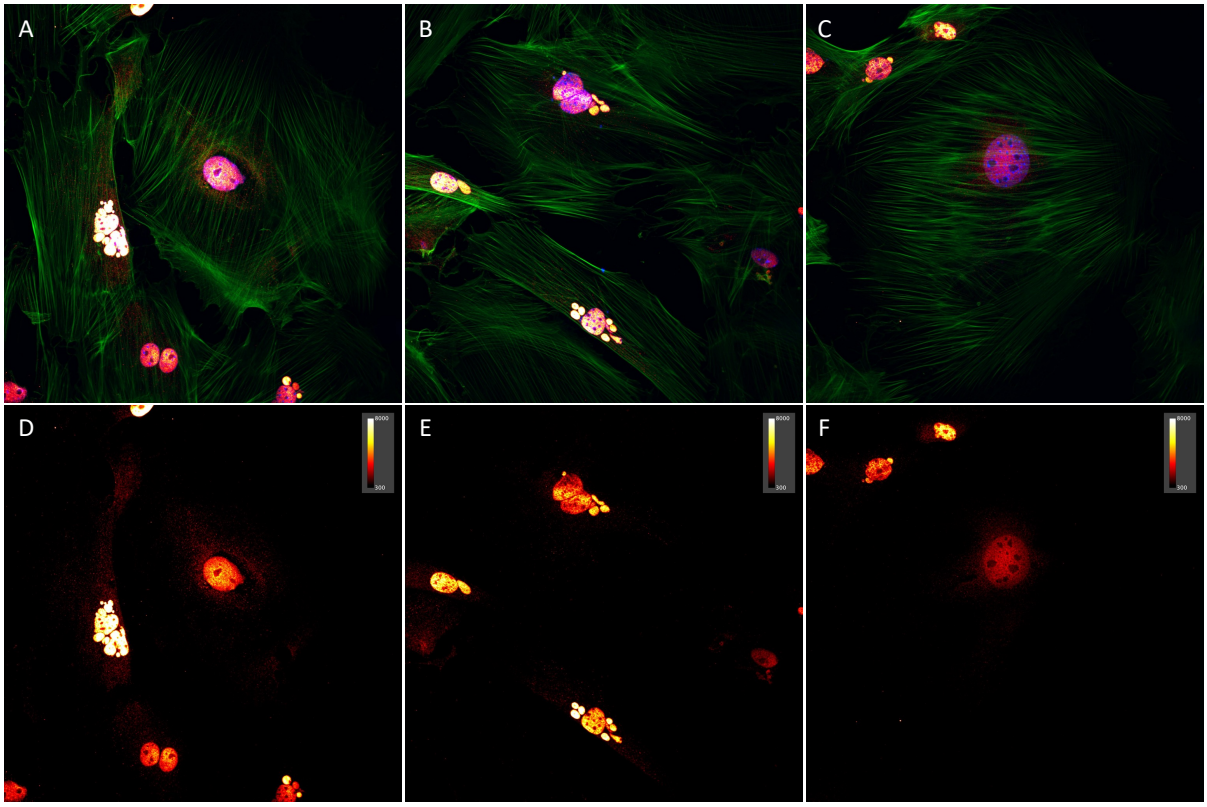

Figure 60. Nuclear localization of p21 in senescent cells. Immunofluorescence staining against p21 (red-white) in senescent cells 8 days after irradiation. Maximum Z-projection of spinning disk confocal microscopy images at 40x magnification. **A-C)** Composite of Dapi (blue), phalloidin (green) and p21 (red to white). **D-F)** p21 signal displayed in a colored scale corresponding to intensity of the signal, from dark red (low) to white (high). Color scale at top-right of the image.

Mass Spectrometry (MS) analysis

A report and a table format document (.xlsx) with the result from this analysis was provided by the proteomic facility. For each detected protein, raw and normalized values of its relative abundance in the 3 technical replicates performed were provided. These values were used to calculate the ratio of detection of the protein in the target samples compared to the background control, in our case, p21 and IgG captured proteins. To confidently determine the specific interactors of p21, the analysis included a statistical analysis (t-test) on the specificity of the binding. In this test, the enrichment of proteins in the elution sample corresponding to p21 partners when compared to unspecific bindings was evaluated. A protein was considered to interact with p21 when this enrichment was statistically significant (p-value <0.05). Since in their analysis samples were analyzed together, I performed additional statistic tests in both experiments separately in order to have more detailed information from each experiment.

A total of 200 proteins (not counting IgG) were detected through MS analysis. Initially, 79 proteins were considered as potential interactors of p21 (Fig. 61A), since they were enriched either in analysis of all samples combined, or in at least one of the experimental replicates when analyzed separately (after filtering out proteins that were significantly enriched in the unspecific elution in one of the experiments). In particular, 61 potential interactors were identified in experiment 1, and 41 in experiment 2, with 13 common proteins in both experiments when analyzed separately (Fig. 61A). When both experiments were analyzed together, as suggested by the platform, 40 proteins passed the significance threshold, including 12 of the 13 proteins commonly present in the separate analysis of the 2 replicates (Fig. 61A). The election of the potential binding partners of p21 was done combining the information from both analyses, and gave a final selection of 41 proteins. This list comprised all of the proteins from analyzing all samples together (40) and the common proteins detected in both experiments analyzed separately (1), which added Hspa5 (Fig. 61A and B).

These 41 interactors, as well as their abundance and the confidence in the identified interaction, was represented in figure 61B. The size of the circles assigned to each protein was determined by their relative abundance (ratio value of detection between specific and unspecific interactions). The confidence in the detected interaction was indicated by the border color of the circle. Proteins were classified in 4 categories depending on how certain their interaction with p21 was (Fig. 61B). A red and pink border was assigned to proteins that were detected in both experiments when analyzed separately, while orange and yellow corresponded to proteins identified only when both experiments were analyzed together. Then, red and orange represent interactions with a p-value <0.01 in the combined analysis. The certainty of the interaction was also reflected by the width of the line connecting each protein to p21 since it was relative to the p-value obtained in the combined analysis, expressed in -log10.

The color of the line between p21 and each partner distinguished novel (grey) from the previously reported (red) interactions, which were manually assess from consulting several mouse and human databases (*String*, *Integrated Interactions Database*, *Pathway Commons Protein-Protein Interactions through Harmonizome* and *Genemania webpage*). The proteins identified in our analysis included 11 known partners of p21: 3 cyclins (Ccnd2, Ccnd3 and Ccnd1), 3 cyclin-dependent kinases (Cdk4, Cdk5 and Cdk2) and another 5 proteins (Txn, Hsp90aa1, Hsp8, Hsp5 and Rab1). Interestingly, to our knowledge, some of the most abundant proteins identified had not been previously reported to be p21 interactors to our

knowledge, such as the cytoskeletal protein spectrin alpha chain (Sptan1), the mitochondrial Hsd17b10, or Serrate RNA effector module (Srrt), which is mainly involved in splicing and the processing of miRNA.

General description of p21 interactors

As a first exploration of this result, I classified the potential p21 interactors depending on their cellular localizations (Fig. 61C), molecular functions (Fig. 61D) biological processes (Fig. 61E) they were involved in. This was done by performing an exploratory pathway analysis through DAVID webpage. Using the results from the Gene Ontology databases, I created representative categories of the most overrepresented terms detected in each section (Fig. 61 C-E). The criterion for category selection was primarily based on the number of proteins associated to it, but the significance of the enrichment (p-value) was also considered. It is to be noted that the relative abundance of the proteins was not taken into account for this analysis. In addition, each protein could be assigned to more than one category.

Since the localization of p21 in senescent cells was observed to be mainly nuclear (Fig. 60), I expected to find many nuclear proteins among its partners. Indeed, 24 out of the 41 interactors were reported to have a nuclear localization (Fig. 61C). Moreover, if the relative abundance had been taken into account (not shown) this result would have been magnified, since some of the most abundant proteins detected could be found in the nucleus. Intriguingly, many of p21 potential interacting proteins could be found extracellularly (28) or in the membrane (21), and 12 of them could be part of adhesion structures.

When the molecular function was considered (Fig. 61D), many p21 interactors presented (or modulated) kinase activity (14). In addition, 10 proteins with the ability to bind ions, especially metals (8) and calcium (4), were noticed. Interestingly, I also observed 11 RNA-binding proteins, suggesting a potential way for p21 to influence gene expression at the level of translation. In line with the fact that 12 proteins could localize to focal or cell-to-cell adhesion structures (Fig. 61C), 6 cadherin binding proteins (Fig. 61D) were found.

As for the other biological functions that were related to the p21 detected interactome (Fig. 61E), cell cycle (8) and proliferation (13) were some of more common represented, supporting the known role of p21 in cell cycle regulation and proliferation inhibition. The regulation of apoptosis is another function described for p21, and accordingly, we found 10 proteins related to it. Another 8 proteins were suggested to regulate gene expression, and 5 to control the nuclear import. The connection between p21 and cellular adhesion was

strengthened by presence of 9 proteins with functions related to "adhesion" among its interactors (Fig. 61E). Surprisingly, 10 proteins with a role in migration were also found.

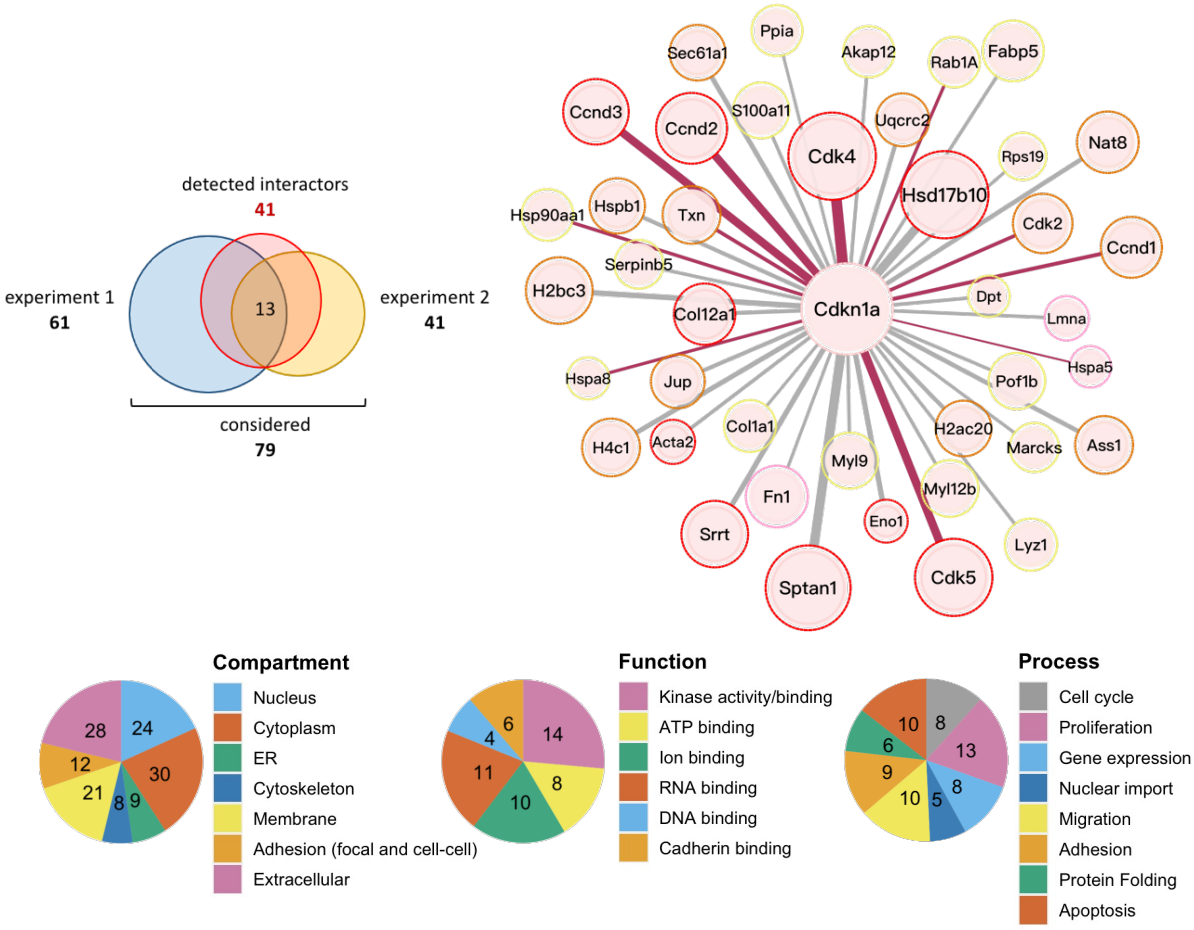

Figure 61. Co-IP MS identified p21 interactors. A) Number of interactors detected in each experiment. A total of 79 proteins were revealed to be potential p21 interactor: 61 in experiment 1 and 41 in experiment 2, when analyzed separately, with an overlap of 13 proteins. The combined analysis of all samples and all the common interactors detected in both experiments generated the final selection of 41 potential interactors that we analyzed in B-D. **B)** Interactors representation. Connecting lines thickness (edges) relative to p-value magnitude (in -log10). Dark red lines for known interactors. Circle (node) size relative to its abundance (not directly proportional), and border color relative to its certainty. Red and pink for interactors that were found in both experiments when analyzed independently (intersection of 13 in A). Red and orange for p-value <0.01 in the combined analysis of both experiments. **C-E)** Number of interactors belonging to the selected categories. Representative terms from Gene Ontology database from performing pathway analysis on p21 and its 41 interactors. Categories were created by grouping similar terms. **C)** Terms from Cellular Component. ER: endoplasmic reticulum. **D)** Terms from Molecular Function. **E)** Terms from Biological Process.

Conclusion of the analysis

The validity of the results was supported by the detection of several known interactors of p21. Although this preliminary analysis only served descriptive purposes, several novel possible interactors of p21 in senescence were identified, which could lead to the finding of new pathways potentially influenced by p21 in senescence. As an example, the 6th most abundant protein detected by Co-Ip MS was Serrate (Srrt), also known as Ars2, which is involved in cell cycle progression through the regulation of miRNA processing, thus influencing gene silencing[473]. Besides this function, Srrt is also necessary and sufficient to promote neural stem cell self-renewal[474]. Therefore, developing and validating these results could provide interesting and novel lines of investigation on pathways controlled by p21 in the future. Nonetheless, at this point a deeper analysis was still required.

DISCUSSION

1. Model considerations

A significant part of this work consisted of the validation of a newly generated mouse line, using primary dermal fibroblasts *in vitro*. The advantages and inconveniences of this model are discussed here. In addition, the problems and implications derived from the presence of areas of proliferation detected in -presumably senescent- irradiated cultures are next examined.

1. 1 Mouse model: p21 conditional knock-down

In this project, a commercially generated transgenic mouse model recently acquired by the laboratory was used to manipulate p21 levels in senescent cells (Mouse provider: Mirimus Inc., https://www.mirimus.com). As previously described, it was designed that doxycycline would induce the expression of a construct encoding for a reporter GFP signal and an shRNA against the transcript of interest (*Cdkn1a*/p21) in all cells from this mouse line. As this model had not previously been used in the lab, I validated the rapid and efficient reduction in p21 protein and transcript level *in vitro* in both proliferating and senescent cultures of primary dermal fibroblasts derived from the skin of newborn pups from this mouse line. Moreover, the reversibility in the expression of the construct was confirmed in proliferating cells, expanding the possibilities of use of this model.

This model of inducible (or **conditional**) **knock-down** of p21 presents some important advantages when compared to other commonly used models, such as constitutive knock-outs. Genetic robustness relies on the ability of cells and organisms to adapt and compensate the loss of a specific gene[475]. This is mainly mediated by either the presence of redundant proteins with overlapping functions or by adaptive changes in the expression of other genes of the same metabolic, signaling or transcriptional network. The compensatory tuning of the networks affected by a disrupted or absent gene is likely to occur early during embryonic development, enabling the adaptation of the organism to the alteration. This may explain why phenotypes related to alterations in specific genes are often observed in conditional models but not in constitutive ones[475]. For this reason, using a conditional approach to disable p21 expression may prevent processes of **compensatory adaptation**, which may mask the effect derived from the extinction of p21 function (reminder: the p21-constitutive knock-out has no major developmental phenotype). In addition, and interestingly, different compensatory mechanisms may become active when a specific gene is disturbed by total ablation (knock-

out) or forced reduction (knock-down). This may be dependent on the level of regulation at which the different feedback loops operate to control the expression and abundance of a protein[475]. Thus, **knock-down** models may be a useful and even more potent **alternative to complete deletion** systems.

The **regulation of p21** is complex: it occurs at multiple levels, affects different pathways and networks and is likely to involve many **feedback loops**. Perhaps one of the most illustrative examples of this complexity is the observation that p21 is actually able to downregulate the expression of its main activator, p53, by promoting its degradation[476,477]. The abundance of regulatory networks for p21 suggests a strong ability for cells to compensate p21 loss in basal conditions. In fact, **compensatory mechanisms** involving specific proteins or changes in the balance of biological processes have been described in p21 knock-out models[81,384,478,479]. Thus, approaches to compromise p21 activity other than the total ablation of the gene may be necessary to unmask the effect of its disruption. Altogether, this suggested that the use of a **knock-down strategy** may be preferred in the study of p21.

In addition, being able to target the expression of p21 in a time-specific manner is a crucial advantage, especially for its investigation in the context of **cellular senescence**. The role of p21 in senescence has been mainly related to its ability to block the cell cycle at the beginning of the senescent response. However, senescence is a highly dynamic program, and the contribution of p21 once the permanent cell cycle arrest has been established remains underexplored. Recently, in an article from 2017, Yosef et al. pointed at the importance of p21 function in **later stages** of senescence. By silencing p21 in fully senescent cells using siRNA with a similar goal to the one in this study, they provided evidence of its role in restricting DNA damage and maintaining cell viability in senescent cells[432].

Altogether, this indicates that **a mouse model** that offers the possibility to **knock-down** p21 in a **time-controlled** manner may provide novel and relevant information on the role of p21 in more advanced stages of the senescence response as well as in other biological contexts. In addition, unlike siRNA approaches, this mouse model allows the possibility to knock-down p21 expression *in vivo*. However, there are some limitations in the use of these models that are worth discussing.

The effect of doxycycline

To achieve a reduction in p21 levels, the expression of a construct containing an shRNA against p21 transcript was induced by the addition of doxycycline to the cell culture media of

cells derived from the described mouse line. Untreated cells from the same genetic background were used as a control for unmanipulated p21 levels. One concern of our model is the lack of a control for a possible **influence of doxycycline** separated from the effect of p21 reduction.

Doxycycline is a tetracycline antibiotic that is also clinically used to inhibit the expression and activity of matrix **metalloproteinases** (MMPs)[480,481]. One of its described targets is MMP9, whose expression is reduced by doxycycline treatment at the transcriptional level[482,483]. However, no reduction in Mmp9 was observed in cells treated with doxycycline in our RNA-seq data. On the contrary, Mmp9 increased its expression with the reduction of p21, upon doxycycline treatment. In addition, I could neither detect any other signal of the anti-inflammatory signature associated with doxycycline treatment described in the literature. Although a direct effect of doxycycline on our cells cannot be totally discarded, no evidence supporting this hypothesis was found in our data.

In order to fully discard a p21-independent effect of doxycycline treatment, samples from cells containing a variation of the same inserted construct but with a modified shRNA directed to an off-target sequence should be ideally used. The inclusion of this **control condition** was originally contemplated in the experimental design. Together with the p21 conditional knock-down mouse model described, another mouse line, generated by the same company, was acquired at the same time. The construct inserted in this line conserved the GFP reporter signal, but the encoded shRNA was modified to target a transcript of the *Luciferase* gene, which is not endogenously expressed in mouse cells. The presence of the construct was verified by genotyping, as advised by the commercial house (data not shown). However, primary dermal fibroblasts derived from the skin of these mice failed to express the reported GFP signal in the presence of doxycycline (data not shown). Since the lack of GFP signal could not be explained and the induction of the construct by doxycycline was not confirmed, this mouse line was considered unreliable and its use was abandoned. As an alternative, primary dermal fibroblasts from wild-type mice could be used as controls, in case it was considered necessary. If an interesting functional or transcriptional alteration associated with p21 knock-down was suspected to be affected by doxycycline, the effect of the drug could be tested in wild-type cells cultured in its presence and absence.

1. 2 *In vitro* skin dermal fibroblasts

All of the experiments in this study were performed *in vitro* using **primary mouse dermal fibroblasts** (MDF) derived from the skin of pups from the inducible p21 knock-down transgenic mouse line. As the principal component of the connective tissue, fibroblasts are present in all tissues and organs. They regulate tissue homeostasis through the synthesis and remodeling of the extracellular matrix (ECM) and the secretion of growth factors. Different stressors causing DNA damage or ROS accumulation can induce senescence in fibroblasts, which is accompanied by the production of a SASP[484,485]. By controlling the **ECM composition** and secreting signaling molecules, senescent fibroblasts affect the behavior of neighboring cells and contribute to a variety of biological processes, such as cancer progression, senescence spreading, wound healing, fibrosis, inflammation and aging[484–486]. In fact, senescent dermal fibroblasts have been proposed to be the main **drivers of aging** in the skin[484]. Because of their physiological relevance in senescence in addition to the previous experience in working with this cell type in the lab, we decided to use primary skin dermal fibroblasts to explore the role of p21 in senescence *in vitro*.

However, the results obtained can be influenced by the use of a specific cell type, MDF in this case. Keeping in mind the **cellular context** where the data was generated is crucial for the interpretation of the biological meaning of the signatures enriched in pathway analysis. For instance, it is not surprising that important processes of MDF were sensitive to senescence induction. Terms related to extracellular matrix composition, such as glycosaminoglycan degradation and extracellular matrix organization, were detected by pathway analysis of genes altered by senescence (Fig. 21). It will be curious to see if other cell types also share the same senescent and p21-loss associated features as those identified here.

In addition, as it occurs with any *in vitro* study, it is difficult to know how the obtained results would translate *in vivo*, in more physiological situations. This is especially relevant with processes that potentially regulate cell signaling and **cell-to-cell interaction** affecting other cell types, such as the immune system. For instance, pathway analysis of our RNA-seq data suggested that the loss of p21 in senescent cells may favor cytokine production and secretion (Fig. 39, 41, 42, 56) or the expression of natural killer ligands (Fig. 43). It would be interesting to know if p21 downregulation in senescence would functionally affect **neighboring immune cells**, either by altering their activation state, migration or their interaction with senescent cells. One type of assay to assess this would be the **co-culturing** of our cells of

interest (senescent MDF from conditional p21 knock-down mice with or without p21) with immune cells (for example Natural Killers) isolated from wild-type mice. Even simpler approaches, such as exposing immune cells to the conditioned media from senescent MDF with or without p21 to test the effect of their **secretome**, could also provide relevant information. However, this kind of experiments can be technically challenging; foreseen complications related to culture media compatibility, optimization of isolation protocols and the maintenance of viable Natural Killers could be expected. Another follow-up experiment that would be promising is the repression of p21 *in vivo*, something which is possible with this mouse model. Nevertheless, *in vivo* or co-culture experiments would only be sensible once more data supporting this line of work has been produced in our current model.

1. 3 Irradiation-induced senescence: a flawed model?

Irradiation was used to induce senescence in primary MDF cultures. **Ionizing irradiation** is commonly used as a radiotherapy treatment in cancer[442]. The exposition to irradiation causes DNA damage, mainly in the form of double-strand breaks. Depending on the level of damage inflicted and the efficiency of the DNA repair mechanisms, irradiation can lead to cell death or senescence in both normal and transformed cells. While high doses of irradiation tend to cause apoptosis, lower doses can cause unresolved DNA damage and the development of **senescence**[441]. In fact, irradiation is a common method to induce senescence *in vitro* in a variety of cell types, including dermal fibroblasts[442].

In order to study the role of p21 in senescent cells, primary proliferating dermal fibroblasts cultures were exposed to 10Gy of X-ray radiation. After 6 days (the chosen timepoint for p21 downregulation), the acquisition of **senescence was confirmed** by their change in morphology, positive SA-ß-gal staining, decreased proliferation (confirmed by decreased EdU incorporation) and the expected transcriptional changes associated with senescence, including the increased expression of the senescent markers p21 (*Cdkn1a*), p16 (*Ink4a*) and p19 (*Arf*) and the reduction of Hmgb2 and Ki67. Senescence acquisition 8 days after irradiation was further confirmed in the RNA-seq analysis. Pathway analysis on the genes differentially expressed in senescent cells compared to proliferating (SC.vs.PC) revealed changes associated with an arrest of proliferation, as well as in other terms related to a senescent phenotype such as lysosomes, cytokine production, extracellular matrix or vacuoles (Results: Fig. 21).

Despite these signs of confirmation of the induction of senescence, I noticed isolated **colonies of proliferating cells** eventually emerging in irradiated plates. These colonies could be detected earlier when p21 was reduced 6 days after irradiation. Over time, p21 knock-down seemed to favor an increase in their incidence and magnitude, as more and bigger dense areas were observed in crystal violet cell proliferation assays (Results: Fig. 48). The interpretations and implications of this observation are rather complex.

Resumed proliferation after irradiation

The appearance of small patches of apparently growing cells in senescent cultures was assessed by **visual observation** of irradiated plates over time and with **crystal violet** proliferation assays. In the latter case, senescent plates were fixed 2-3 weeks after irradiation, stained with crystal violet, and darker areas, corresponding with denser cellular regions, were attributed to proliferating colonies. Although the presence of proliferating cells in long-term irradiated plates seemed obvious, these methods are insufficient to detect them or quantify their incidence.

The **morphological** appearance of cells located in areas of presumed proliferation tended to be smaller than typical senescent cells, but the senescent state could not be determined by visual microscopic evaluation, especially since the cell shape of fibroblasts adapts to cellular confluence. On the other hand, crystal violet cell proliferation assays provide information on the global amount and distribution of cells only **at the moment of fixation**. While these denser spots seemed to expand over time, the contribution of processes other than proliferation, such as cell **migration** or the **selective survival** of the most packed areas, could not be totally discarded. To confidently assess the proliferative capacity of these cellular clusters, cells could be exposed to an **EdU pulse** shortly before fixation, at this later stage after irradiation.

In addition, an accurate **quantification** of proliferating colonies was difficult to achieve, mainly because of their heterogeneity in shape, distribution and size. Small colonies could have been easily dismissed, while bigger ones tended to merge, and colony borders often blurred. Theoretically, **clonogenic assays** (also known as colony of focus formation assays) could be performed for more accurate quantification. In these assays, often used to measure the efficacy of anticancer treatment on cell viability and proliferation capacity, the origin of each colony corresponds to single cells[487,488]. Although they would be useful to quantify and compare the number of non-senescent cells emergent in irradiated plates in different

conditions (unmanipulated and downregulated p21), the principal difference to crystal violet proliferation assays is that they require plating cells sparse enough to isolate them. However, **low density** plating of fibroblasts causes a drastic decrease in cell survival of fibroblasts, especially after irradiation. For this reason, clonogenic assays are **not suitable** in this case.

Effect of p21 knock-down

Due to these methodological limitations, it was difficult to assess the exact effect of p21 downregulation on the appearance of dividing cells observed in senescent cultures. Interestingly, the incidence, growth rate and speed of emergence of **proliferating areas** in irradiated plates remarkably **increased** upon **p21 knock-down**. While small patches of growing cells were only started to be perceptible about 2 weeks after irradiation, when p21 was reduced from day 6 after irradiation, they started to be appreciable about 10 days after irradiation, and were clearly detectable at day 12. Actually, the number and size of growing colonies 3 weeks after irradiation visibly increased in p21 downregulated plates, as observed by crystal violet staining (Results: Fig. 48). However, the **cause** for this is uncertain. While it is possible that p21 loss in irradiated plates favored the emergence of non-senescent cells that either avoided (bypassed) or reversed (escaped) senescence after irradiation, other explanations cannot be fully discarded.

The apparent increase in the **number of separate proliferating areas** could indicate that more cells failed to establish senescence irreversibly upon p21 downregulation. However, due to the technical limitations mentioned above, the number of growing colonies in irradiated plates was difficult to assess. In fact, the detection of proliferating areas is critically determined by their **growth rate**, since they are only spotted once they reach a certain size. In agreement with the literature[400], a boost in growth rate in proliferating fibroblasts upon p21 knock-down had been observed (see *Results:: Model validation:: Induced p21 knock-down validation:: Effective and reversible induction of p21 knock-down in proliferating cells: GFP expression upon doxycycline induction of the silencing construct*). On the other hand, it is possible that the absence of p21 could favor the **migration** on non-senescent cells from a colony, giving rise to separate proliferating clusters in other locations. Although I find this idea unlikely, p21 has indeed been reported to play a role in regulating cell migration[254,349]. In addition, pathway analysis revealed signatures associated to focal and cell-to-cell adhesion to be transcriptionally affected by the loss of p21 in senescent cells, suggesting that migration and adhesion processes might be altered in this condition (Results: Fig. 25 and 34).

Despite changes in proliferation rate and migratory behavior might have contributed to the observation of more non-senescent cells upon p21 knock-down, the overall presence of proliferating cells in irradiated –and presumably senescent- plates could be explained by two distinct mechanisms: **senescence bypass**, where non-fully senescent cells failed to completely establish senescence, or the **senescence escape** (or reversal), where fully senescent cells reversed their proliferation arrest. The downregulation of p21 could have favored these processes.

Senescence bypass

In this model, the establishment of senescence was assessed 6 days after irradiation, when p21 downregulation was induced. However, it is possible that a fraction of the cells considered senescent at that timepoint were actually in an early, **pre-senescent** stage where, despite presenting the associated markers, they were not fully committed to senescence. It has been proposed that different mechanisms are required for the **initiation,** or establishment, and the maintenance of senescence, which upholds its irreversibility[159,489]. While p21 induction mediates senescence establishment, it is thought to be dispensable for senescence maintenance[159,164,166]. Indeed, **p21 absence** has been shown to facilitate senescence **bypass**[372,423,424,490,491]**.** It is then possible that the loss of p21 in pre-senescent cells had favored their ability to avoid senescence. In this case, **delaying** the addition of **doxycycline** and induction of p21 knock-down to later stages could prevent senescence bypass by guaranteeing enough time for cells to fully establish an **irreversible proliferation arrest**. However, this strategy cannot overcome the important limitation that supposes the modest -but not negligible- presence of non-senescent cells observed in irradiated plates when p21 remained unaltered. This baseline of non-senescent cells would be presumably still sensitive to a proliferative boost caused by the loss of p21.

Senescence escape

Another possibility is that the increase in emerging proliferating cells in irradiated plates upon p21 withdrawal was not due to a failure in the establishment of senescence but to an actual **reversal** or escape from the senescence associated **growth-arrest**. In this case, p21 reduction 6 days after irradiation would have favored that some cells that had already developed complete senescence (as reflected by the senescent markers measured) could "reverse" their senescent phenotype and resume proliferation. Although senescence is defined as a state of irreversible arrest of proliferation, cell-cycle re-entry events in seemingly senescent populations have been occasionally described, especially in the context of **cancer**.

Interestingly, **p21 downregulation** has been associated with **resumed proliferation** and tumor progression in oncogene-induced senescence models[492,493]. The idea that senescent cells can re-enter the cell cycle can be typically **confronted** with two main arguments. The first one is that since senescence escape is mostly described as a product of external **experimental manipulation** (such as the genetic ablation of senescence mediators)[159,494,495], it might be a highly **artificial** event that is not representative of any physiological situation. The second objection is based on a circular reasoning by which if a cell is able to resume proliferation, then, by **definition**, it should not have been considered senescent in the first place. This is in fact a strong argument; it is objectively extremely difficult to refute. Most of the studies reporting tumoral proliferation emerging from senescent populations were performed in **mass cultures**. In this scenario, the presence of non-senescent cells cannot be totally discarded, and therefore, the origin of the replicating populations cannot be unequivocally attributed to senescent cells. In order to avoid this terminological and conceptual controversy, terms such as "senescence-like", "pseudo-senescence" or "dormancy" are sometimes used to refer to states that otherwise could be considered as examples of senescence escape[496]. Nevertheless, spontaneous resumption of proliferation in senescent cells in the absence of external interventions is still being claimed, and new compelling evidence supporting this hypothesis is accumulating[19,226,497–499]. Regardless of the exact frame-work and nomenclature adopted, the investigation of processes of spontaneous reversal of (senescence-associated) growth-arrest has made remarkable contributions to our understanding of the mechanisms regulating cell behavior in senescence or senescence related contexts. Thus, it is appropriate to stress that although critical evaluations and conceptual discussions are always legitimate and necessary, the importance and validity of results obtained in these studies should not be dismissed over **terminological** or **essentialist disagreements**.

Impact of re-proliferation

The unexpected presence of proliferating cells in irradiated senescence cultures is a **drawback** of the model, but it should not diminish the relevance of the results obtained. After all, these results still reflect the consequences of p21 loss in the context of senescence. In fact, **cellular heterogeneity** is observed when senescence occurs in more **physiological** situations, where senescent and non-senescent cells are in contact. In addition, knowing the distinction of the specific mechanisms behind the origin of proliferation re-entry may not be relevant for the interpretation of the results. However, this limitation should be evaluated and taken into **consideration** for a critical interpretation of our data. Furthermore, the

conclusions derived from this study should be validated in an **alternative model** of senescence, ideally after the total absence of proliferation under basal conditions could be verified.

Bulk RNA-seq data and pathway analysis

The most important repercussion of the presence of non-senescent cells in irradiated plates concerns the results obtained from the RNA-seq analysis. It is worth noticing that, upon p21 knock-down in senescent cells (SD.vs.SC) I could detect the upregulation of a transcriptional signature associated to proliferation (Fig. 25). There are certain **general limitations** to be considered regarding any pathway analysis of bulk RNA-seq data.

General methodological considerations

The first one is associated to the fact that in a **bulk** RNA-seq, cells are pooled together before their sequencing. For this reason, it is not possible to know if the transcriptional signatures detected respond to robust changes in small subpopulations of cells or reflects a general trend that can be detected in the combination of **heterogeneous** changes in gene expression distributed among the culture. Thus, a proliferation-related signature could be due to either the expansion of a subset of non-senescent cells due to increased proliferation upon p21 reduction, or to the re-expression of proliferation-related genes broadly affecting the majority of the cells.

The second can be applied to any **pathway analysis** process. Pathway analysis is based on statistically relevant associations between transcriptional changes and pre-existing "terms" in databases. Its accuracy is determined by the statistic tests applied and the configuration of the terms of the consulted databases, which in turn are based on the available biological knowledge. For this reason, the kind of biological functions or pathways that can be associated to the observed transcriptional changes depend entirely on the name and configuration of the **pre-existing terms** defined in each database**.** This can be a source of several common confusions. For instance, it is common for databases to contain redundant or overlapping terms. Because of their genes in common, related terms with different names can be simultaneously enriched, causing an **overrepresentation** of signatures referring to the same process when only the most enriched terms are considered. In fact, it was considered to be the case in my analysis, when several signatures related to the cell cycle processes were among the top terms enriched upon p21 knock-down in senescent cells (SD.vs.SC, Fig. 25). On the contrary, considering terms out of context, or unconsciously

focusing solely on terms with names fitting pre-established expectative, can contribute to **confirmation bias**. A common way of enforcing the unbiased interpretation of pathway analysis is the consultation of different databases. Thus, the enrichment of a term was considered to be relevant only when it formed part of a **broader consistent signature**, and when similar or related pathways were detected across **different databases**. Additionally, existing bioinformatic tools (such as certain Cytoscape packages) could be used to explore the composition and proximity of the pathways detected in order to further clarify the biological meaning of the enrichment of a term.

Concerns specific to the performed analysis

When considering the possible interferences that the unforeseen presence of **non-senescent cells** may have had on the RNA-seq analysis, it is worth mentioning that senescent samples were collected **8 days after irradiation**, 2 days after doxycycline addition to induce the knock-down of p21. At that time point, the presence of proliferating cells was unnoticeable by visual examination, and **minimal** as assessed by crystal violet stainings (Fig. 48). Based on these observations, the presence of proliferating fibroblasts 8 days after irradiation was estimated to be extremely rare. In consequence, their impact on the RNA-seq results may have been **negligible**. Yet, the current data is not sufficient to entirely confirm this assumption. Additional information on this could be obtained by performing **single cell sequencing** (scRNA-seq) on senescent cells with unaltered and downregulated p21 levels, which might provide critical information on the cellular heterogeneity of the culture, although at the expense of limiting sequencing depth.

Furthermore, the most relevant results obtained from the RNA-seq analysis were obtained by what was defined as a "**physiological interpretation**" of our data (*Results:: RNA-seq analysis:: Role of p21 in senescence: physiological interpretation*). To consider the effect of p21 loss in senescence besides its role as a mediator of the response, I focused on the genes that were activated or repressed by p21 specifically in senescence which could have an effect on the senescent phenotype when compared to control proliferating cells (Tab. 2, Fig. 36 and 38). In the way these genes were selected, the transcriptional signature associated with senescence that was dampened or reversed by p21 downregulation (Fig. 35) was excluded. In consequence, **this approach** should have **minimized** any alleged transcriptional effect caused by the **expansion of non-senescent cells** upon p21 knock-down.

Nonetheless, the best way to improve the reliability of my analysis would be to validate these results in a senescence model where the **total absence of proliferation** can be confirmed.

This can be achieved either through the optimization of the irradiation protocol, or by the use of an **alternative method** of senescence induction. Any of these approaches should be sufficient to detect any confusion derived from the flaws in our model as well as to corroborate the role of p21 in the regulation of specific functions in senescent cells.

Adriamycin as an alternative inducer of senescence

As an alternative to irradiation, I proposed to induce senescence by treating them with **adriamycin** (also known as doxorubicin), a DNA damaging drug that is also commonly used in the treatment of cancer. In agreement with the literature, preliminary results confirmed that an acute exposure to adriamycin produced the expected phenotypical and transcriptional changes associated with senescence in primary mouse dermal fibroblasts (Fig. 49). In comparison to irradiation, an early increase in cell death was observed. In addition, and importantly, **no proliferation** could be detected in plates treated with adriamycin, even upon the reduction of p21 at 6 days after drug exposure, as shown by crystal violet proliferating assays on cultures fixed 3 weeks after senescence induction (Fig. 48B). For this reason, adriamycin was considered to be a good **alternative model** of damage induced senescence that could be used to validate the results obtained in this work. Unfortunately, the lack of time prevented us from further developing and exploiting this tool.

2. Role of p21 in senescence: hypothesis examination

The principal aim of this thesis was to investigate the role of p21 in senescence independently of its well-known function of mediating cell cycle arrest at the onset of the program. The main set of data of this work consists on the transcriptomic analysis from a bulk RNA-seq on proliferating and senescent dermal fibroblasts with unmanipulated and downregulated p21. Pathway analysis on the changes resulting from comparing each of these conditions indicated that p21 might be regulating several cellular processes in senescence (*Results::RNA-seq analysis*). The involvement of p21 in some of them was further explored in complementary experiments (*Results::Hypothesis exploration*). In this section, I discuss some of the most interesting hypotheses derived from this data.

In my opinion, the principal result of this thesis supports an **anti-inflammatory** and **immunoprotective** role of p21 in senescence. These observations are in agreement with previous literature. A better understanding of the role of p21 in regulating the immunosurveillance of senescent cells may have important implications for the understanding and treatment of the pathological and beneficial processes affected by senescence. In addition, pathway analysis on the RNA-seq data clearly implicate p21 in the transcriptional regulation of processes related to cellular **migration** and **adhesion** [345,348–350,500]. Although it is already known that p21 contributes to the regulation of these functions, the exact mechanisms behind it are not fully understood, especially at the transcriptional level. For this reason, the transcriptional changes associated to the loss of p21 in relation to the regulation of the adhesion and migration of senescent cells are also briefly discussed here. Lastly, senescence induction as well as the loss of p21 in senescent cells altered the expression of several **translation** associated factors. Increasing evidence suggests that changes in the translation machinery (ribosome biogenesis, tRNAs and translation factors) regulate cellular functioning, affecting key molecular pathways in senescence. Thus, the potential importance of translation regulation is briefly commented.

2. 1 Immune clearance of senescent cells

In my opinion, the most interesting outcome of this work is the indication that the **loss of p21** in senescence may promote the detection and **clearance of senescent cells** by the **immune system**. This hypothesis is based on two results. First, the downregulation of p21 in senescent cells favored the transcriptional upregulation of the production and secretion of

cytokines, chemokines and SASP factors (Fig. 41 and 42). Preliminary results (n=2) from performing a **cytokine array** on the conditioned media of senescent fibroblasts confirmed the potent stimulation of the secretion of 3 chemokines (Cxcl9, Cxcl10 and Ccl5/Rantes) upon p21 reduction (Fig. 56). Secondly, p21 downregulation in senescent cells caused an important transcriptional induction of 4 out of the 5 main **ligands** of the Natural Killer (NK) receptor **NKG2D** expressed by our cells, as well as other regulators of NK activity (Il15 and Icam1) that have been implicated in the clearance of senescent cells[79,231,235] (Fig. 43). Mechanistically, the promotion of a pro-inflammatory phenotype that favors immune cell recruitment and senescence clearance could be mediated by the intensification of the **TNF-α** signaling[54,432] (Fig. 44).

p21 as a regulator of inflammation in immune cells

It has been described that p21 participates in the regulation of cells from the immune system in various ways. The absence of p21 in mice (and even in humans[501]) has been shown to promote the development of **autoimmune diseases** such as lupus-like disease and glomerulonephritis[415,502–506]. In these studies, the ability of p21 to suppress the progression of autoimmunity was associated to the regulation of **T cells** proliferation and reactivity, including their production of IFN-γ[504,506]. In addition, p21 also reduced the severity of experimental rheumatoid arthritis by controlling the innate immune response[418]. It has been shown that p21 modulates **macrophage** activation and **cytokine production**[365,416,418,507]. In macrophages, p21 has been shown to shift the balance between pro-inflammatory M1 to anti-inflammatory M2 macrophages by preventing the transcription of NF-κB targets, which is one of the principal pathways activating the SASP[365,507]. Therefore, the role of p21 in the regulation of inflammation goes beyond senescence clearance.

p21-dependent secretome

In 2000, Chang et al. showed that the senescence-like phenotype caused by **p21 overexpression** was accompanied by the transcriptional upregulation of senescence-related genes[325]. Most of the p21-induced genes identified by **microarray** in this study encoded **secreted proteins**, especially components of the extracellular matrix. Last year, Sturmlechner et al. reported that p21, mainly via Rb, activated the transcription of a complex **secretome** that mediated the recruitment of **immune cells**[436]. Although the p21-activated secretory phenotype (**PASP**) was independent from senescence, it partially overlapped with the senescent secretome (about 37% in irradiated MEF), suggesting that p21 may be an

important contributor of the SASP. The PASP had important effects on the **motility** of neighboring cells. PASP was able to attract **macrophages** *in vivo* and *in vitro*, mainly due to the chemokine Cxcl14, although it also stimulated **fibroblast migration** *in vitro*. Importantly, most of the PASP components were not targets of RelA/p65, the homodimerized transcriptionally active subunit of NF-kB, the main transcription factor of the SASP. On the other hand, in 2011, Coppé et al. reported that, although **p21 overexpression** induced a **senescence-like phenotype**, this was not accompanied by the expression of characteristic SASP factors[508]. In fact, their figures indicate that p21 overexpression actually **reduced** the basal levels of certain **SASP** components, such as IL8, IL6, CXCL1/GROa, CXCL3/GROg or OPG/TNFRSF-II (Supp-Fig.1B-C and Fig1A-B in Coppé 2011).

RNA-seq results: transcriptional regulation of the senescent secretome by p21

The results from our **RNA-seq** support and reconcile these previous observations on the role of p21 in establishing a secretome, which might actually not be in contradiction with the increased expression of SASP factors upon p21 knock-down observed in our data. To define the **PASP**, Sturmlechner et al. categorized as "secreted factors" all genes contained in the term "**extracellular space**" from Gene Ontology Cellular Component database. (GO:0005615, included up to the 2015 version of the database). A quick pathway analysis on the genes contained in this term showed functions related to cytokine activity, immune cell regulation, ECM remodeling, migration, angiogenesis, adhesion and proliferation (analysis of 1120 genes in the 2015 version of the term extracted from Enrichr. Gene Ontology 2021 databases were consulted using Enrichr). Some of these functions were enriched among the genes altered by the downregulation of p21 in senescent cells in my analysis (Fig. 25, 34, 37 and 39). While downregulated genes mainly corresponded to focal adhesion and ECM organization (Fig. 34A, Fig. 37), upregulated genes were associated to cell-to-cell interaction and the activation of pro-inflammatory pathways (Fig. 34B, Fig. 39). In this line, in a 2017 article, Yosef et al. already presented evidence of the transcriptional **downregulation** of **focal adhesion** genes following **p21 inactivation** in senescent cells[432] (Fig. 2E in Yosef et al. 2017). Altogether, this suggests that different subsets of secreted factors can be either activated or repressed by p21. My RNA-seq analysis proposes that, while **p21 promotes** the expression of **focal adhesion** proteins and some **extracellular matrix** components, it **limits** the activation of **pro-inflammatory** pathways in senescent cells. Yosef et al. obtained similar conclusions from their microarray analysis, although their work was oriented towards a more mechanistic study[432]. This hypothesis could be further confirmed at the transcriptional level through the **bioinformatic analysis** of other **available datasets**. For instance, to describe the PASP,

Sturmlechner et al. produced and studied RNA-seq data on human and mouse senescent fibroblasts upon p21 downregulation[436]. Since RNA-seq samples from both articles were produced in damage induced senescent fibroblasts (etoposide or irradiation in mouse MEFs and human IMR90), it would be interesting to know if similar conclusions would be obtained in other **senescence models**.

Protein level: regulation of the senescent secretome by p21

The significance of the role of p21 in regulating the senescent secretome at the transcriptional level can be better understood by assessing the impact of these changes at the protein and functional level. In this line, complementary to the transcriptional analysis, I assessed the effect of p21 downregulation on senescent cells analyzing their conditioned media by **cytokine array**. Importantly, the loss of p21 was accompanied by a notable increase in the abundance of Cxcl9, Cxcl10 and Ccl5/Rantes secreted by senescent cells (fold change of 2.02, 1.87 and 1.72 respectively). These chemokines can be secreted by fibroblasts and promote the migration and activation of different immune cells, such as T-cells, NK cells, macrophages and dendritic cells[509,510]. Interestingly, the levels of these chemokines are elevated in a number of inflammatory and autoimmune diseases[511–513].

The **methodology** of this analysis could be improved in different ways. The content of conditioned media can be quite variable, so increasing the **number of replicates** analyzed would help strengthen these results. In addition, the development of the membranes was suboptimal: since the **saturation of the signal** of all dots of the membrane was not reached, the detection range was limited. Increasing the potency of the reagents used to develop the membrane could significantly increase the sensitivity of the test, allowing analysis of the less expressed cytokines included in the membrane. In addition, since the SASP is known to be very variable depending on the model analyzed, other **cytokine array kits** including a higher **number of targets** might be considered. Lastly, and ideally, conditioned media from **wild type** senescent fibroblasts (MDF) treated with **doxycycline** could be analyzed as a control condition to discard any possible effect of doxycycline in my results. These technical improvements could potentiate the strength and the depth of the cytokine analysis of the secretome of senescent cells upon p21 downregulation.

p21-dependent senescence immunosurveillance by Natural Killers

Senescent cells have been shown to attract and interact with different **immune cell types** through their SASP, including Natural Killer cells (NK), monocytes/macrophages,

neutrophils, dendritic cells, T cells and B cells[235,514]. Many of these cell types have been shown to participate in the immunosurveillance and removal of senescent cells *in vivo*. Since several publications demonstrated that **senescent cells** are recognized and removed by **NK**[79,231,515], the presence of terms related in the results of the pathway analysis is particularly relevant (Fig. 33, Fig. 39).

A part from enhancing the expression of a pro-inflammatory secretome, p21 downregulation in senescent cells induced the transcriptional upregulation of ligands of the Natural Killer (NK) NKG2D receptor (Fig. 43). The expression of **NKG2D ligands** by senescent cells is critical for their recognition and elimination by NK[239,516,517]. Although it has been shown that senescent cells upregulate the expression of NKG2D ligands[231,239,517,518], the opposite trend was observed at the transcriptional level in our model (Fig. 43). Instead, NKGD2 ligands (Raet1d, H60b, Raet1e and Ulbp1) were strongly **induced only** upon **p21 reduction** (Fig. 43). This observation raised the question whether the decrease in p21 in later stages in senescence might be responsible for the expression of NKG2D ligands in other models, especially since p21 protein levels tended to decrease over time in irradiation and adriamycin induced senescence (Fig. 57). It would be very interesting to assess the expression of these ligands in later states of senescence at the transcriptional and protein level to see if they actually correlated to those of p21 physiologically.

In 2019, Muñoz et al. observed that some senescent cells expressing NKG2D ligands eluded their clearance by NK[239]. This was attributed to an increase in the expression of certain **matrix metalloproteinases** (MMPs), which shaded these ligands, removing them from the surface of senescent cells. In our data, senescent cells induced the expression of a number of MMPs (10/23), but most of them were **not affected** by p21 knock-down (Supp. Fig. 4). Only 4 MMPs were regulated by p21 in senescence: 1 decreased (Mmp11) and 3 increased (Mmp9, Mmp15 and Mmp24) their expression upon p21 knock-down. Importantly, -and despite the fact that their results were obtained in human cells and the functional equivalence in mouse might not be direct- none of the MMPs that were proposed to mediate the cleaving of the NKG2D ligands in the work of Muñoz et al. were induced after p21 loss. Thus, it is unlikely that the expression of NKG2D ligands upon p21 reduction in senescent cells could be counteracted by enhanced production of MMPs.

Apart from inducing NKGD2 ligands, p21 reduction in senescence was also accompanied by enhanced transcriptional expression of the cytokine **Il15** and the cell adhesion molecule **Icam1** (Fig. 43). Il15 has been shown to potentiate the expression of the NKG2D receptor in

T-cells and NK and to potentiate their cytotoxicity[519,520]. Icam-1 (or CD54) also mediates the adhesion and lysis capacity of NK by binding the LFA-1 ($CD11a^{ITGAL}$/$CD18^{ITGB2}$) and Mac-1^{CR3} ($CD11b^{ITCAM}$/$CD18^{ITGB2}$) heterodimeric integrin receptors expressed by lymphocytes[521–523]. In accordance with our data, the expression of Icam-1 has been shown to increase in senescence[524,525]. This upregulation has been shown to be dependent on **p53** or **NF-κB**, following **TNF-α** activation, which suggests that p21 downregulation might stimulate the transcriptional activity of these transcription factors. In addition, cytokine array of the conditioned media of senescent cells showed that the soluble version of Icam-1, sIcam-1, which has been proposed to be an inflammatory biomarker[523], tended to increase upon p21 reduction (Fig. 56). Moreover, **Cxcl9**, **Cxcl10** and **Ccl5**, the 3 cytokines whose secretion was remarkably enhanced when p21 was knocked-down in senescent cells (Fig. 56), are also known to stimulate the migration of NK, and the two last also potentiate their cytotoxicity[526,527].

Future experiments proposed

This thesis evidenced the ability of p21 to dampen the secretion of pro-inflammatory factors in senescence, as well as to prevent the expression of specific ligands that are crucial for the effective killing of senescent cells by NK. In order to reinforce and explore these hypotheses, these results should be strengthened and further developed. Ideally, the transcriptional effect of p21 downregulation in senescence should be **validated** at the protein level, and ultimately, functionally.

The expression of NK ligands at the protein level could be tested by **Western Blot**, although **immunofluorescence** analysis would be more appropriate to corroborate the expected membrane **localization**. However, due to the complexity of the regulatory molecules affecting immune cells interactions, the conclusions from this staining would be hardly conclusive. For this reason, directly testing the **functional** effect of p21 downregulation in co-cultures with immune cells might be preferable.

To determine the specifications that functional experiments require, I would consider repeating the **cytokine array analysis** of the conditioned media of senescent fibroblasts with and without p21 knock-down with some technical **improvements**: reaching saturation when developing the signal of all cytokines, and testing a broader number of cytokines by using a bigger array kit. To determine the effect of p21 loss in senescence beyond the specificities of the irradiation model (and the possible limitations associated to this approach previously

discussed in the *Model validation:: Irradiation-induced senescence: a flawed model?* section of the discussion), the experiment could be repeated in parallel using **adriamycin** as an alternative senescence inductor after previous **validation** of the transcriptomic results. The conclusion of these experiments could help in defining the target immune cells that could be functionally affected by p21 ablation, as well as to design tests to specifically assess the allegedly altered functions. Based on the current data, two kinds of functional assays should be considered

First, effects of the secretome of senescent cultures with reduced p21 on **motility** could be tested with **transwell migration** assays by exposing immune cells to the conditioned media of these cultures[436]. Immune cells could be obtained from the peritoneal fluid of adult mice, and the subsets of interest, presumably lymphocytes (and ideally NK and T-cells), could be enriched by FACS (Fluorescence Activated Cell Sorting) flow cytometry isolation using specific markers[436,528]. Alternatively, (once sufficiently justified by our data and ethically approved) conditioned media could be directly injected in the mice **peritoneal cavity** for the posterior recollection of the recruited immune cells[436]. Secondly, to assess the effects of p21 loss in senescence on the activation and cytotoxicity of immune cells, they could be **co-cultured** with senescent cells. Based on our data, **NK** would be the preferred cell type to test in this assay. After co-culturing them with senescent fibroblasts with normal or decreased p21, the viability, **activation** and **cytotoxicity** of NK could be quantified using known markers via flow cytometry[529]. Moreover, a complete validation of these hypothesis would involve testing them *in vivo*. The details of the required experiments could be defined based on the results obtained *in vitro*.

However, isolating and maintaining the viability of immune cells is known to be challenging. Due to the foreseen difficulties of these experiments, they would only be considered if robustly supported by previous data. On the other hand, it would be interesting to analyze the mechanism mediating the effect of p21 downregulation in senescence, especially if this was proven to have a functional impact on the recognition and removal of senescent cells. Some of the molecular pathways that could be presumed to be involved are discussed below.

Molecular mechanism behind p21 regulation of the immune response

The molecular mechanisms by which loss of p21 in senescent cells could potentiate the expression of a pro-inflammatory proteome are diverse. In 2017, Yosef et al. showed that the ablation of p21 in senescent cells intensified the **DNA damage response (DDR)**, activating

the TNF-α pathway and enhancing the transcriptional activity of NF-κB[432]. This was due to a resumption of the DNA synthesis, which lead to numerous double-strand breaks and micro-nucleation. In fact, the expression of NKG2D ligands by senescent cells was proposed to be dependent on the DDR[517,530].

Pathway analysis on genes repressed by p21 in senescence revealed their enrichment in **TNF-α** related terms (Fig.39). TNF-α is a pleiotropic pro-inflammatory cytokine that can promote the expression of a pro-inflammatory SASP by activating **NF-κB** as well as JNK/AP1 or p38 MAPK[531,532]. In 2017, Kandhaya-Pillai showed that the exposure to TNF-α causes DNA damage and ROS accumulation, and senescence acquisition in human cells[54]. From the 15 TNF-α targets described in that article and regulated by p21 in our RNA-seq, 12 of them increased upon p21 loss in senescence (Fig. 44). The activation of Tnf-α could be also observed by analyzing the behavior of the genes of the "TNF via NF-kB" term from the Hallmark 2020 database (Supp. Fig. 3). From the 56 genes regulated by p21 in this term, 44 were induced upon p21 downregulation in senescence. The enhancement of **NF-κB** transcriptional targets upon p21 loss in senescence would support the ability of p21 to repress NF-κB, as had been observed in macrophages and discussed here above[507].

The interactome of p21 in senescence could indicate possible molecular mechanisms mediating the activation of Tnf-α signaling upon p21 loss other than a potential direct increase in DNA damage events. The mass spectrometry (MS) analysis of the proteins co-immunoprecipitated with p21 (Co-Ip) in senescent cells revealed some known and novel partners. Among the known interactors of p21, some CDKs (Cdk4, **Cdk5** and **Cdk2**) and cyclins D (Ccnd2, Ccnd3, **Ccnd1**) were detected (Fig. 61). The activity, interactions and even localization of these proteins are likely to be affected by p21 loss in senescence. While Cdk4 and Cdk2 are mostly associated with cell cycle regulation, Cdk5 is considered an atypical CDK, mainly known for its role in the nervous system, which makes it an especially interesting interactor[533]. In fact, most cyclins and CDKs have been recognized to regulate other cellular processes apart from the cell cycle. Among other functions, many cell cycle regulators have been shown to have **immunomodulatory** effects[534]. For instance, a high throughput screening study identified CDK2 and CDK5 as modulators of **NF-κB** activation by **TNF-α**[535]. Kandhaya-Pillai et al. proposed that TNF-α was able to induce senescence by triggering a positive feedback loop with STAT1/3 proteins[54]. Interestingly, **CDK5** has been shown to activate **STAT3** when interacting with p35 (Cdk5r1) [536,537]. **Cyclin D1** has also been shown to modulate **STAT3** activity, by repressing it[538]. The hypothetical stimulation of STAT3 upon

p21 downregulation in senescent cells could also affect other transcriptional regulators of the senescent program. Activation of **STAT3** by CDKs was shown to induce the expression of c-Fos and JunB, members of the **AP-1** family, which is an important regulator of the senescence transcriptome, including the SASP[55,536]. It is worth noticing that **p21** has been directly connected to the reduced **NF-κB** and **STAT3** function for decades, so an increase in the activity of these transcriptional factors upon p21 loss would be expected[357,361]. Altogether, the interaction of p21 with CDKs and cyclins might not only be relevant for cell cycle regulation but also as a potential molecular mechanism regulating the proposed p21 repression of a pro-inflammatory transcriptome in senescence.

Moreover, p21 loss in senescence might potentiate the expression of an immunosensitive phenotype though additional or alternative mechanisms. Due to the multiple and pleiotropic known activities of p21, many pathways might be hypothesized to be involved. Among them, the possible implication of **p53** should not be overlooked. It has been proposed that p53 is mainly an activator of transcription, and its repressive functions are indirect and mediated by its direct targets, such as p21[353]. Interestingly, pathway analysis on the genes repressed by p21 in senescence revealed terms mentioning p53 to be enriched in most consulted databases (Fig. 39). Although this could be due to the de-repression of DREAM targets as indicated in Fig. 40, I wonder if it could also partially be attributed to a direct potentiation of p53 following p21 loss. While p53 is well recognized as the principal transcriptional inductor of p21, the ability of p21 to stimulate p53 degradation is much less discussed[476,477]. Consequently, in a senescence model where p53 is expected to be induced upon DNA damage, it is especially relevant to consider that the transcriptional changes following p21 ablation could be partially due to an increase in p53

2. 2 Cellular adhesion and migration

As mentioned in the introduction, p21 is known to regulate cellular adhesion and migration (*Introduction:: p21-Cdkn1a:: Cellular functions regulated by p21:: Cellular migration and cystoskeleton dynamics*). However, the specific effect of p21 in these processes in the context of **senescence** has been underexplored. For this reason, the **transcriptional** regulation of genes involved in migration and adhesion by p21 as well as the list of its **interactors** in senescence could represent a relevant contribution that is worth mentioning.

It has been suggested that p21 promotes migration and cytoskeleton remodeling **via protein-protein interaction** with cytoskeleton regulators in the **cytoplasm**[344,345,348]. In line

with this, the analysis of the **interactome** of p21 in senescence revealed many of its known and novel partners to be part of the cellular membrane, cytoskeleton, focal and cell to cell adhesions, or to be secreted, possibly and affecting migration and adhesion (Fig. 61C-E). This suggests that, through these interactions, p21 might possibly mediate or influence cellular adhesion and migration in unknown ways. However, and taking into account that p21 localization was found to be mostly nuclear (Fig. 60), it cannot be discarded that these results could be influenced by technical **artifacts**. To gain insight into the cellular context of p21 interactions, the cytoplasm and nucleus of senescent cells could be dissociated using centrifuge-based protocols, and the interactome of p21 in **each compartment** analyzed separately via Co-Ip followed by MS.

On the other side, at the **transcriptional** level, pathway analysis suggested that p21 regulates cell **adhesion**, cytoskeleton remodeling and the **extracellular matrix** (affecting migration and adhesion in turn), in both proliferating (Fig. 23) and senescent cells (Fig. 25). These observations are in agreement with previous publications, where p21 in senescence-related models was shown to affect the expression of genes involved in these processes[325,432,436]. Although these transcriptional changes could be partially due to secondary adaptations to the alterations in cytoskeletal dynamics occurring at a protein level, it is possible that p21 might be controlling the expression of these genes through a more **direct mechanism**. In fact, p21 has been shown to regulate cell migration by interacting with Smad3 and Slug transcription factors and acting as a **co-transcriptional** regulator in cancer cells[349,350]. Therefore, it is likely that other partners of p21 to have similar roles.

Importantly, our Co-Ip MS analysis identified **junction plakoglobin** (Jup) as candidate novel interactor of p21 in senescent cells (Fig. 61B). Junction plakoglobin (also known as PG for plakoglobin, γ-catenin and Ctnng) is a component of **adherens junctions** and desmosomes[539]. Besides being part of cell-to-cell adhesions, Jup controls cellular adhesion and migration by participating in different **signaling pathways**, such as Wnt, Sonic hedgehog, Src and Ras[539]. Moreover, Jup has been shown to regulate **transcription** by binding different transcriptional factors and regulators; either sequestering them in the cytoplasm or promoting/repressing their activity in the nucleus[539]. Remarkably, Jup has been shown to collaborate with **p53** to regulate transcription via direct interaction[540–542]. Since p53 targets were significantly enriched among the genes repressed by p21 in senescence (Fig. 39), it is feasible to think that the putative interaction of Jup with p21 in senescent cells might prevent its association with p53 and the consequent stimulation of p53 transcriptional

activity. Therefore, the previously unreported interaction between p21 and Jup could represent a promising **new mechanism** mediating the transcriptional control of p21 in senescence. As a first step for the exploration of this hypothesis, **immunofluorescent** staining of these proteins could help to infer their interaction in the cell, as well as to assess the localization of Jup in the presence and absence of p21 in senescent cells.

2. 3 Translation and ribosome biogenesis

Pathway analysis on the RNA-seq data indicated that the expression of genes implicated in translation was affected by senescence induction and by p21 loss in senescence (Fig. 26, 37, 45).

Interestingly, translation and ribosome biogenesis are altered in **senescence**. While ribosome biogenesis and translation are globally repressed in senescent cells, the translation of specific proteins is selectively increased, including lysosomal proteins and SASP factors[543]. Increasing evidence suggests that the translation machinery, including tRNAs[544,545], ribosomes[546], and translation factors[547], is a critical **post-transcriptional regulator of gene expression**, determinant for controlling cellular function. For instance, ribosomal biogenesis has been shown to regulate **dsDNA-sensing** and inflammation[548,549], processes implicated in the expression of the SASP in senescent cells[37]. Considering **senescence** specifically, perturbation of **ribosome biogenesis** seems to be required and sufficient to its establishment[550]. In fact, a number of ribosomal and translation factors have been shown or suggested to contribute to the acquisition of senescent phenotypes[543]. For instance, several ribosomal factors (RPL11, RPL5, RPL23, RPL27 and 5S RNP)[551,552] promote **p53** stabilization by interacting with MDM2, RPS14 interacts with CDK4 acting as a **CDKi**[553], and the translation elongation factor eIF2a controls the SASP regulator **NF-κB** [554].

The expression of **translation-related** genes affected by p21 downregulation in senescence was represented in a heatmap, which showed, with some exceptions (including Rpl11), a general transcriptional drop of these factors upon p21 loss, which in most cases accentuated the tendency associated to senescence induction (Fig. 45). Despite that I consider this a result worth mentioning, the possible interpretations are far from being obvious. This is mainly because the study of the non-canonical functions of the expression of translation factors is a complex undeveloped **emerging field**. Nevertheless, it indicates that the modification of the expression of translation factors could represent an additional layer of regulation in p21's control of the senescent phenotype. In line with this, it is interesting to notice the presence of

11 RNA binding proteins among the p21 **partners** identified by **Co-Ip MS** analysis (Fig. 61), which further suggests that p21 may be -direct or indirectly- regulating gene expression at the **post-transcriptional** level by unreported mechanisms.

Rplp0 and housekeeping genes

Unexpectedly, one of the translation genes altered by senescence and p21 was *Rplp0*, the chosen **housekeeping** transcript used as a reference for the normalization of RT-qPCR values. Despite that *Rplp0* was selected as a reference gene precisely because its expression seemed stable across RNA samples of different conditions when analyzed by RT-qPCR, RNA-seq data showed that it was **significantly downregulated** upon senescence induction and after p21 knock-down in senescence (Fig. 45). However, its transcriptional reduction was relatively small in these conditions, a fold change of 0.789 in senescence (SC.vs.PC), 0.904 upon p21 loss in senescence (SD.vs.SC), and not significant when p21 was reduced in proliferating cells (PD.vs.PC).

In order to find a better reference gene for future RT-qPCR analysis, the expression of 14 commonly used housekeeping genes[555] was evaluated in a heatmap, and only 6 of them did not vary significantly in the evaluated comparisons: *Tbp*, *Pgk1*, *Gapdh*, *Ywhaz*, *Sdha* and *Ubc* (Supp. Fig. 5). To assess the impact that the use of *Rplp0* may have had on my results, some RT-qPCRs were repeated with *Gapdh* as a reference gene (data not shown), which did not substantially alter the previous conclusions. Nonetheless, *Rplp0* is not to be used as a RT-qPCR reference gene for future experiments examining changes in senescence in mouse dermal fibroblasts. This result highlights the importance and complexity of finding **adequate** reference **controls** for each experimental technique.

3. Physiological dynamics of p21 in senescence: a promising perspective

Although at a quite variable rate, the level of p21 protein in senescent cultures consistently decreased around 8-9 days after irradiation, as observed by Western Blot (Fig. 57A). Remarkably, preliminary results suggest that this trend was also maintained when senescence was induced by an acute exposure to adriamycin (Fig. 57B), suggesting that this reduction cannot be attributed to an amplification of non-senescent proliferating populations in the irradiated plates. Curiously, among the **interactors** of p21 detected by Co-Ip MS, two regulators of **p21 protein stability** were found: Cdk5, which promotes its degradation, and Hsp90 (as Hsp90aa1), a chaperone that can regulate its stability[307,556]. In my opinion, the **reduction of p21** protein in late stages of senescence is **extremely relevant** to evaluate the potential impact of my results.

Despite that p21 upregulation is commonly used as a marker of senescence, especially *in vivo*, a **decrease in p21 protein** as senescence advances has been repeatedly documented in the **literature**. In fact, it is commonly accepted that while p21 is key for the cell cycle arrest at the beginning of the establishment of senescence, this function is later on maintained by p16, another CDKi, and at that point, the levels of an irrelevant p21 are reduced. When this idea is mentioned, it commonly involves the citation of 3 articles, all from the end of the 90s[164–166]: Alcorta et al. 1996, Robles et al. 1998 and Stein et al. 1999. However, aside from this thesis, this same behavior of p21 levels can be observed in other more recent publications, though it is not specifically discussed. A list of **examples** include Chen and Ozanne 2006, Fig1; Muthna et al. 2010, Fig. 4A; Cmielová et al. 2011, Fig. 4A; Capparelli et al. 2012, Fig.2A; Dalle Pezze et al. 2014, Fig. 1B and E; Kirschner et al. 2015, Fig 1C[25,97,211,328,557,558] (Supp. Fig. 6). It is interesting to notice that all results from the examples previously mentioned were obtained ***in vitro***, and although senescence was triggered by various stimuli, none of them was via oncogene activation. Thus, it is possible that the observed decrease of p21 at later stages of senescence is **restricted** to specific **senescence triggers** or cell types. However, even in situations where p21 is actually reduced in late senescence, it might not return to the basal levels of proliferating cells. In this case, this event could have easily been **underestimated**, since it would be undetectable if comparing a single senescence timepoint to a non-senescent control, which is a common approach in senescence studies.

Since a reduction of p21 in late senescent cells is likely to be a real and common event, it is necessary to wonder what is the **physiological** situation that the forced reduction of p21 6 days after irradiation performed in this work is actually modeling. Would the transcriptional changes associated to p21 knock-down still occur at later timepoints when reduction of p21 occurs naturally? This hypothesis seems fascinating, and it could be **explored** with relative simplicity. For example, by assessing the expression of some interesting genes whose **transcription** was found to be potentially regulated by p21 in the RNA-seq analysis (such as Hmgb2, the NK ligands, Ccl5 or Mmp9) at **later stages** of senescence, 10 and 12 days after damage induction for instance. Since some proliferative colonies emerged in irradiated plates over time, their potential effect should be taken into account, and their presence should be minimized. For instance, these results could be validated in samples with a total absence of non-senescent cells, for which the **adriamycin** induced senescence model would be a great alternative. If transcriptional analysis supported a connection between the unmanipulated drop of p21 and the increase in pro-inflammatory SASP factors at later timepoints, **cytokine array** of the conditioned media could be used to verify it at the protein level.

Through these simple experiments, we could know if the effect of a time-dependent and unmanipulated drop in p21 is functionally comparable to its forced depletion by the knock-down strategy applied at earlier timepoints. If it was not the case, it would be interesting to investigate the **mechanisms** operating during this time window to establish a senescent phenotype **insensitive to p21** levels. In turn, this scenario could help to unravel new pathways and processes critically controlled by p21 during the initiation of senescence establishment.

On the other hand, if the **reduction of p21** was found to exert similar transcriptional (and potentially functional) changes when **occurring naturally** at later stages, it would have significant implications for our understanding of the senescent process. How are the dynamics of p21 in senescence ***in vivo***? Are they similar in **animals** with better **regeneration** capacity such as axolotl, zebrafish or salamander[559], or especially resistant to pathological **aging** such as naked mole rats[149,560]? Is it possible that the impairment of the natural downregulation of p21 in late senescent cells could prevent their elimination by the **immune system**? Is the downregulation of p21 being compromised in aging or in other **pathologies** associated to senescence? If it was the case, could an abnormal stabilization of p21 be part of the underlying causes of the detrimental accumulation of senescent cells observed during **aging**? And if so, could it be averted? This could open the venue for possible **therapeutic**

interventions targeting p21 to improve senescence associated conditions. Moreover, these questions are especially relevant when considering that the transient presence of senescence can be **beneficial** in some contexts, such as in development, tissue regeneration and wound healing[6,559]. Thus, in contrast to, or even in combination with, the use of senolytics, promoting the natural clearance of senescent cells by enforcing the -presumably- physiological downregulation of p21 could allow them to exert their beneficial effects while still avoiding the detrimental consequences of their accumulation. Although all these ideas are based on -educated- speculations, I believe them to be illustrative of the **potential** that I foresee in continuing this line of investigation, in which the results of this thesis may have contributed.

MATERIALS AND METHODS

Mice and genotyping

A bitransgenic mouse model enabling the inducible expression of an interference RNA (iRNA) against *Cdkn1a* was purchased from Mirimus company (C72-0530). Animals were bred into C57B6J strain following company indications at the Institut clinique de la souris (ICS), platform of the IGBMC. The genotyping of the line was performed using a piece of tail tip (Mouse Direct PCR Kit, Bimake) according to the genotyping protocol provided by the company. These animals were used to generate primary cellular cultures of skin dermal fibroblasts.

Isolation and culturing of primary cells

Primary mouse dermal fibroblasts were isolated from the skin of 0-1-day old mice. Newborn pups were euthanatized by anesthetic injection (2:1 ketamine/xylazine in NaCl solution), their skin was dissected and incubated overnight in 2.5mg/mL dispase II (Sigma-Aldrich 04942078001) in PBS at 4°C, floating on the epidermis. Next morning, dermis was separated from epidermis, minced with sterile scissors and incubated in pre-filtered 2.5mg/mL collagenase A (Roche 10103586001) in PBS at 37°C for 30 min. Then, DNase I (NEB) was added at 5mg/mL, and after 5min, the suspension was diluted in 1:4 in culture media (DMEM Gibco 41965, with 10% FBS and 40ug/mL gentamycin), filtered 3 times by pouring it through a 0.7um strainer, and centrifuged for 5min at 1500rpm. After discarding the supernatant, cells were washed in cell culture media and centrifuged 5min at 1500rpm. The resulting pellet was resuspended in culture media and seeded in cell culture dishes at 4-6 15cm plates per skin. Before reaching full confluency, cells were frozen on FBS with 8% DMSO, and preserved in liquid nitrogen. Experiments were performed on primary mouse dermal fibroblasts maintained at a low (2-6) passage number.

Induction of p21 knock-down

To induce the knock-down of p21, doxycycline (doxycycline hyclate, Sigma-Aldrich D9891) was added into the cultured media of proliferating or senescent fibroblasts at 2ug/mL (1x) or 4ug/mL (2x) for the specified number of days. The expression of the construct encoding the shRNA against *Cdkn1a* was verified through the detection of the fluorescent GFP reporter signal in a fluorescent microscope (EVOS FLoid).

Senescence induction

The induction of senescence in MDF by irradiation or acute adriamycin treatment of non-confluent proliferating cultures in plastic dishes. After 3-4 days, pre-senescent cells were split and seeded into plastic dishes, or in gelatin coated glass coverslips (gelatin 0.1% in PBS, Pan Biotech) for immunofluorescence. Senescence was considered to be established 6 days after irradiation or adriamycin exposure. Irradiated plates were exposed to 10Gy of X-irradiation (CellRad+ irradiator from Precision X-Ray Irradiation), culture media was changed 1-3 hours after irradiation. Adriamycin (Sigma-Aldrich 44583) was added into the culture media of proliferating cells at 250nM for 24h, plates were washed twice with PBS and adriamycin-free culture media was supplied.

SA-β-galactosidase

For SA-β-gal staining, proliferating or senescent cultures 6 days after irradiation were washed twice with PBS, fixed with 0.5% glutaraldehyde (Sigma-Aldrich G7651) in PBS for 17min at room temperature, and washed twice with PBS 1mM $MgCl_2$ at pH 5.5. Cells were stained with X-Gal solution (1mg/mL X-Gal, 0.12 mM $K_3Fe(CN)_6$, 0.12 mM $K_4Fe(CN)_6$ in PBS 1mM $MgCl_2$ at pH 5.5) for approximately 8h at 37ºC. Cells were washed tree times with distilled water and imaged in a bright field microscope (EVOS XL Core). Quantification of positive cells was done manually, a minimum of 500 cells per condition in 4 experiments were evaluated.

EdU incorporation

EdU (Lumiprobe) was diluted into fresh cell culture media at a final concentration of 10uM for a pulse of 16h (n=2) or 3h (n=1). Then, cells were washed twice with PBS and fixed with 4% paraformaldehyde in PBS (Thermo Fisher Scientific 28908) for 20min at room temperature, and washed twice with PBS. EdU incorporation was revealed via Click reaction following an *in-house* protocol of the Click-iT EdU Alexa Fluor 488 Imaging Kit (Invitrogen). Nuclei were stained with DAPI 0.1ug/mL (Invitrogen D1306) for 5 min. Cells were imaged using a fluorescent microscope (Leica DM IRB or Zeiss Axio Observer Z1). EdU incorporation was assessed manually or semi-automatically using CellProfiler[561], a minimum of 580 cells per condition in 3 experiments were evaluated.

RNA isolation and RT-qPCR

Proliferating, irradiated or adriamycin-treated MDF cultures were washed with PBS and lysed in Lysis Buffer LBP (Macherey-Nagel) according to the RNA extraction protocol.

Samples were kept at -20°C and experimental batches were processed at once. RNA isolation (RNA isolation NucleoSpin RNA Plus, Macherey-Nagel), cDNA retrotranscription (RT) (qScript cDNA SuperMix, QuantaBio) and quantitative polymerase chain reaction (qPCR) (SYBR Green I Master and LightCycler 480 Instrument, Roche) were performed according to manufacturer's instructions. Relative levels of expression were normalized to *Rplp0*, which was used as the reference housekeeping gene. Primer sequences: *Cdkn1a* (p21): Fwd-gttccgcacaggagcaaagt, Rev- acggcgcaactgctcac; *Hmgb2*: Fwd-gggtgagatgtggtctgagc, Ref-tcctgcttcacttttgccct; *Ink4a* (p16): Fwd- cgtaccccgattcaggtg, Rev- accagcgtgtccaggaag; *Arf* (p19): Qiagen QT01164891; *Ki67*: Fwd- gctgtcctcaagacaatcatca, Rev- ggcgttatcccaggagact; *Rplp0*: Qiagen QT00249375.

RNA-sequencing and analysis

RNA samples were prepared as for RT-qPCR and sent to the GenomEast platform at Institut de Génétique et de Biologie Moléculaire et Cellulaire (IGBMC). Library preparation with TruSeq Stranded mRNA Library preparation (Illumina). Sequencing was performed with HiSeq 4000 technology (Illumina) on single-end 50bp length reads. Reads were pre-processed to remove low quality and short (<40bp) reads using cutadapt[562] 1.10. Remaining reads were mapped onto the mm10 assembly of *Mus musculus* genome with STAR[563] 2.5.3a. Gene expression quantification was performed from unique aligned reads using htseq-count[564] 0.6.1p1 with annotations from Ensembl version 100 and "union" mode and normalized with the median-of-ratios method[565]. Hierarchical clustering for the heatmap of SERE coefficient[566] across samples performed using Unweighted Pair Group Method with arithmetic mean algorithm (UPGMA). Differential gene expression analysis was performed using Wald test considering the experimental batch as a variable[567] in Bioconductor package DESeq2 1.16.1. counts Outlier counts were filtered out based on high Cook's distance for p-value calculation. Low expressed genes were discarded applying independent filtering based on the mean of normalized counts to increase statistical power. P-values were adjusted for multiple testing following the Benjamini and Hochberg method[568]. Genes with and adjusted p-value <0.05 were considered significantly differentially expressed. A report of the sequencing protocol and file with the differential gene expression analysis was generated and provided by Matthieu Jung, from the GenomEast platform. Pathway analysis was performed through the Enrichr webpage[444–446], and the following databases were consulted: BioPlanet 2019, Gene Ontology Databases (Biological Process 2021, Molecular Function 2021, Cellular Component 2018 and 2021), KEGG 2021 Human, KEGG 2019 Mouse and MSigDB Hallmark 2020. A pathway considered significantly enriched when the adjusted p-value was lower than

0.25. Pathway analysis results were shown in dotplots or bar graphs created using ggplot2 package in R studio. The expression of specific gene sets across samples and comparisons was depicted using heatmaps with ComplexHeatmap package in R studio. Heatmaps indicating the basal expression level of each gene, on a grey scale, indicate the average expression level in the proliferating control condition samples (PC) in comparison with the rest of gene considered. Counts of individual samples, depicted in a blue-to-red scale, were corrected per row and relative to all samples. Peroxisomal genes affected by senescence and/or p21 downregulation in senescence were colored in the KEGG reference map of the mouse "Peroxisome" term (map04146) using KEGG pathway maps in the GenomeNet webpage.

Immunofluorescence staining

For immunofluorescence, cells were plated in 11mmØ glass coverslips coated with 0.1% gelatin (Pan Biotech) placed in 24 well plates at least two days before fixation. Cells were washed twice with PBS, fixed with 4% paraformaldehyde (PFA, Electron Microscopy Sciences 15710) for 17min, and washed 3 times with PBS. After 10 min permeabilization with 0.1% triton in PBS, cells were washed with PBS, and blocked in 10% goat serum with 0.5% tween in PBS for 1h at room temperature. Cells were incubated with primary antibody in dilution buffer (1% goat serum and 0.05% tween in PBS) overnight at 4°C. They were washed twice with PBS and incubated with secondary antibody at 1:2000 in dilution buffer for 1h at room temperature. To stain actin cytoskeleton, fluorescent phalloidin (Invitrogen A12379 or A12380) was added at this step in with the secondary antibody dilution. Cells were washed once with PBS, nuclei were counterstained with DAPI (Invitrogen D1306) for 5min, washed twice with PBS and coverslips were mounted with Fluoromount-G (CliniSciences 0100-01) on glass slides. Images were taking using wide field (Zeiss Axio Observer Z1) or spinning disk confocal (Leica CSU-W1) fluorescence microscopes. Peroxisomal aggregates identification was assessed visually based on the signal of Pmp70 primary antibody, and the quantification of cells containing aggregates was performed manually. Primary antibodies used: p21 (1:100, BD Pharmigen 556431), Pmp70 (1:200, Sigma-Aldrich SAB4200181), Catalase (1:250, Invitrogen PA5-95349), p62 (1:300, Progen GP62-C).

Protein isolation

Proliferating, irradiated or adriamycin-treated MDF cultures in were washed twice and scrapped into cold PBS. After centrifugation, cellular pellets were stored at -20°C, and all samples from the same experimental batch were processed together. Frozen cellular pellets

were resuspended in RIPA buffer (Bio Basic RB4476) with PMSF, DTT and PIC (Roche 04693132001), sonicated (Bioruptor Twin, Diagenode) and centrifuged at 4°C. The resulting supernatant was transferred to a new tube, and concentrations were equaled across samples after protein quantification (BioRad 5000112). Samples were boiled 5 min at 99°C in Laemmli buffer with β-mercaptoethanol (BioRad, 1610747), and stored at -20°C.

Western Blotting

Prepared samples in Laemmli buffer were boiled a second time at 99°C for 5 min, resolved on 10-12% polyacrylamide gels (or 4-20% precast gels for Co-IP samples, BioRad 4561094) and transferred to a 0.45um nitrocellulose membrane (GE Healthcare 10600002) using wet transfer cells (BioRad). Ponceu staining of the membranes was used to verify even loading and transfer. Membranes were blocked with 5% milk in TBS-T (25nM Tris-HCl, pH 7.5, 150nM NaCl, 0.05% tween) for 1h at room temperature, and were incubated with primary antibodies in TBS-T with 2,5% milk rocking overnight at 4°C. After washing them three times with TBS-T, they were incubated with secondary antibody coupled to HRP (1:10000 dilution in TBS-T with 2.5% milk) rocking for 1h at room temperature. Membranes were washed three time in TBS-T and developed using standard or pico ECL Western Blotting chemiluminescent substrate (Thermo Scientific 32209 and 34080). Primary antibodies used: p21 (1:200-1:250, BD Pharmigen 556431), α-Tubulin (1:7000, Sigma-Aldrich T6199).

Co-Immunoprecipitation (Co-Ip)

For each experiment, four 15cm plates of senescent MDF at day 8 after irradiation were collected in the same way than for Western Blot experiments. Beads (Protein G Sepharose 4 Fast Flow, GE Healthcare) were washed twice with water and twice with Ip100 buffer (25mM Tris Cl pH 7.9, 10% glycerol, 2mM DTT, 5mM $MgCl_2$, 100mM KCl, 0.1% NP40, PIC (Roche 04693132001)) and incubated with p21 (1:50 dilution, BD Pharmigen 556431) or IgG (1:100 dilution, Antibodies Online ABIN457406) antibodies in Ip100 buffer for 90-120min rocking at room temperature. Before incubation with the input, beads were washed twice with Ip500 buffer (25mM Tris Cl pH 7.9, 10% glycerol, 2mM DTT, 5mM $MgCl_2$, 500mM KCl, 0.1% NP40, PIC) and three times with Ip100 buffer. For protein extraction, cellular pellets were resuspended in the same volume of EB buffer (50mM Tris-HCl pH 7.9, 25% glycerol, 0.2mM EdTA, 0.5mM DTT, 5mM $MgCl_2$, 600mM KCl, 0.5% NP40, PIC), incubated for 5min on ice, sonicated (Bioruptor Twin, Diagenode), resuspended in 3 volumes of Ip0 buffer (25mM Tris-HCl pH 7.9, 5% glycerol, 1mM DTT, 5mM $MgCl_2$, 0.1% NP40, PIC), incubated for 10min on ice, and centrifuged at 18000g for 20min at 4°C. The supernatant was incubated with the beads

rocking for 90-120min at 4ºC. The supernatant (Input) was transferred to the beads bound to p21 or IgG antibodies and incubated overnight rocking at 4ºC. Next morning, supernatants (SN) were stored and beads were washed twice for 5-10min with Ip500 buffer and three times with Ip100 buffer. Elution (El) was performed in 2 rounds of 5min incubation in low pH glycine solution (0.1M glycine pH 2.8) and neutralization with 1.5M Tris buffer pH 8.8. Eluted samples were centrifuged at high speed for 20min at 4ºC to eliminate all insoluble material before sending them for MS analysis. Aliquots from the input, supernatants (SN-p21 and SN-IgG), and eluted fractions (El-p21 and El-IgG) were boiled at 99ºC in Laemmli buffer with β-mercaptoethanol (BioRad, 1610747) and analyzed by Western Blot.

Mass spectrometry (MS)

Eluted fractions of p21 or IgG co-immunoprecipitated (Co-Ip) proteins from senescent MDF extracts from 2 independent experiments were sent to the IGBMC proteomic facility for Mass Spectrometry (MS) analysis. Samples were digested with LysC-Trypsin and analyzed using a C18 Accucore 50cm column (Thermo Scientific) coupled to Orbitrap ELITE instrument (Thermo Scientific) by Top 20 CID method for 2h and in triplicate per each sample. Data was processed using Proteome Discoverer 2.4 and Perseus 1.6.12.0 software. The proteomic facility provided a file with the raw list of proteins detected in each sample, their abundance ratio in p21 Co-Ip vs IgG Co-Ip samples and the certainty of their detection (t-test, grouping samples of the same condition, after global normalization and exclusion of contaminants). In addition, I performed a t-test for each independent experiment in order to evaluate them separately. Significancy threshold was established at p-value <0.05. Proteins were considered to be p21 interactors when they were significantly more abundant in the p21 co-immunoprecipitated than in the IgG co-immunoprecipitated in both experimental replicates, either when they were evaluated grouped or per separate. The interactome of p21 was depicted as a network using Cytoscape. The size of the nodes, corresponding to each protein, were relative to their abundance, and their border color to their significance taking into consideration their p-value when samples were merged for the t-test and if they were found in both experiments when analyzed separately (red: p-value <0.01 and found in both experiments, pink: p-value <0.05 and found in both experiments, orange: p-value <0.01 and present when experiments were analyzed together, yellow: p-value <0.05 and present when experiments were analyzed together). The thickness of the edges (lines) connecting them to p21 was relative to their significance in p-value, and the color indicates if the interaction had been previously reported in at least one of the following databases: String, Integrated Interactions Database, Pathway Commons Protein-Protein Interactions through

Harmonizome and Genemania webpage (red for previously reported interaction). To represent the functions and cellular components associated with p21 interactome, the identified partners were submitted to pathway analysis using DAVID webpage. Gene Ontology databases (Cellular Component, Molecular Function and Cellular process) were consulted.

Cytokine array

The secretome of senescent cells with unmanipulated or reduced p21 levels was compared using a cytokine array panel of 42 cytokines. 8 days after irradiation, senescent cells with unmanipulated (doxycycline-free) or reduced p21 levels (achieved by doxycycline addition into the culture media from day 6 after irradiation) were washed with PBS and provided fresh culture media (DMEM Gibco 41965, with 10% FBS and 40ug/mL gentamycin with or without doxycycline). After 24h, conditioned media from both plates was collected and filtered through a 20um strainer to remove cellular debris (Corning CLS431224 or Minisart 16532-K). The number of cells was counted using a Neubauer chamber in order to verify an equivalent cell number in each condition (50 000 cells/mL). Samples from 2 independent experiments were analyzed at the same time using the Proteome Profiler Mouse Cytokine Array Kit, Panel A (R&D Systems ARY006) following to manufacture instructions. Membranes were developed using standard ECL Western Blotting chemiluminescent substrate (Thermo Scientific 32209) and imaged in Invitrogen iBright CL100 imaging system (Thermo Scientific) at different exposure times. Pixel intensity was determined using FIJI software. While an intermediate exposure time was used to compare the Mean Pixel Density of all cytokines, the best exposure time for each cytokine was used to assess its relative abundance in p21 depleted cultures, normalized to each correspondent control and represented as a relative fold change.

Proliferation assays

Crystal violet cell proliferation assays were used to assess the proliferative capacity of long-term senescent cultures. Irradiated or adriamycin treated pre-senescent cultures were split, counted, and plated at low density (~500-5000 cells/cm^2) 3 to 5 days after damage induction. To induce p21 downregulation, doxycycline was added in the culture media 6 days after damage induction. After 15 to 22 days of senescence induction, plates were washed twice with PBS, fixed in 4% paraformaldehyde (PFA, Electron Microscopy Sciences 15710) in PBS for 17min, washed twice with PBS, stained with crystal violet (0.5% crystal violet (Sigma-Aldrich V5265), 20% methanol in PBS) 20min at room temperate, washed gently 5 times with

water and allowed to air dry. The purple color of stained cells allows the visualization of denser cellular regions corresponding to proliferative populations.

BIBLIOGRAPHY

1. Rhinn, M. *et al.* Aberrant induction of p19Arf-mediated cellular senescence contributes to neurodevelopmental defects. *PLOS Biol.* **20**, e3001664 (2022).

2. Jennings, H. S. (University of C. at L. A. Paramecium Bursaria: Life History. I. Immaturity, Maturity and Age. *Biol. Bull.* **86**, 131–145 (1944).

3. Sonneborn, T. M. The Relation of Autogamy to Senescence and Rejuvenescence in Paramecium aurelia. *J. Protozool.* **1**, 38–53 (1954).

4. Hayflick, L. Moorhead, P. . The serial cultivation of human diploid cell strains. *Exp. Cell Res.* **25**, 585–621 (1961).

5. Hayflick, L. The limited in vitro lifetime of human diploid cell strains. *Exp. Cell Res.* **37**, 614–636 (1965).

6. Rhinn, M., Ritschka, B. & Keyes, W. M. Cellular senescence in development , regeneration and disease. (2019). doi:10.1242/dev.151837

7. Gorgoulis, V. *et al.* Cellular Senescence: Defining a Path Forward. *Cell* **179**, 813–827 (2019).

8. Muñoz-espín, D. & Serrano, M. Cellular senescence : from physiology to pathology. *Nat. Publ. Gr.* **15**, (2014).

9. Hernandez-segura, A., Nehme, J. & Demaria, M. Hallmarks of Cellular Senescence. *Trends Cell Biol.* **28**, 436–453 (2018).

10. Herranz, N., Gil, J., Herranz, N. & Gil, J. Mechanisms and functions of cellular senescence Mechanisms and functions of cellular senescence. **128**, 1238–1246 (2018).

11. Kumari, R., Jat, P., Karimian, A., Ahmadi, Y. & Yousefi, B. Mechanisms of Cellular Senescence: Cell Cycle Arrest and Senescence Associated Secretory Phenotype. *Front. Cell Dev. Biol.* **9**, 1–24 (2021).

12. Muñoz-Espín, D. & Serrano, M. Cellular senescence: from physiology to pathology.

Nat. Rev. Mol. Cell Biol. **15**, 482–496 (2014).

13. Sharpless, N. E. & Sherr, C. J. Forging a signature of in vivo senescence. *Nat. Rev. Cancer* **15**, 397–408 (2015).

14. Di Micco, R., Krizhanovsky, V., Baker, D. & d'Adda di Fagagna, F. Cellular senescence in ageing: from mechanisms to therapeutic opportunities. *Nat Rev Mol Cell Biol* **22**, 75–95 (2021).

15. Malumbres, M. Cyclin-dependent kinases. *Genome Biol.* **15**, 122 (2014).

16. Sherr, C. J. & Roberts, J. M. CDK inhibitors: Positive and negative regulators of G1-phase progression. *Genes Dev.* **13**, 1501–1512 (1999).

17. Fischer, M. & Müller, G. A. Cell cycle transcription control: DREAM/MuvB and RB-E2F complexes. *Crit. Rev. Biochem. Mol. Biol.* **52**, 638–662 (2017).

18. Kuilman, T., Michaloglou, C., Mooi, W. J. & Peeper, D. S. The essence of senescence. *Genes Dev.* **24**, 2463–2479 (2010).

19. Zampetidis, C. P. *et al.* A recurrent chromosomal inversion suffices for driving escape from oncogene-induced senescence via subTAD reorganization. *Mol. Cell* **81**, 4907-4923.e8 (2021).

20. Childs, B. G., Baker, D. J., Kirkland, J. L., Campisi, J. & van Deursen, J. M. Senescence and apoptosis: dueling or complementary cell fates? *EMBO Rep.* **15**, 1139–53 (2014).

21. Campisi, J. & d'Adda di Fagagna, F. Cellular senescence : when bad things happen to good cells. **8**, (2007).

22. Yosef, R. *et al.* Directed elimination of senescent cells by inhibition of BCL-W and BCL-XL. *Nat. Commun.* **7**, (2016).

23. Ryu, S. J., Oh, Y. S. & Park, S. C. Failure of stress-induced downregulation of Bcl-2 contributes to apoptosis resistance in senescent human diploid fibroblasts. *Cell Death Differ.* **14**, 1020–1028 (2007).

24. Sanders, Y. Y. *et al.* Histone modifications in senescence-associated resistance to

apoptosis by oxidative stress. *Redox Biol.* **1**, 8–16 (2013).

25. Kirschner, K. *et al.* Phenotype Specific Analyses Reveal Distinct Regulatory Mechanism for Chronically Activated p53. *PLoS Genet.* **11**, 1–28 (2015).

26. Myrianthopoulos, V. *et al.* Senescence and senotherapeutics: a new field in cancer therapy. *Pharmacol. Ther.* **193**, 31–49 (2019).

27. Zhu, Y. *et al.* The achilles' heel of senescent cells: From transcriptome to senolytic drugs. *Aging Cell* **14**, 644–658 (2015).

28. Fuhrmann-Stroissnigg, H. *et al.* Identification of HSP90 inhibitors as a novel class of senolytics. *Nat. Commun.* **8**, (2017).

29. Druelle, C. *et al.* ATF6a regulates morphological changes associated with senescence in human fibroblasts. *Oncotarget* **7**, 67699–67715 (2016).

30. Cho, K. A. *et al.* Morphological adjustment of senescent cells by modulating caveolin-1 status. *J. Biol. Chem.* **279**, 42270–42278 (2004).

31. Nishio, K. & Inoue, A. Senescence-associated alterations of cytoskeleton: Extraordinary production of vimentin that anchors cytoplasmic p53 in senescent human fibroblasts. *Histochem. Cell Biol.* **123**, 263–273 (2005).

32. Moujaber, O. *et al.* Cellular senescence is associated with reorganization of the microtubule cytoskeleton. *Cell. Mol. Life Sci.* **76**, 1169–1183 (2019).

33. Pathak, R. U., Soujanya, M. & Mishra, R. K. Deterioration of nuclear morphology and architecture: A hallmark of senescence and aging. *Ageing Res. Rev.* **67**, 101264 (2021).

34. Freund, A., Laberge, R. M., Demaria, M. & Campisi, J. Lamin B1 loss is a senescence-associated biomarker. *Mol. Biol. Cell* **23**, 2066–2075 (2012).

35. Shah, P. P. *et al.* Lamin B1 depletion in senescent cells triggers large-scale changes in gene expression and the chromatin landscape. *Genes Dev.* **27**, 1787–1799 (2013).

36. Miller, K. N., Dasgupta, N., Liu, T., Adams, P. D. & Vizioli, M. G. Cytoplasmic chromatin fragments—from mechanisms to therapeutic potential. *Elife* **10**, 1–10 (2021).

37. Yang, H., Wang, H., Ren, U., Chen, Q. & Chena, Z. J. CGAS is essential for cellular senescence. *Proc. Natl. Acad. Sci. U. S. A.* **114**, E4612–E4620 (2017).

38. Glück, S. *et al.* Innate immune sensing of cytosolic chromatin fragments through cGAS promotes senescence. *Nat. Cell Biol.* **19**, 1061–1070 (2017).

39. Dou, Z. *et al.* Cytoplasmic chromatin triggers inflammation in senescence and cancer. *Nature* **550**, 402–406 (2017).

40. Narita, M. *et al.* Rb-mediated heterochromatin formation and silencing of E2F target genes during cellular senescence. *Cell* **113**, 703–716 (2003).

41. Chandra, T. *et al.* Independence of Repressive Histone Marks and Chromatin Compaction during Senescent Heterochromatic Layer Formation. *Mol. Cell* **47**, 203–214 (2012).

42. Zhang, R. *et al.* Formation of macroH2A-containing senescence-associated heterochromatin foci and senescence driven by ASF1a and HIRA. *Dev. Cell* **8**, 19–30 (2005).

43. Di Micco, R. *et al.* Interplay between oncogene-induced DNA damage response and heterochromatin in senescence and cancer. *Nat. Cell Biol.* **13**, 292–302 (2011).

44. Evangelou, K. *et al.* Robust, universal biomarker assay to detect senescent cells in biological specimens. *Aging Cell* **16**, 192–197 (2017).

45. Georgakopoulou, E. *et al.* Specific lipofuscin staining as a novel biomarker to detect replicative and stress-induced senescence. A method applicable in cryo-preserved and archival tissues. *Aging (Albany. NY).* **5**, 37–50 (2012).

46. Herranz, N. & Gil, J. Mechanisms and functions of cellular senescence. *J. Clin. Invest.* **128**, 1238–1246 (2018).

47. Storer, M. *et al.* Senescence Is a Developmental Mechanism that Contributes to Embryonic Growth and Patterning. *Cell* **155**, 1119–1130 (2013).

48. Coppé, J. P., Desprez, P. Y., Krtolica, A. & Campisi, J. The senescence-associated secretory phenotype: The dark side of tumor suppression. *Annu. Rev. Pathol. Mech. Dis.* **5**, 99–118 (2010).

49. Kuilman, T. & Peeper, D. S. Senescence-messaging secretome: SMS-ing cellular stress. *Nat. Rev. Cancer* **9**, 81–94 (2009).

50. Lopes-Paciencia, S. *et al.* The senescence-associated secretory phenotype and its regulation. *Cytokine* **117**, 15–22 (2019).

51. Davalos, A. R. *et al.* p53-dependent release of Alarmin HMGB1 is a central mediator of senescent phenotypes. *J. Cell Biol.* **201**, 613–629 (2013).

52. Freund, A., Patil, C. K. & Campisi, J. P38MAPK is a novel DNA damage response-independent regulator of the senescence-associated secretory phenotype. *EMBO J.* **30**, 1536–1548 (2011).

53. Schafer, M. J. *et al.* The senescence-associated secretome as an indicator of age and medical risk. *JCI Insight* **5**, (2020).

54. Kandhaya-Pillai, R. *et al.* TNFα-senescence initiates a STAT-dependent positive feedback loop, leading to a sustained interferon signature, DNA damage, and cytokine secretion. *Aging (Albany. NY).* **9**, 2411–2435 (2017).

55. Martínez-Zamudio, R. I. *et al.* AP-1 imprints a reversible transcriptional programme of senescent cells. *Nat. Cell Biol.* **22**, 842–855 (2020).

56. Rodier, F. *et al.* Persistent DNA damage signalling triggers senescence-associated inflammatory cytokine secretion. *Nat. Cell Biol.* **11**, 973–979 (2009).

57. Acosta, J. C. *et al.* A complex secretory program orchestrated by the inflammasome controls paracrine senescence. *Nat. Cell Biol.* **15**, 978–990 (2013).

58. Coppé, J. P. *et al.* Senescence-associated secretory phenotypes reveal cell-nonautonomous functions of oncogenic RAS and the p53 tumor suppressor. *PLoS Biol.* **6**, (2008).

59. Lehmann, B. D. *et al.* Senescence-associated exosome release from human prostate cancer cells. *Cancer Res.* **68**, 7864–7871 (2008).

60. Hoare, M. *et al.* NOTCH1 mediates a switch between two distinct secretomes during senescence. *Nat. Cell Biol.* **18**, 979–992 (2016).

61. De Cecco, M. *et al.* L1 drives IFN in senescent cells and promotes age-associated inflammation. *Nature* **566**, 73–78 (2019).

62. Acosta, J. C. *et al.* Chemokine Signaling via the CXCR2 Receptor Reinforces Senescence. *Cell* **133**, 1006–1018 (2008).

63. Wang, X. *et al.* Control of the senescence-associated secretory phenotype by NF-kappaB promotes senescence and enhances Control of the senescence-associated secretory phenotype by NF- k B promotes senescence and enhances chemosensitivi. *Genes Dev.* 2125–2136 (2011). doi:10.1101/gad.17276711

64. Acosta, J. C. *et al.* A complex secretory program orchestrated by the inflammasome controls paracrine senescence. *Nat. Cell Biol.* **15**, 978–990 (2013).

65. Kang, C. *et al.* The DNA damage response induces inflammation and senescence by inhibiting autophagy of GATA4. *Science (80-.).* **349**, (2015).

66. Takahashi, A. *et al.* DNA damage signaling triggers degradation of histone methyltransferases through APC/C Cdh1 in senescent cells. *Mol. Cell* **45**, 123–131 (2012).

67. Hayakawa, T. *et al.* SIRT1 suppresses the senescence-associated secretory phenotype through epigenetic gene regulation. *PLoS One* **10**, 1–16 (2015).

68. Tasdemir, N. *et al.* BRD4 Connects Enhancer Remodeling to Senescence Immune Surveillance. *Cancer Discov.* **6**, 612–629 (2016).

69. Ito, T., Teo, Y. V., Evans, S. A., Neretti, N. & Sedivy, J. M. Regulation of Cellular Senescence by Polycomb Chromatin Modifiers through Distinct DNA Damage- and Histone Methylation-Dependent Pathways. *Cell Rep.* **22**, 3480–3492 (2018).

70. Chen, H. *et al.* MacroH2A1 and ATM Play Opposing Roles in Paracrine Senescence and the Senescence-Associated Secretory Phenotype. *Mol. Cell* **59**, 719–731 (2015).

71. Contrepois, K. *et al.* Histone variant H2A.J accumulates in senescent cells and promotes inflammatory gene expression. *Nat. Commun.* **8**, (2017).

72. Capell, B. C. *et al.* Mll1 is essential for the senescenceassociated secretory phenotype. *Genes Dev.* **30**, 321–336 (2016).

73. Aird, K. M. *et al.* HMGB2 orchestrates the chromatin landscape of senescence-associated secretory phenotype gene loci. *J. Cell Biol.* **215**, 325–334 (2016).

74. Sofiadis, K. *et al.* HMGB1 coordinates SASP-related chromatin folding and RNA homeostasis on the path to senescence. *Mol. Syst. Biol.* **17**, 1–17 (2021).

75. Laberge, R. *et al.* MTOR regulates the pro-tumorigenic senescence-associated secretory phenotype by promoting IL1A translation. *Nat. Cell Biol.* **17**, 1049–1061 (2015).

76. Herranz, N. *et al.* mTOR regulates MAPKAPK2 translation to control the senescence-associated secretory phenotype. *Nat. Cell Biol.* **17**, 1205–1217 (2015).

77. Effenberger, T. *et al.* Senescence-associated release of transmembrane proteins involves proteolytic processing by ADAM17 and microvesicle shedding. *FASEB J.* **28**, 4847–4856 (2014).

78. Parry, A. J. *et al.* NOTCH-mediated non-cell autonomous regulation of chromatin structure during senescence. *Nat. Commun.* **9**, 1840 (2018).

79. Xue, W. *et al.* Senescence and tumour clearance is triggered by p53 restoration in murine liver carcinomas. *Nature* **445**, 656–660 (2007).

80. Franceschi, C. & Campisi, J. Chronic inflammation (Inflammaging) and its potential contribution to age-associated diseases. *Journals Gerontol. - Ser. A Biol. Sci. Med. Sci.* **69**, S4–S9 (2014).

81. Muñoz-Espín, D. *et al.* Programmed Cell Senescence during Mammalian Embryonic Development. *Cell* **155**, 1104–1118 (2013).

82. Demaria, M. *et al.* An essential role for senescent cells in optimal wound healing through secretion of PDGF-AA. *Dev. Cell* **31**, 722–733 (2014).

83. Mosteiro, L. *et al.* Tissue damage and senescence provide critical signals for cellular reprogramming in vivo. *Science (80-.).* **354**, aaf4445 (2016).

84. Mosteiro, L., Pantoja, C., de Martino, A. & Serrano, M. Senescence promotes in vivo reprogramming through p16 INK 4a and IL-6. *Aging Cell* **17**, e12711 (2018).

85. Krtolica, A., Parrinello, S., Lockett, S., Desprez, P. Y. & Campisi, J. Senescent fibroblasts promote epithelial cell growth and tumorigenesis: A link between cancer and aging. *Proc. Natl. Acad. Sci. U. S. A.* **98**, 12072–12077 (2001).

86. Pluquet, O., Pourtier, A. & Abbadie, C. The unfolded protein response and cellular senescence. A Review in the Theme: Cellular Mechanisms of Endoplasmic Reticulum Stress Signaling in Health and Disease. *Am. J. Physiol. Physiol.* **308**, C415–C425 (2015).

87. Matos, L., Gouveia, A. M. & Almeida, H. ER stress response in human cellular models of senescence. *Journals Gerontol. - Ser. A Biol. Sci. Med. Sci.* **70**, 924–935 (2015).

88. Dörr, J. R. *et al.* Synthetic lethal metabolic targeting of cellular senescence in cancer therapy. *Nature* **501**, 421–425 (2013).

89. Cormenier, J. *et al.* The ATF6α arm of the Unfolded Protein Response mediates replicative senescence in human fibroblasts through a COX2/prostaglandin E2 intracrine pathway. *Mech. Ageing Dev.* **170**, 82–91 (2018).

90. Abbadie, C. & Pluquet, O. Unfolded Protein Response (UPR) Controls Major Senescence Hallmarks. *Trends in Biochemical Sciences* **45**, 371–374 (2020).

91. Kim, H. S. *et al.* The p38-activated ER stress-ATF6α axis mediates cellular senescence. *FASEB J.* **33**, 2422–2434 (2019).

92. Korolchuk, V. I., Miwa, S., Carroll, B. & von Zglinicki, T. Mitochondria in Cell Senescence: Is Mitophagy the Weakest Link? *EBioMedicine* **21**, 7–13 (2017).

93. Passos, J. F. *et al.* Feedback between p21 and reactive oxygen production is necessary for cell senescence. *Mol. Syst. Biol.* **6**, 347 (2010).

94. Moiseeva, O., Bourdeau, V., Roux, A., Deschênes-Simard, X. & Ferbeyre, G. Mitochondrial Dysfunction Contributes to Oncogene-Induced Senescence. *Mol. Cell. Biol.* **29**, 4495–4507 (2009).

95. Passos, J. F. *et al.* Mitochondrial dysfunction accounts for the stochastic heterogeneity in telomere-dependent senescence. *PLoS Biol.* **5**, 1138–1151 (2007).

96. Mai, S., Klinkenberg, M., Auburger, G., Bereiter-Hahn, J. & Jendrach, M. Decreased

expression of Drp1 and Fis1 mediates mitochondrial elongation in senescent cells and enhances resistance to oxidative stress through PINK1. *J. Cell Sci.* **123**, 917–926 (2010).

97. Dalle Pezze, P. *et al.* Dynamic Modelling of Pathways to Cellular Senescence Reveals Strategies for Targeted Interventions. *PLoS Comput. Biol.* **10**, (2014).

98. Hoshino, A. *et al.* Cytosolic p53 inhibits Parkin-mediated mitophagy and promotes mitochondrial dysfunction in the mouse heart. *Nat. Commun.* **4**, 1–12 (2013).

99. García-Prat, L. *et al.* Autophagy maintains stemness by preventing senescence. *Nature* **529**, 37–42 (2016).

100. Ogrodnik, M. *et al.* Cellular senescence drives age-dependent hepatic steatosis. *Nat. Commun.* **8**, (2017).

101. Correia-Melo, C. *et al.* Mitochondria are required for pro-ageing features of the senescent phenotype. *EMBO J.* **35**, 724–742 (2016).

102. Wiley, C. D. *et al.* Mitochondrial dysfunction induces senescence with a distinct secretory phenotype. *Cell Metab.* **23**, 303–314 (2016).

103. Kaplon, J. *et al.* A key role for mitochondrial gatekeeper pyruvate dehydrogenase in oncogene-induced senescence. *Nature* **498**, 109–112 (2013).

104. Birch, J. & Passos, J. F. Targeting the SASP to combat ageing: Mitochondria as possible intracellular allies? *BioEssays* **39**, 1–7 (2017).

105. Park, W. Y. *et al.* Up-regulation of caveolin attenuates epidermal growth factor signaling in senescent cells. *J. Biol. Chem.* **275**, 20847–20852 (2000).

106. Inomata, M., Shimada, Y., Hayashi, M., Kondo, H. & Ohno-Iwashita, Y. Detachment-associated changes in lipid rafts of senescent human fibroblasts. *Biochem. Biophys. Res. Commun.* **343**, 489–495 (2006).

107. Ohno-Iwashita, Y., Shimada, Y., Hayashi, M. & Inomata, M. Plasma membrane microdomains in aging and disease. *Geriatr. Gerontol. Int.* **10**, 41–52 (2010).

108. Cho, K. A. *et al.* Senescent phenotype can be reversed by reduction of caveolin

status. *J. Biol. Chem.* **278**, 27789–27795 (2003).

109. Volonte, D. *et al.* Oxidative stress-induced inhibition of Sirt1 by caveolin-1 promotes p53-dependent premature senescence and stimulates the secretion of interleukin 6 (IL-6). *J. Biol. Chem.* **290**, 4202–4214 (2015).

110. Frescas, D. *et al.* Senescent cells expose and secrete an oxidized form of membrane-bound vimentin as revealed by a natural polyreactive antibody. *Proc. Natl. Acad. Sci. U. S. A.* **114**, E1668–E1677 (2017).

111. Althubiti, M. *et al.* Characterization of novel markers of senescence and their prognostic potential in cancer. *Cell Death Dis.* **5**, 1–10 (2014).

112. Kim, K. M. *et al.* Identification of senescent cell surface targetable protein DPP4. *Genes Dev.* **31**, 1529–1534 (2017).

113. Wu, M. *et al.* Metabolomics-Proteomics Combined Approach Identifies Differential Metabolism-Associated Molecular Events between Senescence and Apoptosis. *J. Proteome Res.* **16**, 2250–2261 (2017).

114. Aird, K. M. & Zhang, R. Metabolic alterations accompanying oncogene-induced senescence. *Mol. Cell. Oncol.* **1**, (2014).

115. James, E. L. *et al.* Senescent human fibroblasts show increased glycolysis and redox homeostasis with extracellular metabolomes that overlap with those of irreparable DNA damage, aging, and disease. *J. Proteome Res.* **14**, 1854–1871 (2015).

116. Quijano, C. *et al.* Oncogene-induced senescence results in marked metabolic and bioenergetic alterations. *Cell Cycle* **11**, 1383–1392 (2012).

117. Narita, M. *et al.* Spatial Coupling of mTOR and Autophagy Augments Secretory Phenotypes. *Science (80-.).* **332**, 966–970 (2011).

118. Young, A. R. J. *et al.* Autophagy mediates the mitotic senescence transition. *Genes Dev.* **23**, 798–803 (2009).

119. Wiley, C. D. & Campisi, J. From Ancient Pathways to Aging Cells - Connecting Metabolism and Cellular Senescence. *Cell Metab.* **23**, 1013–1021 (2016).

120. Ryan, K. M. P53 and autophagy in cancer: Guardian of the genome meets guardian of the proteome. *Eur. J. Cancer* **47**, 44–50 (2011).

121. Takebayashi, S. I. *et al.* Retinoblastoma protein promotes oxidative phosphorylation through upregulation of glycolytic genes in oncogene-induced senescent cells. *Aging Cell* **14**, 689–697 (2015).

122. Bengsch, F. *et al.* Comprehensive analysis of the ubiquitinome during oncogene-induced senescence in human fibroblasts. *Cell Cycle* **14**, 1540–1547 (2015).

123. Nacarelli, T. *et al.* NAD + metabolism governs the proinflammatory senescence-associated secretome. *Nat. Cell Biol.* **21**, 397–407 (2019).

124. Harley, C. B., Futcher, A. B. & Greider, C. W. Telomeres shorten during ageing of human fibroblasts. *Nature* **345**, 458–460 (1990).

125. Griffith, J. D. *et al.* Mammalian Telomeres End in a Large Duplex Loop. *Cell* **97**, 503–514 (1999).

126. Palm, W. & de Lange, T. How Shelterin Protects Mammalian Telomeres. *Annu. Rev. Genet.* **42**, 301–334 (2008).

127. D'Adda Di Fagagna, F. *et al.* A DNA damage checkpoint response in telomere-initiated senescence. *Nature* **426**, 194–198 (2003).

128. Fumagalli, M. *et al.* Telomeric DNA damage is irreparable and causes persistent DNA-damage-response activation. *Nat. Cell Biol.* **14**, 355–365 (2012).

129. Collins, K. Mammalian telomeres and telomerase. *Curr. Opin. Cell Biol.* **12**, 378–383 (2000).

130. Cech, T. R. Beginning to Understand the End of the Chromosome. *Mod. Biopharm. Des. Dev. Optim.* **1**, 36–48 (2008).

131. Di Leonardo, A., Linke, S. P., Clarkin, K. & Wahl, G. M. DNA damage triggers a prolonged p53-dependent G1 arrest and long-term induction of Cip1 in normal human fibroblasts. *Genes Dev.* **8**, 2540–2551 (1994).

132. Chen, Q. & Ames, B. N. Senescence-like growth arrest induced by hydrogen

peroxide in human diploid fibroblast F65 cells. *Proc. Natl. Acad. Sci. U. S. A.* **91**, 4130–4134 (1994).

133. Toussaint, O., Medrano, E. E. & Von Zglinicki, T. Cellular and molecular mechanisms of stress-induced premature senescence (SIPS) of human diploid fibroblasts and melanocytes. *Exp. Gerontol.* **35**, 927–945 (2000).

134. Childs, B. G., Durik, M., Baker, D. J. & Van Deursen, J. M. Cellular senescence in aging and age-related disease: From mechanisms to therapy. *Nat. Med.* **21**, 1424–1435 (2015).

135. Petrova, N. V., Velichko, A. K., Razin, S. V. & Kantidze, O. L. Small molecule compounds that induce cellular senescence. *Aging Cell* **15**, 999–1017 (2016).

136. Blagosklonny, M. V. Cell senescence and hypermitogenic arrest. *EMBO Rep.* **4**, 358–362 (2003).

137. Serrano, M., Lin, A. W., McCurrach, M. E., Beach, D. & Lowe, S. W. Oncogenic ras provokes premature cell senescence associated with accumulation of p53 and p16(INK4a). *Cell* **88**, 593–602 (1997).

138. Alimonti, A. *et al.* Subtle variations in Pten dose determine cancer susceptibility. *Nat. Genet.* **42**, 454–458 (2010).

139. Parisotto, M. *et al.* PTEN deletion in luminal cells of mature prostate induces replication stress and senescence in vivo. *J. Exp. Med.* **215**, 1749–1763 (2018).

140. Moiseeva, O., Mallette, F. A., Mukhopadhyay, U. K., Moores, A. & Ferbeyre, G. DNA Damage Signaling and p53-dependent Senescence after Prolonged β-Interferon Stimulation. *Mol. Biol. Cell* **17**, 1583–1592 (2006).

141. Lee, A. C. *et al.* Ras proteins induce senescence by altering the intracellular levels of reactive oxygen species. *J. Biol. Chem.* **274**, 7936–7940 (1999).

142. Di Micco, R. *et al.* Oncogene-induced senescence is a DNA damage response triggered by DNA hyper-replication. *Nature* **444**, 638–642 (2006).

143. Ogrunc, M. *et al.* Oncogene-induced reactive oxygen species fuel hyperproliferation and DNA damage response activation. *Cell Death Differ.* **21**, 998–1012 (2014).

144. Gibaja, A. *et al.* TGFβ2-induced senescence during early inner ear development. *Sci. Rep.* **9**, 1–13 (2019).

145. Chuprin, A. *et al.* Cell fusion induced by ERVWE1 or measles virus causes cellular senescence. *Genes Dev.* **27**, 2356–2366 (2013).

146. Nacher, V. *et al.* The quail mesonephros: A new model for renal senescence? *J. Vasc. Res.* **43**, 581–586 (2006).

147. Villiard, É. *et al.* Senescence gives insights into the morphogenetic evolution of anamniotes. *Biol. Open* **6**, 891–896 (2017).

148. Davaapil, H., Brockes, J. P. & Yun, M. H. Conserved and novel functions of programmed cellular senescence during vertebrate development. *Dev.* **144**, 106–114 (2017).

149. Zhao, Y. *et al.* Naked mole rats can undergo developmental, oncogene-induced and DNA damage-induced cellular senescence. *Proc. Natl. Acad. Sci. U. S. A.* **115**, 1801–1806 (2018).

150. Hubackova, S., Krejcikova, K., Bartek, J. & Hodny, Z. IL1-and TGFβ-Nox4 signaling, oxidative stress and DNA damage response are shared features of replicative, oncogene-induced, and drug-induced paracrine 'Bystander senescence'. *Aging (Albany. NY).* **4**, 932–951 (2012).

151. Vassilieva, I. *et al.* Paracrine senescence of human endometrial mesenchymal stem cells: A role for the insulin-like growth factor binding protein 3. *Aging (Albany. NY).* **12**, 1987–2004 (2020).

152. Chong, M. *et al.* CD 36 initiates the secretory phenotype during the establishment of cellular senescence . *EMBO Rep.* **19**, 1–13 (2018).

153. Victorelli, S. *et al.* Senescent human melanocytes drive skin ageing via paracrine telomere dysfunction. *EMBO J.* **38**, 1–18 (2019).

154. Admasu, T. D., Rae, M. & Stolzing, A. Dissecting primary and secondary senescence to enable new senotherapeutic strategies. *Ageing Res. Rev.* **70**, 101412 (2021).

155. Nelson, G. *et al.* A senescent cell bystander effect: Senescence-induced senescence.

Aging Cell **11**, 345–349 (2012).

156. Shay, J. W., Pereira-Smith, O. M. & Wright, W. E. A role for both RB and p53 in the regulation of human cellular senescence. *Exp. Cell Res.* **196**, 33–39 (1991).

157. He, S. & Sharpless, N. E. Senescence in Health and Disease. *Cell* **169**, 1000–1011 (2017).

158. McConnell, B. B., Starborg, M., Brookes, S. & Peters, G. Inhibitors of cyclin-dependent kinases induce features of replicative senescence in early passage human diploid fibroblasts. *Curr. Biol.* **8**, 351–354 (1998).

159. Beauséjour, C. M. *et al.* Reversal of human cellular senescence: Roles of the p53 and p16 pathways. *EMBO J.* **22**, 4212–4222 (2003).

160. Vogelstein, Bert; Lane, David; J. Levine, A. Surfing p53 Network. *Nature* **408**, 307–310 (2000).

161. Fischer, M., Steiner, L. & Engeland, K. The transcription factor p53: Not a repressor, solely an activator. *Cell Cycle* **13**, 3037–3058 (2014).

162. Kastenhuber, E. R. & Lowe, S. W. Putting p53 in Context. *Cell* **170**, 1062–1078 (2017).

163. El-Deiry, W. *et al.* WAF1, a potential mediator of p53 tumor suppression. *Cell* **75**, 817–825 (1993).

164. Alcorta, D. A. *et al.* Involvement of the cyclin-dependent kinase inhibitor p16 (INK4a) in replicative senescence of normal human fibroblasts. *Proc. Natl. Acad. Sci.* **93**, 13742–13747 (1996).

165. Robles, S. J. & Adami, G. R. Agents that cause DNA double strand breaks lead to p16INK4a enrichment and the premature senescence of normal fibroblasts. *Oncogene* **16**, 1113–1123 (1998).

166. Stein, G. H., Drullinger, L. F., Soulard, A. & Dulić, V. Differential Roles for Cyclin-Dependent Kinase Inhibitors p21 and p16 in the Mechanisms of Senescence and Differentiation in Human Fibroblasts. *Mol. Cell. Biol.* **19**, 2109–2117 (1999).

167. Uchida, C. Roles of pRB in the Regulation of Nucleosome and Chromatin Structures. *Biomed Res. Int.* **2016**, (2016).

168. Bracken, A. P. *et al.* EZH2 is downstream of the pRB-E2F pathway, essential for proliferation and amplified in cancer. *EMBO J.* **22**, 5323–5335 (2003).

169. Serrano, M. *et al.* Role of the INK4a locus in tumor suppression and cell mortality. *Cell* **85**, 27–37 (1996).

170. Quelle, D. E., Zindy, F., Ashmun, R. A. & Sherr, C. J. Alternative reading frames of the INK4a tumor suppressor gene encode two unrelated proteins capable of inducing cell cycle arrest. *Cell* **83**, 993–1000 (1995).

171. Bates, S. *et al.* p14(ARF) links the tumour suppressors RB and p53 [5]. *Nature* **395**, 124–125 (1998).

172. Sherr, C. J. The INK4a/ARF network in tumour suppression. *Nat. Rev. Mol. Cell Biol.* **2**, 731–737 (2001).

173. Sharpless, N. E. INK4a/ARF: A multifunctional tumor suppressor locus. *Mutat. Res. - Fundam. Mol. Mech. Mutagen.* **576**, 22–38 (2005).

174. Sherr, C. J. *et al.* p53-dependent and -independent functions of the Arf tumor suppressor. *Cold Spring Harb. Symp. Quant. Biol.* **70**, 129–137 (2005).

175. Fontana, R. & Vivo, M. Dynamics of p14ARF and focal adhesion kinase-mediated autophagy in cancer. *Cancers (Basel).* **10**, 13–15 (2018).

176. Ozenne, P., Eymin, B., Brambilla, E. & Gazzeri, S. The ARF tumor suppressor: Structure, functions and status in cancer. *Int. J. Cancer* **127**, 2239–2247 (2010).

177. Pollice, A., Vivo, M. & Mantia, G. La. The promiscuity of ARF interactions with the proteasome. *FEBS Lett.* **582**, 3257–3262 (2008).

178. Serrano, M., Hannon, G. J. & Beach, D. A new regulatory motif in cell-cycle control causing specific inhibition of cyclin D/CDK4. *Nature* **366**, 704–707 (1993).

179. Krishnamurthy, J. *et al.* Ink4a/Arf expression is a biomarker of aging. *J. Clin. Invest.* **114**, 1299–1307 (2004).

180. Herbig, U., Ferreira, M., Condel, L., Carey, D. & Sedivy, J. M. Cellular senescence in aging primates. *Science (80-.).* **311**, 1257 (2006).

181. Ressler, S. *et al.* p16INK4A is a robust in vivo biomarker of cellular aging in human skin. *Aging Cell* **5**, 379–389 (2006).

182. Hernandez-Segura, A. *et al.* Unmasking Transcriptional Heterogeneity in Senescent Cells. *Curr. Biol.* **27**, 2652-2660.e4 (2017).

183. Gil, J. & Peters, G. Regulation of the INK4b-ARF-INK4a tumour suppressor locus: All for one or one for all. *Nat. Rev. Mol. Cell Biol.* **7**, 667–677 (2006).

184. Cheng, L. Q., Zhang, Z. Q., Chen, H. Z. & Liu, D. P. Epigenetic regulation in cell senescence. *J. Mol. Med.* **95**, 1257–1268 (2017).

185. Yang, N. & Sen, P. The senescent cell epigenome. *Aging (Albany. NY).* **10**, 3590–3609 (2018).

186. Sen, P. *et al.* Histone Acetyltransferase p300 Induces De Novo Super-Enhancers to Drive Cellular Senescence. *Mol. Cell* **73**, 684-698.e8 (2019).

187. Zirkel, A. *et al.* HMGB2 Loss upon Senescence Entry Disrupts Genomic Organization and Induces CTCF Clustering across Cell Types. *Mol. Cell* **70**, 730-744.e6 (2018).

188. Scelfo, A., Piunti, A. & Pasini, D. The controversial role of the Polycomb group proteins in transcription and cancer: How much do we not understand Polycomb proteins? *FEBS J.* **282**, 1703–1722 (2015).

189. Gil, J., Bernard, D., Martínez, D. & Beach, D. Polycomb CBX7 has a unifying role in cellular lifespan. *Nat. Cell Biol.* **6**, 67–72 (2004).

190. Jacobs, J. L., Kieboom, K., Marino, S., DePinho, R. A. & Van Lohuizen, M. The oncogene and Polycombgroup gene bmi-1 regulates cell proliferation and senescence through the ink4a locus. *Nature* **397**, 164–168 (1999).

191. Bracken, A. P. *et al.* The Polycomb group proteins bind throughout the INK4A-ARF locus and are disassociated in senescent cells. *Genes Dev.* **21**, 525–530 (2007).

192. Agherbi, H. *et al.* Polycomb mediated epigenetic silencing and replication timing at

the INK4a/ARF locus during senescence. *PLoS One* **4**, 1–10 (2009).

193. Rai, T. S. *et al.* Human CABIN1 Is a Functional Member of the Human HIRA/UBN1/ASF1a Histone H3.3 Chaperone Complex. *Mol. Cell. Biol.* **31**, 4107–4118 (2011).

194. Banumathy, G. *et al.* Human UBN1 Is an Ortholog of Yeast Hpc2p and Has an Essential Role in the HIRA/ASF1a Chromatin-Remodeling Pathway in Senescent Cells. *Mol. Cell. Biol.* **29**, 758–770 (2009).

195. Funayama, R., Saito, M., Tanobe, H. & Ishikawa, F. Loss of linker histone H1 in cellular senescence. *J. Cell Biol.* **175**, 869–880 (2006).

196. Narita, M. *et al.* A Novel Role for High-Mobility Group A Proteins in Cellular Senescence and Heterochromatin Formation. *Cell* **126**, 503–514 (2006).

197. Zhu, H. *et al.* SPOP E3 Ubiquitin Ligase Adaptor Promotes Cellular Senescence by Degrading the SENP7 deSUMOylase. *Cell Rep.* **13**, 1183–1193 (2015).

198. Boumendil, C., Hari, P., Olsen, K. C. F., Acosta, J. C. & Bickmore, W. A. Nuclear pore density controls heterochromatin reorganization during senescence. 144–149 (2019). doi:10.1101/gad.321117.118.

199. Chandra, T. *et al.* Global reorganization of the nuclear landscape in senescent cells. *Cell Rep.* **10**, 471–483 (2015).

200. Adams, P. D. Remodeling chromatin for senescence. *Aging Cell* **6**, 425–427 (2007).

201. Swanson, E. C., Manning, B., Zhang, H. & Lawrence, J. B. Higher-order unfolding of satellite heterochromatin is a consistent and early event in cell senescence. *J. Cell Biol.* **203**, 929–942 (2013).

202. Ferbeyre, G. *et al.* PML is induced by oncogenic ras and promotes premature senescence. *Genes Dev.* **14**, 2015–2027 (2000).

203. Parry, A. J. & Narita, M. Old cells, new tricks: chromatin structure in senescence. *Mamm. Genome* **27**, 320–331 (2016).

204. Sadaie, M. *et al.* Redistribution of the Lamin B1 genomic binding profile affects

rearrangement of heterochromatic domains and SAHF formation during senescence. *Genes Dev.* **27**, 1800–1808 (2013).

205. Van Deursen, J. M. The role of senescent cells in ageing. *Nature* **509**, 439–446 (2014).

206. Sulli, G., Di Micco, R. & Di Fagagna, F. D. A. Crosstalk between chromatin state and DNA damage response in cellular senescence and cancer. *Nat. Rev. Cancer* **12**, 709–720 (2012).

207. Barascu, A. *et al.* Oxidative stress induces an ATM-independent senescence pathway through p38 MAPK-mediated lamin B1 accumulation. *EMBO J.* **31**, 1080–1094 (2012).

208. Bhaumik, D. *et al.* MicroRNAs miR-146a/b negatively modulate the senescence-associated inflammatory mediators IL-6 and IL-8. *Aging (Albany. NY).* **1**, 402–411 (2009).

209. De Cecco, M. *et al.* Genomes of replicatively senescent cells undergo global epigenetic changes leading to gene silencing and activation of transposable elements. *Aging Cell* **12**, 247–256 (2013).

210. Ivanov, A. *et al.* Lysosome-mediated processing of chromatin in senescence. **202**, 129–143 (2013).

211. Chen, J.-H. & Ozanne, S. E. Deep senescent human fibroblasts show diminished DNA damage foci but retain checkpoint capacity to oxidative stress. *FEBS Lett.* **580**, 6669–6673 (2006).

212. Shimi, T. *et al.* The role of nuclear lamin B1 in cell proliferation and senescence. *Genes Dev.* **25**, 2579–2593 (2011).

213. Neurohr, G. E. *et al.* Excessive Cell Growth Causes Cytoplasm Dilution And Contributes to Senescence. *Cell* **176**, 1083-1097.e18 (2019).

214. Kuilman, T. *et al.* Oncogene-Induced Senescence Relayed by an Interleukin-Dependent Inflammatory Network. *Cell* **133**, 1019–1031 (2008).

215. Bavik, C. *et al.* The gene expression program of prostate fibroblast senescence

modulates neoplastic epithelial cell proliferation through paracrine mechanisms. *Cancer Res.* **66**, 794–802 (2006).

216. Banito, A. *et al.* Senescence impairs successful reprogramming to pluripotent stem cells. *Genes Dev.* **23**, 2134–2139 (2009).

217. Utikal, J. *et al.* Immortalization eliminates a roadblock during cellular reprogramming into iPS cells. *Nature* **460**, 1145–1148 (2009).

218. Li, H. *et al.* The Ink4/Arf locus is a barrier for iPS cell reprogramming. *Nature* **460**, 1136–1139 (2009).

219. Hong, H. *et al.* Suppression of induced pluripotent stem cell generation by the p53-p21 pathway. *Nature* **460**, 1132–1135 (2009).

220. Kawamura, T. *et al.* Linking the p53 tumour suppressor pathway to somatic cell reprogramming. *Nature* **460**, 1140–1144 (2009).

221. Marión, R. M. *et al.* A p53-mediated DNA damage response limits reprogramming to ensure iPS cell genomic integrity. *Nature* **460**, 1149–1153 (2009).

222. Mosteiro, L. *et al.* Tissue damage and senescence provide critical signals for cellular reprogramming in vivo. *Science (80-.).* **354**, (2016).

223. Chiche, A. *et al.* Injury-Induced Senescence Enables In Vivo Reprogramming in Skeletal Muscle. *Cell Stem Cell* **20**, 407-414.e4 (2017).

224. Ritschka, B. *et al.* The senescence-associated secretory phenotype induces cellular plasticity and tissue regeneration. *Genes Dev.* **31**, 172–183 (2017).

225. Mario Gonzalez-Meljem, J. *et al.* Stem cell senescence drives age-attenuated induction of pituitary tumours in mouse models of paediatric craniopharyngioma. *Nat. Commun.* **8**, 1–14 (2017).

226. Milanovic, M. *et al.* Senescence-associated reprogramming promotes cancer stemness. *Nature* **553**, 96–100 (2018).

227. Liu, D. & Hornsby, P. J. Senescent human fibroblasts increase the early growth of xenograft tumors via matrix metalloproteinase secretion. *Cancer Res.* **67**, 3117–

3126 (2007).

228. Ghosh, D. *et al.* Senescent mesenchymal stem cells remodel extracellular matrix driving breast cancer cells to more invasive phenotype. *J. Cell Sci.* **133**, (2020).

229. Coppe, J. P., Kauser, K., Campisi, J. & Beauséjour, C. M. Secretion of vascular endothelial growth factor by primary human fibroblasts at senescence. *J. Biol. Chem.* **281**, 29568–29574 (2006).

230. Ksiazek, K., Jörres, A. & Witowski, J. Senescence induces a proangiogenic switch in human peritoneal mesothelial cells. *Rejuvenation Res.* **11**, 681–683 (2008).

231. Krizhanovsky, V. *et al.* Senescence of Activated Stellate Cells Limits Liver Fibrosis. *Cell* **134**, 657–667 (2008).

232. Jun, J. Il & Lau, L. F. The matricellular protein CCN1 induces fibroblast senescence and restricts fibrosis in cutaneous wound healing. *Nat. Cell Biol.* **12**, 676–685 (2010).

233. Schafer, M. J. *et al.* Cellular senescence mediates fibrotic pulmonary disease. *Nat. Commun.* **8**, (2017).

234. Freund, A., Orjalo, A. V., Desprez, P. Y. & Campisi, J. Inflammatory networks during cellular senescence: causes and consequences. *Trends Mol. Med.* **16**, 238–246 (2010).

235. Sagiv, A. & Krizhanovsky, V. Immunosurveillance of senescent cells: The bright side of the senescence program. *Biogerontology* **14**, 617–628 (2013).

236. Kang, T.-W. *et al.* Senescence surveillance of pre-malignant hepatocytes limits liver cancer development. *Nature* **479**, 547–551 (2011).

237. Di Mitri, D. *et al.* Tumour-infiltrating Gr-1 + myeloid cells antagonize senescence in cancer. *Nature* **515**, 134–137 (2014).

238. Eggert, T. *et al.* Distinct Functions of Senescence-Associated Immune Responses in Liver Tumor Surveillance and Tumor Progression. *Cancer Cell* **30**, 533–547 (2016).

239. Muñoz, D. P. *et al.* Targetable mechanisms driving immunoevasion of persistent

senescent cells link chemotherapy-resistant cancer to aging. *JCI Insight* **4**, (2019).

240. Baker, D. J. *et al.* Clearance of p16 Ink4a-positive senescent cells delays ageing-associated disorders. *Nature* **479**, 232–236 (2011).

241. Campisi, J. Aging , Cellular Senescence , and Cancer. 1–21 (2013). doi:10.1146/annurev-physiol-030212-183653

242. Calcinotto, A. *et al.* Cellular senescence: Aging, cancer, and injury. *Physiol. Rev.* **99**, 1047–1078 (2019).

243. Baker, D. J. *et al.* Naturally occurring p16Ink4a-positive cells shorten healthy lifespan. *Nature* **530**, 184–189 (2016).

244. Warfel, N. A. & El-Deiry, W. S. p21WAF1 and tumourigenesis. *Curr. Opin. Oncol.* **25**, 52–58 (2013).

245. Lim, S. & Kaldis, P. Cdks, cyclins and CKIs: Roles beyond cell cycle regulation. *Dev.* **140**, 3079–3093 (2013).

246. Besson, A., Dowdy, S. F. & Roberts, J. M. CDK Inhibitors: Cell Cycle Regulators and Beyond. *Dev. Cell* **14**, 159–169 (2008).

247. Xiong, Y. *et al.* P21 is a universal inhibitor of cyclin kinases. *Nature* **366**, 701–704 (1993).

248. Harper, J. W., Adami, G. R., Wei, N., Keyomarsi, K. & Elledge, S. J. The p21 Cdk-interacting protein Cip1 is a potent inhibitor of G1 cyclin-dependent kinases. *Cell* **75**, 805–16 (1993).

249. Noda, A., Ning, Y., Venable, S. F., Pereira-Smith, O. M. & Smith, J. R. Cloning of senescent cell-derived inhibitors of dna synthesis using an expression screen. *Experimental Cell Research* **211**, 90–98 (1994).

250. Xiong, Y., Zhang, H. & Beach, D. D type cyclins associate with multiple protein kinases and the DNA replication and repair factor PCNA. *Cell* **71**, 505–514 (1992).

251. Gu, Y., Turck, C. W. & Morgan, D. O. Inhibition of CDK2 activity in vivo by an associated 20K regulatory subunit. *Nature* **366**, 707–710 (1993).

252. Zhang, H., Xiong, Y. & Beach, D. Proliferating cell nuclear antigen and p21 are components of multiple cell cycle kinase complexes. *Mol. Biol. Cell* **4**, 897–906 (1993).

253. Dulić, V. *et al.* p53-dependent inhibition of cyclin-dependent kinase activities in human fibroblasts during radiation-induced G1 arrest. *Cell* **76**, 1013–1023 (1994).

254. Kreis, Louwen & Yuan. The Multifaceted p21 (Cip1/Waf1/CDKN1A) in Cell Differentiation, Migration and Cancer Therapy. *Cancers (Basel).* **11**, 1220 (2019).

255. Al Bitar, S. & Gali-Muhtasib, H. The role of the cyclin dependent kinase inhibitor p21cip1/waf1 in targeting cancer: Molecular mechanisms and novel therapeutics. *Cancers (Basel).* **11**, 1–21 (2019).

256. Karimian, A., Ahmadi, Y. & Yousefi, B. Multiple functions of p21 in cell cycle , apoptosis and transcriptional regulation after DNA damage. *DNA Repair (Amst).* **42**, 63–71 (2016).

257. Gartel, A. L., Radhakrishnan, S. K., Serfas, M. S., Kwon, Y. H. & Tyner, A. L. A novel p21WAF1/CIP1 transcript is highly dependent on p53 for its basal expression in mouse tissues. *Oncogene* **23**, 8154–8157 (2004).

258. Radhakrishnan, S. K., Gierut, J. & Gartel, A. L. Multiple alternate p21 transcripts are regulated by p53 in human cells. *Oncogene* **25**, 1812–1815 (2006).

259. Nozell, S. & Chen, X. p21B, a variant of p21Waf1/Cip1, is induced by the p53 family. *Oncogene* **21**, 1285–1294 (2002).

260. Collier, A. E., Spandau, D. F. & Wek, R. C. Translational control of a human CDKN1A mRNA splice variant regulates the fate of UVB-irradiated human keratinocytes. *Mol. Biol. Cell* **29**, 29–41 (2018).

261. Jung, Y.-S., Qian, Y. & Chen, X. Examination of the expanding pathways for the regulation of p21 expression and activity. *Cell. Signal.* **22**, 1003–1012 (2010).

262. Lehman, S. L. *et al.* Translational Upregulation of an Individual p21Cip1 Transcript Variant by GCN2 Regulates Cell Proliferation and Survival under Nutrient Stress. *PLoS Genet.* **11**, 1–21 (2015).

263. López-Domínguez, J. A. *et al.* Cdkn1a Transcript Variant 2 is a Marker of Aging and Cellular Senescence. *Aging (Albany. NY).* **13**, 13380–13392 (2021).

264. Dutto, I., Tillhon, M., Cazzalini, O., Stivala, L. A. & Prosperi, E. Biology of the cell cycle inhibitor p21CDKN1A: molecular mechanisms and relevance in chemical toxicology. *Arch. Toxicol.* **89**, 155–178 (2015).

265. Bateman, A. *et al.* UniProt: The universal protein knowledgebase in 2021. *Nucleic Acids Res.* **49**, D480–D489 (2021).

266. Yoon, M.-K., Mitrea, D. M., Ou, L. & Kriwacki, R. W. Cell cycle regulation by the intrinsically disordered proteins p21 and p27. *Biochem. Soc. Trans.* **40**, 981–988 (2012).

267. Wang, Y. *et al.* Intrinsic disorder mediates the diverse regulatory functions of the Cdk inhibitor p21. *Nat. Chem. Biol.* **7**, 214–221 (2011).

268. Macleod, K. F. *et al.* p53-dependent and independent expression of p21 during cell growth, differentiation, and DNA damage. *Genes Dev.* **9**, 9335–9344 (1995).

269. Shahbaz, A. J. The Guardian of the Genome: p53. *J. Pakistan Assoc. Dermatologists* **14**, 107–109 (2004).

270. Harms, K., Nozell, S. & Chen, X. The common and distinct target genes of the p53 family transcription factors. *Cell. Mol. Life Sci.* **61**, 822–842 (2004).

271. Gartel, A. L. & Radhakrishnan, S. K. Lost in transcription: p21 repression, mechanisms, and consequences. *Cancer Res.* **65**, 3980–3985 (2005).

272. Abbas, T. & Dutta, A. p21 in cancer: intricate networks and multiple activities. *Nat. Rev. Cancer* **9**, 400–414 (2009).

273. Chai, Y. L., Cui, J. Q., Shao, N., Reddy, E. S. P. & Rao, V. N. The second BRCT domain of BRCA1 proteins interacts with p53 and stimulates transcription from the p21(WAF1/CIP1) promoter. *Oncogene* **18**, 263–268 (1999).

274. Sherr, C. J. Tumor surveillance via the ARF-p53 pathway. *Genes Dev.* **12**, 2984–2991 (1998).

275. Calvisi, D. F. *et al.* NORE1A Tumor Suppressor Candidate Modulates p21 CIP1 via p53. *Cancer Res.* **69**, 4629–4637 (2009).

276. Takahashi, K. & Yamanaka, S. Induction of Pluripotent Stem Cells from Mouse Embryonic and Adult Fibroblast Cultures by Defined Factors. *Cell* **126**, 663–676 (2006).

277. Rowland, B. D., Bernards, R. & Peeper, D. S. The KLF4 tumour suppressor is a transcriptional repressor of p53 that acts as a context-dependent oncogene. *Nat. Cell Biol.* **7**, 1074–1082 (2005).

278. Zhang, W. *et al.* The gut-enriched Kruppel-like factor (Kruppel-like factor 4) mediates the transactivating effect of p53 on the p21(WAF1)/(Cip)1 promoter. *J. Biol. Chem.* **275**, 18391–18398 (2000).

279. Yoon, H. S., Chen, X. & Yang, V. W. Krüppel-like Factor 4 Mediates p53-dependent G1/S Cell Cycle Arrest in Response to DNA Damage. *J. Biol. Chem.* **278**, 2101–2105 (2003).

280. Rowland, B. D. & Peeper, D. S. KLF4, p21 and context-dependent opposing forces in cancer. *Nat. Rev. Cancer* **6**, 11–23 (2006).

281. Gévry, N., Ho, M. C., Laflamme, L., Livingston, D. M. & Gaudreau, L. p21 transcription is regulated by differential localization of histone H2A.Z. *Genes Dev.* **21**, 1869–1881 (2007).

282. Gartel, A. L. & Tyner, A. L. Transcriptional Regulation of the p21(WAF1/CIP1)Gene. *Exp. Cell Res.* **246**, 280–289 (1999).

283. Datto, M. B. *et al.* Transforming growth factor β induces the cyclin-dependent kinase inhibitor p21 through a p53-independent mechanism. *Proc. Natl. Acad. Sci. U. S. A.* **92**, 5545–5549 (1995).

284. Pardali, K. *et al.* Role of Smad proteins and transcription factor Sp1 in p21Waf1/Cip1 regulation by transforming growth factor-β. *J. Biol. Chem.* **275**, 29244–29256 (2000).

285. Mitchell, K. O. & El-Deiry, W. S. Overexpression of c-Myc inhibits p21(WAF1/CIP1)

expression and induces S-phase entry in 12-O-tetradecanoylphorbol-13-acetate (TPA)-sensitive human cancer cells. *Cell Growth Differ.* **10**, 223–230 (1999).

286. Brenner, C. *et al.* Myc represses transcription through recruitment of DNA methyltransferase corepressor. *EMBO J.* **24**, 336–346 (2005).

287. Fang, J. Y. & Lu, Y. Y. Effects of histone acetylation and DNA methylation on p21WAF1 regulation. *World J. Gastroenterol.* **8**, 400–405 (2002).

288. Ocker, M. & Schneider-Stock, R. Histone deacetylase inhibitors: Signalling towards p21cip1/waf1. *Int. J. Biochem. Cell Biol.* **39**, 1367–1374 (2007).

289. Shamloo, B. & Usluer, S. P21 in cancer research. *Cancers (Basel).* **11**, 1–19 (2019).

290. Filipowicz, W., Bhattacharyya, S. N. & Sonenberg, N. Mechanisms of post-transcriptional regulation by microRNAs: Are the answers in sight? *Nat. Rev. Genet.* **9**, 102–114 (2008).

291. Nie, M., Balda, M. S. & Matter, K. Stress- and Rho-activated ZO-1-associated nucleic acid binding protein binding to p21 mRNA mediates stabilization, translation, and cell survival. *Proc. Natl. Acad. Sci. U. S. A.* **109**, 10897–10902 (2012).

292. Davidovic, L. *et al.* A Novel Role for the RNA-Binding Protein FXR1P in Myoblasts Cell-Cycle Progression by Modulating p21/Cdkn1a/Cip1/Waf1 mRNA Stability. *PLoS Genet.* **9**, (2013).

293. Jiang, Y. *et al.* Rbm24, an RNA-binding Protein and a Target of p53, Regulates p21 Expression via mRNA Stability. *J. Biol. Chem.* **289**, 3164–3175 (2014).

294. Peters, D. *et al.* The DEAD-box RNA helicase DDX41 is a novel repressor of p21WAF1/CIP1 mRNA translation. *J. Biol. Chem.* **292**, 8831–8841 (2017).

295. Li, Q. *et al.* NSUN2-Mediated m5C Methylation and METTL3/METTL14-Mediated m6A Methylation Cooperatively Enhance p21 Translation. *J. Cell. Biochem.* **118**, 2587–2598 (2017).

296. Nakakido, M. *et al.* PRMT6 increases cytoplasmic localization of p21CDKN1A in cancer cells through arginine methylation and makes more resistant to cytotoxic agents. *Oncotarget* **6**, 30957–30967 (2015).

297. Lee, M.-S. *et al.* Stabilization of p21 (Cip1/WAF1) following Tip60-dependent acetylation is required for p21-mediated DNA damage response. *Cell Death Differ.* **20**, 620–629 (2013).

298. Li, B. *et al.* Sirt1-inducible deacetylation of p21 promotes cardiomyocyte proliferation. *Aging (Albany. NY).* **11**, 12546–12567 (2019).

299. Sheaff, R. J. *et al.* Proteasomal turnover of p21(Cip1) does not require p21(Cip1) ubiquitination. *Mol. Cell* **5**, 403–410 (2000).

300. Glickman, M. H. & Ciechanover, A. The ubiquitin-proteasome proteolytic pathway: Destruction for the sake of construction. *Physiol. Rev.* **82**, 373–428 (2002).

301. Starostina, N. G. & Kipreos, E. T. Multiple degradation pathways regulate versatile CIP/KIP CDK inhibitors. *Trends Cell Biol.* **22**, 33–41 (2012).

302. Kreis, N.-N., Louwen, F. & Yuan, J. Less understood issues: p21Cip1 in mitosis and its therapeutic potential. *Oncogene* **34**, 1758–1767 (2015).

303. Starostina, N. G., Simpliciano, J. M., McGuirk, M. A. & Kipreos, E. T. CRL2LRR-1 Targets a CDK Inhibitor for Cell Cycle Control in C. elegans and Actin-Based Motility Regulation in Human Cells. *Dev. Cell* **19**, 753–764 (2010).

304. Park, M. H. *et al.* Parkin Knockout Inhibits Neuronal Development via Regulation of Proteasomal Degradation of p21. *Theranostics* **7**, 2033–2045 (2017).

305. Lee, E.-W. *et al.* Differential regulation of p53 and p21 by MKRN1 E3 ligase controls cell cycle arrest and apoptosis. *EMBO J.* **28**, 2100–2113 (2009).

306. Zhi, X. *et al.* E3 Ubiquitin Ligase RNF126 Promotes Cancer Cell Proliferation by Targeting the Tumor Suppressor p21 for Ubiquitin-Mediated Degradation. *Cancer Res.* **73**, 385–394 (2013).

307. Jascur, T. *et al.* Regulation of p21WAF1/CIP1 Stability by WISp39, a Hsp90 Binding TPR Protein. *Mol. Cell* **17**, 237–249 (2005).

308. Coleman, M. L., Marshall, C. J. & Olson, M. F. Ras promotes p21(Waf1/Cip1) protein stability via a cyclin D1-imposed block in proteasome-mediated degradation. *EMBO J.* **22**, 2036–46 (2003).

309. Xiao, J. *et al.* Nucleophosmin/B23 interacts with p21WAF1/CIP1 and contributes to its stability. *Cell Cycle* **8**, 889–895 (2009).

310. Oh, H. *et al.* Negative regulation of cell growth and differentiation by TSG101 through association with p21Cip1/WAF1. *Proc. Natl. Acad. Sci.* **99**, 5430–5435 (2002).

311. Timchenko, N. A. *et al.* CCAAT/enhancer binding protein alpha regulates p21 protein and hepatocyte proliferation in newborn mice. *Mol. Cell. Biol.* **17**, 7353–7361 (1997).

312. Cazzalini, O., Scovassi, A. I., Savio, M., Stivala, L. A. & Prosperi, E. Multiple roles of the cell cycle inhibitor p21CDKN1A in the DNA damage response. *Mutat. Res. - Rev. Mutat. Res.* **704**, 12–20 (2010).

313. Saha, P., Eichbaum, Q., Silberman, E. D., Mayer, B. J. & Dutta, A. p21CIP1 and Cdc25A: competition between an inhibitor and an activator of cyclin-dependent kinases. *Mol. Cell. Biol.* **17**, 4338–4345 (1997).

314. Luo, Y., Hurwitz, J. & Massagué, J. Cell-cycle inhibition by independent CDK and PCNA binding domains in p21Cip1. *Nature* **375**, 159–161 (1995).

315. Chen, J., Jackson, P. K., Kirschner, M. W. & Dutta, A. Separate domains of p21 involved in the inhibition of Cdk kinase and PCNA. *Nature* **374**, 386–388 (1995).

316. Labaer, J. *et al.* New functional activities for the p21 family of CDK inhibitors. *Genes Dev.* **11**, 847–862 (1997).

317. Cheng, M. *et al.* The p21(Cip1) and p27(Kip1) CDK 'inhibitors' are essential activators of cyclin D-dependent kinases in murine fibroblasts. *EMBO J.* **18**, 1571–1583 (1999).

318. Dash, B. C. & El-Deiry, W. S. Phosphorylation of p21 in G 2 /M Promotes Cyclin B-Cdc2 Kinase Activity . *Mol. Cell. Biol.* **25**, 3364–3387 (2005).

319. Lai, L., Shin, G. Y. & Qiu, H. The Role of Cell Cycle Regulators in Cell Survival—Dual Functions of Cyclin-Dependent Kinase 20 and p21Cip1/Waf1. *Int. J. Mol. Sci.* **21**, 8504 (2020).

320. Gartel, A. L. & Tyner, A. L. The role of the cyclin-dependent kinase inhibitor p21 in apoptosis. *Mol. Cancer Ther.* **1**, 639–649 (2002).

321. Jänicke, R. U., Sohn, D., Essmann, F. & Schulze-Osthoff, K. The Multiple Battles Fought by Anti-Apoptotic p21. *Cell Cycle* **6**, 407–413 (2007).

322. Suzuki, A., Tsutomi, Y., Akahane, K., Araki, T. & Miura, M. Resistance to Fas-mediated apoptosis: activation of Caspase 3 is regulated by cell cycle regulator p21WAF1 and IAP gene family ILP. *Oncogene* **17**, 931–939 (1998).

323. Asada, M. *et al.* Apoptosis inhibitory activity of cytoplasmic p21(Cip1/WAF1) in monocytic differentiation. *EMBO J.* **18**, 1223–1234 (1999).

324. Shim, J., Lee, H., Park, J., Kim, H. & Choi, E.-J. A non-enzymatic p21 protein inhibitor of stress-activated protein kinases. *Nature* **381**, 804–807 (1996).

325. Chang, B. *et al.* Effects of p21 Waf1 / Cip1 / Sdi1 on cellular gene expression : Implications for carcinogenesis , senescence , and age-related diseases. *PNAS* **97**, (2000).

326. Gartel, A. L. The conflicting roles of the cdk inhibitor p21(CIP1/WAF1) in apoptosis. *Leuk. Res.* **29**, 1237–1238 (2005).

327. Fujiwara, K. *et al.* Pivotal role of the cyclin-dependent kinase inhibitor p21 WAF1/CIP1 in apoptosis and autophagy. *J. Biol. Chem.* **283**, 388–397 (2008).

328. Capparelli, C. *et al.* CDK inhibitors (p16/p19/p21) induce senescence and autophagy in cancer-associated fibroblasts, 'fueling' tumor growth via paracrine interactions, without an increase in neo-angiogenesis. *Cell Cycle* **11**, 3599–3610 (2012).

329. Mohapatra, P. *et al.* Quinacrine-Mediated Autophagy and Apoptosis in Colon Cancer Cells Is Through a p53- and p21-Dependent Mechanism. *Oncol. Res. Featur. Preclin. Clin. Cancer Ther.* **20**, 81–91 (2012).

330. Xu, M. *et al.* Oridonin protects against cardiac hypertrophy by promoting P21-related autophagy. *Cell Death Dis.* **10**, (2019).

331. Kwon, Y. H., Jovanovic, A., Serfas, M. S. & Tyner, A. L. The Cdk inhibitor p21 is

required for necrosis, but it inhibits apoptosis following toxin-induced liver injury. *J. Biol. Chem.* **278**, 30348–30355 (2003).

332. Waga, S., Hannon, G. J., Beach, D. & Stillman, B. The p21 inhibitor of cyclin-dependent kinases controls DNA replication by interaction with PCNA. *Nature* **369**, 574–578 (1994).

333. Tom, S., Ranalli, T. A., Podust, V. N. & Bambara, R. A. Regulatory Roles of p21 and Apurinic/Apyrimidinic Endonuclease 1 in Base Excision Repair. *J. Biol. Chem.* **276**, 48781–48789 (2001).

334. Avkin, S. *et al.* p53 and p21 Regulate Error-Prone DNA Repair to Yield a Lower Mutation Load. *Mol. Cell* **22**, 407–413 (2006).

335. Cazzalini, O. *et al.* Interaction of p21CDKN1A with PCNA regulates the histone acetyltransferase activity of p300 in nucleotide excision repair. *Nucleic Acids Res.* **36**, 1713–1722 (2008).

336. Soria, G., Speroni, J., Podhajcer, O. L., Prives, C. & Gottifredi, V. p21 differentially regulates DNA replication and DNA-repair-associated processes after UV irradiation. *J. Cell Sci.* **121**, 3271–3282 (2008).

337. Cazzalini, O. *et al.* p21CDKN1A participates in base excision repair by regulating the activity of poly(ADP-ribose) polymerase-1. *DNA Repair (Amst).* **9**, 627–635 (2010).

338. Mauro, M. *et al.* P21 promotes error-free replication-coupled DNA double-strand break repair. *Nucleic Acids Res.* **40**, 8348–8360 (2012).

339. Perucca, P. *et al.* Spatiotemporal dynamics of p21CDKN1A protein recruitment to DNA-damage sites and interaction with proliferating cell nuclear antigen. *J. Cell Sci.* **119**, 1517–1527 (2006).

340. Mansilla, S. F. *et al.* Cyclin Kinase-independent role of p21CDKN1A in the promotion of nascent DNA elongation in unstressed cells. *Elife* **5**, 1–26 (2016).

341. Georgakilas, A. G., Martin, O. A. & Bonner, W. M. p21: A Two-Faced Genome Guardian. *Trends Mol. Med.* **23**, 310–319 (2017).

342. Mansilla, S. F. *et al.* UV-triggered p21 degradation facilitates damaged-DNA replication and preserves genomic stability. *Nucleic Acids Res.* **41**, 6942–6951 (2013).

343. Galanos, P. *et al.* Chronic p53-independent p21 expression causes genomic instability by deregulating replication licensing. *Nat. Cell Biol.* **18**, 777–789 (2016).

344. Tanaka, H. *et al.* Cytoplasmic p21Cip1/WAF1 regulates neurite remodeling by inhibiting Rho-kinase activity. *J. Cell Biol.* **158**, 321–329 (2002).

345. Lee, S. & Helfman, D. M. Cytoplasmic p21Cip1 Is Involved in Ras-induced Inhibition of the ROCK/LIMK/Cofilin Pathway. *J. Biol. Chem.* **279**, 1885–1891 (2004).

346. Qian, X. *et al.* p21CIP1 mediates reciprocal switching between proliferation and invasion during metastasis. *Oncogene* **32**, 2292–2303 (2013).

347. Romanov, V. S., Pospelov, V. A. & Pospelova, T. V. Cyclin-dependent kinase inhibitor p21Waf1: Contemporary view on its role in senescence and oncogenesis. *Biochem.* **77**, 575–584 (2012).

348. Bouchet, B. P., Fauvet, F., Grelier, G., Galmarini, C. M. & Puisieux, A. P21 Cip1 regulates cell-substrate adhesion and interphase microtubule dynamics in untransformed human mammary epithelial cells. *Eur. J. Cell Biol.* **90**, 631–641 (2011).

349. Dai, M. *et al.* A novel function for p21Cip1 and acetyltransferase p/CAF as critical transcriptional regulators of TGFβ-mediated breast cancer cell migration and invasion. *Breast Cancer Res.* **14**, 3055 (2012).

350. Kim, J. *et al.* Cooperative actions of p21 WAF 1 and p53 induce Slug protein degradation and suppress cell invasion . *EMBO Rep.* **15**, 1062–1068 (2014).

351. Löhr, K., Möritz, C., Contente, A. & Dobbelstein, M. p21/CDKN1A mediates negative regulation of transcription by p53. *J. Biol. Chem.* **278**, 32507–32516 (2003).

352. Shiyanov, P. *et al.* p21 Disrupts the interaction between cdk2 and the E2F-p130 complex. *Mol. Cell. Biol.* **16**, 737–744 (1996).

353. Quaas, M., Müller, G. A. & Engeland, K. p53 can repress transcription of cell cycle

genes through a p21 WAF1/CIP1-dependent switch from MMB to DREAM protein complex binding at CHR promoter elements. *Cell Cycle* **11**, 4661–4672 (2012).

354. Engeland, K. Cell cycle arrest through indirect transcriptional repression by p53: I have a DREAM. *Cell Death Differ.* **25**, 114–132 (2018).

355. Delavaine, L. & La Thangue, N. B. Control of E2F activity by p21(Waf1/Cip1). *Oncogene* **18**, 5381–5392 (1999).

356. Kitaura, H. *et al.* Reciprocal Regulation via Protein-Protein Interaction between c-Myc and p21 in DNA Replication and Transcription. *J. Biol. Chem.* **275**, 10477–10483 (2000).

357. Coqueret, O. & Gascan, H. Functional interaction of STAT3 transcription factor with the cell cycle inhibitor p21(WAF1/CIP1/SDI1). *J. Biol. Chem.* **275**, 18794–18800 (2000).

358. Chen, W. *et al.* Direct Interaction between Nrf2 and p21Cip1/WAF1 Upregulates the Nrf2-Mediated Antioxidant Response. *Mol. Cell* **34**, 663–673 (2009).

359. Fritah, A., Saucier, C., Mester, J., Redeuilh, G. & Sabbah, M. p21 WAF1 / CIP1 Selectively Controls the Transcriptional Activity of Estrogen Receptor α . *Mol. Cell. Biol.* **25**, 2419–2430 (2005).

360. Snowden, A. W., Anderson, L. A., Webster, G. A. & Perkins, N. D. A Novel Transcriptional Repression Domain Mediates p21 WAF1/CIP1 Induction of p300 Transactivation. *Mol. Cell. Biol.* **20**, 2676–2686 (2000).

361. Perkins, N. D. *et al.* Regulation of NF-κB by Cyclin-Dependent Kinases Associated with the p300 Coactivator. *Science (80-.).* **275**, 523–527 (1997).

362. Devgan, V., Mammucari, C., Millar, S. E., Brisken, C. & Dotto, G. P. p21WAF1/Cip1 is a negative transcriptional regulator of Wnt4 expression downstream of Notch1 activation. *Genes Dev.* **19**, 1485–1495 (2005).

363. Tan, H. H. & Porter, A. G. p21WAF1 negatively regulates DNMT1 expression in mammalian cells. *Biochem. Biophys. Res. Commun.* **382**, 171–176 (2009).

364. Yao, H. *et al.* Disruption of p21 attenuates lung inflammation induced by cigarette

smoke, LPS, and fMLP in mice. *Am. J. Respir. Cell Mol. Biol.* **39**, 7–18 (2008).

365. Trakala, M. *et al.* Regulation of macrophage activation and septic shock susceptibility via p21 (WAF1/CIP1). *Eur. J. Immunol.* **39**, 810–819 (2009).

366. Parker, S. B. *et al.* p53-independent expression of p21Cip1 in muscle and other terminally differentiating cells. *Science (80-.).* **267**, 1024–1027 (1995).

367. Di Cunto, F. *et al.* Inhibitory Function of p21 Cip1/WAF1 in Differentiation of Primary Mouse Keratinocytes Independent of Cell Cycle Control. *Science (80-.).* **280**, 1069–1072 (1998).

368. Zezula, J. *et al.* p21 cip1 is required for the differentiation of oligodendrocytes independently of cell cycle withdrawal. *EMBO Rep.* **2**, 27–34 (2001).

369. Ghanem, L. & Steinman, R. A. p21Waf1 inhibits granulocytic differentiation of 32Dcl3 cells. *Leuk. Res.* **30**, 1285–1292 (2006).

370. Bellosta, P., Masramon, L., Mansukhani, A. & Basilico, C. p21WAF1/CIP1 Acts as a Brake in Osteoblast Differentiation. *J. Bone Miner. Res.* **18**, 818–826 (2003).

371. Missero, C. *et al.* Involvement of the cell-cycle inhibitor Cip1/WAF1 and the E1A-associated p300 protein in terminal differentiation. *Proc. Natl. Acad. Sci.* **92**, 5451–5455 (1995).

372. Topley, G. I., Okuyama, R., Gonzales, J. G., Conti, C. & Dotto, G. P. p21WAF1/Cip1 functions as a suppressor of malignant skin tumor formation and a determinant of keratinocyte stem-cell potential. *Proc. Natl. Acad. Sci. U. S. A.* **96**, 9089–9094 (1999).

373. Cheng, T. *et al.* Hematopoietic Stem Cell Quiescence Maintained by p21 cip1/waf1. *Science (80-.).* **287**, 1804–1808 (2000).

374. Kippin, T. E., Martens, D. J. & van der Kooy, D. p21 loss compromises the relative quiescence of forebrain stem cell proliferation leading to exhaustion of their proliferation capacity. *Genes Dev.* **19**, 756–767 (2005).

375. Viale, A. *et al.* Cell-cycle restriction limits DNA damage and maintains self-renewal of leukaemia stem cells. *Nature* **457**, 51–56 (2009).

376. Kawamura, T. *et al.* Linking the p53 tumour suppressor pathway to somatic cell reprogramming. *Nature* **460**, 1140–1144 (2009).

377. Hong, H. *et al.* Suppression of induced pluripotent stem cell generation by the p53–p21 pathway. *Nature* **460**, 1132–1135 (2009).

378. Yamamizu, K., Schlessinger, D. & Ko, M. S. H. SOX9 accelerates ESC differentiation to three germ layer lineages by repressing SOX2 expression through P21 (WAF1/CIP1). *Development* **141**, 4254–4266 (2014).

379. Bedelbaeva, K. *et al.* Lack of p21 expression links cell cycle control and appendage regeneration in mice. *Proc. Natl. Acad. Sci.* **107**, 5845–5850 (2010).

380. Gawriluk, T. R. *et al.* Comparative analysis of ear-hole closure identifies epimorphic regeneration as a discrete trait in mammals. *Nat. Commun.* **7**, (2016).

381. Wu, H. *et al.* Targeted in vivo expression of the cyclin-dependent kinase inhibitor p21 halts hepatocyte cell-cycle progression, postnatal liver development and regeneration. *Genes Dev.* **10**, 245–260 (1996).

382. Stepniak, E. *et al.* c-Jun/AP-1 controls liver regeneration by repressing p53/p21 and p38 MAPK activity. *Genes Dev.* **20**, 2306–2314 (2006).

383. Lehmann, K. *et al.* Liver Failure After Extended Hepatectomy in Mice Is Mediated by a p21-Dependent Barrier to Liver Regeneration. *Gastroenterology* **143**, 1609-1619.e4 (2012).

384. Buitrago-Molina, L. E. *et al.* The degree of liver injury determines the role of p21 in liver regeneration and hepatocarcinogenesis in mice. *Hepatology* **58**, 1143–1152 (2013).

385. Ritschka, B. *et al.* The senotherapeutic drug ABT-737 disrupts aberrant p21 expression to restore liver regeneration in adult mice. *Genes Dev.* **34**, 489–494 (2020).

386. Premnath, P. *et al.* p21−/− mice exhibit enhanced bone regeneration after injury. *BMC Musculoskelet. Disord.* **18**, 435 (2017).

387. Jablonski, C. L., Besler, B. A., Ali, J. & Krawetz, R. J. p21−/− Mice Exhibit Spontaneous

Articular Cartilage Regeneration Post-Injury. *Cartilage* **13**, 1608S-1617S (2021).

388. Ibaraki, K. *et al.* Deletion of p21 expression accelerates cartilage tissue repair via chondrocyte proliferation. *Mol. Med. Rep.* **21**, 2236–2242 (2020).

389. Jiang, D. *et al.* Local and transient inhibition of p21 expression ameliorates age-related delayed wound healing. *Wound Repair Regen.* **28**, 49–60 (2020).

390. Lv, X. *et al.* The cell cycle inhibitor P21 promotes the development of pulmonary fibrosis by suppressing lung alveolar regeneration. *Acta Pharm. Sin. B* **12**, 735–746 (2022).

391. Torbenson, M. *et al.* Stat-3 overexpression and p21 up-regulation accompany impaired regeneration of fatty livers. *Am. J. Pathol.* **161**, 155–161 (2002).

392. Arthur, L. M. & Heber-Katz, E. The role of p21 in regulating mammalian regeneration. *Stem Cell Res. Ther.* **2**, 30 (2011).

393. Chinzei, N. *et al.* P21 Deficiency Delays Regeneration of Skeletal Muscular Tissue. *PLoS One* **10**, e0125765 (2015).

394. Tanaka, H. *et al.* Cytoplasmic p21Cip1/WAF1 enhances axonal regeneration and functional recovery after spinal cord injury in rats. *Neuroscience* **127**, 155–164 (2004).

395. Barboza, J. A., Liu, G., Ju, Z., El-Naggar, A. K. & Lozano, G. P21 delays tumor onset by preservation of chromosomal stability. *Proc. Natl. Acad. Sci. U. S. A.* **103**, 19842–19847 (2006).

396. Efeyan, A., Collado, M., Velasco-Miguel, S. & Serrano, M. Genetic dissection of the role of p21Cip1/Waf1 in p53-mediated tumour suppression. *Oncogene* **26**, 1645–1649 (2007).

397. Deng, C., Zhang, P., Wade Harper, J., Elledge, S. J. & Leder, P. Mice Lacking p21CIP1/WAF1 undergo normal development, but are defective in G1 checkpoint control. *Cell* **82**, 675–684 (1995).

398. Martín-Caballero, J., Flores, J. M., García-Palencia, P. & Serrano, M. Tumor Susceptibility of p21 Waf1/Cip1-deficient Mice 1. *Cancer Res.* **61**, 6234–6238

(2001).

399. Jackson, R. J. *et al.* Loss of the cell cycle inhibitors p21Cip1 and p27Kip1 enhances tumorigenesis in knockout mouse models. *Oncogene* **21**, 8486–8497 (2002).

400. Missero, C., Kiyokawa, H. & Hospital, M. G. The absence of p21Cipl / wAF1 alters keratinocyte growth and differentiation and promotes r a s - t u m o r progression. 3065–3075 (1996).

401. Brugarolas, J., Bronson, R. T. & Jacks, T. p21 is a critical CDK2 regulator essential for proliferation control in Rb-deficient cells. *J. Cell Biol.* **141**, 503–514 (1998).

402. Adnane, J. *et al.* Loss of p21(WAF1/CIP1) accelerates Ras oncogenesis in a transgenic/knockout mammary cancer model. *Oncogene* **19**, 5338–5347 (2000).

403. Martín-Caballero, J., Flores, J. M., García-Palencia, P., Collado, M. & Serrano, M. Different cooperating effect of p21 or p27 deficiency in combination with INK4a/ARF deletion in mice. *Oncogene* **23**, 8231–8237 (2004).

404. Carbone, C. J., Graña, X., Reddy, E. P. & Haines, D. S. p21 loss cooperates with INK4 inactivation facilitating immortalization and Bcl-2-mediated anchorage-independent growth of oncogene-transduced primary mouse fibroblasts. *Cancer Res.* **67**, 4130–4137 (2007).

405. Bearss, D. J., Lee, R. J., Troyer, D. A., Pestell, R. G. & Windle, J. J. Differential effects of p21(WAF1/CIP1) deficiency on MMTV-ras and MMTV-myc mammary tumor properties. *Cancer Res.* **62**, 2077–84 (2002).

406. De La Cueva, E. *et al.* Tumorigenic activity of p21Waf1/Cip1 in thymic lymphoma. *Oncogene* **25**, 4128–4132 (2006).

407. Roninson, I. B. Oncogenic functions of tumour suppressor p21Waf1/Cip1/Sdi1: Association with cell senescence and tumour-promoting activities of stromal fibroblasts. *Cancer Lett.* **179**, 1–14 (2002).

408. Abukhdeir, A. M. & Park, B. H. p21 and p27: roles in carcinogenesis and drug resistance. *Expert Rev. Mol. Med.* **10**, e19 (2008).

409. Blagosklonny, M. V. Are p27 and p21 Cytoplasmic Oncoproteins? *Cell Cycle* **1**, 391–

393 (2002).

410. Liu, S., Bishop, W. R. & Liu, M. Differential effects of cell cycle regulatory protein p21WAF1/Cip1 on apoptosis and sensitivity to cancer chemotherapy. *Drug Resist. Updat.* **6**, 183–195 (2003).

411. Gartel, A. L. p21 WAF1/CIP1 and cancer: A shifting paradigm? *BioFactors* **35**, 161–164 (2009).

412. Rodier, F. & Campisi, J. Four faces of cellular senescence. *J. Cell Biol.* **192**, 547–556 (2011).

413. Milanovic, M., Yu, Y. & Schmitt, C. A. The Senescence–Stemness Alliance – A Cancer-Hijacked Regeneration Principle. *Trends Cell Biol.* **28**, 1049–1061 (2018).

414. Liu, Y. *et al.* Somatic cell type specific gene transfer reveals a tumor-promoting function for p21Waf1/Cip1. *EMBO J.* **26**, 4683–4693 (2007).

415. Balomenos, D. *et al.* The cell cycle inhibitor p21 controls T-cell proliferation and sex- linked lupus development. *Nat. Med.* **6**, 171–176 (2000).

416. Scatizzi, J. C. *et al.* The CDK domain of p21 is a suppressor of IL-1β-mediated inflammation in activated macrophages. *Eur. J. Immunol.* **39**, 820–825 (2009).

417. Woods, J. M. *et al.* A cell-cycle independent role for p21 in regulating synovial fibroblast migration in rheumatoid arthritis. *Arthritis Res. Ther.* **8**, 1–8 (2006).

418. Mavers, M. *et al.* Cyclin-Dependent Kinase Inhibitor p21 , via Its C-Terminal Domain , Is Essential for Resolution of Murine Inflammatory Arthritis. **64**, 141–152 (2012).

419. Hayashi, S. *et al.* p21 deficiency is susceptible to osteoarthritis through STAT3 phosphorylation. *Arthritis Res. Ther.* **17**, 1–11 (2015).

420. Fang, L. *et al.* p21Waf1/Cip1/Sdi1 induces permanent growth arrest with markers of replicative senescence in human tumor cells lacking functional p53. *Oncogene* **18**, 2789–2797 (1999).

421. Wang, Y., Blandino, G. & Givol, D. Induced p21waf expression in H1299 cell line promotes cell senescence and protects against cytotoxic effect of radiation and

doxorubicin. *Oncogene* **18**, 2643–2649 (1999).

422. Macip, S. *et al.* Inhibition of p21-mediated ROS accumulation can rescue p21-induced senescence. *EMBO J.* **21**, 2180–2188 (2002).

423. Brugarolas, J. *et al.* Radiation-induced cell cycle arrest compromised by p21 deficiency. *Nature* **377**, 552–557 (1995).

424. Brown, J. P., Wei, W. & Sedivy, J. M. Bypass of senescenoe after disruption of p21(CIP1)/(WAF1) gene in normal diploid human fibroblasts. *Science (80-.).* **277**, 831–834 (1997).

425. Dulić, V., Beney, G.-E., Frebourg, G., Drullinger, L. F. & Stein, G. H. Uncoupling between Phenotypic Senescence and Cell Cycle Arrest in Aging p21-Deficient Fibroblasts. *Mol. Cell. Biol.* **20**, 6741–6754 (2000).

426. Borgdorff, V. *et al.* Multiple microRNAs rescue from Ras-induced senescence by inhibiting p21Waf1/Cip1. *Oncogene* **29**, 2262–2271 (2010).

427. Pantoja, C. & Serrano, M. Murine fibroblasts lacking p21 undergo senescence and are resistant to transformation by oncogenic Ras. *Oncogene* **18**, 4974–4982 (1999).

428. Chang, B.-D. *et al.* Molecular determinants of terminal growth arrest induced in tumor cells by a chemotherapeutic agent. *Proc. Natl. Acad. Sci.* **99**, 389–394 (2002).

429. Castro, M. E., Guijarro, M. D. V., Moneo, V. & Carnero, A. Cellular senescence induced by p53-ras cooperation is independent of p21waf1 in murine embryo fibroblasts. *J. Cell. Biochem.* **92**, 514–524 (2004).

430. te Poele, R. H., Okorokov, A. L., Jardine, L., Cummings, J. & Joel, S. P. DNA damage is able to induce senescence in tumor cells in vitro and in vivo. *Cancer Res.* **62**, 1876–83 (2002).

431. Hsu, C. H., Altschuler, S. J. & Wu, L. F. Patterns of Early p21 Dynamics Determine Proliferation-Senescence Cell Fate after Chemotherapy. *Cell* **178**, 361-373.e12 (2019).

432. Yosef, R. *et al.* p21 maintains senescent cell viability under persistent DNA damage response by restraining JNK and caspase signaling. *EMBO J.* **36**, 2280–2295 (2017).

433. Villeneuve, N. F., Sun, Z., Chen, W. & Zhang, D. D. Nrf2 and p21 regulate the fine balance between life and death by controlling ROS levels. *Cell Cycle* **8**, 3255–3256 (2009).

434. Inoue, T. *et al.* Level of reactive oxygen species induced by p21WAF(1)/CIP(1) is critical for the determination of cell fate. *Cancer Sci.* **100**, 1275–1283 (2009).

435. Kim, H. K. *et al.* Transcriptional repression of high-mobility group box 2 by p21 in radiation-induced senescence. *Mol. Cells* **41**, 362–372 (2018).

436. Sturmlechner, I. *et al.* p21 produces a bioactive secretome that places stressed cells under immunosurveillance. *Science (80-.).* **374**, (2021).

437. Jaisser, F. Inducible Gene Expression and Gene Modification in Transgenic Mice. *J. Am. Soc. Nephrol.* **11**, S95–S100 (2000).

438. Premsrirut, P. K. *et al.* A rapid and scalable system for studying gene function in mice using conditional RNA interference. *Cell* **145**, 145–158 (2011).

439. Dow, L. E. *et al.* A pipeline for the generation of shRNA transgenic mice. *Nat. Protoc.* **7**, 374–393 (2012).

440. Kutter, C. & Svoboda, P. miRNA, siRNA, piRNA: Knowns of the unknown. *RNA Biol.* **5**, 181–188 (2008).

441. Wang, Y., Boerma, M. & Zhou, D. Ionizing Radiation-Induced Endothelial Cell Senescence and Cardiovascular Diseases. *Radiat. Res.* **186**, 153–161 (2016).

442. Chen, Z. *et al.* Cellular senescence in ionizing radiation (Review). *Oncol. Rep.* **42**, 883–894 (2019).

443. Xie, J., Nair, A. & Hermiston, T. W. A comparative study examining the cytotoxicity of inducible gene expression system ligands in different cell types. *Toxicol. Vitr.* **22**, 261–266 (2008).

444. Chen, E. Y. *et al.* Enrichr: interactive and collaborative HTML5 gene list enrichment analysis tool. *BMC Bioinformatics* **14**, 128 (2013).

445. Kuleshov, M. V. *et al.* Enrichr: a comprehensive gene set enrichment analysis web

server 2016 update. *Nucleic Acids Res.* **44**, W90–W97 (2016).

446. Xie, Z. *et al.* Gene Set Knowledge Discovery with Enrichr. *Curr. Protoc.* **1**, 1–51 (2021).

447. Butte, A. J. & Kohane, I. S. Mutial Information relevance networks: functional genomic clustering using pairwise entropy measurements. *Biocomput. 2000* 418–429 (1999). doi:10.1142/9789814447331_0040

448. Benson, E. K. *et al.* p53-dependent gene repression through p21 is mediated by recruitment of E2F4 repression complexes. *Oncogene* **33**, 3959–3969 (2014).

449. Fischer, M., Quaas, M., Steiner, L. & Engeland, K. The p53-p21-DREAM-CDE/CHR pathway regulates G2/M cell cycle genes. *Nucleic Acids Res.* **44**, 164–174 (2016).

450. Ferrándiz, N. *et al.* P21 as a transcriptional co-repressor of S-phase and mitotic control genes. *PLoS One* **7**, (2012).

451. Samarakoon, A., Chu, H. & Malarkannan, S. Murine NKG2D ligands: 'Double, double toil and trouble'. *Mol. Immunol.* **46**, 1011–1019 (2009).

452. Schrader, M. & Fahimi, H. D. The peroxisome: Still a mysterious organelle. *Histochem. Cell Biol.* **129**, 421–440 (2008).

453. Islinger, M., Voelkl, A., Fahimi, H. D. & Schrader, M. The peroxisome: an update on mysteries 2.0. *Histochem. Cell Biol.* **150**, 443–471 (2018).

454. Giordano, C. R. & Terlecky, S. R. Peroxisomes, cell senescence, and rates of aging. *Biochim. Biophys. Acta - Mol. Basis Dis.* **1822**, 1358–1362 (2012).

455. Di Cara, F. *et al.* Peroxisomes in Immune Response and Inflammation. *Int. J. Mol. Sci.* **20**, 3877 (2019).

456. Kim, J. & Bai, H. Peroxisomal Stress Response and Inter-Organelle Communication in Cellular Homeostasis and Aging. *Antioxidants* **11**, (2022).

457. Legakis, J. E. *et al.* Peroxisome senescence in human fibroblasts. *Mol. Biol. Cell* **13**, 4243–4255 (2002).

458. Pommier, Y., Leo, E., Zhang, H. & Marchand, C. DNA Topoisomerases and Their

Poisoning by Anticancer and Antibacterial Drugs. *Chem. Biol.* **17**, 421–433 (2010).

459. Ewald, J. A., Desotelle, J. A., Wilding, G. & Jarrard, D. F. Therapy-induced senescence in cancer. *J. Natl. Cancer Inst.* **102**, 1536–1546 (2010).

460. Thorn, C. F. *et al.* Doxorubicin pathways. *Pharmacogenet. Genomics* **21**, 440–446 (2011).

461. Jackson, J. G. *et al.* p53-Mediated Senescence Impairs the Apoptotic Response to Chemotherapy and Clinical Outcome in Breast Cancer. *Cancer Cell* **21**, 793–806 (2012).

462. Demaria, M. *et al.* Cellular Senescence Promotes Adverse Effects of Chemotherapy and Cancer Relapse. *Cancer Discov.* **7**, 165–176 (2017).

463. Islinger, M., Grille, S., Fahimi, H. D. & Schrader, M. The peroxisome: An update on mysteries. *Histochem. Cell Biol.* **137**, 547–574 (2012).

464. Uzor, N. E., McCullough, L. D. & Tsvetkov, A. S. Peroxisomal Dysfunction in Neurological Diseases and Brain Aging. *Front. Cell. Neurosci.* **14**, 1–10 (2020).

465. Schrader, M. & Fahimi, H. D. Peroxisomes and oxidative stress. *Biochim. Biophys. Acta - Mol. Cell Res.* **1763**, 1755–1766 (2006).

466. Terlecky, S. R., Koepke, J. I. & Walton, P. A. Peroxisomes and aging. *Biochim. Biophys. Acta - Mol. Cell Res.* **1763**, 1749–1754 (2006).

467. Koepke, J. I., Wood, C. S., Terlecky, L. J., Walton, P. A. & Terlecky, S. R. Progeric effects of catalase inactivation in human cells. *Toxicol. Appl. Pharmacol.* **232**, 99–108 (2008).

468. Deosaran, E. *et al.* NBR1 acts as an autophagy receptor for peroxisomes. *J. Cell Sci.* **126**, 939–952 (2013).

469. Defourny, J. *et al.* Pejvakin-mediated pexophagy protects auditory hair cells against noise-induced damage. *Proc. Natl. Acad. Sci. U. S. A.* **116**, 8010–8017 (2019).

470. Li, J. & Wang, W. Mechanisms and functions of pexophagy in mammalian cells. *Cells* **10**, (2021).

471. Ammit, A. J. *et al.* Tumor necrosis factor-α-induced secretion of RANTES and interleukin-6 from human airway smooth-muscle cells modulation by cyclic adenosine monophosphate. *Am. J. Respir. Cell Mol. Biol.* **23**, 794–802 (2000).

472. Hardaker, E. L. *et al.* Regulation of TNF-alpha- and IFN-gamma-induced CXCL10 expression: participation of the airway smooth muscle in the pulmonary inflammatory response in chronic obstructive pulmonary disease. *FASEB J.* **18**, 191–193 (2004).

473. Gruber, J. J. *et al.* Ars2 Links the Nuclear Cap-Binding Complex to RNA Interference and Cell Proliferation. *Cell* **138**, 328–339 (2009).

474. Andreu-Agullo, C., Maurin, T., Thompson, C. B. & Lai, E. C. Ars2 maintains neural stem-cell identity through direct transcriptional activation of Sox2. *Nature* **481**, 195–200 (2012).

475. El-Brolosy, M. A. & Stainier, D. Y. R. Genetic compensation: A phenomenon in search of mechanisms. *PLOS Genet.* **13**, e1006780 (2017).

476. Broude, E. V. *et al.* p21 (CDKN1A) is a Negative Regulator of p53 Stability. *Cell Cycle* **6**, 1467–1470 (2007).

477. Lee, J. *et al.* p21WAF1/CIP1 promotes p53 protein degradation by facilitating p53-Wip1 and p53-Mdm2 interaction. *Biochem. Biophys. Res. Commun.* **543**, 23–28 (2021).

478. Zhang, P. *et al.* p21CIP1 and p57KIP2 control muscle differentiation at the myogenin step. *Genes Dev.* **13**, 213–224 (1999).

479. Franklin, D. S., Godfrey, V. L., O'Brien, D. A., Deng, C. & Xiong, Y. Functional Collaboration between Different Cyclin-Dependent Kinase Inhibitors Suppresses Tumor Growth with Distinct Tissue Specificity. *Mol. Cell. Biol.* **20**, 6147–6158 (2000).

480. Stechmiller, J., Cowan, L. & Schultz, G. The Role of Doxycycline as a Matrix Metalloproteinase Inhibitor for the Treatment of Chronic Wounds. *Biol. Res. Nurs.* **11**, 336–344 (2010).

481. Griffin, M. O., Ceballos, G. & Villarreal, F. J. Tetracycline compounds with non-antimicrobial organ protective properties: Possible mechanisms of action. *Pharmacol. Res.* **63**, 102–107 (2011).

482. Kim, H.-S., Luo, L., Pflugfelder, S. C. & Li, D.-Q. Doxycycline Inhibits TGF-β1–Induced MMP-9 via Smad and MAPK Pathways in Human Corneal Epithelial Cells. *Investig. Opthalmology Vis. Sci.* **46**, 840 (2005).

483. Pereira, J. A., Matsumura, C. Y., Minatel, E., Marques, M. J. & Santo Neto, H. Understanding the beneficial effects of doxycycline on the dystrophic phenotype of the mdx mouse. *Muscle Nerve* **50**, 283–286 (2014).

484. Wlaschek, M., Maity, P., Makrantonaki, E. & Scharffetter-Kochanek, K. Connective Tissue and Fibroblast Senescence in Skin Aging. *J. Invest. Dermatol.* **141**, 985–992 (2021).

485. Lee, Y. I., Choi, S., Roh, W. S., Lee, J. H. & Kim, T.-G. Cellular Senescence and Inflammaging in the Skin Microenvironment. *Int. J. Mol. Sci.* **22**, 3849 (2021).

486. Fedintsev, A. & Moskalev, A. Stochastic non-enzymatic modification of long-lived macromolecules - A missing hallmark of aging. *Ageing Res. Rev.* **62**, 101097 (2020).

487. Bourguignon, M. H. *et al.* Genetic and epigenetic features in radiation sensitivity: Part II: Implications for clinical practice and radiation protection. *Eur. J. Nucl. Med. Mol. Imaging* **32**, 351–368 (2005).

488. Vandersickel, V., Slabbert, J., Thierens, H. & Vral, A. Comparison of the colony formation and crystal violet cell proliferation assays to determine cellular radiosensitivity in a repair-deficient MCF10A cell line. *Radiat. Meas.* **46**, 72–75 (2011).

489. Fiorentino, F. P., Symonds, C. E., Macaluso, M. & Giordano, A. Senescence and p130/Rbl2: a new beginning to the end. *Cell Res.* **19**, 1044–1051 (2009).

490. Vigneron, A., Roninson, I. B., Gamelin, E. & Coqueret, O. Src Inhibits Adriamycin-Induced Senescence and G 2 Checkpoint Arrest by Blocking the Induction of p21waf1. *Cancer Res.* **65**, 8927–8935 (2005).

491. Oskarsson, T. *et al.* Skin epidermis lacking the c-myc gene is resistant to Ras-driven tumorigenesis but can reacquire sensitivity upon additional loss of the p21 Cip1 gene. *Genes Dev.* **20**, 2024–2029 (2006).

492. Carné Trécesson, S. De *et al.* Escape from p21-mediated oncogene-induced senescence leads to cell dedifferentiation and dependence on anti-apoptotic Bcl-xL and MCL1 proteins. *J. Biol. Chem.* **286**, 12825–12838 (2011).

493. Guillon, J. *et al.* Regulation of senescence escape by TSP1 and CD47 following chemotherapy treatment. *Cell Death Dis.* **10**, (2019).

494. Sage, J., Miller, A. L., Pérez-Mancera, P. A., Wysocki, J. M. & Jacks, T. Acute mutation of retinoblastoma gene function is sufficient for cell cycle re-entry. *Nature* **424**, 223–228 (2003).

495. Dirac, A. M. G. & Bernards, R. Reversal of senescence in mouse fibroblasts through lentiviral suppression of p53. *J. Biol. Chem.* **278**, 11731–11734 (2003).

496. Saleh, T., Tyutyunyk-Massey, L. & Gewirtz, D. A. Tumor cell escape from therapy-induced senescence as a model of disease recurrence after dormancy. *Cancer Res.* **79**, 1044–1046 (2019).

497. Puig, P. E. *et al.* Tumor cells can escape DNA-damaging cisplatin through DNA endoreduplication and reversible polyploidy. *Cell Biol. Int.* **32**, 1031–1043 (2008).

498. Patel, P. L., Suram, A., Mirani, N., Bischof, O. & Herbig, U. Derepression of hTERT gene expression promotes escape from oncogene-induced cellular senescence. *Proc. Natl. Acad. Sci. U. S. A.* **113**, E5024–E5033 (2016).

499. Saleh, T. *et al.* Tumor cell escape from therapy-induced senescence. *Biochem. Pharmacol.* **162**, 202–212 (2019).

500. Kreis, N. N. *et al.* Function of p21 (Cip1/Waf1/CDKN1A) in migration and invasion of cancer and trophoblastic cells. *Cancers (Basel).* **11**, 1–17 (2019).

501. Kong, E. K. P. *et al.* p21 gene polymorphisms in systemic lupus erythematosus. *Rheumatology* **46**, 220–226 (2006).

502. Salvador, J. M. *et al.* Mice lacking the p53-effector gene Gadd45a develop a lupus-

like syndrome. *Immunity* **16**, 499–508 (2002).

503. Goulvestre, C. *et al.* A Mimic of p21 WAF1/CIP1 Ameliorates Murine Lupus. *J. Immunol.* **175**, 6959–6967 (2005).

504. Arias, C. F. *et al.* p21 CIP1/WAF1 Controls Proliferation of Activated/Memory T Cells and Affects Homeostasis and Memory T Cell Responses . *J. Immunol.* **178**, 2296–2306 (2007).

505. Zhu, B. *et al.* Early growth response gene 2 (Egr-2) controls the self-tolerance of T cells and prevents the development of lupuslike autoimmune disease. *J. Exp. Med.* **205**, 2295–2307 (2008).

506. Daszkiewicz, L. *et al.* Distinct p21 requirements for regulating normal and self-reactive T cells through IFN-γ production. *Sci. Rep.* **5**, 7691 (2015).

507. Rackov, G. *et al.* P21 mediates macrophage reprogramming through regulation of p50-p50 NF-κB and IFN-β. *J. Clin. Invest.* **126**, 3089–3103 (2016).

508. Coppé, J.-P. *et al.* Tumor Suppressor and Aging Biomarker p16INK4a Induces Cellular Senescence without the Associated Inflammatory Secretory Phenotype. *J. Biol. Chem.* **286**, 36396–36403 (2011).

509. Appay, V. & Rowland-Jones, S. L. RANTES: A versatile and controversial chemokine. *Trends Immunol.* **22**, 83–87 (2001).

510. Tokunaga, R. *et al.* CXCL9, CXCL10, CXCL11/CXCR3 axis for immune activation – A target for novel cancer therapy. *Cancer Treat. Rev.* **63**, 40–47 (2018).

511. Stanczyk, J. *et al.* RANTES and chemotactic activity in synovial fluids from patients with rheumatoid arthritis and osteoarthritis. *Mediators Inflamm.* **2005**, 343–348 (2005).

512. Lee, E. Y., Lee, Z. H. & Song, Y. W. CXCL10 and autoimmune diseases. *Autoimmun. Rev.* **8**, 379–383 (2009).

513. Levy, J. A. The Unexpected Pleiotropic Activities of RANTES. *J. Immunol.* **182**, 3945–3946 (2009).

514. Lujambio, A. To clear, or not to clear (senescent cells)? That is the question. *Insid. Cell* **1**, 87–95 (2016).

515. Sagiv, A. *et al.* Granule exocytosis mediates immune surveillance of senescent cells. *Oncogene* **32**, 1971–1977 (2013).

516. Iannello, A., Thompson, T. W., Ardolino, M., Lowe, S. W. & Raulet, D. H. p53-dependent chemokine production by senescent tumor cells supports NKG2D-dependent tumor elimination by natural killer cells. *J. Exp. Med.* **210**, 2057–2069 (2013).

517. Sagiv, A. *et al.* NKG2D ligands mediate immunosurveillance of senescent cells. *Aging (Albany. NY).* **8**, 328–344 (2016).

518. Soriani, A. *et al.* ATM-ATR-dependent up-regulation of DNAM-1 and NKG2D ligands on multiple myeloma cells by therapeutic agents results in enhanced NK-cell susceptibility and is associated with a senescent phenotype. *Blood* **113**, 3503–3511 (2009).

519. Roberts, A. I. *et al.* Cutting Edge: NKG2D Receptors Induced by IL-15 Costimulate CD28-Negative Effector CTL in the Tissue Microenvironment. *J. Immunol.* **167**, 5527–5530 (2001).

520. Zhang, C., Zhang, J., Niu, J., Zhang, J. & Tian, Z. Interleukin-15 improves cytotoxicity of natural killer cells via up-regulating NKG2D and cytotoxic effector molecule expression as well as STAT1 and ERK1/2 phosphorylation. *Cytokine* **42**, 128–136 (2008).

521. Barber, D. F. & Long, E. O. Coexpression of CD58 or CD48 with Intercellular Adhesion Molecule 1 on Target Cells Enhances Adhesion of Resting NK Cells. *J. Immunol.* **170**, 294–299 (2003).

522. Barber, D. F., Faure, M. & Long, E. O. LFA-1 Contributes an Early Signal for NK Cell Cytotoxicity. *J. Immunol.* **173**, 3653–3659 (2004).

523. Bui, T. M., Wiesolek, H. L. & Sumagin, R. ICAM-1: A master regulator of cellular responses in inflammation, injury resolution, and tumorigenesis. *J. Leukoc. Biol.* **108**, 787–799 (2020).

524. Gorgoulis, V. G. *et al.* p53-Dependent ICAM-1 overexpression in senescent human cells identified in atherosclerotic lesions. *Lab. Investig.* **85**, 502–511 (2005).

525. Chien, Y. *et al.* Control of the senescence-associated secretory phenotype by NF-κB promotes senescence and enhances chemosensitivity. *Genes Dev.* **25**, 2125–2136 (2011).

526. Robertson, M. J. Role of chemokines in the biology of natural killer cells. *J. Leukoc. Biol.* **71**, 173–83 (2002).

527. Maghazachi, A. A. Role of Chemokines in the Biology of Natural Killer Cells. in *Assessment & Evaluation in Higher Education* **37**, 37–58 (2010).

528. Ray, A. & Dittel, B. N. Isolation of Mouse Peritoneal Cavity Cells. *J. Vis. Exp.* 9–11 (2010). doi:10.3791/1488

529. Biran, A. *et al.* Senescent cells communicate via intercellular protein transfer. *Genes Dev.* **29**, 791–802 (2014).

530. Gasser, S., Orsulic, S., Brown, E. J. & Raulet, D. H. The DNA damage pathway regulates innate immune system ligands of the NKG2D receptor. *Nature* **436**, 1186–1190 (2005).

531. Aggarwal, B. B. Signalling pathways of the TNF superfamily: a double-edged sword. *Nat. Rev. Immunol.* **3**, 745–756 (2003).

532. Hayden, M. S. & Ghosh, S. Regulation of NF-κB by TNF family cytokines. *Semin. Immunol.* **26**, 253–266 (2014).

533. Sharma, S. & Sicinski, P. A kinase of many talents: non-neuronal functions of CDK5 in development and disease. *Open Biol.* **10**, 190287 (2020).

534. Laphanuwat, P. & Jirawatnotai, S. Immunomodulatory Roles of Cell Cycle Regulators. *Front. Cell Dev. Biol.* **7**, 1–8 (2019).

535. Choudhary, S. *et al.* High throughput short interfering RNA (siRNA) screening of the human kinome identifies novel kinases controlling the canonical nuclear factor-κB (NF-κB) activation pathway. *J. Biol. Chem.* **286**, 37187–37195 (2011).

536. Fu, A. K. Y. *et al.* Cyclin-dependent kinase 5 phosphorylates signal transducer and activator of transcription 3 and regulates its transcriptional activity. *Proc. Natl. Acad. Sci. U. S. A.* **101**, 6728–6733 (2004).

537. Courapied, S. *et al.* The cdk5 kinase regulates the STAT3 transcription factor to prevent DNA damage upon topoisomerase I inhibition. *J. Biol. Chem.* **285**, 26765–26778 (2010).

538. Bienvenu, F., Gascan, H. & Coqueret, O. Cyclin D1 Represses STAT3 Activation through a Cdk4-independent Mechanism. *J. Biol. Chem.* **276**, 16840–16847 (2001).

539. Aktary, Z., Alaee, M. & Pasdar, M. Beyond cell-cell adhesion: Plakoglobin and the regulation of tumorigenesis and metastasis. *Oncotarget* **8**, 32270–32291 (2017).

540. Aktary, Z., Kulak, S., Mackey, J., Jahroudi, N. & Pasdar, M. Plakoglobin interacts with the transcription factor p53 and regulates the expression of 14-3-3σ. *J. Cell Sci.* **126**, 3031–3042 (2013).

541. Aktary, Z. & Pasdar, M. Plakoglobin represses SATB1 expression and decreases in Vitro proliferation, migration and invasion. *PLoS One* **8**, 1–13 (2013).

542. Alaee, M., Padda, A., Mehrabani, V., Churchill, L. & Pasdar, M. The physical interaction of p53 and plakoglobin is necessary for their synergistic inhibition of migration and invasion. *Oncotarget* **7**, 26898–26915 (2016).

543. Payea, M. J., Anerillas, C., Tharakan, R. & Gorospe, M. Translational Control during Cellular Senescence. *Mol. Cell. Biol.* **41**, (2021).

544. Gingold, H. *et al.* A dual program for translation regulation in cellular proliferation and differentiation. *Cell* **158**, 1281–1292 (2014).

545. Goodarzi, H. *et al.* Modulated expression of specific tRNAs drives gene expression and cancer progression. *Cell* **165**, 1416–1427 (2016).

546. Genuth, N. R. & Barna, M. The Discovery of Ribosome Heterogeneity and Its Implications for Gene Regulation and Organismal Life. *Mol. Cell* **71**, 364–374 (2018).

547. Liu, B. & Qian, S. B. Translational reprogramming in cellular stress response. *Wiley*

Interdiscip. Rev. RNA **5**, 301–305 (2014).

548. Danilova, N. *et al.* Innate immune system activation in zebrafish and cellular models of Diamond Blackfan Anemia. *Sci. Rep.* **8**, 1–11 (2018).

549. Bianco, C. & Mohr, I. Ribosome biogenesis restricts innate immune responses to virus infection and DNA. *Elife* **8**, 1–21 (2019).

550. Nishimura, K. *et al.* Perturbation of Ribosome Biogenesis Drives Cells into Senescence through 5S RNP-Mediated p53 Activation. *Cell Rep.* **10**, 1310–1323 (2015).

551. Donati, G., Montanaro, L. & Derenzini, M. Ribosome biogenesis and control of cell proliferation: p53 is not alone. *Cancer Res.* **72**, 1602–1607 (2012).

552. Donati, G., Peddigari, S., Mercer, C. A. & Thomas, G. 5S Ribosomal RNA Is an Essential Component of a Nascent Ribosomal Precursor Complex that Regulates the Hdm2-p53 Checkpoint. *Cell Rep.* **4**, 87–98 (2013).

553. Lessard, F. *et al.* Senescence-associated ribosome biogenesis defects contributes to cell cycle arrest through the Rb pathway. *Nat. Cell Biol.* **20**, 789–799 (2018).

554. Jiang, H.-Y. & Wek, R. C. GCN2 phosphorylation of eIF2α activates NF-κB in response to UV irradiation. *Biochem. J.* **385**, 371–380 (2005).

555. Yokoyama, T. *et al.* Identification of reference genes for quantitative PCR analyses in developing mouse gonads. *J. Vet. Med. Sci.* **80**, 1534–1539 (2018).

556. Huang, P. H. *et al.* Cdk5 directly targets nuclear p21CIP1 and promotes cancer cell growth. *Cancer Res.* **76**, 6888–6900 (2016).

557. Muthna, D. *et al.* Irradiation of adult human dental pulp stem cells provokes activation of p53, cell cycle arrest, and senescence but not apoptosis. *Stem Cells Dev.* **19**, 1855–1862 (2010).

558. Cmielová, J. *et al.* DNA damage caused by ionizing radiation in embryonic diploid fibroblasts WI-38 induces both apoptosis and senescence. *Physiol. Res.* **60**, 667–677 (2011).

559. Antelo-Iglesias, L., Picallos-Rabina, P., Estévez-Souto, V., Da Silva-Álvarez, S. & Collado, M. The role of cellular senescence in tissue repair and regeneration. *Mech. Ageing Dev.* **198**, (2021).

560. Seluanov, A., Gladyshev, V. N., Vijg, J. & Gorbunova, V. Mechanisms of cancer resistance in long-lived mammals. *Nat. Rev. Cancer* **18**, 433–441 (2018).

561. Stirling, D. R. *et al.* CellProfiler 4: improvements in speed, utility and usability. *BMC Bioinformatics* **22**, 433 (2021).

562. Martin, M. Cutadapt removes adapter sequences from high-throughput sequencing reads. *EMBnet.journal* **17**, 10 (2011).

563. Dobin, A. *et al.* STAR: ultrafast universal RNA-seq aligner. *Bioinformatics* **29**, 15–21 (2013).

564. Anders, S., Pyl, P. T. & Huber, W. HTSeq--a Python framework to work with high-throughput sequencing data. *Bioinformatics* **31**, 166–169 (2015).

565. Anders, S. & Huber, W. Differential expression analysis for sequence count data. *Genome Biol.* **11**, R106 (2010).

566. Schulze, S. K., Kanwar, R., Gölzenleuchter, M., Therneau, T. M. & Beutler, A. S. SERE: Single-parameter quality control and sample comparison for RNA-Seq. *BMC Genomics* **13**, 524 (2012).

567. Love, M. I., Huber, W. & Anders, S. Moderated estimation of fold change and dispersion for RNA-seq data with DESeq2. *Genome Biol.* **15**, 1–21 (2014).

568. Benjamini, Y. & Hochberg, Y. Controlling the False Discovery Rate: A Practical and Powerful Approach to Multiple Testing. *J. R. Stat. Soc. Ser. B* **57**, 289–300 (1995).

RÉSUMÉ – SUMMARY (FRENCH)

Introduction

1. La sénescence cellulaire

La sénescence cellulaire est définie comme un état d'arrêt prolifératif permanent accompagné de altérations phénotypiques caractéristiques affectant la morphologie, le métabolisme et la sécrétion ou les cellules, qui est généralement - mais pas exclusivement – induit par les dommages et le stress cellulaire.

Bien que les caractéristiques spécifiques de la sénescence varient en fonction du type cellulaire, le stimulus inducteur et d'autre contextes (par exemple si se produit *in vitro* ou *in vivo*), certaines caractéristiques sont couramment utilisées comme **marqueurs** pour l'identification des cellules sénescentes. Premièrement, les cellules sénescentes subissent une **perte permanente de la capacité proliférative**, même lorsqu'elles sont exposées à des signaux pro-prolifératifs, car elles expriment des inhibiteurs du cycle cellulaire. Deuxièmement, elles expriment des protéines anti-apoptotique et inhibent des gènes pro-apoptotique, de sorte qu'els sont **résistants à l'apoptose**. En troisième lieu, les cellules sénescentes subissent des **modifications morphologiques** caractéristiques. Cela comprend des changements dans la forme (qui deviennent plus grandes, plates et irrégulières), une vacuolisation accrue, le réarrangement de leur cytosquelette et des altérations de l'adhésion. De plus, leurs **noyaux se déforment** et perdent leur intégrité et présentent des altérations au niveau de la chromatine, telles que la présence de **fragments de chromatine dans le cytoplasme** (CCF) et la formation de **foyers d'hétérochromatine associée à la sénescence** (SAHF), qui sont des régions riches en marques répressives. Fait important, les cellules sénescentes présentent également un **contenu lysosomal accru**, qui a été utilisé pour leur identification par la **coloration SA-ß-gal** (ou ß-galactosidase associée à la sénescence). Cette réaction colorimétrique donne un bleu en présence d'une enzyme lysosomale, marquant positivement les cellules sénescentes. Une autre caractéristique importante de la sénescence est l'activation d'une **réponse persistante aux dommages à l'ADN** (**DDR**). Le DDR est connu pour induire la sénescence, et il a été démontré qu'il maintient et renforce ce phénotype en favorisant le blocage du cycle cellulaire et l'expression d'un sécrétome pro-inflammatoire. En

effet, et outre ces modifications intrinsèques, les cellules sénescentes deviennent hautement sécrétoires, et affectent de manière extrinsèque leur environnement par la production du **phénotype sécrétoire associé à la sénescence**, ou SASP. Bien que sa composition change dynamiquement, soit très variable et hétérogène, la SASP est formée de facteurs de croissance, de chimiokines et de cytokines, d'espèces réactives de l'oxygène (ROS) et de composants et de remodeleurs de la matrice extracellulaire, entre autres facteurs. Plusieurs voies sont impliquées dans l'établissement de SASP, mais elles convergent dans l'activation de deux principaux facteurs de transcription : **NF-κB** et **C/EBPβ**, bien qu'il ait été démontré que de nombreuses autres protéines régulent les composants de SASP. Le SASP est responsable de nombreuses fonctions biologiques de la sénescence, car il influence la composition des tissus et signale les cellules voisines. Enfin, il convient de mentionner que l'acquisition d'un phénotype sénescent affecte la plupart des organites cellulaires, qui subissent des modifications spécifiques afin de s'adapter aux nouvelles exigences transcriptionnelles, protéomiques et métaboliques. Par exemple, en raison d'une augmentation des protéines mal repliées (en partie causée par la synthèse de facteurs SASP), le **réticulum endoplasmique** (ER) se dilate. Pour faire face au stress du ER, la réponse protéique dépliée (UPR) et les voies de dégradation des protéines (ERAD) sont activées, ce qui influence l'expression de SASP et la forme cellulaire. De plus, les cellules sénescentes présentent une accumulation de **mitochondries dysfonctionnelles**, ce qui accentue la production de ROS, induisant ou renforçant la réponse de sénescence. De plus, la composition de la **membrane plasmique** est également altérée, et l'expression de certaines protéines (cavéoline-1, DPP4) a été proposée comme marqueurs de sénescence. Plus généralement, le **métabolisme** et la **protéostase** sont largement affectés dans les cellules sénescentes, qui présentent une augmentation de la glycolyse et de l'autophagie, et une altération du métabolisme lipidique et de la traduction.

L'établissement de la sénescence est un processus complexe qui peut être déclenchée par une large gamme de stimuli, classés en 3 groupes. En premier lieu, la sénescence est normalement causée par **des dommages cellulaires**, qui activent le DDR. La sénescence induite par les dommages peut survenir à la suite d'une accumulation de cycles réplicatifs (**sénescence réplicative**), qui provoque des dommages en raccourcissant progressivement les télomères. D'autres stimuli dommageables peuvent également provoquer un stress cellulaire et des **dommages à l'ADN**, tels que des agents génotoxiques ou une irradiation. Fait intéressant, la surexpression d'oncogènes ou le maintien de signaux mitogènes peuvent également entraîner une hyperprolifération et un stress cellulaire, déclenchant le DDR. Dans la

sénescence induite par un oncogène, le blocage intrinsèque de la prolifération agit comme un mécanisme suppresseur de tumeur. Étonnamment, la sénescence peut se produire en l'absence de dommages, en réponse à l'activation physiologique des voies de signalisation développementales. Au cours du **développement embryonnaire**, des cellules présentant de nombreuses caractéristiques de sénescence (absence de prolifération, positivité SA-ß-gal, expression de certains inhibiteurs du cycle cellulaire et facteurs SASP) ont été identifiées dans plusieurs organismes, dont la souris, l'homme, le poulet, le poisson zèbre et la grenouille. La présence de ces cellules est transitoire et la sénescence du développement semble contribuer à la normale structuration embryonnaire. Enfin, la sénescence peut se propager aux cellules voisines, ce que l'on appelle la **sénescence secondaire**. Cela peut être médié soit par l'effet **paracrine** des facteurs SASP, soit de manière **juxtracrine** via un contact de cellule à cellule, où les communications intercellulaires permettent le transfert de ROS et l'activation du récepteur NOTCH1.

Les principaux inducteurs moléculaires de la sénescence cellulaire appartiennent aux voies suppresseurs de tumeurs p53/p21 et p16, et en plus, la réponse est renforcée par des modifications épigénétiques spécifiques. Typiquement, le suppresseur de tumeur **p53** est activé en réponse à un stress ou à des dommages cellulaires. Entre autres fonctions, ce maître régulateur peut bloquer le cycle cellulaire en transcrivant l'un de ses médiateurs les plus importants, **p21**. En perturbant la formation des complexes cycline-CDK, p21 favorise l'activation des protéines de la famille des rétinoblastomes (**RB**). Lorsqu'elles sont actives, ces protéines forment les complexes répressifs RB-E2F et DREAM, qui empêchent l'expression des gènes nécessaires à la progression du cycle cellulaire, la bloquent et induisent l'arrêt prolifératif associé à la sénescence. L'action de p21 converge avec un autre inhibiteur du cycle cellulaire, **p16^{Ink4a}**, également capable de perturber les complexes cycline-CDK et d'activer les protéines RB. Fait intéressant, p16^{Ink4a} est codé **avec p19^{Arf}** (p14^{Arf} chez l'humain), dans le locus *Cdkn2a*. Bien que p16 et p19Arf partagent une part de leur séquence nucléotidique, ils produisent des protéines totalement différentes en raison d'un décalage du cadre de lecture de la traduction. Étonnamment, p19^{Arf} est connu pour favoriser la stabilité de p53, ainsi le locus *Cdkn2a* code pour 2 protéines différentes capables d'influencer séparément les 2 axes principaux responsables de l'induction de la sénescence. Outre l'activation de ces voies, le programme transcriptionnel des cellules sénescentes est contrôlé par des **modifications épigénétiques**. Certains des principaux régulateurs épigénétiques de la sénescence sont la protéine HMGB2, les membres des complexes répressifs Polycomb 1 et 2 (PRC1 et PRC2), les chaperons du complexe HIRA ou la perte de

LaminB1. Les marques épigénétiques propagées par ces facteurs contrôlent la formation des SAHF, l'activation des DDR et l'expression des facteurs SASP. En conclusion : l'acquisition de la sénescence est un processus **complexe** et **en plusieurs étapes** contrôlé par un **croisement** de voies interdépendantes et de rétroactions positives qui renforcent les programmes impliqués dans sa progression. Bien que l'activation de différents facteurs soit souvent expliquée selon un ordre linéaire et chronologique, des déséquilibres à n'importe quel niveau des différents **réseaux interconnectés** impliqués dans la régulation de la sénescence peuvent être à l'origine et propager cette réponse. De plus, il a été démontré que la composition des SASP change avec le temps, et la sénescence est considérée comme un processus **dynamique**, avec différentes caractéristiques dans les stades « précoces » ou « tardifs/profonds » de la réponse.

La présence de cellules sénescentes peut avoir un impact important sur la santé de l'organisme, et de nombreux processus biologiques peuvent être impactés par les **fonctions intrinsèques et extrinsèques** de la sénescence. Par exemple, bien que la sénescence représente un blocage intrinsèque de la **prolifération** qui agit comme un mécanisme suppresseur de tumeur, les cellules sénescentes peuvent favoriser la prolifération de manière extrinsèque par la sécrétion de la SASP, qui peut contribuer au développement tumoral. De même, il a été proposé que la sénescence agit comme une barrière intrinsèque à la **reprogrammation**, mais la SASP peut stimuler la plasticité et la reprogrammation dans les cellules voisines. De plus, étant donné que certains composants de la SASP sont des composants ou des remodeleurs de la matrice extracellulaire, ils contribuent au r**emodelage tissulaire**, à la fibrose et à la structuration embryonnaire. De plus, les cytokines et chimiokines de la SASP peuvent attirer et moduler l'action des **cellules immunitaires**. Selon sa composition exacte, la SASP peut avoir des effets immunosuppresseurs ou immunostimulants qui, lorsqu'ils sont persistants, contribuent à l'inflammation chronique ou « inflammaging ». Ainsi, les cellules sénescentes contribuent au développement de nombreux états **physiologiques** et **pathologiques**, souvent de manière contradictoire. De manière générale, on considère que l'expression transitoire des cellules sénescentes, qui sont généralement éliminées par le système immunitaire, est **bénéfique**, alors que leur persistance chronique est davantage associée à leurs effets **délétères**. Afin de limiter leur influence négative, des médicaments **sénolytiques** et **sénomorphes**, visant respectivement à éliminer ou à moduler l'action des cellules sénescentes, sont à l'étude.

2. p21 – *Cdkn1a*

p21, également connu sous le nom de Cip1 et Waf1, a été décrit indépendamment par plusieurs groupes au début des années 1990. C'est le premier membre décrit de la **famille Cip/Kip**, qui comprend également $p27^{Kip1}$ et $p57^{Kip2}$, codés par les gènes *Cdkn1b* et *Cdkn1c* respectivement. Les familles Cip/Kip et Ink4 (qui comprend $p15^{Ink4b}$, $p16^{Ink4a}$, $p18^{Ink4c}$ et $p19^{Ink4d}$) sont des inhibiteurs du cycle cellulaire. Ils **bloquent le cycle cellulaire** en inhibant l'action des kinases dépendantes des cyclines (CDK) qui le contrôlent, pour lesquelles ils sont appelés inhibiteurs de CDK (CDKi). Les membres de Cip/Kip sont des protéines de **promiscuité**, capables d'interagir avec différents complexes CDK-cycline, affectant différentes phases du cycle cellulaire. De plus, ils interagissent également avec d'autres facteurs et sont également impliqués dans la régulation **d'autres processus cellulaires**.

Chez la souris, **la protéine p21** est composée de 159 acides aminés et à un pois moléculaire de 18KDa. Il est codé par les 2e et 3e exons du **gène *Cdkn1a***. Plusieurs domaines fonctionnels ont été décrits, comme les domaines d'interaction des cyclines, CDKs et PCNA, et des signaux de localisation et d'exportation nucléaires. Puisqu'elle n'a pas de structure tertiaire stable, p21 est considérée comme une protéine **intrinsèquement désordonnée**, ce qui facilite son interaction avec de multiples partenaires.

L'expression de p21 est régulée à plusieurs niveaux. Son **principal activateur transcriptionnel est p53**, qui est normalement activé lors de dommages à l'ADN ou de signaux oncogènes. Cependant, il a été démontré que de nombreux **autres facteurs de transcription** et régulateurs épigénétiques favorisent (et répriment) la transcription de *Cdkn1a* indépendamment de p53, y compris d'autres répondeurs au stress ou des membres de la voie de développement du TGF-ß. **Post-transcriptionnellement**, la stabilité et l'efficacité de la traduction de l'ARNm de *Cdkn1a* sont influencées par les micro-ARN (mi-RNAs), les protéines de liaison à l'ARN (RBPs) et le facteur de traduction eIF2α. Enfin, plusieurs **modifications post-traductionnelles** déterminent la stabilité de la protéine p21. Des marques spécifiques de phosphorylation, de méthylation et d'acétylation favorisent ou empêchent la **dégradation** de p21, qui se produit par des mécanismes dépendants et indépendants de l'ubiquitine.

Fonctionnellement, p21 est une protéine pléiotrope, impliquée dans de multiples activités cellulaires. En plus de bloquer le **cycle cellulaire** par différents mécanismes, p21 régule également la mort cellulaire et **l'apoptose**, contribue à la **réparation de l'ADN et à la**

stabilité du génome, influence la **dynamique du cytosquelette**, la migration et l'adhérence cellulaires et contrôle la **transcription**. La contribution spécifique de p21 dans ces processus est souvent controversée, car elle peut jouer des **rôles contradictoires** selon sa localisation cellulaire, son contexte et ses partenaires d'interaction.

En raison de ses nombreuses fonctions, p21 influence plusieurs processus biologiques. Par exemple, l'induction de p21 est impliquée dans la **différenciation** de nombreux types cellulaires, le maintien du **renouvellement des cellules souches** de certaines populations et la **reprogrammation** des cellules souches pluripotentes induites. De plus, l'expression de p21 est normalement considérée comme une barrière à la **régénération** de différents organes et tissus, bien qu'elle puisse être nécessaire dans d'autres cas spécifiques. Dans le **cancer**, p21 joue un double rôle, agissant soit comme un suppresseur de tumeur, soit comme un promoteur de la résistance, de l'agressivité et de l'invasion tumorale. De plus, le déficit en p21 a été associé au développement de **maladies auto-immunes**, bien que p21 puisse favoriser l'expression de gènes associés à des pathologies inflammatoires et neurodégénératives. Enfin, p21 est un contributeur important un marqueur de la **sénescence cellulaire**. En fait, c'est l'un des médiateurs de la sénescence exprimés au cours de la **sénescence développementale**. Alors que son rôle a été principalement associé au début de l'établissement de la sénescence, où il intervient dans **l'arrêt prolifératif**, on pense également que p21 maintient la **viabilité cellulaire** des cellules sénescentes en les protégeant de l'apoptose. De plus, l'expression de p21 médie et renforce la réponse sénescente en augmentant la **production de ROS**. Enfin, p21 contribue également à l'acquisition du **programme transcriptionnel** sénescent en régulant la sénescence et les régulateurs SASP, tels que les protéines HMGB2 ou RB.

Résultats

1. Validation du modèle

La première partie de la section des résultats décrit la **validation *in vitro*** du modèle de souris qui permet le knock-down inductible de p21 utilisé dans ce projet. Dans ce modèle, l'ajout de doxycycline au milieu de culture cellulaire a induit la transcription de la construction contenant un signal rapporteur GFP et un shRNA (short hairpin ARN) contre le transcrit de

notre protéine d'intérêt, p21. Les expériences décrites dans ce projet ont été réalisées sur des fibroblastes dermiques primaires isolés et cultivés dérivés de la peau de nouveau-nés de cette lignée de souris.

Pour valider le **knock-down de p21 dans les cellules en prolifération**, j'ai confirmé l'expression de la construction via la visualisation par fluorescence du signal GFP, ainsi que la diminution de l'expression de p21 au niveau du transcrit et de la protéine via RT-qPCR (PCR quantitative) et Western Blot, respectivement. Ensuite, j'ai utilisé l'irradiation pour induire la sénescence. Six jours après l'irradiation, **l'établissement de la sénescence** a été confirmé par l'observation des changements morphologiques et transcriptionnels caractéristiques, le blocage de la prolifération et l'augmentation de l'activité lysosomale. Ces changements ont été mesurés par l'observation microscopique à contraste de phase, des RT-qPCR sur des marqueurs de sénescence (p21, $p19^{Arf}$, $p16^{Ink4a}$, Ki67 et Hmgb2), l'incorporation réduite d'EdU, et le signal au bleu positive avec la coloration SA-ß-gal. L'induction efficace du **knock-down de p21 dans les cultures sénescentes** a été confirmée aux niveaux transcriptionnel (RT-qPCR), protéique (Western Blot) et fonctionnel (dérépression transcriptionnelle de Hmgb2 évaluée par RT-qPCR).

Une fois l'induction du knock-down de p21 validée dans des cultures proliférantes et sénescentes, j'ai **optimisé** les conditions expérimentales (temps après irradiation et dose de doxycycline) pour générer des échantillons d'ARN à analyser via « **bulk RNA-seq** » (séquençage en vrac de l'ARN). Pour induire le knock-down de p21, les cellules proliférantes et sénescentes ont été complétées avec 2 ug/mL de doxycycline pendant 2 jours avant le prélèvement de l'échantillon, et des échantillons de cellules sénescentes ont été prélevés au jour 8 après irradiation. Pour la sélection des échantillons optimaux, la sénescence et la régulation négative de p21 ont été évaluées dans 7 réplicats biologiques et techniques par analyse RT-qPCR des marqueurs de la sénescence et de la fonction p21 (p21, $p16^{Ink4a}$ et Hmgb2). Cela a conduit à la sélection d'échantillons correspondant à 4 conditions, et produits en 4 répétitions techniques et biologiques. Chaque condition a été définie par la combinaison de 2 variables : proliférante/sénescente (P : proliférante vs S : sénescente) et p21 non altérée/réduite par l'induction du knock-down avec le traitement à la doxycycline (C : contrôle vs D : traitées avec doxycycline ou « p21 knock-down »). Par conséquent, un total de 16 échantillons d'ARN correspondant à 4 répétitions de chacune des 4 conditions d'intérêt (PC, PD, SC et SD) ont été envoyés à la plateforme GenomEast pour leur séquençage.

2. Analyse du bulk RNA-seq (séquençage en vrac de l'ARN)

La deuxième partie de la section des résultats consiste en l'analyse bioinformatique des données du séquençage en vrac d'ARN. Après séquençage, la plateforme GenomEast nous a fourni un rapport du processus et une analyse de l'expression différentielle des gènes dans la comparaison des conditions d'intérêt. Dans un premier temps, une **description générale des données** a été réalisée à partir des informations fournies par la plateforme dans leur rapport. Ensuite, afin d'explorer et d'interpréter les changements transcriptionnels associés à la réduction de p21 dans la sénescence, j'ai effectué une **analyse de voie** (pathway analysis) sur des listes de gènes créées à partir de leur analyse de l'expression génique différentielle à l'aide de la page Web Enrichr, un outil d'analyse de voie. Les résultats ont été représentés graphiquement à l'aide de packages de visualisation dans R studio. L'interprétation de l'analyse des voies s'est avérée assez complexe, donc a été divisée en 4 sections.

Tout d'abord, les gènes différentiellement exprimés dans les **principales comparaisons** ont été analysés. Cela a permis de confirmer l'induction de la sénescence, et a fourni une description des programmes transcriptionnels altérés en sénescence (SC.vs.PC), ainsi que ceux associés à la diminution de p21 dans les cultures proliférantes (PD.vs.PC) et sénescentes (SD. vs SC). Étant donné que cette analyse s'est avérée insuffisante pour démêler de nouveaux rôles spécifiques associés à la fonction p21 dans les cellules sénescentes, j'ai décidé de subdiviser les gènes différentiellement exprimés de la comparaison de notre intérêt principal (SD.vs.SC) en sous-catégories en fonction de leur **comportement transcriptionnel dans autres comparaisons**. D'une part, j'ai cherché à déterminer quels processus étaient affectés de manière similaire et différentielle par la réduction de p21 dans les cellules proliférantes ou sénescentes. D'autre part, je voulais distinguer l'effet de la perte de p21 dans les changements transcriptionnels associés au programme de sénescence, ainsi que détecter son impact dans d'autres fonctions non altérées par l'établissement de la sénescence. Cette analyse de « comparaison de comparaisons » m'a aidé à définir le rôle de p21 dans différents contextes, mais l'approche méthodologique appliquée a également entraîné une perte de puissance statistique importante.

À ce moment-là, j'ai réalisé qu'une **interprétation physiologique** de nos conditions expérimentales était nécessaire pour une interprétation profonde et significative de nos données. En considérant les changements transcriptionnels des gènes dans plusieurs comparaisons, j'ai développé un critère pour déterminer les gènes **activés ou réprimés par**

p21 qui pourraient avoir un impact pertinent sur le phénotype des cellules sénescentes. L'analyse des voies sur ces ensembles de gènes a révélé un nouvel ensemble de fonctions biologiques associées à la diminution de p21 dans la sénescence. Pour terminer l'analyse bioinformatique, j'ai exploré certains des processus non couverts potentiellement contrôlés par p21 dans la sénescence qui pourraient avoir un impact physiologique intéressant. J'ai représenté le comportement du gène impliqué dans ces programmes à l'aide de graphes ***heatmap***. Tout d'abord, le rôle de p21 en tant que médiateur de la sénescence et de la fonction de p53 a été validé en observant son contrôle de l'activité du complexe répresseur **DREAM**. Étant donné que plusieurs voies liées au système immunitaire se sont révélées enrichies parmi les gènes affectés par p21, j'ai ensuite analysé comment p21 affectait certains composants **SASP**, la sécrétion générale de **chimiokines et de cytokines** et les médiateurs de l'activité des **Natural Killers**. La voie de signalisation du **TNF- α** était affectée par la régulation négative de p21 dans la sénescence, je l'ai donc explorée comme un mécanisme potentiel par lequel p21 pourrait exercer un contrôle sur les programmes transcriptionnels impliqués dans la régulation du système immunitaire. Enfin, les changements dans la machinerie liée à la **traduction** des protéines et les gènes **peroxysomaux** ont attiré notre attention et ont été brièvement explorés.

3. Exploration d'hypothèses

Quelques hypothèses intéressantes issues de l'analyse transcriptomique. Premièrement, il a été observé que la perte de p21 dans les cellules sénescentes provoquait une inversion partielle des modifications transcriptionnelles associées à la sénescence, y compris la réexpression de gènes liés à la prolifération. Pour cette raison, j'ai décidé d'explorer l'irréversibilité de l'arrêt prolifératif des cultures sénescentes. À ma grande surprise, de petites plaques **de cellules proliférantes ont émergé dans les plaques irradiées** lorsqu'elles ont été cultivées sur des périodes prolongées. Le nombre, la taille et le taux de croissance de ces grappes ont été intensifiés par la régulation négative de p21 dans les cellules sénescentes. Des essais de prolifération de cristal violet ont été effectués afin d'évaluer l'incidence de cellules non sénescentes dans des cultures irradiées avec p21 non manipulé ou ablaté 2 à 3 semaines après l'irradiation. En raison du biais possible de travailler avec des cultures sénescentes non complètement arrêtées, je suis arrivé à la conclusion qu'un modèle alternatif d'induction de la sénescence sera éventuellement nécessaire pour la validation de mes résultats. Dans ce contexte, l'utilisation de **l'adriamycine** comme modèle alternatif de sénescence induite par les dommages a été proposée et évaluée. Les résultats

préliminaires ont montré que les cellules exposées de manière aiguë à l'adriamycine arrêtaient la prolifération, adoptaient une morphologie sénescente et acquéraient les modifications transcriptionnelles attendues associées à la sénescence (testait par RT-qPCR sur p21, $p16^{Ink4a}$, Hmgb2 et Ki67). De plus, l'ajout de doxycycline a également induit la chute des niveaux et de l'activité de p21 dans ce modèle (RT-qPCR sur p21 et Hmgb2). Fait important, une **absence totale de cellules proliférantes** non sénescentes a été observée dans toutes les cultures sénescentes induites par l'adriamycine grâce à leur examen visuel jusqu'à 3 semaines après l'induction de la sénescence, même lorsque p21 était régulé à la baisse. Ceci a été préalablement vérifié dans des essais de prolifération du cristal violet. Ainsi, la sénescence induite par l'adriamycine est un modèle alternatif, où l'effet d'une présence résiduelle de cellules non sénescentes dans des cultures irradiées pourrait être évalué afin de valider mes résultats dans le futur.

Ensuite, nous avons décidé d'explorer certaines des fonctions associées à p21 qui ont été révélées par l'analyse du séquençage d'ARN (ARN-seq). D'un côté, nous avons décidé d'évaluer l'effet de la sénescence et de la perte de p21 sur les **peroxysomes**. Pour ce faire, j'ai réalisé une **immunofluorescence** sur le marqueur peroxysomal Pmp70 et j'ai imagé des peroxysomes dans des cellules proliférantes et sénescentes. Dans ces colorations, la présence de grappes de signal peroxysomal ressemblant à des agrégats peroxysomaux a été remarquée. Fait intéressant, les cellules contenant des agrégats étaient plus fréquentes dans les plaques sénescentes, soit induites par irradiation ou adriamycine. Cependant, la perte ou l'absence de p21 ne semble pas affecter leur incidence. Afin d'étudier l'impact fonctionnel ou la cause des agrégats, j'ai réalisé des colorations par immunofluorescence sur l'enzyme catalase et le marqueur d'autophagie p62. Les résultats de ces expériences n'ont pas été concluants. Cette voie de recherche a été abandonnée, et à l'heure actuelle, la nature, l'origine et l'impact fonctionnel de ces structures restent inconnus.

L'analyse des voies sur les gènes potentiellement réprimés par p21 dans la sénescence a suggéré que sa perte favorise le recrutement et l'interaction avec le **système immunitaire**. Une analyse plus approfondie a suggéré que la production et la sécrétion de plusieurs cytokines et facteurs SASP pourraient être potentialisées lors de la perte de p21 dans la sénescence, au moins de manière transcriptionnelle. Pour cette raison, la **sécrétion de cytokine**s par des cellules sénescentes avec p21 non manipulé ou régulé négativement a été analysée. L'abondance de 40 cytokines dans le milieu conditionné de cellules sénescentes du 8e au 9e jour après l'irradiation a été évaluée à l'aide d'un kit de réseau de cytokines

commercial (cytokine array). Parmi les 24 cytokines exprimées à une plage suffisamment élevée pour être mesurées de manière fiable, seules 3 ont changé dans le même sens dans les deux expériences analysées et ont montré un changement moyen de plus de 25 % lors de la réduction de p21. Remarquablement, ces cytokines -Cxcl9/Mig, Cxcl10/Ip10/Crg2 et Ccl5/Rantes- ont été incrémentées à plus de 70 % en moyenne. Au niveau transcriptionnel, l'expression de Cxcl10 et Ccl5 (les deux cibles rapportées de Tnf-α) a également augmenté de manière significative lors de l'inactivation de p21 en sénescence. Cette expérience a soutenu l'idée que la régulation négative de p21 dans les cellules sénescentes intensifie l'expression d'un **sécrétome pro-inflammatoire**, également au niveau protéique.

Enfin, une observation intéressante de l'analyse d'ARN-seq était l'accentuation des changements transcriptionnels associés à l'établissement de la sénescence suite au knock-down de p21. D'une certaine manière, cela semblait indiquer que la perte de p21 conduit à l'acquisition d'un phénotype « plus sénescent ». Curieusement, j'avais observé lors de Western Blot précédents que le niveau de protéine p21 dans les plaques irradiées avait tendance à diminuer avec le temps. Cela a conduit à l'hypothèse que la **régulation négative de p21 à des stades tardifs de la sénescence** pourrait se produire naturellement dans le cadre de la réponse sénescente physiologique. Pour tester cette idée, j'ai mesuré **l'expression temporelle** de la protéine p21 en sénescence par **Western Blot** jusqu'au jour 12 ou 15 après irradiation (n = 7) ou traitement à l'adriamycine (n = 2). Bien que la variabilité entre les échantillons ait été notable, toutes les expériences ont confirmé une réduction de la protéine p21 au fil du temps, commençant vers le jour 8-9 (ou même plus tôt) après l'induction de la sénescence. Ce résultat a eu des implications importantes pour l'interprétation de mes résultats d'ARN-seq, puisque l'ablation forcée de p21 à des moments antérieurs (jour 6 post-irradiation) pourrait refléter les changements transcriptionnels se produisant naturellement aux stades ultérieurs de la sénescence en raison de la réduction physiologique de p21.

4. Approche alternative : l'interactome de p21

Parallèlement à l'exploration de l'impact transcriptionnel de la déplétion de p21 dans la sénescence, nous avons décidé d'étudier son interactome dans les cellules sénescentes. Nous avons émis l'hypothèse que les informations sur les partenaires d'interaction de p21 pourraient compléter l'analyse de l'ARN-seq et même suggérer d'éventuels mécanismes moléculaires impliqués dans la fonction de p21 dans la sénescence, y compris son rôle sur la

régulation de la transcription. Les partenaires de liaison de p21 ont été identifiés par analyse par spectrométrie de masse (MS) sur les protéines co-immunoprécipitées (Co-Ip) avec p21 dans des extraits protéiques de cellules sénescentes 8 jours après irradiation. L'analyse MS a été réalisée par la plate-forme protéomique de l'IGBMC, et complétée par une analyse statistique supplémentaire par moi-même. Parmi les **41 protéines détectées**, 11 étaient des interacteurs connus de p21, dont plusieurs CDK et des cyclines. Fait intéressant, certains des **potentielles partenaires nouveaux**, tels que Sptan1, figuraient parmi les résultats les plus abondants et les plus identifiés avec confiance (basés sur des tests statistiques) de l'analyse. L'interactome de p21 a été soumis à une analyse des voies afin d'effectuer une analyse descriptive de sa composition. Les protéines ont été classées en fonction de la **localisation cellulaire**, de la **fonction moléculaire** et du **processus biologique** dans lequel elles étaient impliquées. Afin d'avoir un **aperçu visuel** des données, les interactions les plus fréquentes dans chacune de ces 3 variables ont été représentées de manière quantitative. Cela a révélé que les interacteurs de p21 se trouvaient couramment dans le noyau de la cellule, mais aussi dans le cytoplasme, la membrane, les structures d'adhésion ou l'espace extracellulaire. Concernant les fonctions moléculaires, elles présentent souvent une activité kinase, ainsi que la capacité de liaison aux ions et aux ARN. De plus, outre leur implication attendue dans la prolifération, le cycle cellulaire et l'apoptose, les partenaires de p21 étaient souvent liés aux processus d'adhésion et de migration. Bien que ce résultat n'ait pas été développé davantage, plusieurs nouveaux interacteurs potentiels de p21 dans les cellules sénescentes ont été dévoilés et ont fourni la base d'une meilleure compréhension mécaniste de ses activités moléculaires à l'avenir.

Discussion

1. Considérations sur le modèle

Les résultats obtenus dans ce travail ont été générés *in vitro*, à l'aide de cultures cellulaires de fibroblastes dermiques primaires isolés d'une lignée commerciale de souris transgéniques qui permet la réduction **(knock-down) inductible de p21**. Cette stratégie présente des avantages importants par rapport aux autres modèles précédemment utilisés pour étudier le rôle de p21, notamment dans le domaine de la sénescence. En raison de la robustesse

génétique, les organismes s'adaptent et compensent souvent les perturbations moléculaires expérimentales ou spontanées. Ces mécanismes compensatoires peuvent donc masquer l'effet fonctionnel causé par la manipulation génétique. Puisque l'existence d'un mécanisme compensatoire a été décrite dans les modèles de knock-out (déplétion total) de p21, l'adoption d'une **stratégie de knock-down** (réduction) pourrait aider à les éviter. De plus, les **interventions conditionnelles** (comment les inductibles), contrairement aux interventions constitutives, offrent la possibilité de perturber une cible de manière contrôlée dans l'espace ou dans le temps. Dans le modèle inductible utilisé dans ce travail, la réduction de p21 pourrait être induite au moment souhaité par l'administration de doxycycline. Étant donné que p21 est bien connu pour participer aux premières étapes de la réponse sénescente en médiant l'arrêt du cycle cellulaire, la capacité de **le réduire à des stades tardifs**, sans altérer l'établissement sénescent normal, a une importance critique. La **principale limite** à l'utilisation de ce modèle dans cette étude pourrait être l'absence d'une **condition de contrôle pour les effets de la doxycycline**, qui est un médicament antibiotique avec une activité connue d'inhibition de la métalloprotéinase matricielle. Cependant, ces préoccupations n'étaient absolument pas étayées par nos données.

Les **fibroblastes dermiques** sont couramment utilisés pour l'étude *in vitro* de la sénescence et ont été proposés comme moteurs du vieillissement cutané *in vivo*. Comme dans toute étude *in vitro*, l'utilisation d'un **type cellulaire spécifique** influence les résultats obtenus, et ne peut représenter l'impact physiologique que le phénotype étudié pourrait avoir au niveau des tissus ou de l'organisme *in vivo*. Ainsi, il serait intéressant de savoir si l'analyse des voies liées aux changements transcriptionnels associés à la régulation négative de p21 dans les fibroblastes sénescents serait également détectée dans d'autres cellules sénescentes, ou même comment ces changements pourraient affecter leur **interaction avec les cellules voisines**, par exemple avec le système immunitaire.

Dans ce travail, le modèle principal utilisé était la **sénescence induite par l'irradiation**. L'irradiation est utilisée comme radiothérapie pour le traitement du cancer et est couramment utilisée comme déclencheur dans l'étude de la sénescence. Dans mes expériences, l'induction de la sénescence 6 jours après l'irradiation a été confirmée par la réduction de la prolifération, la positivité SA-β-gal et la détection de marqueurs transcriptionnels. Cela a été confirmé lors de l'analyse des voies sur les données d'ARN-seq, lorsque les termes attendus liés à la sénescence ont été significativement enrichis 8 jours après l'irradiation. Malgré cela, **l'apparition de colonies proliférantes** a été repérée à

plusieurs reprises environ 2 semaines après l'irradiation. Lorsque p21 a été régulé à la baisse, 6 jours après l'irradiation, ces colonies ont été détectées plus tôt et se sont considérablement agrandies. La cause de ceci est incertaine. Il est possible que la déplétion de p21 puisse augmenter le taux de prolifération des cellules résiduelles non sénescentes dans les plaques irradiées. Cependant, la contribution d'autres processus ne peut être exclue, comme l'expansion des colonies proliférantes due à une migration accrue lors de la perte de p21, ou la réversion de la sénescence. La possibilité **que l'épuisement de p21 puisse améliorer l'évasion de la sénescence** dans les cellules non complètement sénescentes (contournement) ou permettre aux cellules sénescentes de **revenir à un état prolifératif** (évasion) est discutée. Pour clarifier ces spéculations, il serait nécessaire de caractériser davantage la présence de cellules prolifératives dans des plaques irradiées avec p21 non manipulé ou appauvri, ce qui pourrait être fait en quantifiant l'incorporation d'EdU à différents moments et conditions.

Fait intéressant, les termes liés à la prolifération de détection enrichis parmi les gènes régulés positivement lors de la perte de p21 dans la sénescence pourraient s'expliquer par l'amplification présumée de la population non sénescente dans cette condition. Bien que **l'impact que la présence de cellules non sénescentes** dans les plaques irradiées ait pu avoir **sur l'interprétation des résultats d'ARN-seq** doive être pris en compte, **il a été estimé qu'il était minime** pour 2 raisons. Premièrement, parce que sur la base de l'examen visuel et de la coloration au cristal violet, la présence de cellules non sénescentes dans les cellules irradiées 8 jours après l'irradiation (le point de temps analysé dans l'ARN-seq) est estimée négligeable. Deuxièmement, parce que les résultats les plus intéressants de l'analyse ont été obtenus en appliquant ce qu'on a appelé une « interprétation physiologique » des données. Dans cette approche, l'accent a été mis sur les gènes activés ou réprimés par p21 spécifiquement dans la sénescence qui pourraient avoir un effet sur le phénotype sénescent par rapport aux cellules proliférantes témoins. En raison de la façon dont ces sous-ensembles de gènes ont été déterminés, la signature transcriptionnelle censée être associée à l'amplification des cellules proliférantes lors de la régulation négative de p21 dans nos échantillons sénescents aurait été exclue. Par conséquent, et malgré le fait que la présence de populations non totalement sénescentes ait pu contribuer à masquer les changements transcriptionnels dus à la perte de p21 dans les cellules sénescentes, leur effet a probablement été minimisé dans mon analyse. En outre, d'autres **limitations générales** de l'exécution **de l'analyse des voies sur les données d'ARN-seq en vrac** (telles que l'hétérogénéité cellulaire ou les biais méthodologiques) sont également discutées.

Enfin, l'utilisation de **l'adriamycine comme déclencheur alternatif de la sénescence** est discutée. Compte tenu des résultats préliminaires, le traitement à l'adriamycine est proposé comme un bon modèle pour valider mes résultats afin d'écarter définitivement l'influence que la présence de cellules non-sénescentes dans des échantillons sénescents aurait pu avoir sur mon analyse.

2. Rôle de p21 dans la sénescence

Le résultat le plus intéressant de l'analyse RNA-seq était l'indication de la capacité de p21 à limiter la **clairance des cellules sénescentes par le système immunitaire**. Fait intéressant, il a été démontré que p21 régule l'activité du système immunitaire de plusieurs manières. Par exemple, son absence a été associée à plusieurs reprises au développement de **maladies auto-immunes** et à l'exacerbation d'un environnement pro-inflammatoire. Parmi les processus affectés par p21 dans les cellules immunitaires, il a été démontré qu'il inhibe l'activité transcriptionnelle du **NF-κB**, un régulateur clé du SASP, dans les macrophages.

Mon analyse d'ARN-seq avait suggéré que la régulation négative de p21 dans les cellules sénescentes intensifiait la production et la sécrétion de plusieurs cytokines et facteurs SASP. Ce résultat a été partiellement confirmé au niveau protéique via l'analyse des cytokines du sécrétome des cellules sénescentes après réduction de p21. En fait, la **capacité de p21 à réguler la sécrétion de facteurs immunomodulateurs** dans des cellules non immunitaires a déjà été rapportée. Bien que certaines des conclusions publiées sur ce sujet puissent sembler en contradiction avec mon analyse d'ARN-seq, ces idées pourraient être réconciliées grâce à un examen approfondi des données et de la méthodologie expérimentale appliquée dans ces articles et d'autres. En plus de favoriser l'expression d'un phénotype pro-inflammatoire, la régulation négative de p21 dans les cellules sénescentes a **induit l'expression des ligands NKGD2**, qui n'étaient pas régulés positivement uniquement lors de l'établissement de la sénescence. Étant donné que les ligands NKGD2 avaient déjà démontré qu'ils intervenaient dans la reconnaissance et l'élimination des cellules sénescentes par les cellules Natural Killer (NK), ce résultat était considéré comme particulièrement pertinent. La production de plusieurs **métalloprotéases matricielles** (MMP) par des cellules sénescentes a été proposée pour inhiber la reconnaissance de leurs ligands NKG2 par NK, empêchant ainsi leur élimination. Fait important, la transcription des MMP n'a généralement pas augmenté lors de la perte de p21. Afin de poursuivre l'exploration du rôle de p21 dans la régulation de la clairance immunitaire des cellules sénescentes, de

futures expériences in vitro et in vivo ont été proposées. Enfin, les résultats de l'analyse des données d'ARN-seq et les interacteurs potentiels de p21 identifiés par MS Co-Ip ont été examinés et comparés à la littérature afin de déduire **le possible mécanisme moléculaire** par lequel p21 pourrait limiter la transcription d'un pro -phénotype inflammatoire dans les cellules sénescentes. L'accentuation possible de la réponse aux dommages de l'ADN (**DDR**), l'activation des **voies TNF-α et NF-κB**, et les modifications de l'activité STAT3 et des niveaux de **p53** lors de la perte de p21 dans la sénescence ont été discutées.

D'autre part, l'analyse des voies sur les gènes affectés par la réduction de p21 a montré l'enrichissement des termes liés à la **matrice extracellulaire**, au remodelage du cytosquelette et à **l'adhésion cellulaire** (influençant donc la **migration**). Bien que la capacité de p21 à réguler ces processus ait été rapportée, l'information sur les mécanismes moléculaires qui la sous-tendent sont rares, en particulier au niveau transcriptionnel. Fait intéressant, **junction plakoglobin** (Jup) a été identifiée comme un nouvel interacteur de p21 dans les cellules sénescentes par l'analyse MS Co-Ip. En plus de participer à la formation de **structures d'adhésion**, il a été démontré que Jup participe à plusieurs voies de signalisation et r**égule la transcription** des gènes liés à l'adhésion et à la migration lorsqu'il se localise dans le noyau, où il interagit et collabore avec p53. Au total, l'interaction non signalée auparavant entre p21 et Jup dans les cellules sénescentes pourrait être un **potentiel nouveau mécanisme** par lequel p21 pourrait réguler l'adhésion et la migration cellulaires au niveau de la transcription.

Enfin, un certain nombre de gènes impliqués dans la traduction des protéines se sont avérés être affectés par la régulation négative de p21 dans la sénescence. La **traduction et la biogenèse des ribosomes** sont connues pour être altérées au cours de la sénescence. Bien qu'il s'agisse d'un domaine émergent, il existe des preuves suggérant que les changements dans l'expression des ARNt (ARN de transfert), des ribosomes et des facteurs de traduction sont des **régulateurs post-transcriptionnels clés de plusieurs processus cellulaires**, y compris l'inflammation ou l'établissement de la sénescence. Ainsi, il est possible qu'en affectant la transcription de nombreux facteurs de la machinerie de traduction, p21 puisse influencer ces fonctions et d'autres, par le contrôle post-transcriptionnel indirect de l'expression génétique. De plus, p21 pourrait influencer la traduction plus directement en interagissant avec plusieurs **facteurs dotés d'une capacité de liaison à l'ARN** identifiés par l'analyse MS Co-Ip.

Sur une autre note, il convient de mentionner que l'un des gènes liés à la traduction régulés par p21 dans la sénescence était ***Rplp0***, qui avait été considéré comme un housekeeping gène (gène ménager ou constitutif) **et utilisé pour normaliser** les valeurs dans les expériences précédentes de RT-qPCR. Bien que les tests préliminaires aient indiqué que les résultats précédents n'étaient pas susceptibles d'être affectés de manière critique par cela (probablement en raison de l'effet faible - mais significatif - de l'établissement de la sénescence et de la régulation négative de p21 dans l'expression de *Rplp0*), ce résultat a souligné l'importance **de choisir des contrôles adéquats** pour les conditions expérimentales évaluées, ce qui peut être particulièrement délicat dans l'étude de la sénescence.

3. Dynamique physiologique de l'expression de p21 dans la sénescence

Fait intéressant, il a été observé que les **niveaux de protéine p21** d**iminuaient aux stades tardifs de la sénescence**, environ 8 à 9 jours après l'irradiation ou le traitement avec l'adriamycine, comme était montré par Western Blot. Il est curieux de remarquer que 2 régulateurs connus de la stabilité de p21, Hsp90 et Cdk5, ont été identifiés par Co-Ip MS comme des interacteurs de p21 en sénescence. Fait important, la régulation négative des niveaux de p21 à des stades tardifs de la sénescence a **déjà été rapportée dans la littérature** dans différents types de cellules et modèles d'induction de la sénescence *in vitro*. Cela suggère que, même lorsque p21 est bien connu pour être régulé positivement au début de l'induction de la sénescence et est largement considéré comme un marqueur de sénescence, ses niveaux pourraient subir une **baisse physiologique à des stades ultérieurs**. Même s'il est possible que cela ne se produise que dans des types de cellules ou des modèles ou des scénarios déterminés (*in vitro* mais non *in vivo*), cela pourrait avoir des **implications importantes dans l'interprétation de mes résultats**.

Dans le cas où la réduction des niveaux de p21 en fin de sénescence était un événement courant, il serait important de savoir si les mêmes changements transcriptionnels observés dans notre modèle, lorsque sa déplétion a été forcée du jour 6 au jour 8 après l'irradiation, se sont également produits plus tard, lorsqu'elle était naturellement régulée à la baisse, au jour 10 ou 12 après une irradiation ou un traitement à l'adriamycine par exemple. La transcription de Hmgb2, des ligands de NK, des cytokines comme Ccl5 ou des métalloprotéinases comme Mmp9 augmente-t-elle aux derniers stades de la sénescence, lorsque les niveaux de p21

tombent ? Cela pourrait être testé en analysant l'expression de ces gènes au niveau transcriptionnel et protéique par RT-qPCR ou « cytokine array » sur **d'échantillons de cellules sénescentes à des moments ultérieurs**, lorsque le niveau de p21 a diminué. Si l'effet de la diminution de p21 dans les cellules sénescentes n'était pas le même lorsqu'il se produisait naturellement à des stades ultérieurs et lorsqu'il était forcé plus tôt, il serait intéressant de savoir quels sont les mécanismes moléculaires agissant pendant cette fenêtre temporelle pour l'empêcher.

Cependant, si des changements similaires sont observés lors de l'épuisement de p21 lorsqu'il est induit artificiellement au jour 6 après l'irradiation et lorsqu'il se produit naturellement à des moments ultérieurs, cela pourrait découvrir de **nouveaux facteurs dont l'expression dépend des niveaux de p21** dans la sénescence. Ainsi, une meilleure compréhension de **l'effet physiologique de la régulation négative de p21** dans la sénescence et des mécanismes qui la contrôlent serait essentielle pour évaluer l'impact de la régulation de p21 dans les processus biologiques et les pathologies associées à la sénescence in vivo. Par exemple, si la chute de p21 favorise réellement la **clairance des cellules sénescentes** par le système immunitaire à des stades ultérieurs de la sénescence, l'altération de la régulation négative de p21 pourrait-elle être associée à **l'effet nocif que les cellules sénescentes persistantes** ont dans des conditions pathologiques ? Les mécanismes de régulation de p21 sont-ils altérés dans les organismes âgés, où les cellules sénescentes s'accumulent ? Si l'efficacité de la diminution de p21 en fin de sénescence était véritablement associée aux effets négatifs de la sénescence, elle pourrait devenir une cible intéressante pour des **interventions thérapeutiques** visant à renforcer les bénéfices et limiter les méfaits associés à la présence de cellules sénescentes dans différents processus, comme l'amélioration la cicatrisation et la régénération des plaies, l'amélioration des pathologies liées à l'âge ou la prévention de la croissance tumorale et de la récidive du cancer.

SUMMARY (ENGLISH)

Introduction

1. Cellular senescence

Cellular senescence is defined as a state of permanent proliferative arrest accompanied by characteristic phenotypical changes affecting the morphology, metabolism and secretion of cells, that is typically -but not exclusively- adopted in response to a damaging stimulus.

Although the specific characteristics of senescence vary depending on the cell type, inductor and other contexts (such as if it occurs *in vitro* or *in vivo*), there are some **hallmarks** that are commonly used as markers for the identification of senescent cells. First, senescent cells experience a **permanent loss of the proliferative capacity**, even when exposed to pro-proliferative signals, due to the expression **of cell cycle inhibitors**. Second, they upregulate antiapoptotic proteins and inhibit pro-apoptotic genes, so they are **resistant to apoptosis**. In the third place, senescent cells undergo characteristic **morphological modifications**. This includes changes in **cell shape** (which becomes larger, flat and irregular), increased vacuolization, rearrangement of their cytoskeleton and alterations in cellular adhesion. Moreover, their **nuclei** become unshaped and lose integrity and present alterations at the level of the chromatin, such as the presence of **chromatin fragments in the cytoplasm** (CCFs) and the formation of **senescence-associated heterochromatin foci** (SAHFs), regions enriched in repressive marks. Importantly, senescent cells also present an **increased lysosomal content**, which has been used for their identification through the **SA-ß-gal** (or senescence associated ß-galactosidase) staining. This colorimetric reaction gives a blue in the presence of a lysosomal enzyme, marking senescent cells. Another important hallmark of senescence is the activation of a **persistent DNA damage response** (DDR). The DDR is known to induce senescence, and it has been shown to maintain and reinforce this phenotype by promoting the block of the cell cycle and expression of a pro-inflammatory secretome. In fact, and besides this intrinsic modifications, senescent cells become highly secretory, and extrinsically affect their surroundings through the production of the senescence-associated secretory phenotype, or **SASP**. Although its composition is dynamically changing, highly variable and heterogenous, the SASP is formed by growth factors, chemokines and cytokines,

reactive oxygen species (ROS), and extracellular matrix components and remodelers among other factors. Multiple pathways are involved in the SASP establishment, but they converge in the activation of two main transcriptional factors: **NF-κB** and **C/EBPβ**, although many other proteins have been shown to regulate SASP components. The SASP is responsible for many of the **biological functions** of senescence, since it influences tissue composition and signals neighboring cells. Finally, it is worth mentioning that the acquisition of a senescent phenotype affects most of the cellular organelles, which undergo specific modifications in order to adapt to new transcriptional, proteomic and metabolic requirements. For instance, due to an increase in misfolded proteins (partially caused by the synthesis of SASP factors), the **endoplasmic reticulum** (ER) expands. To deal with ER stress, the unfolded protein response (UPR) and protein degradation pathways (ERAD) get activated, which influences SASP expression and cell shape. In addition, senescent cells present an accumulation of **dysfunctional mitochondria**, which accentuates the production of ROS, inducing or reinforcing the senescence response. Moreover, the composition of the **plasma membrane** is also altered, and the expression of some proteins (caveolin-1, DPP4) has been proposed as markers of senescence. More generally, the **metabolism** and the **proteostasis** broadly affected in senescent cells, which present an increased glycolysis and autophagy, and altered lipid metabolism and translation.

The **establishment of senescence** is a complex process that can be triggered by a wide range of stimuli, classified in 3 groups. In the first place, senescence is normally caused by cellular damage, which activates the DDR. **Damage-induced senescence** can happen as consequence of an accumulation of replicative cycles (**replicative senescence**), which causes damage by gradually shorten telomeres. Other **damaging stimuli** can also cause cellular stress and DNA damage, such as genotoxic agents or irradiation. Interestingly, the overexpression of oncogenes or maintained mitogenic signals can also lead to hyperproliferation and cellular stress, triggering the DDR. In **oncogenic-induced senescence**, the intrinsic block of proliferation acts as a tumor suppressor mechanism. Surprisingly, senescence can occur in the absence of damage, in response to the physiological activation of developmental pathways. During **embryonic development**, cells presenting many hallmarks of senescence (absence of proliferation, SA-ß-gal positivity, expression of some cell cycle inhibitors and SASP factors) have been identified in several organisms, including mouse, human, chicken, zebra fish and frog. The presence of these cells is transient, and developmental senescence seems to contribute to normal embryonic patterning. Finally, senescence can spread to neighboring cells, which is known as **secondary senescence**. This can be mediated either by

the **paracrine** effect of SASP factors, or in a **juxtracrine** manner via cell-to-cell contact, where gap junctions enable ROS transfer and NOTCH1 receptor activation.

The main molecular drivers of cellular senescence belong to the p53/p21 and p16 tumor suppressor pathways, and the response is reinforced with specific epigenetic modifications. Typically, the tumor suppressor **p53** is activated in response to stress or cellular damage. Among other functions, this master regulator can block the cell cycle by inducing the transciption of one of its most important mediators, **p21.** By disrupting the formation of cyclin-CDK complexes, p21 promotes the activation of proteins from the retinoblastoma family (**RB**). When active, these proteins form the RB-E2F and DREAM repressive complexes, which prevent the expression of genes necessary for the cell cycle progression, blocking it and inducing the **senescence-associated proliferative arrest.** The action of p21 converges with another cell cycle inhibitor, **p16^{Ink4a}**, also able to disrupt cyclin-CDK complexes and activate RB proteins. Interestingly, p16^{Ink4a} is encoded **together with p19^{Arf}** (p14^{Arf} in humans), in the *Cdkn2a* locus. Although p16 and p19^{Arf} share part of their nucleotide sequence, they produce totally different proteins due to a shift in the translation reading frame. Surprisingly, p19^{Arf} is known to promote the stability of p53, so the *Cdkn2a* locus encodes 2 different proteins able to separately influence the 2 main axes responsible for senescence induction. In addition to the activation of these pathways, the transcriptional program of senescent cells is controlled by **epigenetic modifications**. Some of the main epigenetic regulators of senescence are the protein HMGB2, the members of the repressive Polycomb complexes 1 and 2 (PRC1 and PRC2), the chaperones of the HIRA complex, or the loss of LaminB1. The epigenetic marks spread by these factors control the formation of the SAHFs, the activation of the DDR and the expression of SASP factors. In conclusion: senescence acquisition is a **complex and multi-step process** controlled by a **crosstalk** of interrelated pathways and positive feed-backs that reinforce the programs involved in its progression. Although the activation of different factors is often explained following a linear and chronologic order, unbalances in any level of the different **interconnected networks** involved in senescence regulation can initiate and propagate this response. In addition, the SASP composition has been shown to change over time, and senescence is considered a **dynamic** process, with different features in “early” or “late/deep” stages of the response.

The presence of senescent cells can have an important impact in the organism health, and many biological processes can be impacted by the **intrinsic and extrinsic functions** of senescence. For instance, although senescence represents an intrinsic block of **proliferation**

that acts as a tumor suppressor mechanism, senescent cells can promote proliferation extrinsically through the secretion of the SASP, which can contribute to tumor development. Similarly, it has been proposed that senescence acts as an intrinsic barrier for **reprogramming**, but the SASP can boost plasticity and reprogramming in neighboring cells. Moreover, since some components of the SASP are extracellular matrix components or remodelers, it contributes to **tissue remodeling**, fibrosis, and embryonic patterning. Also, the cytokines and chemokines of the SASP can attract and modulate the action of **immune cells**. Depending on its exact composition, the SASP can have immunosuppressive or immunostimulant effects, which when persistent, contribute to chronic inflammation or "inflammaging". Therefore, senescent cells contribute to the development of many **physiological** and **pathological** states, often in contradictory ways. In general, it is considered that the transient expression of senescent cells, which are generally removed by the immune system, is **beneficial**, while their chronic persistence is more associated to their **detrimental** effects. In order to limit their negative influence, **senolytic** and **senomorphic** drugs, aiming to eliminate or modulate the action of senescent cells respectively, are being investigated.

2. p21 – *Cdkn1a*

p21, also known as Cip1 and Waf1, was independently described by several groups at the beginning of the 1990s. It is the first described member of the **Cip/Kip family**, which also includes $p27^{Kip1}$ and $p57^{Kip2}$, encoded by the *Cdkn1b* and *Cdkn1c* genes respectively. The Cip/Kip and the Ink4 families (which includes $p15^{Ink4b}$, $p16^{Ink4a}$, $p18^{Ink4c}$ and $p19^{Ink4d}$) are cell cycle inhibitors. They **block the cell cycle** by inhibiting the action of the cyclin-dependent kinases (CDKs) that control it, for which they are called CDK inhibitors (CDKi). Cip/Kip members are **promiscuous** proteins, able to interact with different CDK-cyclin complexes, affecting different phases of the cell cycle. Moreover, they also interact with other factors, and are also involved in the regulation of **other cellular processes**.

In mice, **p21 protein** is composed by 159 amino acids, and has a molecular weight of 18KDa. It is encoded by the 2nd and 3rd exon of the ***Cdkn1a* gene**. Several functional domains have been described, like cyclins, CDKs, and PCNA interaction domains, and nuclear localization and export signals. Since it lacks a stable tertiary structure, p21 is considered an **intrinsically disordered protein**, which facilitates its interaction with multiple partners.

The expression of p21 is regulated at multiple levels. Its main **transcriptional activator is p53**, which is normally activated upon DNA damage or oncogenic signals. However, many **other transcription factors** and epigenetic regulators have been shown to promote (or repress) *Cdkn1a* transcription independently of p53, including other responders to stress or members of TGF-ß developmental pathway. **Post-transcriptionally**, the stability and translation efficiency of *Cdkn1a* mRNA is influenced by micro-RNAs (mi-RNAs), RNA-binding proteins (RBPs), and the translation factor eIF2α. Finally, **several post-translational** modifications determine the stability of p21 protein. Specific phosphorylation, methylation and acetylation marks promote or prevent the **degradation** of p21, which occurs through ubiquitin-dependent and independent mechanisms.

Functionally, p21 is a pleiotropic protein, involved in multiple cellular activities. Besides blocking the **cell cycle** through different mechanisms, p21 also regulates cell death and **apoptosis**, contributes to **DNA repair and genome stability**, influences **cytoskeleton dynamics**, cell migration and adhesion, and controls **transcription**. The specific contribution of p21 in these processes is often controversial, since it can play **contradictory roles** depending on its cellular localization, context and interaction partners.

Because of its numerous functions, p21 influences several biological processes. For instance, the induction of p21 is involved in the **differentiation** of many cell types, the maintenance of the **renewal of stem cells** of some populations, and the **reprogramming** of induced pluripotent stem cells. Also, p21 expression is normally considered a barrier to the **regeneration** of different organs and tissues, although it might be required in other specific cases. In **cancer**, p21 plays a dual role, acting either as a tumor suppressor or a promoter of tumor resistance, aggressiveness and invasion. Moreover, p21 deficiency has been associated with the development of **autoimmune diseases**, although p21 could promote the expression of genes associated with inflammatory and neurodegenerative pathologies. Finally, p21 is an important contributor and marker of **cellular senescence**. In fact, it is one of the senescence mediators expressed during **developmental senescence**. While its role has been primarily associated with the onset of senescence establishment, where it mediates the **proliferative arrest**, p21 is also thought to maintain the cell viability of senescent cells by protecting them from **apoptosis**. In addition, p21 expression mediates and reinforces the senescent response by enhancing **ROS production**. Finally, p21 also contributes to the acquisition of the senescent **transcriptional program** by regulating senescence and SASP regulators, such as HMGB2 or RB proteins.

Results

1. Model validation

The first part of the results section describes the ***in vitro* validation** of the inducible knock-down mouse model used in this project. In this model, the addition of doxycycline to the cell culture media induced the transcription of the construct containing a GFP reporter signal and a shRNA against the transcript of our protein of interest, p21. The experiments described in this project were carried out in isolated and cultured primary dermal fibroblasts derived from the skin of newborn pups from this mouse line.

To validate the **knock-down of p21 in proliferating cells**, I confirmed the expression of the construct via fluorescence visualization of the GFP signal, as well as the decreased expression of p21 at the transcript and protein level through RT-qPCR and Western Blot, respectively. Next, I used irradiation to induce senescence. Six days after irradiation, **senescence establishment** was confirmed by the observation of the characteristic morphological and transcriptional changes, proliferation blockage and increased lysosomal activity. These changes were measured by phase contrast microscopic observation, RT-qPCR on senescence markers (p21, $p19^{Arf}$, $p16^{Ink4a}$, Ki67 and Hmgb2), reduced EdU incorporation, and positive-blue SA-ß-gal staining. The efficient induction of **p21 knock-down in senescent cultures** was confirmed at the transcriptional (RT-qPCR), protein (Western Blot) and functional (Hmgb2 transcriptional de-repression assessed by RT-qPCR) levels.

Once the induction of p21 knock-down was validated in proliferating and senescent cultures, I **optimized** the experimental conditions (day after irradiation and doxycycline dose) to generate RNA samples to analyze via **bulk RNA-seq**. To induce the knock-down of p21, proliferating and senescent cells were supplemented with 2ug/mL of doxycycline for 2 days before sample collection, and samples from senescent cells were collected at post-irradiation day 8. For the selection of the optimal samples, senescence and p21 downregulation were evaluated in 7 biological and technical replicates though RT-qPCR analysis of markers of senescence and p21 function (p21, $p16^{Ink4a}$ and Hmgb2). This led to the selection of samples corresponding to 4 conditions, and produced in 4 technical and biological replicates. Each condition was defined by the combination of 2 variables: proliferating/senescent (P: proliferating vs S: senescent) and unaltered/reduced p21 via knock-down induction with doxycycline treatment (C: control vs D: doxycycline or p21 knock-down). Therefore, total of

16 RNA samples corresponding 4 replicates of each of the 4 conditions of interest (PC, PD, SC and SD) were sent to the GenomEast Platform for their sequencing.

2. Bulk RNA-seq analysis

The second part of the results section consists on the bioinformatic analysis of the data from the bulk RNA-sequencing. After sequencing, the GenomEast platform provided us with a report of the process and an analysis of differential gene expression in the comparison of the conditions of interest. First, a general **description of the data** was performed using the information provided by the platform in their report. Then, in order to explore and interpret the transcriptional changes associated to p21 reduction in senescence, I performed **pathway analysis** on gene lists created from their differential gene expression analysis using Enrichr webpage, a pathway analysis tool. Results were graphed using visualization packages in R studio. The interpretation of the pathway analysis turned out to be rather complex, so it was divided in 4 sections.

First, the differentially expressed genes in the **main comparisons** were analyzed. This allowed the confirmation of senescence induction, and provided a description of the transcriptional programs altered in senescence (SC.vs.PC), as well as those associated with p21 decrease in proliferating (PD.vs.PC) and senescent cultures (SD.vs.SC). Since this analysis proved to be insufficient to unravel specific novel roles associated to p21 function in senescent cells, I decided to subdivide the differentially expressed genes of the comparison of our main interest (SD.vs.SC) in subcategories depending on their **transcriptional behavior in other comparisons**. On one hand, I aimed to determine which processes were similarly and differentially impacted by p21 reduction in either proliferating or senescent cells. On the other, I wanted to distinguish the effect of p21 loss in the transcriptional changes associated to the senescent program, as well as to detect its impact in other functions not altered by the establishment of senescence. This “comparison of comparisons” analysis helped me to define the role of p21 in different contexts, but the methodological approach applied also led to a significant loss of statistical power.

At that point, I realized that a **physiological interpretation** of our experimental conditions was necessary for a deep and meaningful interpretation of our data. By considering the transcriptional changes of genes in several comparisons, I developed a criterion to determine the genes **activated or repressed by p21** that could have a relevant impact on the phenotype of senescent cells. Pathway analysis on these gene sets revealed a novel set of biological

functions associated to p21 decrease in senescence. To finish the bioinformatic analysis, I explored some of the uncovered processes potentially controlled by p21 in senescence that could have an interesting physiological impact. I represented the behavior of the gene involved in these programs using **heatmap** graphs. First, the role of p21 as a mediator of senescence and p53 function was validated by observing its control of the activity of the **DREAM** repressor complex. Since several immune-related pathways were shown to be enriched among genes affected by p21, I then analyzed how p21 affected some **SASP** components, general **chemokine and cytokine secretion** and mediators of **Natural Killers** activity. **TNF-α** signaling was affected by p21 downregulation in senescence, so I explored it as a potential mechanism by which p21 could exert a control over transcriptional programs involved in the regulation of the immune system. Lastly, changes in **translation** related machinery and **peroxisomal** genes caught our attention and were briefly explored.

3. Hypotheses exploration

Some interesting hypotheses raised from the transcriptomic analysis. First, it had been observed that the loss of p21 in senescent cells caused a partial reversion of the transcriptional changes associated to senescence, including the re-expression of proliferation related genes. For this reason, I decided to explore the irreversibility of the proliferative arrest of senescent cultures. To our surprise, small patches of **proliferating cells emerged from irradiated plates** when cultured over prolonged periods of time. The number, size and growth rate of these clusters was intensified by the downregulation of p21 in senescent cells. Crystal violet proliferation assays were performed in order to assess the incidence of non-senescent cells in irradiated cultures with unmanipulated or ablated p21 at 2-3 weeks after irradiation. Due to the possible bias of working with not completely arrested senescent cultures, I arrived to the conclusion that an alternative model of senescence induction will be eventually required for the validation of my results. In this context, the use of **adriamycin** as an alternative model of damage induced senescence was proposed and evaluated. Preliminary results showed that cells acutely exposed to adriamycin arrested proliferation, adopted a senescent morphology, and acquired the expected transcriptional changes associated to senescence (RT-qPCR on p21, $p16^{Ink4a}$, Hmgb2 and Ki67). Moreover, the addition of doxycycline also induced the drop of p21 levels and activity in this model (RT-qPCR on p21 and Hmgb2). Importantly, a total **absence of non-senescent proliferating cells** was observed in all adriamycin-induced senescent cultures through their visual examination up to 3 weeks after senescence induction, even when p21 was downregulated.

This was preliminarily verified in crystal violet proliferation assays. Thus, adriamycin-induced-senescence is an alternative model, where the effect of a residual presence of non-senescent cells in irradiated cultures could be evaluated in order to validate my results in the future.

Next, we decided to explore some of the functions associated to p21 that were unraveled by the RNA-seq analysis. On one side, we decided to assess the effect of senescence and p21 loss on **peroxisomes**. To do so, I performed **immunofluorescence** on the peroxisomal marker Pmp70 and I imaged peroxisomes in proliferating and senescent cells. In this stainings, the presence of clusters of peroxisomal signal resembling peroxisomal aggregates was noticed. Interestingly, cells containing aggregates were more frequent in senescent plates, either induced by irradiation or adriamycin. However, the loss or absence of p21 seemed not to affect their incidence. In order to investigate the functional impact or the cause of aggregates, I performed immunofluorescence stainings on the enzyme catalase and the autophagy marker p62. The results of these experiments were inconclusive. This line of research was abandoned, and at the current moment, the nature, origin and functional impact of these structures remains unknown.

Pathway analysis on the genes potentially repressed by p21 in senescence suggested that its loss favors the recruitment and interaction with the **immune system**. Further analysis suggested that the production and secretion of several cytokines and SASP factors might be potentiated upon p21 loss in senescence, at least transcriptionally. For this reason, the **secretion of cytokines** by senescent cells with unmanipulated or downregulated p21 was analyzed. The abundance of 40 cytokines in the conditioned media of senescent cells from day 8 to 9 after irradiation was assessed using a commercial **cytokine array** kit. Among the 24 of cytokines that were expressed at a range high enough to be reliably measured, only 3 changed in the same direction in the two experiments analyzed, and showed an average change of more than 25% upon p21 reduction. Remarkably, these cytokines -**Cxcl9**/Mig, **Cxcl10**/Ip10/Crg2 and **Ccl5**/Rantes- were **upregulated** more than 70% on average. At the transcriptional level, the expression of Cxcl10 and Ccl5 (both reported targets of Tnf-α) also increased significantly upon p21 knock-down in senescence. This experiment supported the idea that the downregulation of p21 in senescent cells intensifies the expression of a **pro-inflammatory secretome**, also at the protein level.

Finally, an interesting observation from the RNA-seq analysis was the **accentuation** of the transcriptional changes associated to **senescence** establishment following the knock-down

of p21. In a way, this seemed to indicate that the loss of p21 leads to the acquisition of a "more senescent" phenotype. Intriguingly, I had observed in previous Western Blot that the level of p21 protein in irradiated plates tended to decrease over time. This led to the hypothesis that the **downregulation of p21 at later stages of senescence** could by naturally occurring as part of the physiological senescent response. To test this idea, I measured the **time-course** expression of p21 protein in senescence by **Western Blot** up to day 12 or 15 after irradiation (n=7) or adriamycin treatment (n=2). Although the variability among samples was notable, all experiments confirmed a reduction in p21 protein over time, starting around day 8-9 (or even earlier) after senescence induction. This result had important implications for the interpretation of my RNA-seq results, since the forced ablation of p21 at earlier timepoints (post-irradiation day 6) could be reflecting the transcriptional changes naturally occurring at later stages of senescence due to the physiological reduction of p21.

4. Alternative approach: p21 interactome

In parallel to the exploration of the transcriptional impact of p21 depletion in senescence, we decided to investigate its **interactome** in senescent cells. We hypothesized that the information on p21 interacting partners could complement the analysis of the RNA-seq and even suggest possible molecular mechanisms implicated in p21 function in senescence, including its role on transcription regulation. The binding partners of p21 were identified by **Mass Spectrometry** (MS) analysis on the proteins **co-immunoprecipitated** (Co-Ip) with **p21** in protein extracts from **senescent cells** 8 days after irradiation. The MS analysis was performed by the Proteomic platform at the IGBMC, and complemented with additional statistical analysis by myself. Among the **41 proteins detected**, 11 were known interactors of p21, including several CDKs and cyclins. Interestingly, some of the **novel potential partners**, such as Sptan1, were among the most abundant and confidently identified (based on statistical test) hits of the analysis. The interactome of p21 was subjected to **pathway analysis** in order to perform a descriptive analysis of its composition. Proteins were categorized depending on the **cellular localization**, **molecular function** and **biological process** in which they were involved. In order to have a **visual overview** of the data, the most frequent interactions in each of these 3 variables were represented in a quantitative manner. This revealed that p21 interactors where commonly found in the nucleus of the cell, but also in the cytoplasm, membrane, adhesion structures or the extracellular space. Regarding molecular functions, they often presented a kinase activity, as well the ability to ion and RNA binding. Moreover, apart from their expected involvement in proliferation, cell

cycle and apoptosis, p21's partners were often related to adhesion and migration processes. Although this result was not further developed, several potential new interactors of p21 in senescent cells were unraveled, and provided the basis for a better mechanistic understanding of its molecular activities in the future.

Discussion

1. Model considerations

The results obtained in this work were generated *in vitro*, using cell cultures of primary dermal fibroblasts isolated from a commercial **transgenic mouse line** that allows the **inducible knock-down** of p21. This strategy presents some important advantages over other models previously used to study the role of p21, especially in the field of senescence. Due to genetic robustness, organisms often adapt and compensate experimental or spontaneous molecular disturbances. These compensatory mechanisms can therefore mask the functional effect caused by genetic manipulation. Since the existence of compensatory mechanism has been described in p21 knock-out models, adopting a **knock-down strategy** could help averting them. Moreover, **conditional interventions**, in contraposition to constitutive ones, offer the possibility of disturbing a target in a spatial or temporal controlled manner. In the inducible model used in this work, the reduction of p21 could be induced at the desired timepoint through the administration of doxycycline. Since p21 is well known to participate in the first stages of the senescent response by mediating the cell cycle arrest, the capacity of **downregulating it at later stages**, without altering the normal senescence establishment, has a critical importance. The **main limitation** in the use of this model in this study might **be the lack of a control condition for the effects of doxycycline**, which is an antibiotic drug with known matrix metalloproteinase inhibition activity. However, these concerns were totally unsupported by our data.

Dermal fibroblasts are commonly used for the *in vitro* study of senescence, and have been proposed to be drivers of skin aging *in vivo*. As in any *in vitro* study, the use of a **specific cell type** influences the obtained results, and cannot represent the physiological impact that the studied phenotype could have at the tissue or organism level *in vivo*. Thus, it would be

interesting to know if the pathways related with the transcriptional changes associated to the downregulation of p21 in senescent fibroblasts would be also detected in other senescent cells, or even how these changes might affect their **interaction with neighboring cells**, for instance with the immune system.

In this work, the main model used was **irradiation-induced senescence**. Irradiation is used as radiotherapy for cancer treatment, and is commonly used as a trigger in the study of senescence. In my experiments, the establishment of senescence 6 days after irradiation was confirmed by the reduction in proliferation, SA-β-gal positivity, and the detection of transcriptional markers. This was further confirmed when performing pathway analysis on the RNA-seq data, when the expected terms related with senescence were significantly enriched 8 days after irradiation. In spite of this, **proliferating colonies** were repeatedly spotted around 2 weeks after irradiation. When p21 was downregulated, 6 days after irradiation, these colonies were detected earlier and grew notably bigger. The cause of this is uncertain. It is possible that the depletion of p21 could boost the proliferation rate of residual non-senescent cells in irradiated plates. However, the contribution of other processes cannot be excluded, such as the expansion of proliferating colonies due to enhanced migration upon p21 loss, or the reversion of senescence. The possibility that **the depletion of p21 could enhance senescence evasion** in non-fully senescent cells (bypass) or enable senescent cells to **reverse to a proliferative state** (escape) are discussed. To clarify these speculations, it would be necessary to further characterize the presence of proliferative cells in irradiated plates with both unmanipulated and depleted p21, which could be done by quantifying EdU incorporation at different timepoints and conditions.

Interestingly, the detection proliferation-related terms enriched among the upregulated genes upon p21 loss in senescence could be explained by the presumed amplification of non-senescent population in this condition. While **the impact of the presence of non-senescent cells** in irradiated plates **on the interpretation of the RNA-seq results** should be considered, it was **estimated to be minimal** for two reasons. First, because based on visual examination and crystal violet staining, the presence of non-senescent cells in irradiated cells 8 days after irradiation (the **timepoint** analyzed in the RNA-seq) is estimated to be negligible. Secondly, because the most interesting results from the analysis were performed by applying what was called a "**physiological interpretation**" of the data. In this approach, the focus was put on the genes that were activated or repressed by p21 specifically in senescence. Because of how these gene subsets were determined, the transcriptional signature expected to be

associated with the amplification of proliferating cells upon p21 downregulation in our senescent samples would have been excluded. Therefore, and despite the fact that the presence of non-fully senescent populations might have contributed to mask the transcriptional changes due to p21 loss in senescent cells, their effect was probably minimized in my analysis. In addition, **other general limitations** of performing **pathway analysis on bulk RNA-seq** data (such as cellular heterogenicity or methodological biases) are also discussed.

Finally, the use of **adriamycin as an alternative senescence trigger** is discussed. Considering preliminary results, adriamycin treatment is proposed as a good model to validate my results in order to definitively discard the influence that the presence of non-senescent cells in senescent samples might have had in my analysis.

2. Role of p21 in senescence

The most interesting result from the RNA-seq analysis was the indication of p21's capacity of limiting the **clearance of senescent cells by the immune system**. Interestingly, p21 has been shown to regulate the activity of the immune system in several ways. For instance, its absence has been repeatedly associated to the development of **autoimmune diseases**, and the exacerbation of a pro-inflammatory environment. Among the processes affected by p21 in immune cells, it has been shown to inhibit the transcriptional activity of the **NF-κB**, a key SASP regulator, in macrophages.

My RNA-seq analysis had suggested that the downregulation of p21 in senescent cells intensified the production and secretion of several cytokines and SASP factors. This result was partially confirmed at the protein level via cytokine array analysis of the secretome of senescent cells after p21 reduction. In fact, the **ability of p21 to regulate the secretion of immunomodulating factors** in non-immune cells has been previously reported. Although some of the published conclusions on this topic may appear to be in contradiction with my RNA-seq analysis, these ideas could be reconciliated through a close examination of the data and the experimental methodology applied in these and other articles. In addition to promoting the expression of a pro-inflammatory phenotype, downregulation of p21 in senescent cells induced the **expression of NKGD2 ligands**, which were not upregulated solely upon the establishment of senescence. Since NKGD2 ligands had been previously shown to mediate the recognition and elimination of senescent cells by natural killers (NK), this result was considered especially relevant. The production of several **matrix**

metalloproteases (MMPs) by senescent cells has been proposed to inhibit the recognition of their NKG2 ligands by NK, therefore preventing their removal. Importantly, the transcription of MMPs did not generally increase upon p21 loss. To continue the exploration of the role of p21 in regulating the immune clearance of senescent cells, some **future *in vitro* and *in vivo* experiments were proposed**. Finally, the results from the analysis of the RNA-seq data and the potential p21 interactors identified through MS Co-Ip were examined and contrasted with the literature in order to infer the **potential molecular mechanism** by which p21 might be limiting the transcription of a pro-inflammatory phenotype in senescent cells. The possible accentuation of the DNA damage response (**DDR**), the activation of the **TNF-α and NF-κB pathways**, and changes in STAT3 activity and in **p53** levels upon the loss of p21 in senescence were discussed.

On the other hand, pathway analysis on the genes affected by p21's downregulation showed the enrichment of terms related to the **extracellular matrix**, cytoskeleton remodeling and cellular **adhesion** (therefore influencing **migration**). Although the capacity of p21 to regulate these processes has been reported, the information about the molecular mechanisms behind it is scarce, especially at the transcriptional level. Interestingly, **junction plakoglobin** (Jup) was identified as a novel interactor of p21 in senescent cells by the MS Co-Ip analysis. Apart from participating in the formation of **adhesion structures**, Jup has been shown to participate in several signaling pathways, and to **regulate transcription** of adhesion and migration related genes when localizing in the nucleus, where interacts and collaborates with p53. Altogether, the previously unreported interaction between p21 and Jup in senescent cells might be **a potential new mechanism** by which p21 could regulate cellular adhesion and migration at the transcriptional level.

Finally, a number of genes implicated in protein translation were found to be affected by p21 downregulation in senescence. **Translation** and **ribosome biogenesis** are known to be **altered in senescence**. Although it is an emerging field, there is evidence suggesting that the changes in the expression of tRNAs, ribosomes and translation factors are key post-transcriptional **regulators of several cellular processes**, including inflammation or the establishment of senescence. Thus, it is possible that, by affecting the transcription of many factors from the translation machinery, p21 could influence these and other functions, through the indirect post-transcriptional control of gene expression. Additionally, p21 might influence translation more directly by interacting with several factors with **RNA-binding capacity** identified by MS Co-Ip analysis. On another note, it is to mention that one of the

translation-related genes regulated by p21 in senescence was ***Rplp0***, which had been considered a housekeeping and **used to normalize** the values in previous RT-qPCR experiments. Although preliminary tests indicated that previous results were not likely to be critically affected by this (probably because of the small effect of senescence establishment and p21 downregulation in *Rplp0* expression), this result highlighted the importance of **choosing adequate controls** for the experimental conditions evaluated, which can be particularly tricky in the study of senescence.

3. Physiological dynamics of p21 expression in senescence

Interestingly, the **levels of p21 protein** were observed to **decrease at later stages** of senescence, around 8 to 9 days after irradiation or adriamycin treatment, as shown by Western Blot. It is curious to notice that two known regulators of p21 stability, Hsp90 and Cdk5, were identified by Co-Ip MS as p21 interactors in senescence. Importantly, the downregulation of p21 levels at later stages of senescence has been **already reported in the literature** in different cell types and models of senescence induction *in vitro*. This suggests that, even when p21 is well known to be upregulated at the beginning of senescence induction, and is widely considered a senescence marker, its levels might experience a **physiological drop at later stages**. Even though it is possible that this only occurs in specific cell types or models or scenarios (*in vitro* but not *in vivo*), it could have **important implications in the interpretation of my results**.

In case that the reduction of p21 levels in late senescence is really common event, it would be important to know if the same transcriptional changes observed in our model, when its depletions was forced from day 6 to 8 after irradiation, also occurred later on, when it was naturally downregulated, at day 10 or 12 after irradiation or adriamycin treatment for instance. Does the transcription of Hmgb2, NK ligands, cytokines like Ccl5 or metalloproteinases like Mmp9 increase at later stages of senescence, when p21 levels dropped? This could be tested by analyzing the expression of these genes at the transcriptional and protein level by performing RT-qPCR or cytokine array on **samples of senescent cells at later timepoints**, when the level of p21 has lowered. If the effect of p21 decrease in senescent cells was not the same when naturally occurring at later stages and when forced earlier on, it would be interesting to know which are the molecular mechanisms operating during this time-window to prevent it.

However, if similar changes are observed upon p21 depletion when artificially induced at day 6 after irradiation and when naturally occurring at later time-points, this could uncover **novel factors whose expression is dependent on p21 levels** in senescence. A better understanding of the **physiological effect of p21 downregulation** in senescence and the mechanisms controlling it would be key in assessing the impact of p21 regulation in the biological processes and pathologies associated with senescence *in vivo*. For instance, if p21 drop is actually promoting the **clearance of senescent cells** by the immune system at later stages of senescence, could the impairment of p21's downregulation be associated with the **detrimental effect that persistent senescent cells** have in pathological conditions? Are the regulatory mechanisms of p21 altered in aged organisms, where senescent cells accumulate? If the impairment of p21 decrease in late senescence was truly associated with negative effects of senescence, it could become an interesting target for **therapeutic interventions** aiming to enhance the benefits and limit the harms associated with the presence of senescent cells in different processes, such as improving wound healing and regeneration, improving age-associated pathologies, or preventing tumor growth and cancer relapse.

ANNEXES

1. Supplementary Figures

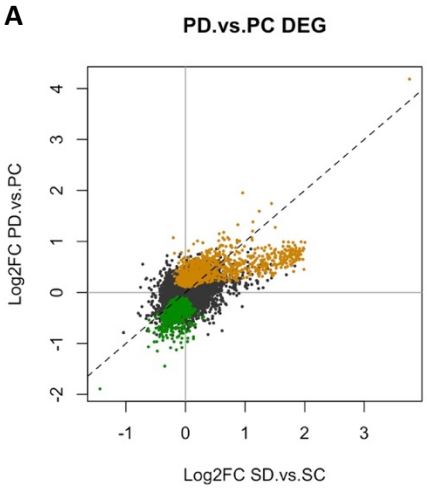

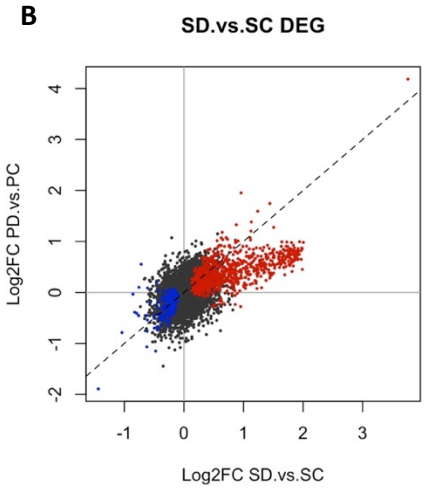

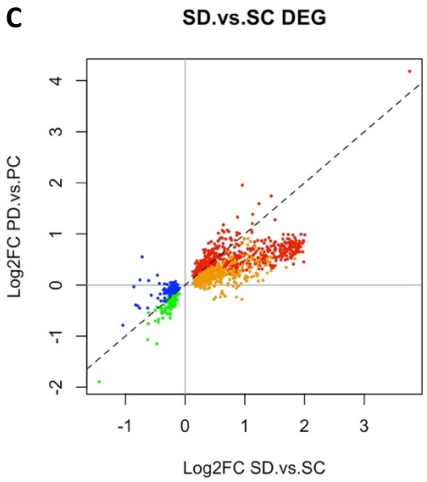

D

		SD.vs.SC			
		Up	NS	Down	
PD.vs.PC	Up	535	562	0	1097
	NS	350	30843	134	31327
	Down	0	599	135	734
		885	32004	269	33158

Supplementary Figure 1. Gene expression change in PD.vs.PC and SD.vs.SC conditions. A-C) Scatter plot of gene expression change (log2 fold change) in each comparison. One dot per gene. **A)** Differentially expressed genes in PD.vs.PC (adjusted p-value <0.05) are colored: upregulated in orange, downregulated in green. All genes are represented. **B)** Differentially expressed genes in SD.vs.SC (adjusted p-value <0.05) are colored: upregulated in red, downregulated in blue. All genes are represented. **C)** Figure 28A. Only differentially expressed genes in SD.vs.SC (adjusted p-value <0.05) are colored. Color based on gene expression change in both comparisons (see Fig. 28A). **D)** Number of genes not significantly changing (NS), differentially up or downregulated (adjusted p-value <0.05) in each comparison.

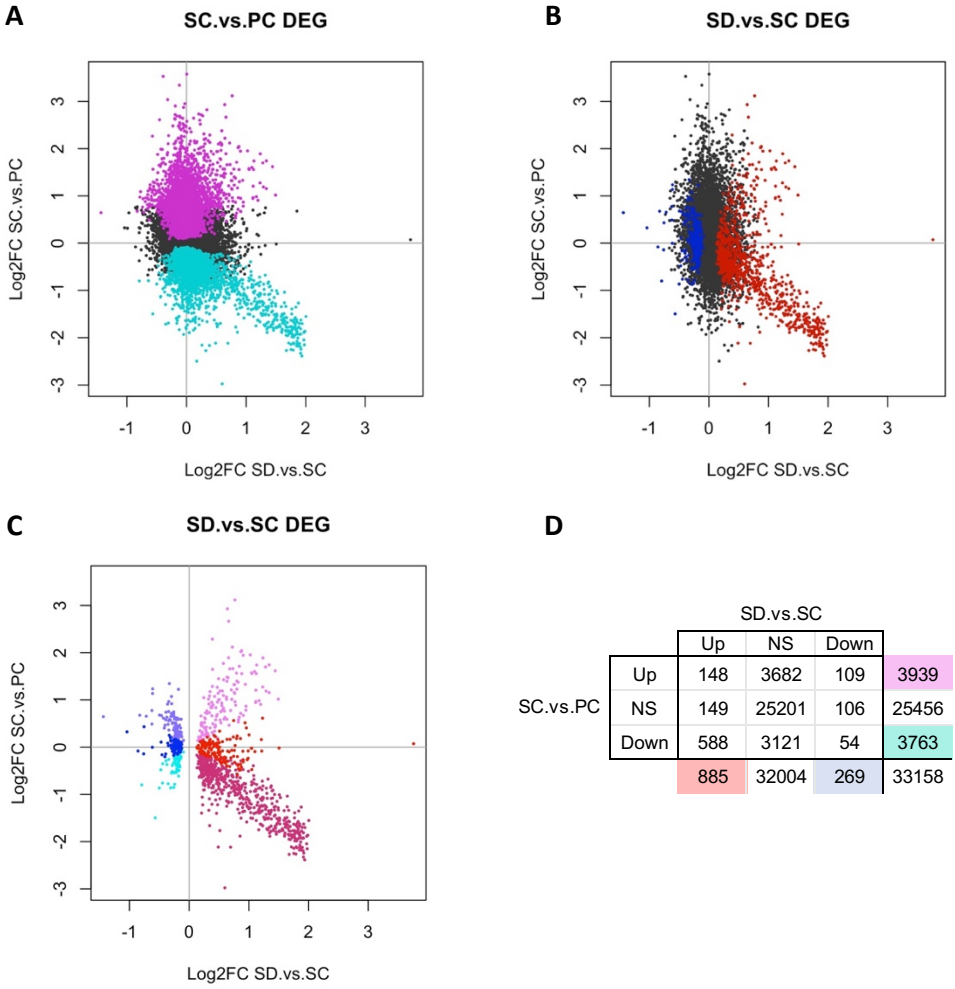

Supplementary Figure 2. Gene expression change in SC.vs.PC and SD.vs.SC conditions. A-C) Scatter plot of gene expression change (log2 fold change) in each comparison. One dot per gene. **A)** Differentially expressed genes in SC.vs.PC (adjusted p-value <0.05) are colored: upregulated in purple, downregulated in cyan. All genes are represented. **B)** Differentially expressed genes in SD.vs.SC (adjusted p-value <0.05) are colored: upregulated in red, downregulated in blue. All genes are represented. **C)** Figure 31A. Only differentially expressed genes in SD.vs.SC (adjusted p-value <0.05) are colored. Color based on gene expression change in both comparisons (see Fig. 31A). **D)** Number of genes not significantly changing (NS), differentially up or downregulated (adjusted p-value <0.05) in each comparison.

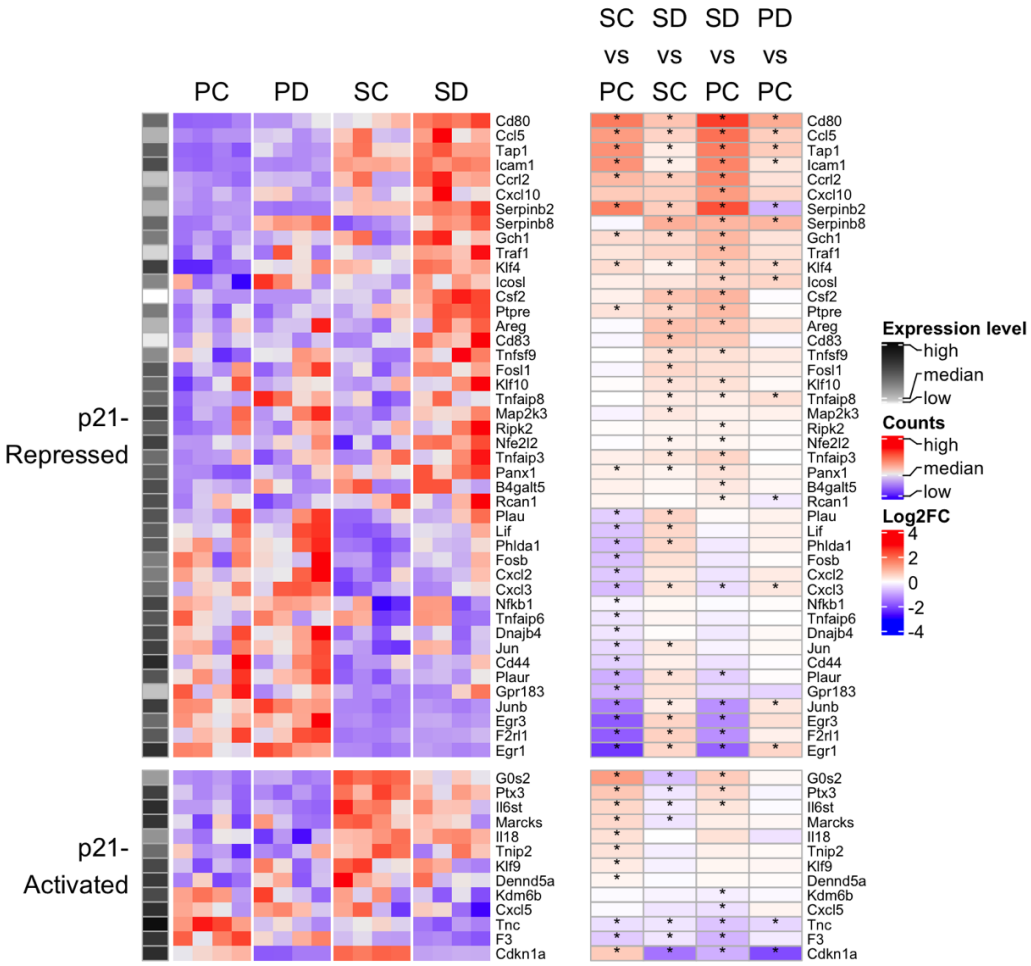

Supplementary Figure 3. Heatmap of TNF via NFKb term. Genes affected by p21 in senescence in "TNF via NKFb" term from Hallmarks 2020 database**.** Figure including 3 heatmaps. Left: relative expression level of the gene in comparison to the rest of transcripts in proliferating cells. Middle: expression in the 16 individual samples, grouped by condition and scaled by row. Right: expression fold change in log2 in the 4 analyzed comparisons. Significant change marked by an asterisk (p-value <0.05).

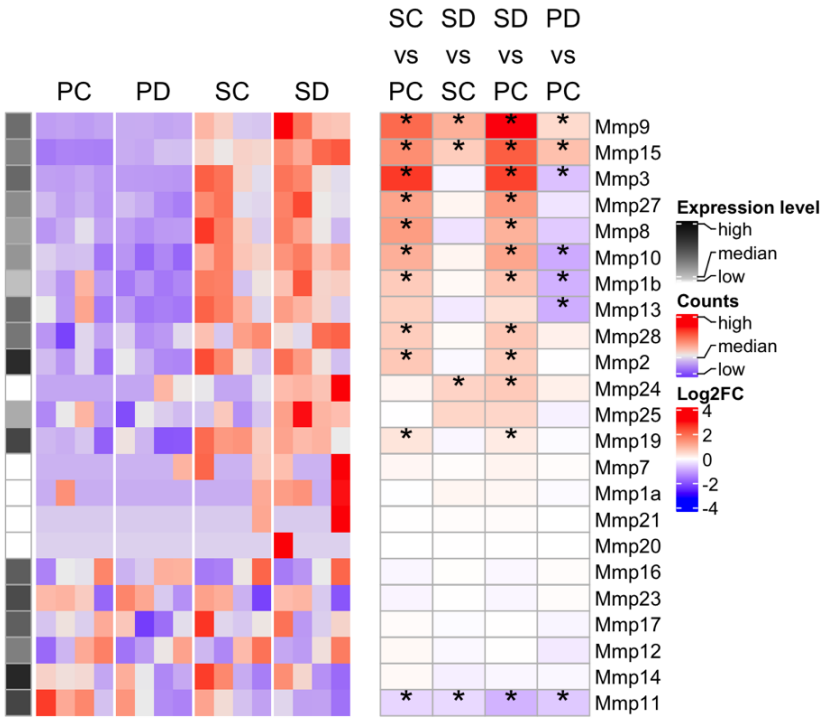

Supplementary Figure 4. Heatmap of metalloproteinases. Expression of 23 genes encoding for matrix metalloproteases. Selection was based on gene description containing the words "matrix metallopeptidase". 11 genes were significantly altered in senescence (10 up and 1 downregulated in SC.vs.PC comparison). 4 genes were affected by p21 downregulation in senescence (Mmp9, Mmp15 and Mmp24 upregulated, and Mmp11 downregulated upon p21 loss in senescence). Figure including 3 heatmaps. Left: relative expression level of the gene in comparison to the rest of transcripts in proliferating cells. Middle: expression in the 16 individual samples, grouped by condition and scaled by row. Right: expression fold change in log2 in the 4 analyzed comparisons. Significant change marked by an asterisk (p-value <0.05).

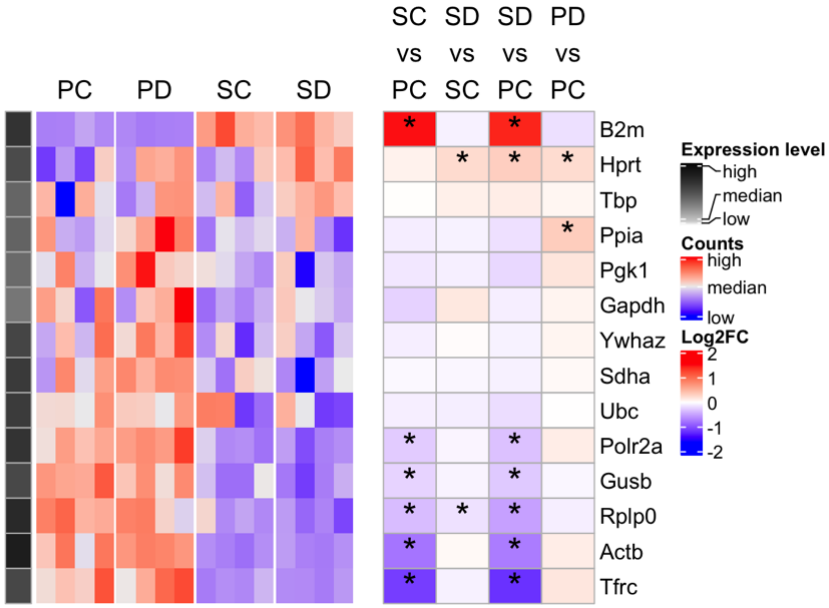

Supplementary Figure 5. Heatmap of housekeeping genes. Selection of 14 housekeeping genes commonly used to normalize mRNA expression levels in qPCR analysis from Yokoyama et al., 2018. Figure including 3 heatmaps. Left: relative expression level of the gene in comparison to the rest of transcripts in proliferating cells. Middle: expression in the 16 individual samples, grouped by condition and scaled by row. Right: expression fold change in log2 in the 4 analyzed comparisons. Significant change marked by an asterisk (p-value <0.05).

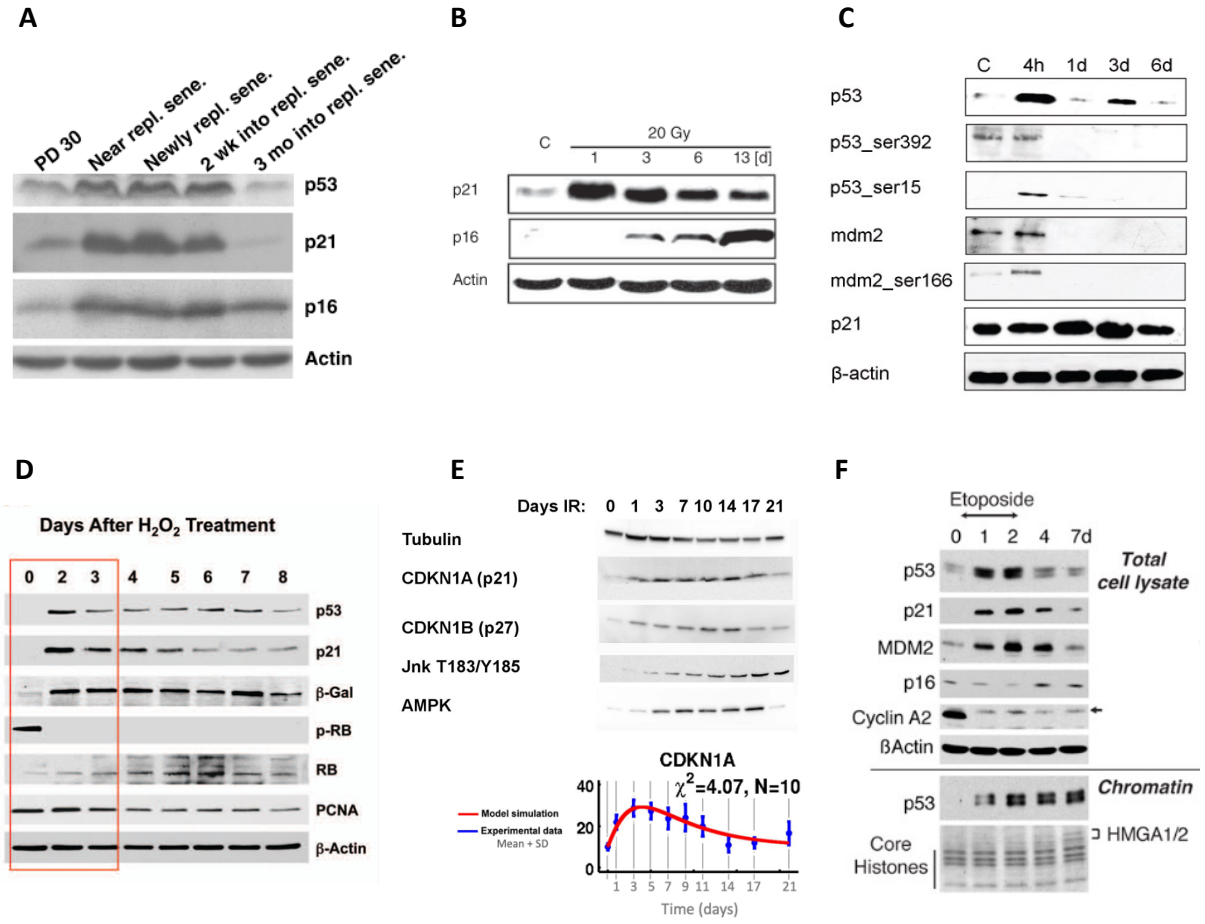

G

	Reference	Cell type	Senescence inductor	Range of time after senescence induction
A	Chen and Ozanne 2006 Fig. 1	Human dermal fibroblasts (IMR90)	Replication	Proliferating to 3 months into senescence
B	Muthna et al. 2010 Fig. 4A	Human dental pulp stem cells	Irradiation (20Gy)	0-13 days
C	Cmielová et al. 2011 Fig. 4A	Human embryonic lung fibroblasts (WI-38)	Irradiation (20Gy)	0-6 days
D	Capparelli et al. 2012 Fig. 2A	Immortalized human fibroblasts (hTERT-BJ1)	Hydrogen peroxide	0-8 days
E	Dalle Pezze et al. 2014 Fig. 1B, E (adapted)	Human embryonic lung fibroblasts (MRC5)	Irradiation (20Gy)	0-21 days
F	Kirschner et al. 2015 Fig. 1C	Human dermal fibroblasts (IMR90)	Etoposide	0-7 days

Supplementary Figure 6. Time course of p21 protein in senescence. Examples of p21 protein decrease at later senescent timepoints from the literature. All experiments were performed *in vitro* in damage induced senescence models. **A-F)** Western Blots showing p21 protein level at different timepoints after senescence induction. **E-bottom)** Modeling of p21 levels after irradiation (red) fitted using experimental datapoints (blue, mean and standard deviation)**.** Adapted image. **G)** Legend table specifying the origin of the figures (Reference), cell type, inductor of senescence and range of time of the analyzed samples in each experiment.

2. Annex 2: Publication (Rhinn *et al.* 2022)

Rhinn, M., Zapata-Bodalo, I., Klein, A., Plassat, J. L., Knauer-Meyer, T., & Keyes, W. M. (2022). Aberrant induction of p19Arf-mediated cellular senescence contributes to neurodevelopmental defects. *PLoS biology, 20*(6), e3001664.
https://doi.org/10.1371/journal.pbio.3001664

PLOS BIOLOGY

RESEARCH ARTICLE

Aberrant induction of p19^{Arf}-mediated cellular senescence contributes to neurodevelopmental defects

Muriel Rhinn[1,2,3,4]*, Irene Zapata-Bodalo[1,2,3,4], Annabelle Klein[1,2,3,4], Jean-Luc Plassat[1,2,3,4], Tania Knauer-Meyer[1,2,3,4], William M. Keyes[1,2,3,4]*

1 Institut de Génétique et de Biologie Moléculaire et Cellulaire (IGBMC), Illkirch, France, **2** UMR7104, Centre National de la Recherche Scientifique (CNRS), Illkirch, France, **3** U1258, Institut National de la Santé et de la Recherche Médicale (INSERM), Illkirch, France, **4** Université de Strasbourg, IGBMC UMR 7104- UMR-S 1258, Illkirch, France

* rhinn@igbmc.fr (MR); bill.keyes@igbmc.fr (WMK)

Check for updates

OPEN ACCESS

Citation: Rhinn M, Zapata-Bodalo I, Klein A, Plassat J-L, Knauer-Meyer T, Keyes WM (2022) Aberrant induction of p19^{Arf}-mediated cellular senescence contributes to neurodevelopmental defects. PLoS Biol 20(6): e3001664. https://doi.org/10.1371/journal.pbio.3001664

Academic Editor: Judith Campisi, Buck Institute for Research on Aging, UNITED STATES

Received: October 29, 2021

Accepted: May 6, 2022

Published: June 14, 2022

Peer Review History: PLOS recognizes the benefits of transparency in the peer review process; therefore, we enable the publication of all of the content of peer review and author responses alongside final, published articles. The editorial history of this article is available here: https://doi.org/10.1371/journal.pbio.3001664

Copyright: © 2022 Rhinn et al. This is an open access article distributed under the terms of the Creative Commons Attribution License, which permits unrestricted use, distribution, and reproduction in any medium, provided the original author and source are credited.

Data Availability Statement: RNA sequencing data is available at GEO (GSE175680). All other relevant data are within the paper.

Abstract

Valproic acid (VPA) is a widely prescribed drug to treat epilepsy, bipolar disorder, and migraine. If taken during pregnancy, however, exposure to the developing embryo can cause birth defects, cognitive impairment, and autism spectrum disorder. How VPA causes these developmental defects remains unknown. We used embryonic mice and human organoids to model key features of VPA drug exposure, including exencephaly, microcephaly, and spinal defects. In the malformed tissues, in which neurogenesis is defective, we find pronounced induction of cellular senescence in the neuroepithelial (NE) cells. Critically, through genetic and functional studies, we identified p19^{Arf} as the instrumental mediator of senescence and microcephaly, but, surprisingly, not exencephaly and spinal defects. Together, these findings demonstrate that misregulated senescence in NE cells can contribute to developmental defects.

Introduction

Cellular senescence is a form of permanent cell cycle arrest induced in response to a variety of stimuli. Senescence arrest is mediated by activation of cell cycle inhibitors including p21, p16^{Ink4a}, and p19^{Arf} [1–3]. In addition, the arrested cells are highly secretory, producing a complex cocktail of cytokines, growth factors, extracellular matrix, and other proteins, collectively known as the senescence-associated secretory phenotype (SASP). This can exert significant functional effects on the microenvironment, prominently including the activation and recruitment of immune cells to remove the senescent population. However, the SASP can also exert other effects including promoting cell proliferation, angiogenesis, and epithelial–mesenchymal transition (EMT), in addition to cell plasticity and stemness [4–6]. Although senescence is mostly associated with aging and disease, other studies have shown how senescent cells can have beneficial functions in various settings including embryonic development, tissue repair and regeneration, and tumor suppression and reprogramming [1,2,7,8]. Therefore, the

Funding: This work was supported by grants from La Fondation pour la Recherche Medicale (FRM) (AJE20160635985), Fondation ARC pour la Recherche sur le Cancer (PJA20181208104), IDEX Attractivité - University of Strasbourg (IDEX2017), La Fondation Schlumberger pour l'Education et la Recherche FSER 19 (Year 2018)/FRM, Agence Nationale de la Recherche (ANR) (ANR-19-CE13-0023-03) and Ligue Contre le Cancer (all to W.M. K.). I.Z.B. was supported by a 4th year fellowship from the Fondation ARC pour la Recherche sur le Cancer, and a PhD fellowship from INSERM and Conseil Regional Grand-Est. A.K. was supported by fellowship from Eur IMCBiO. The work was also supported by an institutional grant to the IGBMC, ANR-10-LABX-0030-INRT, a French State fund managed by the Agence Nationale de la Recherche under the frame program Investissements d'Avenir ANR-10-IDEX-0002-02. Sequencing was performed by the GenomEast platform, a member of the "France Génomique" consortium (ANR-10-INBS-0009). The funders had no role in study design, data collection and analysis, decision to publish, or preparation of the manuscript.

Competing interests: The authors have declared that no competing interests exist.

Abbreviations: AER, apical ectodermal ridge; ASD, autism spectrum disorder; BP, basal progenitor; E, embryonic day; EMT, epithelial–mesenchymal transition; HDACi, histone deacetylase inhibitor; NE, neuroepithelial; PHH3, phospho-histone H3; qRT-PCR, quantitative real-time PCR; RG, radial glial; RNA-seq, RNA sequencing; SASP, senescence-associated secretory phenotype; SA-β-gal, senescence-associated beta-galactosidase; TUNEL, TdT-mediated dUTP nick end-labeling; VPA, valproic acid; VZ, ventricular zone.

current view is that timely, controlled, and efficiently cleared senescent cells can have beneficial effects on tissue development and regeneration. However, when there is mistimed or chronic induction of senescence, then this contributes to aging and disease including neurodegenerative disease, fibrosis, and arthritis [2,3,9].

During embryonic development, cells exhibiting features of senescence are detected in precise areas and at critical stages of development, including in the apical ectodermal ridge (AER) of the limb, the hindbrain roofplate, the mesonephros, and the endolymphatic sac [10,11]. Here, it is thought that the controlled induction of senescence contributes to cell fate patterning and tissue development, while the efficient removal of these cells aids in tissue remodeling [1,2,12]. In the embryo, senescence is mediated by p21, but appears not to involve the induction of $p16^{Ink4a}$ and $p19^{Arf}$, which are both expressed from the *Cdkn2a* gene (Ink4a/Arf locus). Indeed, in the embryo, this locus is epigenetically silenced and becomes active in adult life in response to oncogene expression or the aging process [13–15]. Therefore, as mistimed induction of senescence is linked with many adult diseases, we wanted to explore whether aberrant senescence might be implicated in developmental disease.

As a first model to investigate such a possible association, we investigated embryonic exposure to valproic acid (VPA). This drug is widely used to treat a number of illnesses, including epilepsy and bipolar disorder. However, since its initial use, there have been many thousands of cases of women taking VPA during pregnancy, subsequently giving birth to children with birth defects [16–18]. In many cases, these were inadequately counseled about the associated risks, and drug use during pregnancy has continued. Common associated congenital malformations include spina bifida, facial alterations, and heart malformation, with additional risk of limb defects, smaller head size (microcephaly), cleft palate, and more, with higher doses associated with increased risk [16–18]. However, the most widespread consequences of VPA exposure are cognitive impairment and autism spectrum disorder (ASD), which occur in 30% to 40% of exposed infants, and which can occur without any major physical deformity [16,19–21].

The connection between VPA exposure and birth defects has been aided significantly by studies in rodent and primate models, leading to the hypothesis that cognitive defects arise from disruption of early neurodevelopment, around the stage of neural tube closure [21–24]. During this period (approximately embryonic day (E) 8.5 to E9.5 in mice), the early neuroepithelium amplifies, bends, and closes to generate the neural tube, which is lined by neuroepithelial (NE) cells. During neural tube closure, the NE cells divide symmetrically to self-renew and expand [25]. With the onset of neurogenesis, they differentiate into radial glial (RG) cells, which then undergo symmetric proliferative divisions to amplify their pool in the ventricular zone (VZ) of the neuroepithelium [26]. As development proceeds, they transition to asymmetric neurogenic divisions to produce cortical neurons directly or indirectly by amplifying progenitors including the basal progenitors (BPs) [26–28]. These steps must be tightly coordinated, and any perturbation of NE or progenitor function may have consequences on later cortical neuron development that could contribute to microcephaly and other neurodevelopmental disorders including cognitive impairment and ASD.

The molecular mechanisms by which VPA perturbs development are mostly unknown, but likely result from its function as a histone deacetylase inhibitor (HDACi) [29]. Interestingly, in this capacity, VPA is also broadly used in cancer therapy and has been shown to induce cellular senescence in certain settings, through direct activation of key senescence mediators including p21, $p16^{Ink4a}$, and $p19^{Arf}$ [30]. Given these associations, we investigated whether aberrant activation of senescence by VPA exposure might contribute to the associated developmental defects.

Results

Valproic acid induces exencephaly, microcephaly, and spinal cord defects in mice

Drawing from earlier VPA exposure studies in mice [23,31], we established a time-course paradigm for assessing acute and developmental phenotypes caused by VPA during embryonic development (see experimental scheme Fig 1A). Although it has been shown that acute dosing of mice can model many key features of drug exposure in humans, mice have high drug tolerance and clearance capacity, and as such, comparatively higher doses are used to model exposure. Also, although in humans VPA causes spina bifida, a posterior neural tube closure defect where part of the spinal cord and nerves are exposed, in mice, exencephaly, a defect of anterior neural tube closure where the brain is located outside of the skull, has been noted [32]. Here, we first analyzed E13.5 embryos from pregnant female mice that had been dosed 3 times around E8. As previously observed, we identified prominent and recurrent defects, such as exencephaly (Fig 1B). However, we also observed that a large proportion of the mice displayed a small brain phenotype resembling microcephaly, a finding which was previously underestimated in mice (Fig 1B). Next, we analyzed VPA-exposed embryos at earlier developmental

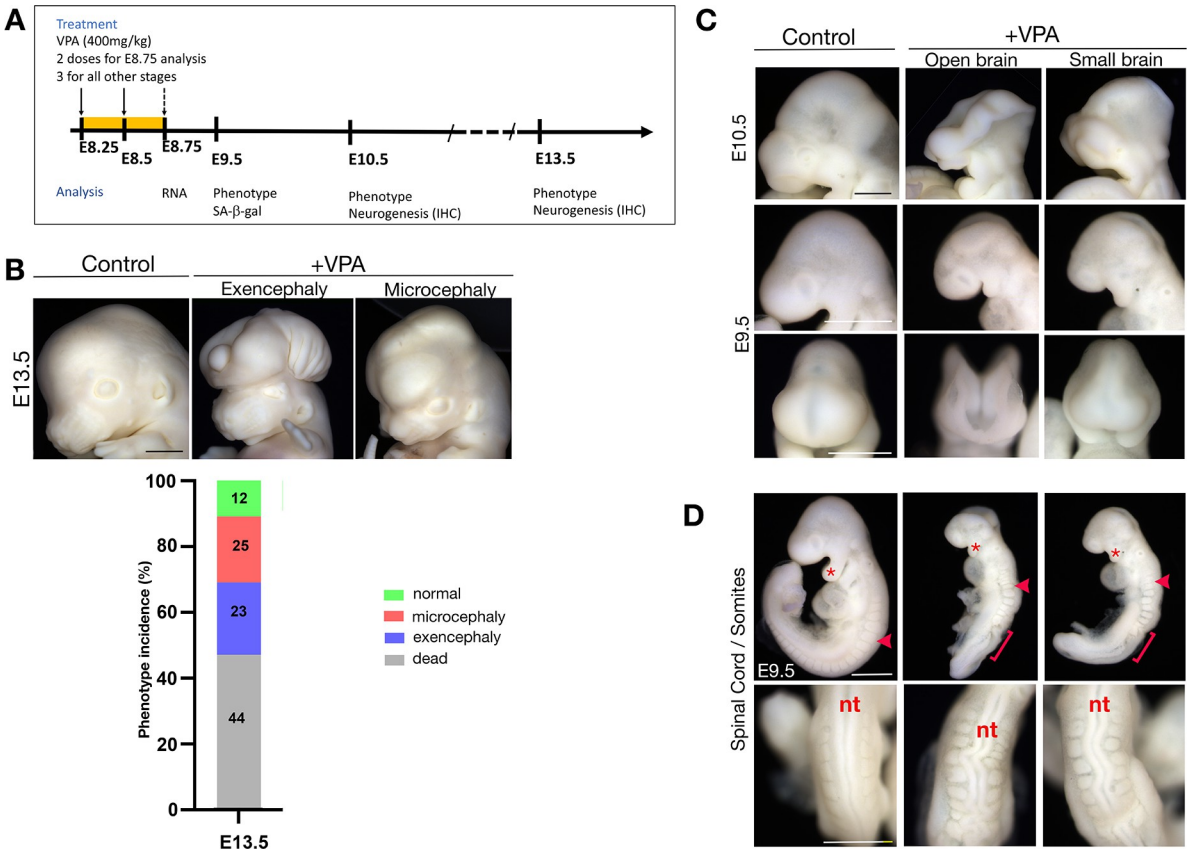

Fig 1. VPA treatment induces developmental defects, including exencephaly, microcephaly, and abnormal spinal cord development. **(A)** Schematic of experimental treatment of mice with VPA and timeline of analysis. **(B)** Top: embryonic head phenotypes in CD1 mice at E13.5 resulting from VPA exposure. Scale bar, 1 mm. Bottom: phenotype incidence at E13.5 ($n = 45$ embryos from 4 litters). **(C)** Embryonic head phenotypes in CD1 mice at E10.5 and E9.5. Scale bar, 500 μm. **(D)** Lateral views (top) and dorsal views (bottom) of control and VPA-treated embryos dissected at E9.5, illustrating the pronounced curve in the nt and abnormally shaped somites observed (arrowhead and brackets), and hypoplastic pharyngeal arches (asterisks). Scale bar, 500 μm. E, embryonic day; IHC, Immunohistochemistry; nt, neural tube; VPA, valproic acid.

https://doi.org/10.1371/journal.pbio.3001664.g001

stages and could visually distinguish these same phenotypes at E10.5 (Fig 1C). When we examined even earlier embryos at E9.5, they also presented with characteristic phenotypes, but at these early stages, care needs to be taken with regard to potential differences in developmental timing. In general, these embryos frequently presented with open neural tube (approximately 29%) and/or smaller brains (approximately 39%) (Fig 1C), suggesting that these may ultimately give rise to, respectively, the exencephaly and microcephaly phenotypes observed at later stages. Furthermore, at these earlier stages, additional deformations were obvious, including somite absence, fusion or gross misalignment (Fig 1D), kinked neural tubes, and hypoplastic pharyngeal arches. Critically, quantitative measurements showed that VPA-treated embryos, just like controls, had all turned, but were significantly shorter in length, and had fewer quantifiable somites as a result of the malformations (S1 Fig). This analysis uncovers distinct separate responses to VPA that were not previously characterized and demonstrate that VPA can cause early phenotypic changes during mouse brain development that recapitulate features of VPA exposure in humans.

Valproic acid induces ectopic senescence in neuroepithelial cells

Next, we investigated whether cellular senescence was a feature in VPA-exposed mouse embryos. First, we performed wholemount staining to assess for activity of the senescence marker senescence-associated beta-galactosidase (SA-β-gal) on E9.5 control or VPA-exposed embryos presenting with the open-brain or small-brain phenotypes. We found that ectopic SA-β-gal activity was prominent in the forebrain and hindbrain in both open-brain and small-brain embryos (Fig 2A, arrow). Notably, this ectopic staining was absent in both the spinal cord and the malformed somites. When we sectioned the embryos, we found that SA-β-gal activity was localized in the NE cells, the embryonic precursors of neurons and glia in the brain (Fig 2B). Interestingly, the SA-β-gal staining was predominantly localized at the apical border of the NE cells. We next assessed proliferation in these cells to confirm their senescent status. Measuring EdU incorporation, we confirmed that VPA-exposed mouse embryos had a significant decrease in staining throughout the forebrain, which was noticeably reduced in the apical borders (Figs 2C, S2A, and S2B). To confirm this, we also performed anti-phospho-histone H3 (PHH3) staining, which labels apical NE cell proliferation, and which again showed a significant reduction in proliferation in the NE cells of VPA-treated embryos (S2C Fig). Next, we assessed cell death levels by wholemount TUNEL staining. Here, the VPA-exposed embryos had a visible increase of cell death in the forebrain regions, while, as expected, both control and VPA-exposed embryos had cell death at the neural fold tips. However, when sectioned, we did not detect any cell death in the NE cells where the senescence staining was located, further supporting that VPA induces senescence in the NE cells (S3 Fig). Finally, we dissected the forebrain and midbrain regions from wild-type or VPA-exposed small-brain embryos at E8.75 and performed quantitative real-time PCR (qRT-PCR) for senescence genes, including cell cycle inhibitors and secreted components of the SASP. We found that *p21*, $p19^{Arf}$, and $p16^{Ink4a}$ and the SASP genes *IL6*, *IL1a*, *IL1b*, and *Pai1* were strongly induced in VPA-exposed embryos (Fig 2D). Together, these data uncover that VPA induces ectopic senescence in NE cells during developmental neurogenesis.

Neural differentiation is reduced by valproic acid exposure

To investigate the potential impact of such aberrant senescence on later cortical development, we analyzed telencephalic corticogenesis at subsequent developmental stages. NE cells undergo differentiation into progenitors, which will then give rise to neurons and glia. When we performed immunostaining in small-brain embryos for the neural progenitor markers Pax6

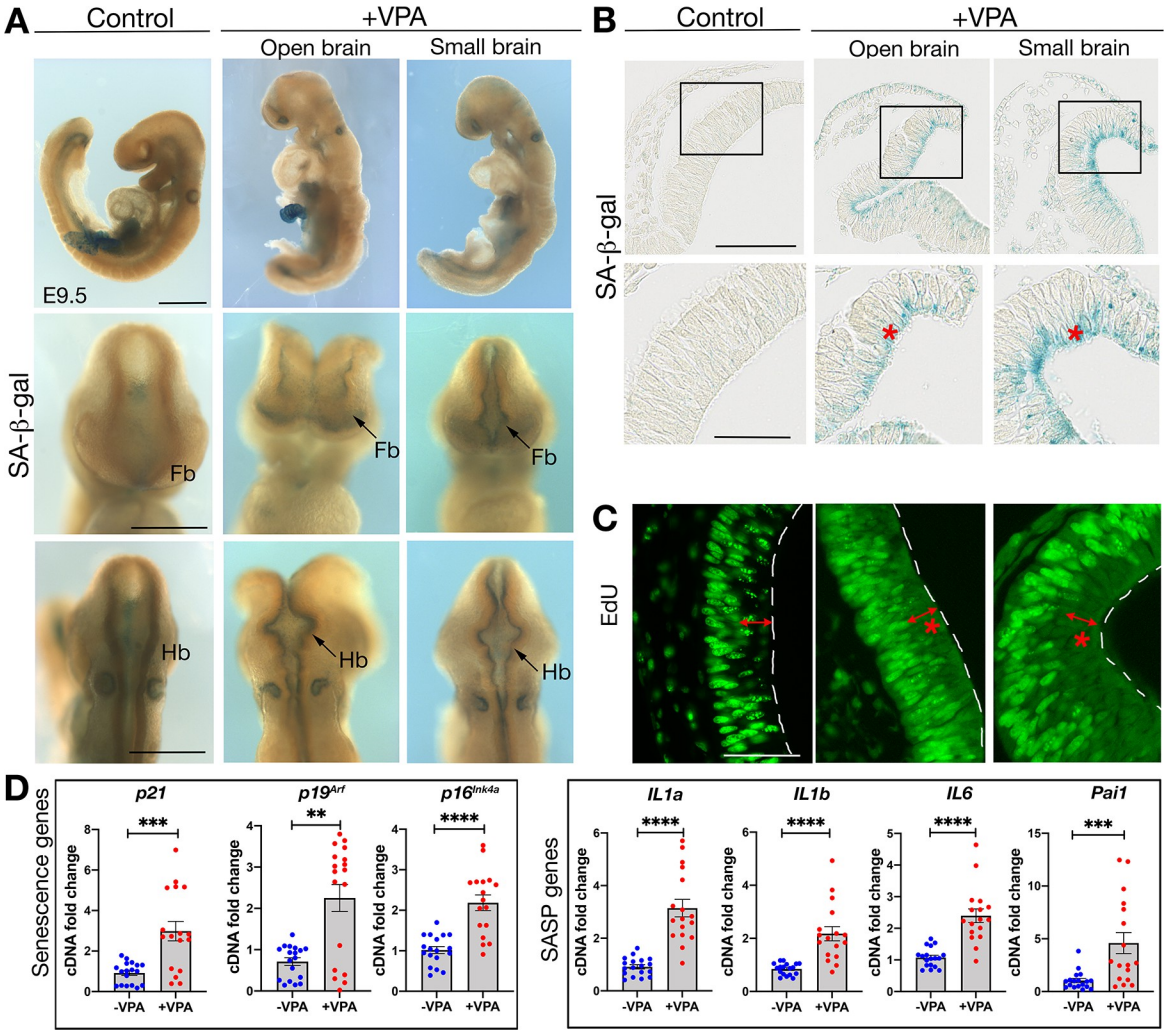

Fig 2. Senescence is induced in the forebrain and hindbrain neuroepithelium of VPA-treated embryos. (A) Whole mount SA-β-gal staining in control and VPA-treated embryos at E9.5 ($n = 18$ embryos from 7 litters). Top row, lateral views. Scale bar, 500 μm. Middle row, frontal views and bottom row, dorsal views. Scale bars, 50 μm. Fb, forebrain. Hb, Hindbrain. **(B)** Sections through whole mount SA-β-gal stained forebrains (scale bar, 100 μm). Box shows the region imaged in lower panel (scale bar, 50 μm). Red asterisks highlight senescent cells. ($n = 8$ embryos from 4 litters). **(C)** EdU incorporation in NE cells. Red asterisks indicate location of senescent cells ($n = 6$ embryos from 5 litters), and the double arrows highlight the apical zone. White dashed lines indicate apical surface of the neural tube. EdU, 5-ethynyl-2′-deoxyuridine. Scale bar, 50 μm. **(D)** qRT-PCR analysis on E8.75 forebrain + midbrain, for senescence markers (p21, $p19^{Arf}$, and $p16^{Ink4a}$) and SASP genes (IL1a, IL1b, IL6, and Pai1) ($n = 17$ to 18 embryos from 3 different litters). Data bars represent mean ± SEM. Mann–Whitney test: $^{**}p \leq 0.01$, $^{***}p \leq 0.001$, and $^{****}p \leq 0.0001$. The data underlying this figure can be found in S1 Data. E, embryonic day; NE, neuroepithelial; qRT-PCR, quantitative real-time PCR; SA-β-gal, senescence-associated beta-galactosidase; VPA, valproic acid.

https://doi.org/10.1371/journal.pbio.3001664.g002

(apical progenitors) and Tbr2 (intermediate progenitors), and for the neuronal differentiation marker Tuj1, we found a significant decrease in progenitors and neurons in VPA-exposed embryos at E10.5 (S4 Fig) and E13.5 (Fig 3). Overall, these data associate early aberrant senescence in NE cells of the embryo with decreased neurogenesis and impaired cortical development.

Human cerebral organoids exhibit senescence in response to valproic acid treatment

We next sought to assess if VPA exposure might similarly induce senescence in human NE cells and used cerebral organoids to investigate this possibility. We grew human organoids as

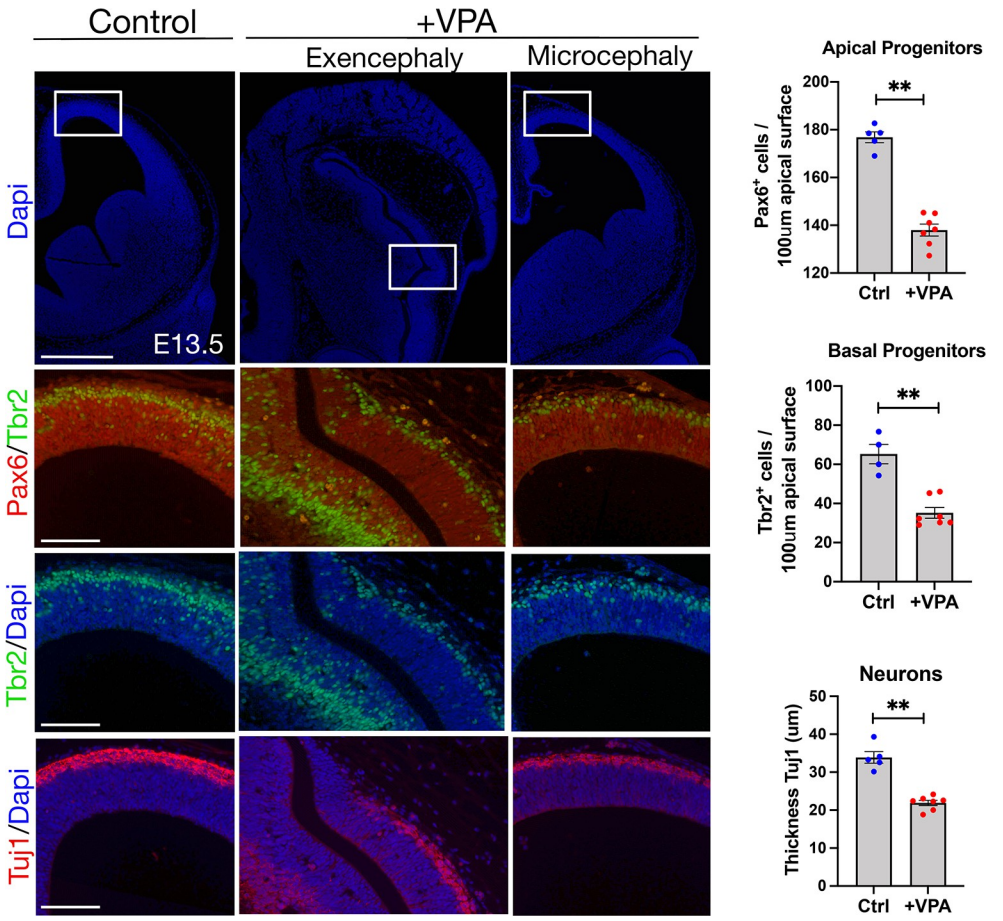

Fig 3. VPA treatment and senescence induction is associated with decreased neurogenesis. Immunostaining for Pax6, Tbr2, and Tuj1 on cortical sections (coronal) of E13.5 embryos. Box highlights the region in lower images. Scale bar, 500 μm (top row), 100 μm (rest). Quantification of Pax6 and Tbr2 positive progenitors or the thickness of the neuronal layer in the microcephalic cortical vesicles (for each condition, 5 embryos from at least 4 different mothers were analyzed). Data bars represent mean ± SEM. Mann–Whitney test: $^{**}p \leq 0.01$. The data underlying this figure can be found in S1 Data. E, embryonic day; VPA, valproic acid.

https://doi.org/10.1371/journal.pbio.3001664.g003

previously described [33] and exposed these to different concentrations of VPA at time points equivalent to the same developmental stages in mouse. Specifically, we treated cultures with 1 to 2 mM VPA from day 18 to 25 and analyzed the organoids upon VPA removal at day 25, or allowed the organoids to develop until day 42, when neuronal differentiation could be assessed (Fig 4A).

Exposure to VPA caused a significant decrease in organoid growth that persisted after drug removal (Fig 4B). As in mice, we assessed cortical neurogenesis in VPA-treated organoids and found a significant reduction in neural rosette size and progenitor number, as measured by Pax6 and Sox1/Tbr2 staining, respectively (Figs 4C and S5), and impaired differentiation of neurons, as measured by Tuj1 (Fig 4C). When we assessed senescence using wholemount SA-β-gal staining, we detected a strong induction in the organoids following VPA treatment, which upon sectioning was found to be present specifically in the NE cells (Fig 4D). Proliferation was also decreased in these cells, as measured by anti-PHH3 staining (Fig 4E). Of course, while it may be considered that rosette size is smaller owing to the decreased total organoid size, we believe that the reduction in rosette size is likely a determinant of the overall size

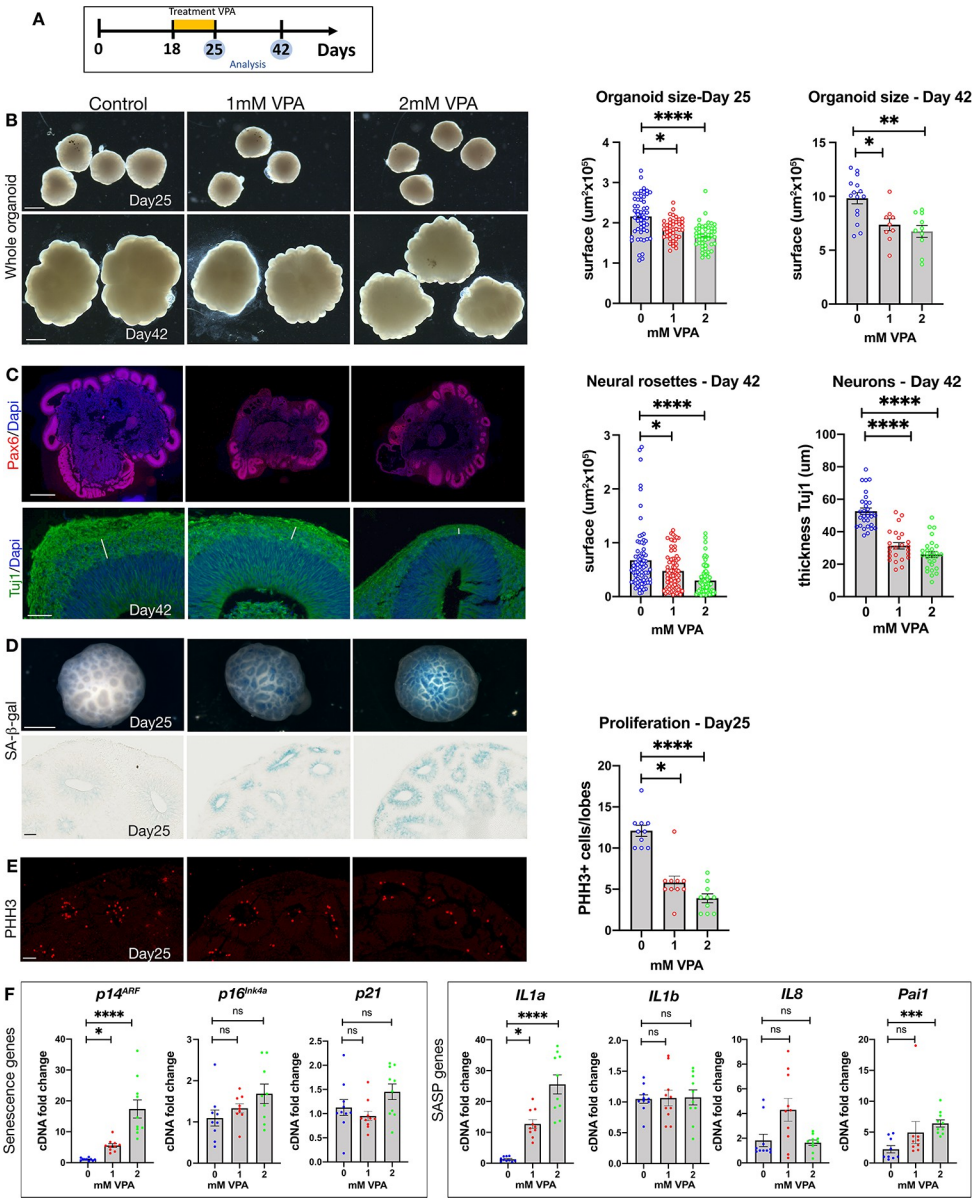

Fig 4. Human cerebral organoids treated with VPA show a decreased size, impaired neurogenesis, and induction of senescence in NE cells. (A) Schematic for organoid cultures experiments. **(B)** Left: Bright field images of cerebral organoids at days 25 and day 42. Scale bar, 1 mm. Right: organoid size (μm^2) at day 25 ($n = 52$ (Control), 41 (1 mM VPA), 45 (2 mM VPA), 4 independent experiments) and day 42 ($n = 15$ (Control), 9 (1 mM VPA), 10 (2 mM VPA), 4 independent experiments). Data bars represent mean ± SEM. Kruskal–Wallis test: $^{*}p \leq 0.05$, $^{**}p \leq 0.01$ and $^{****}p \leq 0.0001$. **(C)** Left: Immunostaining on sections of control and VPA-treated organoids for Pax6 (red) or Tuj1 (green), counterstained with Dapi (blue). Scale bar, 500 μm (Pax6) and 50 μm (Tuj1). Right: Neural rosette area at day 42 ($n = 79$ (Control), 76 (1mM VPA), 79 (2 mM VPA), 4 independent experiments), and neuron layer thickness (μm) at day 42 ($n = 30$ (Control), 24 (1 mM VPA), 28 (2 mM VPA), 4 independent experiments). Data bars represent mean ± SEM. Kruskal–Wallis test: $^{*}p \leq 0.05$, and $^{****}p \leq 0.0001$. **(D)** Whole mount SA-β-gal staining of day 25 organoids (scale bar, 500 μm). Sections show SA-β-gal staining in the neuroepithelium (scale bar, 50 μm) ($n = 5$ (Control), 5 (1 mM VPA), 5 (2 mM VPA), 3 independent experiments). **(E)** Left: Immunostaining on sections of control and VPA-treated organoids for PHH3 (red) at day 25. Scale bar, 50 μm. Right: Proliferation quantification at day 25. ($n = 10$ (Control), 10 (1 mMVPA), 10 (2 mMVPA), 2 independent experiments). Data bars represent mean ± SEM. Kruskal–Wallis test: $^{*}p \leq 0.05$ and $^{****}p \leq 0.0001$. **(F)** qRT-PCR analysis for senescence markers (*p21*, $p14^{ARF}$, $p16^{INK4A}$) and for SASP genes (*IL1a*, *IL1b*, *IL8*, and *Pai1*) ($n = 10$ organoids from 4 independent experiments). Data bars represent mean ± SEM. Kruskal–Wallis test: ns, not significant, $^{*}p \leq 0.05$, $^{***}p \leq 0.001$ and $^{****}p \leq 0.0001$. The data underlying this figure can be found in S1 Data. NE, neuroepithelial; PHH3, phospho-histone H3; SA-β-gal, senescence-associated beta-galactosidase; VPA, valproic acid.

https://doi.org/10.1371/journal.pbio.3001664.g004

impairment, especially as senescence was detected specifically in the NE cells. Finally, we assessed expression of key senescence mediators by qRT-PCR at day 25. Interestingly, we observed a significant induction of $p14^{ARF}$ (human ortholog of $p19^{Arf}$) and the SASP genes *IL1a* and *Pai1*, but no change in $p16^{INK4A}$ or *p21* expression (Fig 4F).

$p19^{Arf}$ deficiency rescues senescence and microcephaly induced by valproic acid

Thus far, our experiments uncovered that exposure to VPA causes a pronounced induction of senescence in NE cells that is associated with a marked decrease in proliferation and neurogenesis. However, we wanted to investigate if aberrant senescence is functionally coupled to the observed phenotypes and impaired neurogenesis. To address this, we employed genetic loss of function models deficient in the main senescence mediators *p21*, $p19^{Arf}$, or $p16^{Ink4a}$ and treated pregnant mice, each individually deficient for these genes, with VPA, and assessed the E9.5 embryo phenotypes. Surprisingly, we found that *p21*- and $p16^{Ink4a}$-deficient embryos had no visible improvement in any phenotype (S6 Fig). With regard to $p19^{Arf}$-deficient embryos exposed to VPA, these displayed no rescue of open-brain incidence, nor somite number and spinal curvature defects relative to wild-type mice (S7 Fig). Interestingly, however, they were noticeably improved, with regard to the incidence and/or severity of the small-brain phenotype (Fig 5A and 5B). To validate our observations, we measured the combined forebrain and midbrain area in all embryos. At this early stage (1 day after VPA exposure), we found that the forebrain/midbrain size in $p19^{Arf}$-deficient embryos was significantly larger compared to wild-type VPA-exposed embryos, an effect that was not present in *p21*- and $p16^{Ink4a}$ -deficient embryos (Fig 5A). The lessened size reduction $p19^{Arf}$-deficient embryos was also evident with in situ hybridization for the forebrain marker *Six3* (S8 Fig). To assess whether the size difference phenotype correlated with changes in senescence, we again assessed SA-β-gal staining and found that VPA-exposed $p19^{Arf}$-deficient mice had reduced expression in the NE cells relative to VPA-exposed wild-type embryos (Fig 5C). Again, this decrease was not detectable in *p21*- and $p16^{Ink4a}$-deficient embryos (S9 Fig). Furthermore, when assessed by qRT-PCR, $p19^{Arf}$ deficiency was associated with a decrease in $p16^{Ink4a}$ and a reduced SASP response (S10 Fig). In agreement with the results from human organoids, this data points to $p19^{Arf}$ as a mediator of VPA-induced senescence in the embryo.

To further investigate this association and to determine if ectopic $p19^{Arf}$ expression is sufficient to induce senescence and cause developmental defects when aberrantly expressed in the neuroepithelium, we electroporated mouse $p19^{Arf}$ into the NE cells of chick embryo forebrains. In comparison to GFP-control plasmid, we found that $p19^{Arf}$ expression caused a unilateral perturbation of development, decreasing forebrain size, and induced strong ectopic SA-β-gal activity in the NE cells (Figs 5D, 5E and S11). These data demonstrate that aberrant $p19^{Arf}$ expression is sufficient to induce senescence and developmental defects.

Finally, to conclusively demonstrate that aberrant senescence contributes to impaired neurodevelopment, we asked whether $p19^{Arf}$ deficiency would rescue some of the major defects caused by VPA exposure. To answer this question, we measured progenitor and neuronal status during cortical neurogenesis at later stages, when neurodevelopment has progressed further. As $p19^{Arf}$ deficiency only rescued the small-brain phenotype at early stages, here now we analyzed the microcephaly phenotype. As before, wild-type embryos exposed to VPA and examined at E13.5 presented with characteristic features of microcephaly, and with a significant reduction in the number of progenitors and neurons (Fig 5F). Strikingly, however, $p19^{Arf}$-deficient mice were not as susceptible to VPA exposure, and presented with a rescue of the microcephalic features, and significantly increased numbers of progenitors, and increased

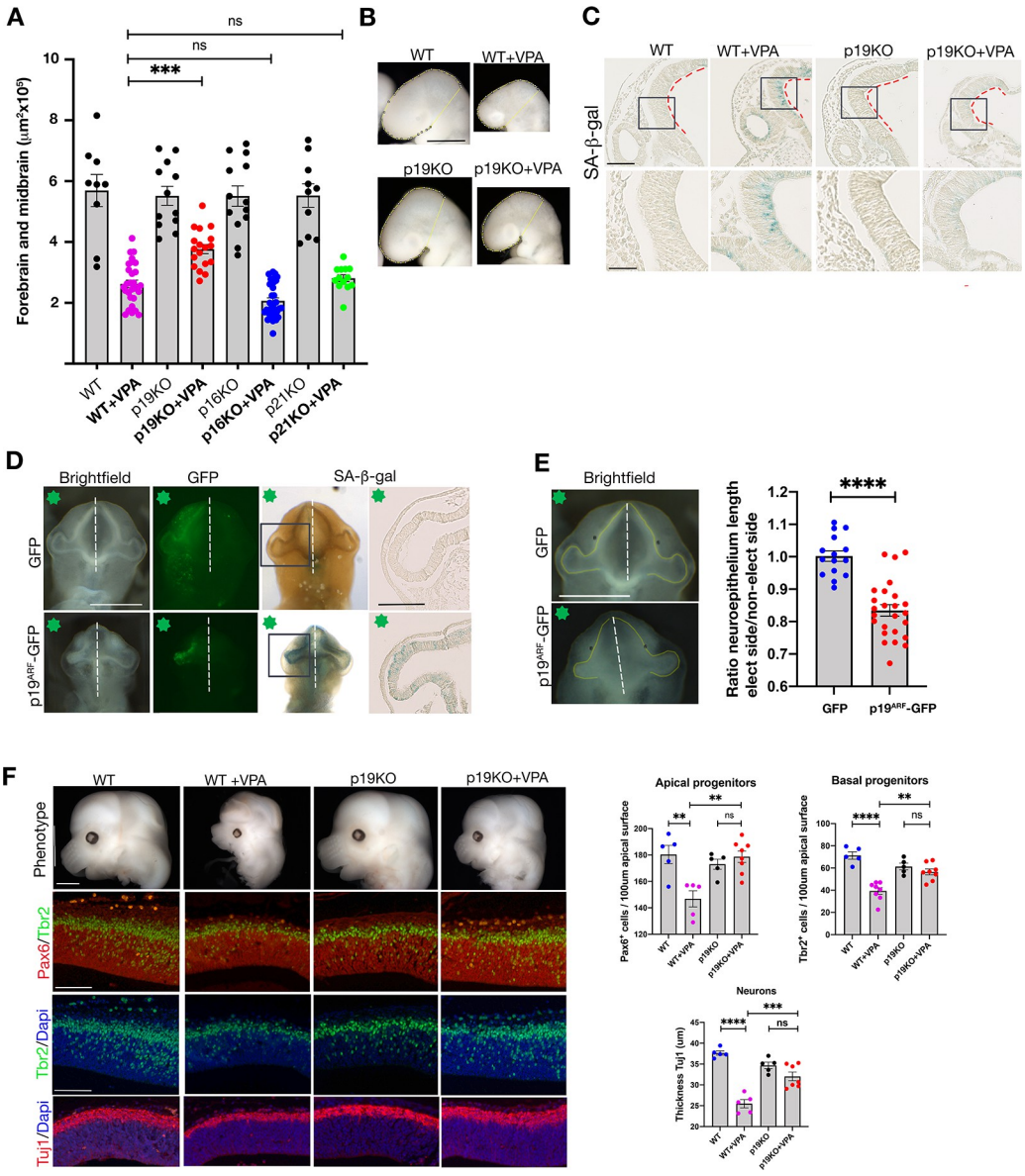

Fig 5. p19^{Arf} expression causes senescence and VPA-induced microcephaly. (A) Graph shows surface area of forebrain and midbrain in each condition, WT, $n = 9$ embryos from 4 litters, WT+VPA, $n = 29$ embryos from 14 litters, p19KO, $n = 12$ embryos from 4 litters, p19KO + VPA, $n = 18$ embryos from 7 litters, p16KO, $n = 13$ embryos from 4 litters, p16KO + VPA, $n = 34$ embryos from 8 litters, p21KO, $n = 11$ embryos from 4 litters, p21KO + VPA, $n = 13$ embryos from 8 litters. Data bars represent mean ± SEM. Kruskal–Wallis test: ns, not significant, $^{**}p \leq 0.01$ and $^{****}p \leq 0.0001$. **(B)** Bright field images of E9.5 embryonic heads, indicating area of the forebrain and midbrain (yellow line). Scale bar, 500 μm. **(C)** Representative brain sections of E9.5 SA-β-gal stained WT or p19KO (scale bar, 100 μm). Box shows the region imaged in lower panel (scale bar, 50 μm). Red dashed lines indicate apical surface of the neural tube. WT, $n = 5$ embryos from 3 litters, WT+VPA, $n = 6$ embryos from 4 litters, p19KO $n = 5$ embryos from 3 litters for p19KO, p19KO + VPA $n = 9$ embryos from 3litters. **(D)** Ventral views of chick embryos at stage HH12, electroporated with a GFP or a p19^{Arf}-GFP plasmid. Green star indicates electroporated side. Scale bar, 500 μm. Embryos were stained for SA-β-gal activity. Boxes indicate sectioned area of forebrain neuroepithelium shown. Scale bar, 100 μm **(E)** Brightfield embryos with yellow line shows length of neuroepithelium. Scale bar, 500 μm. Graph shows ratio of length of neuroepithelium in electroporated side compared to control side. GFP, $n = 15$ embryos from 4 different electroporations, p19^{Arf}-GFP, $n = 25$ embryos from 9 different electroporations. Data bars represent mean ± SEM. Unpaired t test: $^{****}p \leq 0.0001$. **(F)** Images showing the cortical vesicles from microcephaly embryos. Scale bar, 1 mM. Immunostaining on cortical sections, E.13.5, for Pax6, Tbr2, Tuj1, and counterstained with Dapi. Scale bar, 100 μm. Graphs showing number of Pax6 and Tbr2 positive progenitors or the thickness of the Tuj1 neuronal layer in the cortical vesicles (for each condition, minimum 5 embryos from at least 4 different mothers were analyzed). Data bars represent mean ± SEM. One-way ANOVA plus

Tukey post hoc test: ns, no significant, $^{**}p \leq 0.01$, $^{***}p \leq 0.001$ and $^{****}p \leq 0.0001$. The data underlying this figure can be found in S1 Data. E, embryonic day; KO, knockout; SA-β-gal, senescence-associated beta-galactosidase; VPA, valproic acid; WT, wild-type.

https://doi.org/10.1371/journal.pbio.3001664.g005

thickness of the neuronal zone relative to wild-type embryos. These experiments conclusively demonstrate that $p19^{Arf}$, in response to VPA, drives a senescence-mediated block in neurogenesis.

Pathways associated with neurodevelopmental defects are rescued in $p19^{Arf}$-deficient mice

Given that $p19^{Arf}$ deficiency is protective for early VPA-induced embryonic developmental defects, we wanted to begin to understand the underlying mechanism at a molecular level. To this end, we performed RNA sequencing (RNA-seq) on the forebrain/midbrain region from both wild-type and $p19^{Arf}$-deficient embryos, either treated or untreated with VPA. Through phenotype pathway analysis of differentially expressed genes, it was evident that many neurodevelopmental and ASD-related phenotypes, including exencephaly and microcephaly, were associated with significantly down-regulated genes in VPA-exposed wild-type mice (Fig 6A). Specifically, these gene signatures were associated with Wnt and Hippo signaling [34] (S12A Fig). In $p19^{Arf}$-deficient animals, however, most of these signatures were significantly less affected, confirming our phenotypic observations of the genetic backgrounds (Figs 6A and S12A).

Genetic population studies have identified candidate genes associated with microcephaly and ASD [35,36]. Many of these genes are significantly decreased in both the forebrain and midbrain of VPA-exposed wild-type embryos, including Chd8, Dyrk1a, Fmr1, Cep63, and others. However, most were not restored upon $p19^{Arf}$ loss (S12B and S12C Fig), suggesting that senescence may be regulated independently or downstream of these specific genes. Therefore, to get a better understanding of how $p19^{Arf}$ might induce these ectopic phenotypes, we analyzed the subset of genes that were significantly down-regulated in VPA-exposed wild-type embryos, but that were not significantly decreased in $p19^{Arf}$-deficient embryos (genes depicted in red in Fig 6B). Within this $p19^{Arf}$-dependent gene set, we identified tRNA aminoacylation and tRNA export (Figs 6C and S12D). Interestingly, perturbation of tRNAs or their regulatory mechanisms is linked to microcephaly and neurodevelopmental defects [37]. This suggests that $p19^{Arf}$-mediated senescence and repression of these genes may contribute to microcephaly and cognitive impairment.

Discussion

Together, these findings demonstrate that aberrantly induced senescence perturbs embryonic development, leading to developmental defects, and advances our understanding of how VPA causes neurodevelopmental disorders.

A major finding of this work is that it makes an exciting functional connection between aberrant cellular senescence and developmental defects. While abnormal induction or chronic accumulation of senescent cells has been linked to many adult and age-related diseases, we demonstrate here a causative role for senescence in neurodevelopmental defects. Interestingly, we identify that the NE cells are the site of senescence induction. As this population of cells is a critical precursor of all mature cell types in the brain, it stands to reason that this is one of the most perturbed population of cells in neurodevelopmental disorders. We demonstrate that induction of senescence in the NE cells correlates with a subsequent impairment in

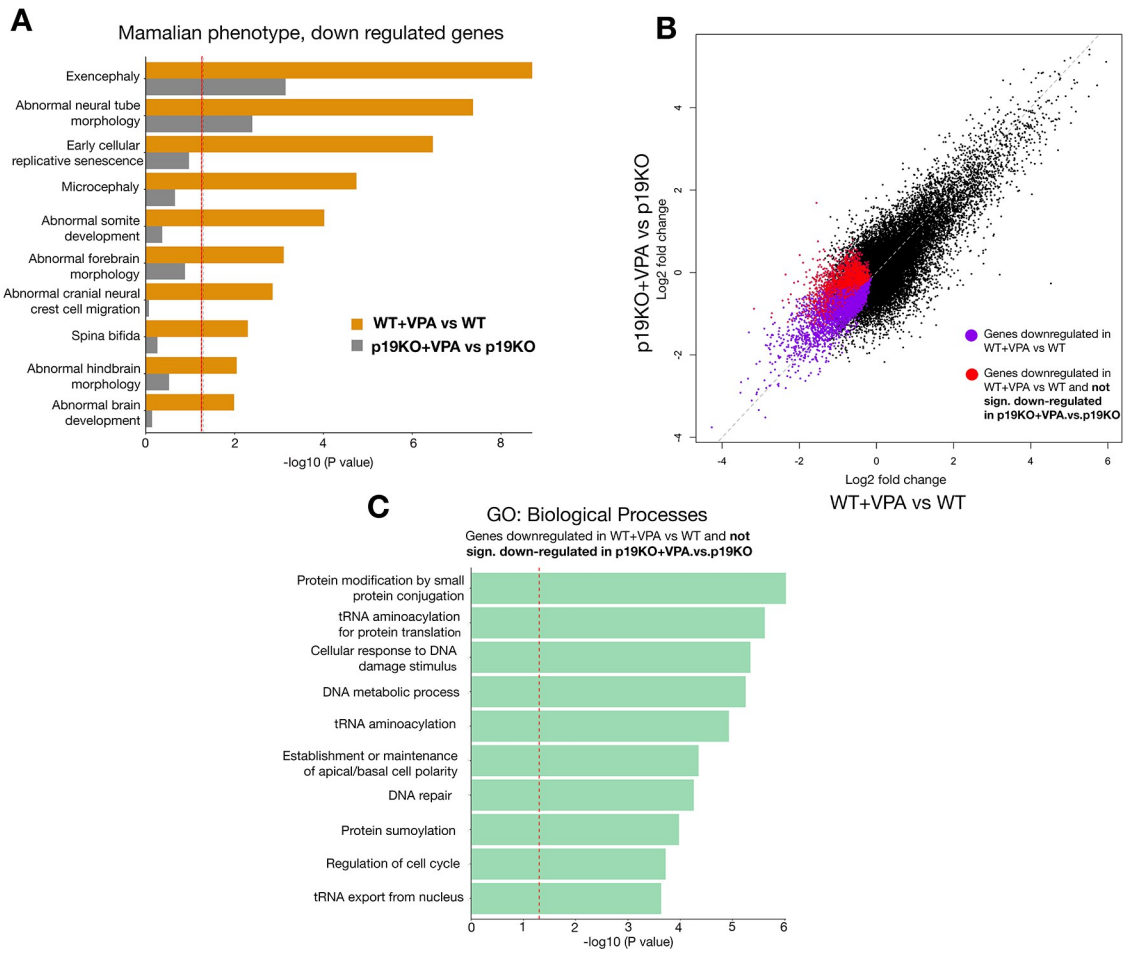

Fig 6. *p19*^{Arf} deficiency rescues VPA-induced gene signatures associated with neurodevelopmental defects. (A) Selected Mammalian Phenotype pathway analysis terms on the down-regulated genes from RNA-seq of the forebrain and midbrain **(B)** Scatter plot showing mRNA fold changes for the genes in WT+VPA compared to WT, and in p19KO + VPA compared to p19KO. **(C)** GO Biological Process pathway analysis on genes highlighted in E with red dot. The data underlying this figure can be found in S1 Data. KO, knockout; RNA-seq, RNA sequencing; VPA, valproic acid; WT, wild-type.

https://doi.org/10.1371/journal.pbio.3001664.g006

corticogenesis and neural differentiation, which is rescued in the absence of a key senescence gene. This demonstrates that this induction of senescence effectively blocks the development of the affected NE cells. As the majority of infants with problems associated with VPA exposure have cognitive defects, including developmental delay and ASD, this suggests that senescence in the NE cells could be a significant contributor to these outcomes.

This study also links aberrant senescence in the NE cells with a small-brain phenotype, characteristic of microcephaly. Indeed, microcephaly is a feature of VPA exposure in infants, and the strategy used here in mice of an acute model of VPA exposure, mimics many associated features of VPA exposure in humans [16,23]. Such high-dose acute treatment is necessary to avoid the low penetrance of developmental defects seen in mice. Of course, it is possible that this may exaggerate some of the features found in humans. However, as shown by VPA treatment of human organoids during week-long exposure, the outcome of senescence in NE cells is conserved, correlating with increased expression of *p14*^{Arf} and decreased neurogenesis. As affected human embryos are chronically exposed to the drug during development, it is possible that this would cause a lower, but longer incidence of senescence in NE cells or their

derivatives, but which may perturb differentiation in specific areas or at different stages of development, yet without always manifesting as microcephaly. Interestingly, however, there is a strong correlation between microcephaly at birth and lower cognitive ability in ASD patients [38–42], suggesting that further exploration for possible connections between mistimed senescence during development and ASD is warranted.

How VPA causes birth defects has remained unclear, but exposure during the first trimester, around the stages of neural tube closure, is suggested as being critical in driving the phenotypes associated with this drug, and with higher doses associated with increased risk [16,21,24]. Our findings identify that the drug can affect individual embryos differently, causing severe physical defects such as exencephaly in some, while causing different effects such as microcephaly in others. The reasons for this varied response remain unknown, but is likely related to cell type–specific responses. For example, while we did not detect aberrant cell death in the NE cells, apoptosis was apparent on the surface ectoderm after VPA treatment, suggesting that in some cases, VPA-induced cell death could contribute to the phenotypes. Interestingly, our study also identifies early and severe posterior neural tube and somite defects in mice, which may improve as development proceeds, as these were not as severe at E13.5. However, these were not associated with senescence, nor were they rescued in $p19^{Arf}$-deficient mice. Together, this supports that aberrant senescence may be more associated with neurodevelopmental defects, as opposed to major congenital deformations.

It might also be considered surprising that the senescence-induced phenotypes are mediated by $p19^{Arf}$, and not p21 or $p16^{Ink4a}$, the latter of which is often considered a primary mediator of adult and age-associated senescence [1,2,13]. One possibility may be because the *Ink4a/Arf* locus is directly repressed by HDACs, which contributes to the normal silencing of these genes in the embryo. However, HDACis including VPA can directly derepress this locus, and it appears that VPA has preferential ability for activating $p19^{Arf}$ over $p16^{Ink4a}$ [43,44]. In support of this association, we demonstrate that ectopic expression of $p19^{Arf}$ is sufficient and able to cause senescence, impaired neurogenesis, and developmental defects. Another possibility may relate to the timing and duration of senescence. Interestingly, in senescence induced in cells in culture, $p16^{Ink4a}$ expression often appears later in the program. Perhaps, in this case in the embryo, the senescent cells are transiently induced following VPA exposure and are ultimately cleared before expression of $p16^{Ink4a}$ can manifest. Therefore, it is possible that $p16^{Ink4a}$, or even misexpressed p21, could contribute to other developmental defects.

An outstanding question as to why there is such a restricted pattern of senescence induced in the embryo by VPA is likely related to the pattern of expression of HDAC genes. As an HDACi, VPA interferes in particular with HDACs 1 and 2. HDACs have distinct patterns of expression in the embryo, with HDAC 1 and 2 being prominent in the early brain, thereby likely making cells in this region susceptible to effects of the drug [45–47]. Furthermore, although VPA is an HDACi, which are typically associated with gene activation, we find, as did others, that the developmental phenotypes are associated with the down-regulated and not the up-regulated genes [36]. This suggests that VPA induction of $p19^{Arf}$-mediated senescence causes a broad repression of key developmental pathways, which impact NE fate and contribute to the developmental phenotypes, as many of these were rescued in the absence of $p19^{Arf}$. Among these, we identify tRNA regulation as one of the most significantly restored pathways in the absence of $p19^{Arf}$. Importantly, $p19^{Arf}$ can directly block tRNA synthesis [48], while disruption of tRNA function is strongly associated with microcephaly and neurodevelopmental disorders [37,49–53]. Interestingly, recent findings also show that induction of senescence involves disruption of tRNA expression, further reinforcing this link [54]. It will be interesting to determine whether such inhibition of tRNA function contributes to specific, or global

alterations in protein translation in senescent cells, either in VPA-induced developmental defects, or other settings.

Overall, the discovery that atypical activation of senescence in the embryo can perturb development raises the intriguing possibility that it may also contribute to defects in developmental contexts beyond those we studied here and highlights how the study of mistimed senescence in developmental disorders merits further study.

Materials and methods

Animal maintenance and VPA administration

Pregnant CD1, C57Bl6/J, *p21*–/–, $p19^{Arf}$–/–, and $p16^{Ink4a}$–/– were maintained in a temperature- and humidity-controlled animal facility with a 12-hour light/dark cycle. We administrated 400 mg/kg VPA (Sigma-Aldrich, (Missouri, USA) P4543) or PBS as control, intraperitoneally to timed-pregnant females, at E8 (3 times (9 AM, 1 PM, and 4 PM). The *p21* –/–, $p19^{Arf}$–/–, and $p16^{Ink4a}$ –/– mice were on a C57Bl6J background, so were compared to C57Bl6J wild-type as control. We observed that the C57Bl6J mice are more sensitive than the CD1 mice to induction of microcephaly. For qRT-PCR and RNA-seq analysis, only the first 2 doses were administered, and samples were collected at E8.75. All the experimental procedures were in full compliance with the institutional guidelines of the accredited IGBMC/ICS animal house, in compliance with French and EU regulations on the use of laboratory animals for research, under the supervision of Dr. Bill Keyes who holds animal experimentation authorizations from the French Ministry of Agriculture and Fisheries (#12840).

Organoids

Cerebral organoids were generated from the iPSC line HPSI0214i-kucg_2 (Catalog# 77650065, HipSci) using the STEMdiff Cerebral Organoid Kit (Catalog nos. 08570 and 08571) from STEMCELL Technologies (Vancouver, Canada). Representative pictures were acquired with a LEICA DMS 1000. We acknowledge Wellcome Trust Sanger Institute as the source of HPSI0214i-kucg_2 human induced pluripotent cell line, which was generated under the Human Induced Pluripotent Stem Cell Initiative funded by a grant from the Wellcome Trust and Medical Research Council, supported by the Wellcome Trust (WT098051) and the NIHR/Wellcome Trust Clinical Research Facility, and acknowledges Life Science Technologies Corporation as the provider of "Cyto tune." Cultures were exposed to unbuffered VPA, diluted in medium. Analysis of the medium showed no pH change in response to VPA.

Immunofluorescence

Embryos and organoids were fixed in 4% PFA for 30 minutes at 4˚C, washed in PBS, and processed for paraffin embedding. Sections were obtained using a microtome (8 μm, Leica 2035 Biocut). After antigen unmasking in citrate buffer (0.01 M, pH 6) for 15 minutes in a microwave oven, slides were blocked with 5% donkey serum, 0.1% TritonX-100 in PBS, and incubated overnight with the following primary antibodies: PHH3 (1:500, Upstate (Merck, Darmstadt, Germany) #05–806); Pax6 (1:300, Covance (New jersey, US) #PRB-278P); Tbr2 (1:300, eBioscience (Thermo Fisher Scientific, Massachusetts, USA) #14–4875); (1:300, Millipore (Massachusetts, USA), #AB2283); Sox1 (1:50, R&D Systems (Minnesota, USA) #AF3369); βIII-tubulin/Tuj1 (1:200, Covance #MMS-435P-100); $p19^{Arf}$ (5-C3-1) rat monoclonal antibody (Santa Cruz (Texas, USA) #sc-32748); and GFP 2A3 (IGBMC (Illkirch, France)). Primary antibodies were visualized by immunofluorescence using secondary antibodies from donkey (1:400, Invitrogen (California, USA): Alexa Fluor 568 donkey anti-mouse IgG #A-100037,

Alexa Fluor 488 donkey anti-rat IgG #A-21208, Alexa Fluor 488 donkey anti-rabbit #A-21206, Alexa Fluor 568 donkey anti-Goat IgG #A-11057) and from goat (1:400, Invitrogen: Alexa Fluor 568 goat anti-rabbit IgG #A-110111, Alexa Fluor 488 goat anti-mouse IgG #A11001, Alexa Fluor 568 anti-rat IgG #A11077), and cell nuclei were identified using DAPI (1:2,000). Stained sections were digitized using a slide scanner (Nanozoomer 2.0-HT, Hamamatsu, Japan), and measurements (thickness of the neuronal layer) were performed using the NDPview software of the digital scanner.

SA-β-gal staining

Whole-mount SA-β-gal was detected as previously described [10]. Incubation with X-gal was performed overnight for mouse embryos and 1 hour and 30 minutes for organoids. For determination of specific localization of senescence in embryonic tissue, embryos stained with SA-β-gal were postfixed in 4% PFA overnight at 4˚ C, embedded in paraffin and sectioned. Representative pictures were acquired using a macroscope (Leica M420) and stained sections were digitized using a slide scanner (Nanozoomer 2.0-HT, Hamamatsu).

EdU

To assess cell proliferation in embryos, pregnant female mice at E9.5 were injected intraperitoneally with 5-ethynyl-2′-deoxyuridine (EdU; 50 mg/kg body weight) for 1 hour. Click-iT EdU Alexa Fluor 488 Imaging Kit (Thermo Fisher (Massachusetts, USA)) was used as per manufacturer's protocol. Representative pictures were acquired using a microscope (DM4000B).

TUNEL

Cell death was assessed using the TdT-mediated dUTP nick end-labeling (TUNEL) method (ApopTagPeroxidase In Situ Apoptosis detection kit, Millipore) as per manufacturer's instructions. Representative pictures were acquired using a macroscope (Leica M420) and a microscope (DM4000B).

RT-qPCR and analysis

The combined forebrain and midbrain region was manually dissected from E8.75 embryos, and snap-frozen. RNA was extracted from individual embryos using the RNAeasy mini kit (QIAGEN (Hilden, Germany)). Moreover, 10 ng RNA were used for analysis with the LUNA one-step RT-qPCR kit (LUNA E3005L BioLabs (Massachusetts, USA)). The relative expression levels of the mRNA of interest were determined by real-time PCR using Quantifast SYBR Green Mix (QIAGEN) with specific primers listed in S1 Table and a LightCycler 480 (Roche (Basel, Switzerland)). Samples were run in triplicate and gene of interest expression was normalized to human Gapdh or mouse Rplp0.

In ovo electroporation

Fertilized chicken embryos were obtained from local farmers. Chick eggs were incubated in a humidified chamber at 37˚C. Moreover, 1.5 μg/μL DNA constructs (*pCAGGS-GFP* [a gift from Dr. J. Godin, IGBMC] or *pCAGGS-p19^{ARF}-GFP* [*p19^{Arf}* coding sequence was cloned in XhoI/NheI multiple cloning sites in the *pCAGGS-GFP*]) mixed with 0.05% Fast Green (Sigma-Aldrich, (Missouri, USA)) were injected into neural tubes of stage HH8 chick embryos and electroporated on the right side, leaving the left side as untreated control. Electroporation was performed using a square wave electroporator (BTX ECM 830 electroporation system) and the parameters applied: 3 pulses of 15V for 30 ms with an interval of 1 second. Embryos were

harvested 24 hours after electroporation and processed for SA-β-gal, histology and immunohistochemistry. Representative pictures were acquired using a macroscope (Leica Z16 APO) and a microscope (Leica DM4000B).

Whole-mount in situ hybridization

RNA probes were prepared by in vitro transcription using the Digoxigenin-RNA labeling mix (Roche). Template plasmids were kindly provided by Drs G. Oliver (*Six3*) and S.L. Ang (*Mox1*). Mouse embryos were dissected in ice-cold PBS and fixed O/N in 4% PFA/PBS. After several washes in PBS1X/0.1% Tween-20 (PBT), embryos were bleached for 1 hour in 3% H_2O_2/PBT and washed in PBT before being digested with Proteinase K (10mg/ml) for 2 minutes. Digestion was stopped by 5-minute incubation in 2 mg/ml glycine/PBT. Embryos were washed again in PBT before postfixing for 20 minutes in 0.2% glutaraldehyde/4% PFA/PBS. After further washes they were incubated in prewarmed hybridization buffer (50% deionized formamide, 5XSSC, 1%SDS, 100μg/ml tRNA) and prehybridized for 2 hours at 65˚C. The buffer was then replaced with fresh prewarmed hybridization buffer containing the digoxigenin labeled RNA probes and incubated O/N at 65˚C. The next day, embryos were washed twice in buffer 1 (50% formamide; 5XSSC; 1%SDS) at 65˚C then in buffer 2 (NaCl 500mM, 10mM TrisHCl pH = 7.5, 0.1%Tween20) at room temperature before treating them with RNaseA (100 mg/ml) to reduce background. The embryos were rinsed in buffer 2, then in buffer 3 (50% formamide, 2XSSC). Finally, the embryos are rinsed in TBS/0.1% Tween-20 (TBST) then blocked for 2 hours in 2% blocking solution (Roche) and incubated O/N in the same solution containing 1:2,500 anti-digoxigenin antibody (Roche). The next day, the embryos were washed in TBST, before washing them in NTMT (NaCl 100mM, Tris-HCl 100mM pH = 9,5, $MgCl_2$ 50mM, Tween20 at 0.1%) and developing the signal in the dark with staining solution (4.5 μl/ml NBT and 3.5 μl/ml BCIP (Roche) in NTMT buffer).

RNA sequencing

RNA was collected as for qRT-PCR. Full-length cDNA was generated from 10 ng of total RNA from 4 individual embryos per treatment, using Clontech SMART-Seq v4 Ultra Low Input RNA kit for Sequencing (Takara Bio Europe, Saint Germain en Laye, France) according to the manufacturer's instructions with 8 cycles of PCR for cDNA amplification by Seq-Amp polymerase. A total of 600 pg of preamplified cDNA were then used as input for Tn5 transposon tagmentation by the Nextera XT DNA Library Preparation Kit (96 samples) (Illumina, San Diego, California, USA) followed by 12 cycles of library amplification. Following purification with Agencourt AMPure XP beads (Beckman-Coulter, Villepinte, France), the size and concentration of libraries were assessed by capillary electrophoresis using the Agilent 2100 Bioanalyzer.

Sequencing was performed on an Illumina HiSeq 4000 in a 1x50bp single end format. Reads were preprocessed using cutadapt 1.10 in order to remove adaptors and low-quality sequences, and reads shorter than 40 bp were removed from further analysis. Remaining reads were mapped to Homo sapiens rRNA sequences using bowtie 2.2.8, and reads mapped to those sequences were removed from further analysis. Remaining reads were aligned to mm10 assembly of Mus musculus with STAR 2.5.3a. Gene quantification was performed with htseq-count 0.6.1p1, using "union" mode and Ensembl 101 annotations. Differential gene expression analysis was performed using DESeq2 1.16.1 Bioconductor R package on previously obtained counts (with default options). *p*-Values were adjusted for multiple testing using the Benjamini and Hochberg method. Adjusted *p*-value <0.05 was taken as statistically significant.

Pathway analysis was performed using Enrichr (http://amp.pharm.mssm.edu/Enrichr) with Gene Ontology 2018 and MGI Mammalian Phenotype Level 4 2019 databases. Adjusted *p*-value of <0.25 was used as a threshold to select the significant enrichment (Fig 6A, all terms significant in WT, with only "exencephaly," significantly enriched in p19KO (adj. <0.25): Fig 6C, all terms significant (adj. <0.25): S12 Fig, all terms significant in WT, and not in p19KO (adj. <0.25)). RNA sequencing data are available at GEO (GSE175680). All other relevant data are within the paper.

Counting and statistical analysis

For cell number quantification, positive cells for a given marker (Pax6, Sox1, Tbr2, Tuj1, and PHH3) were counted in a 100-μm wide columnar area from the VZ to the apical surface in similar regions in the cortex. Edu was counted similarly, in a 50-μm wide columnar area. Immunofluorescence analyses, area measurements, and RNA expression were statistically analyzed using Prism (GraphPad, San Diego, California, USA). At least 5 animals of each treatment from 3 different litters were analyzed. Cell counting was performed on 3 adjacent sections. Results are presented as mean ± SEM. Statistical analysis was carried out employing the Mann–Whitney test for unpaired variables. For 3 or more groups, normal multiple comparisons were tested with 1-way ANOVA plus Tukey post hoc test and nonnormal multiple comparisons were tested using Kruskal–Wallis test followed by a Dunn test. *p*-Values < 0.05 were considered significant ($^{*}p \leq 0.05$, $^{**}p \leq 0.01$, $^{***}p \leq 0.001$, and $^{****}p \leq 0.0001$).

Supporting information

S1 Fig. VPA treatment affects somite number and embryo length. (A) Quantification of visibly intact somite number (Control, $n = 27$ from 12 litters; (OB), Open brain, $n = 22$ from 10 litters; (SB) Small brain, $n = 25$ from 16 litters). Data bars represent mean ± SEM. Kruskal–Wallis test: ns, no significant and $^{***}p \leq 0.001$. **(B)** Measurements of the length of the embryo (from the otic vesicle to the tail tip) (Control, $n = 24$ from 12 litters; Open brain, $n = 22$ from 10 litters; Small brain, $n = 25$ from 16 litters. Data bars represent mean ± SEM. Kruskal–Wallis test: ns, no significant and $^{****}p \leq 0.0001$. The data underlying this figure can be found in S1 Data. VPA, valproic acid.
(TIF)

S2 Fig. VPA decreases cell proliferation. (A) Quantification of total EdU positive cells present at E9.5 (Control, n = 9 from 5 litters; Open brain, $n = 4$ from 3 litters; Small brain, $n = 5$ from 3 litters). Data bars represent mean ± SEM. Kruskal–Wallis test: $^{*}p \leq 0.05$. **(B)** Quantification of EdU positive cells in the apical zone at E9.5 (Control, $n = 9$ from 5 litters; Open brain, $n = 4$ from 3 litters; Small brain, $n = 5$ from 3 litters). Data bars represent mean ± SEM. Kruskal–Wallis test: $^{*}p \leq 0.05$ and $^{**}p \leq 0.01$. **(C)** Left: Immunostaining on sections of control and VPA-treated embryos for PHH3 (red) at E9.5. The square indicates the counted area. Scale bar, 100 μm. Right: PHH3 positive cells quantification at E9.5. (Control, $n = 4$ from 2 litters; Open brain, $n = 3$ from 3 litters; Small brain, $n = 4$ from 3 litters from 3 litters); 3 levels have been counted per embryo. Data bars represent mean ± SEM. Kruskal–Wallis test: $^{**}p \leq 0.01$ and $^{****}p \leq 0.0001$. The data underlying this figure can be found in S1 Data. E, embryonic day; PHH3, phospho-histone H3; VPA, valproic acid.
(TIF)

S3 Fig. VPA does not induce apoptosis in the forebrain neuroepithelium. Control and VPA-treated embryos were stained with whole mount TUNEL assay, to assess cell death. (Left) Lateral views and frontal views of control and VPA-treated embryos dissected at E8.5. Scale

bar, 500 μm. Corresponding horizontal sections at the forebrain level (3 embryos from at least 2 litters were analyzed). Scale bar, 100 μm. (Right) Lateral views and frontal views of control and VPA-treated embryos dissected at E9.5 (6 embryos from at least 5 litters were analyzed). Scale bar, 500 μm. Corresponding horizontal sections at the forebrain level. Scale bar, 100 μm. Some apoptotic cells are observed in the surface ectoderm. Positive cells are seen in the neural fold tips in all conditions (asterisk). E, embryonic day; ne, neuroepithelium; se, surface ectoderm; VPA, valproic acid.
(TIF)

S4 Fig. Impaired neurogenesis after VPA treatment is already observed at E10.5. Cortical sections (coronal) of E10.5 embryos were immunoassayed for Pax6, Tbr2, Tuj1, and counterstained with Dapi. Scale bar, 250 μm (top row), 50 μm. Graphs show quantification of Pax6 and Tbr2 positive progenitors or the thickness of the neuronal layer in the microcephalic cortical vesicles (5 embryos from at least 4 different mothers were analyzed). Data bars represent mean ± SEM Mann–Whitney test: $^{*}p \leq 0.05$ and $^{**}p \leq 0.01$. The data underlying this figure can be found in S1 Data. E, embryonic day; VPA, valproic acid.
(TIF)

S5 Fig. Neurogenesis is impaired in human cerebral organoids treated with VPA. Sections through control and VPA-treated organoids were immunostained with Sox1(red), Tbr2 (green), and Dapi (blue) at day 42 (scale bar, 50 μm), (n = 15 (Control), 12 (1 mM VPA), 13 (2 mM VPA), 4 independent experiments). Kruskal–Wallis test: $^{***}p \leq 0.001$ and $^{****}p \leq 0.0001$. The data underlying this figure can be found in S1 Data. VPA, valproic acid.
(TIF)

S6 Fig. Genetic deficiency of $p16^{Ink4a}$ or *p21* does not rescue VPA-induced phenotypes. Lateral views of control and VPA-treated embryos deficient for $p16^{Ink4a}$ or *p21* (top row). Scale bar, 500 μm. Higher magnification of the heads in lateral (middle row) and frontal views (bottom row). Scale bar, 500 μm. An open neural tube or a smaller brain, as well as a gross misalignment of the neural tube and somites are still observed after VPA treatment in the absence of $p16^{Ink4a}$ or *p21*. VPA, valproic acid.
(TIF)

S7 Fig. The impaired somite number and reduced length is not rescued in $p19^{Arf}$-deficient mice after VPA treatment. (A) Quantification of visibly intact somite number (WT, n = 8 embryos from 4 litters, WT+VPA, n = 30 embryos from 11 litters, p19KO, n = 14 embryos from 4 litters, p19KO + VPA, n = 17 embryos from 8 litters). Data bars represent mean ± SEM. Kruskal–Wallis test: ns, no significant, $^{*}p \leq 0.05$ and $^{****}p \leq 0.0001$. **(B)** Measurements of the length of the embryo (from the otic vesicle to the tail tip (WT, n = 8 embryos from 4 litters, WT+VPA, n = 28 embryos from 11 litters, p19KO, n = 14 embryos from 4 litters, p19KO + VPA, n = 22 embryos from 8 litters). Data bars represent mean ± SEM. Kruskal–Wallis test: ns, not significant and $^{****}p \leq 0.000$. **(C)** Lateral views (top) and dorsal views (bottom) of control and VPA-treated embryos dissected at E9.5, illustrating the pronounced curve in the neural tube and abnormally shaped somites observed (control embryo is same as shown in S6 Fig). Scale bar, 500 μm. The data underlying this figure can be found in S1 Data. E, embryonic day; VPA, valproic acid; WT, wild-type.
(TIF)

S8 Fig. Improved forebrain phenotype in $p19^{Arf}$-deficient mice after VPA treatment. Whole mount in situ hybridization for *Six3* (forebrain) and *Mox1* (somites), showing an increased size of the forebrain in $p19^{Arf}$-deficient, VPA-treated mice in comparison to the *WT*

mice treated with VPA. Scale bar, 500 μm (top row) and 50 μm (bottom row). The number of embryos examined are indicated ($n = 10$ from at least 5 different litters). VPA, valproic acid; WT, wild-type.
(TIF)

S9 Fig. Senescence is induced in the forebrain neuroepithelium in *p16*^{Ink4a}- or *p21* -deficient mice treated with VPA. Whole mount SA-β-gal staining in control and VPA-treated embryos with small-brain phenotypes at E9.5 (WT, $n = 9$ embryos from 4 litters, WT+VPA, $n = 10$ embryos from 5 litters, p16KO, $n = 2$ embryos from 1 litter, p16KO + VPA, $n = 10$ embryos from 5 litters, p21KO, $n = 6$ embryos from 3 litters, p21KO + VPA, $n = 5$ embryos from 2 litters). Scale bar, 500 μm. Higher magnification of the heads in lateral (second row) and frontal views (third row). Scale bar, 50 μm. Bottom row, Sections through whole mount SA-β-gal stained forebrains (scale bar, 100 μm). Red asterisks highlight senescent cells. (WT, $n = 5$ embryos from 3 litters, WT+VPA, $n = 10$ embryos from 5 litters, p16KO, $n = 2$ embryos from 1 litter, p16KO + VPA, $n = 10$ embryos from 5 litters, p21KO, $n = 6$ embryos from 3 litters, p21KO + VPA, $n = 5$ embryos from 2 litters). E, embryonic day; WT, wild-type.
(TIF)

S10 Fig. Senescence and SASP genes are less induced in *p19*^{Arf}-deficient embryos with VPA treatment. qRT-PCR analysis on E8.75 forebrain and midbrain, from control and *p19*^{Arf}-deficient mice, treated with VPA or left untreated. Graphs show fold change expression for the senescence markers (*p21* and *p16*^{Ink4a}) and for SASP genes (*IL6*, *IL1a*, *IL1b*, and *Pai1*), normalized to untreated control ($n = 12$ (Control), $n = 12$ (Control+VPA), $n = 20$ (*p19KO*), $n = 20$ (*p19KO*+VPA), from at least 3 different litters). Data bars represent mean ± SEM. Kruskal–Wallis test: ns, no significant, $^{**}p \leq 0.01$, $^{***}p \leq 0.001$ and $^{****}p \leq 0.0001$. The data underlying this figure can be found in S1 Data. E, embryonic day; qRT-PCR, quantitative real-time PCR; SASP, senescence-associated secretory phenotype; VPA, valproic acid.
(TIF)

S11 Fig. Ectopic expression of *p19*^{Arf}*-GFP* in the chicken neural tube. Sections through the neural tube of *p19*^{Arf}*-GFP* electroporated chicken embryos electroporated at stage HH12, immunostained for p19^{Arf} (red) and GFP (green), with Dapi counterstaining (blue). The green star shows the electroporated side. Scale bar, 100 μm.
(TIF)

S12 Fig. RNA-seq data analysis uncovers neurodevelopmental and tRNA-related signatures as being less affected by VPA treatment in *p19*^{Arf}-deficient mice. (A) GO Biological Processes pathway analysis on the down-regulated genes from RNA-seq of the forebrain and midbrain. Heat maps showing the relative expression of representative genes associated with **(B)** microcephaly (list generated from [35]), **(C)** autism (list generated from [35]) and **(D)** tRNA (list of genes identified in Fig 6C pathway analysis). The data underlying this figure can be found in S1 Data. RNA-seq, RNA sequencing; VPA, valproic acid.
(TIF)

S1 Table. Primers used for qRT-PCR in the study. qRT-PCR, quantitative real-time PCR.
(DOCX)

S1 Data. Excel spreadsheet containing, in separate sheets, the underlying numerical data for Figs 2D, 3, 4B, 4C, 4E, 4F, 5A, 5E, 5F, 6A, 6C, S1A, S1B, S2A, S2B, S2C, S4, S5A, S7A, S7B, S10, S12A, S12B, S12C and S12D.
(XLSX)

Acknowledgments

We thank Travis Stracker, Juliette Godin, Michele Studer, Pura Munoz, Birgit Ritschka, Christina Lilliehook (Life Science Editors), and members of the Keyes lab for comments on the manuscript. We thank the core facilities at the IGBMC for excellent technical support, including the Sequencing, Cell Culture and Microscopy platforms, the mouse facilities of the IGBMC and the Mouse Clinical Institute (ICS), and in particular Sylvie Falcone, Amélie Freismuth, Marion Humbert, Jean-Marie Garnier, and Olivia Wendling for technical assistance.

Author Contributions

Conceptualization: Muriel Rhinn, William M. Keyes.

Data curation: Muriel Rhinn, Irene Zapata-Bodalo.

Formal analysis: Muriel Rhinn, Irene Zapata-Bodalo, Annabelle Klein.

Funding acquisition: William M. Keyes.

Investigation: Muriel Rhinn, Annabelle Klein, Jean-Luc Plassat, Tania Knauer-Meyer, William M. Keyes.

Methodology: Muriel Rhinn, Irene Zapata-Bodalo, Annabelle Klein, Jean-Luc Plassat, Tania Knauer-Meyer.

Project administration: Muriel Rhinn, William M. Keyes.

Supervision: William M. Keyes.

Validation: Muriel Rhinn, Annabelle Klein, Jean-Luc Plassat.

Visualization: Muriel Rhinn, Irene Zapata-Bodalo.

Writing – original draft: Muriel Rhinn, William M. Keyes.

Writing – review & editing: Muriel Rhinn, Irene Zapata-Bodalo, Annabelle Klein, Jean-Luc Plassat, Tania Knauer-Meyer.

References

1. Muñoz-Espín D, Serrano M. Cellular senescence: From physiology to pathology. Nat Rev Mol Cell Biol. 2014; 15: 482–496. https://doi.org/10.1038/nrm3823 PMID: 24954210
2. Rhinn M, Ritschka B, Keyes WM. Cellular senescence in development, regeneration and disease. Dev. 2019; 146: 1–10. https://doi.org/10.1242/dev.151837 PMID: 31575608
3. Childs BG, Durik M, Baker DJ, Van Deursen JM. Cellular senescence in aging and age-related disease: From mechanisms to therapy. Nat Med. 2015; 21: 1424–1435. https://doi.org/10.1038/nm.4000 PMID: 26646499
4. Coppé JP, Patil CK, Rodier F, Sun Y, Muñoz DP, Goldstein J, et al. Senescence-associated secretory phenotypes reveal cell-nonautonomous functions of oncogenic RAS and the p53 tumor suppressor. PLoS Biol. 2008; 6. https://doi.org/10.1371/journal.pbio.0060301 PMID: 19053174
5. Ritschka B, Storer M, Mas A, Heinzmann F, Ortells MC, Morton JP, et al. The senescence-associated secretory phenotype induces cellular plasticity and tissue regeneration. Genes Dev. 2017; 31: 172–183. https://doi.org/10.1101/gad.290635.116 PMID: 28143833
6. Mosteiro L, Pantoja C, Alcazar N, Marión RM, Chondronasiou D, Rovira M, et al. Tissue damage and senescence provide critical signals for cellular reprogramming in vivo. Science. 2016; 354. https://doi.org/10.1126/science.aaf4445 PMID: 27884981
7. Demaria M, Ohtani N, Youssef SA, Rodier F, Toussaint W, Mitchell JR, et al. An essential role for senescent cells in optimal wound healing through secretion of PDGF-AA. Dev Cell. 2014; 31: 722–733. https://doi.org/10.1016/j.devcel.2014.11.012 PMID: 25499914

8. Antelo-Iglesias L, Picallos-Rabina P, Estévez-Souto V, Da Silva-Álvarez S, Collado M. The role of cellular senescence in tissue repair and regeneration. Mech Ageing Dev. 2021;198. https://doi.org/10.1016/j.mad.2021.111528 PMID: 34181964

9. Baker DJ, Petersen RC. Cellular senescence in brain aging and neurodegenerative diseases: Evidence and perspectives. J Clin Invest. 2018; 128: 1208–1216. https://doi.org/10.1172/JCI95145 PMID: 29457783

10. Storer M, Mas A, Robert-Moreno A, Pecoraro M, Ortells MC, Di Giacomo V, et al. Senescence is a developmental mechanism that contributes to embryonic growth and patterning. Cell. 2013; 155. https://doi.org/10.1016/j.cell.2013.10.041 PMID: 24238961

11. Muñoz-Espín D, Cañamero M, Maraver A, Gómez-López G, Contreras J, Murillo-Cuesta S, et al. Programmed cell senescence during mammalian embryonic development. Cell. 2013; 155: 1104. https://doi.org/10.1016/j.cell.2013.10.019 PMID: 24238962

12. Da Silva-Álvarez S, Picallos-Rabina P, Antelo-Iglesias L, Triana-Martínez F, Barreiro-Iglesias A, Sánchez L, et al. The development of cell senescence. Exp Gerontol. 2019; 128: 110742. https://doi.org/10.1016/j.exger.2019.110742 PMID: 31648013

13. Liu JY, Souroullas GP, Diekman BO, Krishnamurthy J, Hall BM, Sorrentino JA, et al. Cells exhibiting strong p16 INK4a promoter activation in vivo display features of senescence. Proc Natl Acad Sci U S A. 2019; 116: 2603–2611. https://doi.org/10.1073/pnas.1818313116 PMID: 30683717

14. Krishnamurthy J, Torrice C, Ramsey MR, Kovalev GI, Al-regaiey K, Su L, et al. Ink4a/Arf expression is a biomarker of aging. J Clin Invest. 2004; 114: 1299–1307. https://doi.org/10.1172/JCI22475 PMID: 15520862

15. Milstone ZJ, Lawson G, Trivedi CM. Histone deacetylase 1 and 2 are essential for murine neural crest proliferation, pharyngeal arch development, and craniofacial morphogenesis. Dev Dyn. 2017; 246: 1015–1026. https://doi.org/10.1002/dvdy.24563 PMID: 28791750

16. Clayton-Smith J, Bromley R, Dean J, Journel H, Odent S, Wood A, et al. Diagnosis and management of individuals with Fetal Valproate Spectrum Disorder; a consensus statement from the European Reference Network for Congenital Malformations and Intellectual Disability. Orphanet J Rare Dis. 2019; 14: 1–21. https://doi.org/10.1186/s13023-019-1064-y

17. Jentink J, Loane MA, Dolk H, Barisic I, Garne E, Morris JK, et al. Valproic acid monotherapy in pregnancy and major congenital malformations. N Engl J Med. 2010; 362: 2185–93. https://doi.org/10.1056/NEJMoa0907328 PMID: 20558369

18. Margulis A V., Hernandez-Diaz S, McElrath T, Rothman KJ, Plana E, Almqvist C, et al. Relation of in-utero exposure to antiepileptic drugs to pregnancy duration and size at birth. PLoS ONE. 2019; 14: e0214180. https://doi.org/10.1371/journal.pone.0214180 PMID: 31381574

19. Meador KJ, Baker GA, Browning N, Cohen MJ, Bromley RL, Clayton-Smith J, et al. Fetal antiepileptic drug exposure and cognitive outcomes at age 6 years (NEAD study): A prospective observational study. Lancet Neurol. 2013; 12: 244–252. https://doi.org/10.1016/S1474-4422(12)70323-X PMID: 23352199

20. Christensen J, Grønborg TK, Sørensen MJ, Schendel D, Parner ET, Pedersen LH. Prenatal valproate exposure and risk of autism spectrum disorders and childhood autism. JAMA. 2013; 309: 1696–1703. https://doi.org/10.1001/jama.2013.2270 PMID: 23613074

21. Roullet FI, Lai JKY, Foster JA. In utero exposure to valproic acid and autism—A current review of clinical and animal studies. Neurotoxicol Teratol. 2013; 36: 47–56. https://doi.org/10.1016/j.ntt.2013.01.004 PMID: 23395807

22. Varghese M, Keshav N, Jacot-Descombes S, Warda T, Wicinski B, Dickstein DL, et al. Autism spectrum disorder: neuropathology and animal models. Acta Neuropathol. 2017; 134: 537–566. https://doi.org/10.1007/s00401-017-1736-4 PMID: 28584888

23. Nicolini C, Fahnestock M. The valproic acid-induced rodent model of autism. Exp Neurol. 2018; 299: 217–227. https://doi.org/10.1016/j.expneurol.2017.04.017 PMID: 28472621

24. Zhao H, Wang Q, Yan T, Zhang Y, Xu H-j, Yu H-p, et al. Maternal valproic acid exposure leads to neurogenesis defects and autism-like behaviors in non-human primates. Transl Psychiatry. 2019; 9: 1–13. https://doi.org/10.1038/s41398-019-0608-1

25. Chenn A, McConnell SK. Cleavage Orientation and the Asymmetric Inheritance of Notch1 Immunoreactivity in Mammalian Neurogenesis. Cell. 1995; 82: 631–641. https://doi.org/10.1016/0092-8674(95)90035-7 PMID: 7664342

26. Götz M, Huttner WB. The cell biology of neurogenesis. Nat Rev Mol Cell Biol. 2005; 6: 777–788. https://doi.org/10.1038/nrm1739 PMID: 16314867

27. Noctor SC, Martinez-Cerdeño V, Ivic L, Kriegstein AR. Cortical neurons arise in symmetric and asymmetric division zones and migrate through specific phases. Nat Neurosci. 2004; 7: 136–144. https://doi.org/10.1038/nn1172 PMID: 14703572

28. Miyata T, Kawaguchi A, Okano H, Ogawa M. Asymmetric inheritance of radial glial fibers by cortical neurons. Neuron. 2001; 31: 727–741. https://doi.org/10.1016/s0896-6273(01)00420-2 PMID: 11567613

29. Moldrich RX, Leanage G, She D, Dolan-Evans E, Nelson M, Reza N, et al. Inhibition of histone deacetylase in utero causes sociability deficits in postnatal mice. Behav Brain Res. 2013; 257: 253–264. https://doi.org/10.1016/j.bbr.2013.09.049 PMID: 24103642

30. Li XN, Shu Q, Su JMF, Perlaky L, Blaney SM, Lau CC. Valproic acid induces growth arrest, apoptosis, and senescence in medulloblastomas by increasing histone hyperacetylation and regulating expression of p21Cip1, CDK4, and CMYC. Mol Cancer Ther. 2005; 4: 1912–1922. https://doi.org/10.1158/1535-7163.MCT-05-0184 PMID: 16373706

31. Ehlers K, Sturje H, Merker HJ, Nau H. Vaproic acid-induced spina bifida: a mouse model. Teratology. 1992; 45: 145–154. https://doi.org/10.1002/tera.1420450208 PMID: 1377411

32. Nau H, Hauck R-S, Ehlers K. Valproic Acid-Induced Neural Tube Defects in Mouse and Human: Aspects of Chirality, Alternative Drug Development, Pharmacokinetics and Possible Mechanisms. Pharmacol Toxicol. 1991; 69: 310–321. https://doi.org/10.1111/j.1600-0773.1991.tb01303.x PMID: 1803343

33. Lancaster MA, Renner M, Martin CA, Wenzel D, Bicknell LS, Hurles ME, et al. Cerebral organoids model human brain development and microcephaly. Nature. 2013; 501: 373–379. https://doi.org/10.1038/nature12517 PMID: 23995685

34. Kwan V, Unda BK, Singh KK. Wnt signaling networks in autism spectrum disorder and intellectual disability. J Neurodev Disord. 2016; 8: 1–10. https://doi.org/10.1186/s11689-016-9176-3

35. Jayaraman D, Bae B II, Walsh CA. The genetics of primary microcephaly. Annu Rev Genomics Hum Genet. 2018; 19: 177–200. https://doi.org/10.1146/annurev-genom-083117-021441 PMID: 29799801

36. Takata A, Miyake N, Tsurusaki Y, Fukai R, Miyatake S, Koshimizu E, et al. Integrative Analyses of De Novo Mutations Provide Deeper Biological Insights into Autism Spectrum Disorder. Cell Rep. 2018; 22: 734–747. https://doi.org/10.1016/j.celrep.2017.12.074 PMID: 29346770

37. Schaffer AE, Pinkard O, Coller JM. TRNA Metabolism and Neurodevelopmental Disorders. Annu Rev Genomics Hum Genet. 2019; 20: 359–387. https://doi.org/10.1146/annurev-genom-083118-015334 PMID: 31082281

38. Mraz KD, Green J, Dumont-mathieu T, Makin S, Fein D. Correlates of Head Circumference Growth. J Child Neurol. 2007; 7–9. https://doi.org/10.1177/0883073807304005 PMID: 17641255

39. Zachor DA, Ben-Itzchak E. Specific medical conditions are associated with unique behavioral profiles in autism spectrum disorders. Front Neurosci. 2016; 10: 1–11. https://doi.org/10.3389/fnins.2016.00410

40. Courchesne E, Carper R, Akshoomoff N. Evidence of Brain Overgrowth in the First Year of Life in Autism. J Am Med Assoc. 2003; 290: 337–344. https://doi.org/10.1001/jama.290.3.337 PMID: 12865374

41. Fombonne E, Rogé B, Claverie J, Courty S, Frémolle J. Microcephaly and macrocephaly in autism. J Autism Dev Disord. 1999; 29: 113–119. https://doi.org/10.1023/a:1023036509476 PMID: 10382131

42. Courchesne E, Pierce K, Schumann CM, Redcay E, Buckwalter JA, Kennedy DP, et al. Mapping early brain development in autism. Neuron. 2007; 56: 399–413. https://doi.org/10.1016/j.neuron.2007.10.016 PMID: 17964254

43. Matheu A, Klatt P, Serrano M. Regulation of the INK4a/ARF locus by histone deacetylase inhibitors. J Biol Chem. 2005; 280: 42433–42441. https://doi.org/10.1074/jbc.M508270200 PMID: 16251190

44. Soriano-Cantón R, Perez-Villalba A, Morante-Redolat JM, Marqués-Torrejón MÁ, Pallás M, Pérez-Sánchez F, et al. Regulation of the p19Arf/p53 pathway by histone acetylation underlies neural stem cell behavior in senescence-prone SAMP8 mice. Aging Cell. 2015; 14: 453–462. https://doi.org/10.1111/acel.12328 PMID: 25728253

45. Murko C, Lagger S, Steiner M, Seiser C, Schoefer C, Pusch O. Expression of class I histone deacetylases during chick and mouse development. Int J Dev Biol. 2010; 54: 1527–1537. https://doi.org/10.1387/ijdb.092971cm PMID: 20979029

46. D'Mello SR. Regulation of Central Nervous System Development by Class i Histone Deacetylases. Dev Neurosci. 2020; 75275: 149–165. https://doi.org/10.1159/000505535 PMID: 31982872

47. Jaworska J, Ziemka-Nalecz M, Zalewska T. Histone deacetylases 1 and 2 are required for brain development. Int J Dev Biol. 2015; 59: 171–177. https://doi.org/10.1387/ijdb.150071tz PMID: 26198144

48. Morton JP, Kantidakis T, White RJ. RNA polymerase III transcription is repressed in response to the tumour suppressor ARF. Nucleic Acids Res. 2007; 35: 3046–3052. https://doi.org/10.1093/nar/gkm208 PMID: 17439968

49. Wang L, Li Z, Sievert D, Smith DEC, Mendes MI, Chen DY, et al. Loss of NARS1 impairs progenitor proliferation in cortical brain organoids and leads to microcephaly. Nat Commun. 2020; 11: 1–12. https://doi.org/10.1038/s41467-020-17454-4

50. Hoye ML, Silver DL. Decoding mixed messages in the developing cortex: translational regulation of neural progenitor fate. Curr Opin Neurobiol. 2021; 66: 93–102. https://doi.org/10.1016/j.conb.2020.10.001 PMID: 33130411

51. Kuo ME, Theil AF, Kievit A, Malicdan MC, Introne WJ, Christian T, et al. Cysteinyl-tRNA Synthetase Mutations Cause a Multi-System, Recessive Disease That Includes Microcephaly, Developmental Delay, and Brittle Hair and Nails. Am J Hum Genet. 2019; 104: 520–529. https://doi.org/10.1016/j.ajhg.2019.01.006 PMID: 30824121

52. Zhang X, Ling J, Barcia G, Jing L, Wu J, Barry BJ, et al. Mutations in QARS, encoding glutaminyl-trna synthetase, cause progressive microcephaly, cerebral-cerebellar atrophy, and intractable seizures. Am J Hum Genet. 2014; 94: 547–558. https://doi.org/10.1016/j.ajhg.2014.03.003 PMID: 24656866

53. Blanco S, Dietmann S, Flores J V, Hussain S, Kutter C, Humphreys P, et al. Aberrant methylation of t RNA s links cellular stress to neuro-developmental disorders. EMBO J. 2014; 33: 2020–2039. https://doi.org/10.15252/embj.201489282 PMID: 25063673

54. Guillon J, Toutain B, Boissard A, Guette C, Coqueret O. tRNA biogenesis and specific Aminoacyl-tRNA Synthetases regulate senescence stability under the control of mTOR. bioRxiv Prepr Serv Biol. 2020. https://doi.org/10.1101/2020.04.30.068114

Supp. Fig. 1. VPA treatment affects somite number and embryo length.
(A) Quantification of visibly intact somite number (Control, $n = 27$ from 12 litters; (OB), Open brain, $n = 22$ from 10 litters; (SB) Small brain, $n = 25$ from 16 litters). Data bars represent mean ± SEM. Kruskal–Wallis test: ns, no significant and ***$p \leq 0.001$. **(B)** Measurements of the length of the embryo (from the otic vesicle to the tail tip) (Control, $n = 24$ from 12 litters; Open brain, $n = 22$ from 10 litters; Small brain, $n = 25$ from 16 litters. Data bars represent mean ± SEM. Kruskal–Wallis test: ns, no significant and ****$p \leq 0.0001$. The data underlying this figure can be found in S1 Data. VPA, valproic acid.
https://doi.org/10.1371/journal.pbio.3001664.s001

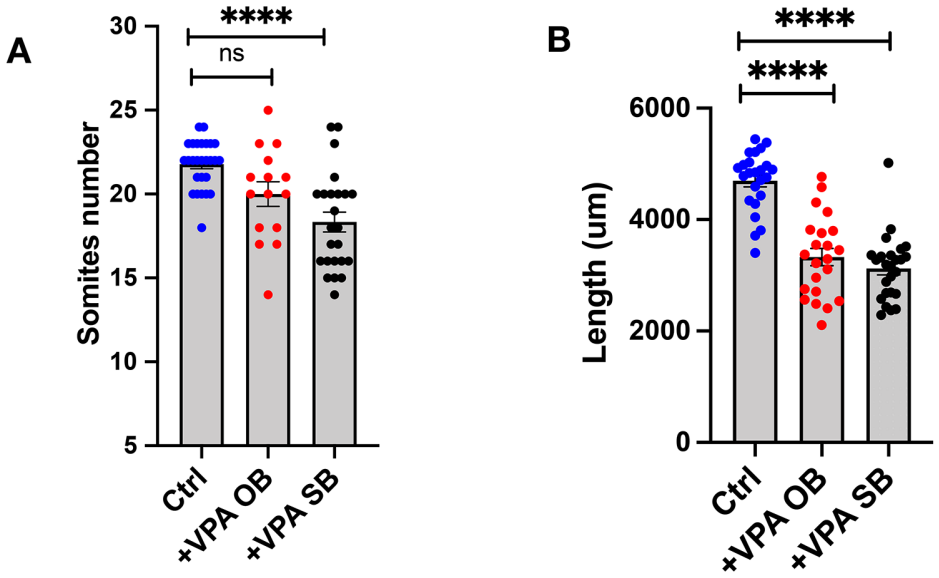

Supp. Fig. 2. VPA decreases cell proliferation.
(A) Quantification of total EdU positive cells present at E9.5 (Control, n = 9 from 5 litters; Open brain, *n* = 4 from 3 litters; Small brain, *n* = 5 from 3 litters). Data bars represent mean ± SEM. Kruskal–Wallis test: **p* ≤ 0.05. **(B)** Quantification of EdU positive cells in the apical zone at E9.5 (Control, *n* = 9 from 5 litters; Open brain, *n* = 4 from 3 litters; Small brain, *n* = 5 from 3 litters). Data bars represent mean ± SEM. Kruskal–Wallis test: **p* ≤ 0.05 and ***p* ≤ 0.01. **(C)** Left: Immunostaining on sections of control and VPA-treated embryos for PHH3 (red) at E9.5. The square indicates the counted area. Scale bar, 100 μm. Right: PHH3 positive cells quantification at E9.5. (Control, *n* = 4 from 2 litters; Open brain, *n* = 3 from 3 litters; Small brain, *n* = 4 from 3 litters from 3 litters); 3 levels have been counted per embryo. Data bars represent mean ± SEM. Kruskal–Wallis test: ***p* ≤ 0.01 and *****p* ≤ 0.0001. The data underlying this figure can be found in S1 Data. E, embryonic day; PHH3, phospho-histone H3; VPA, valproic acid.
https://doi.org/10.1371/journal.pbio.3001664.s002

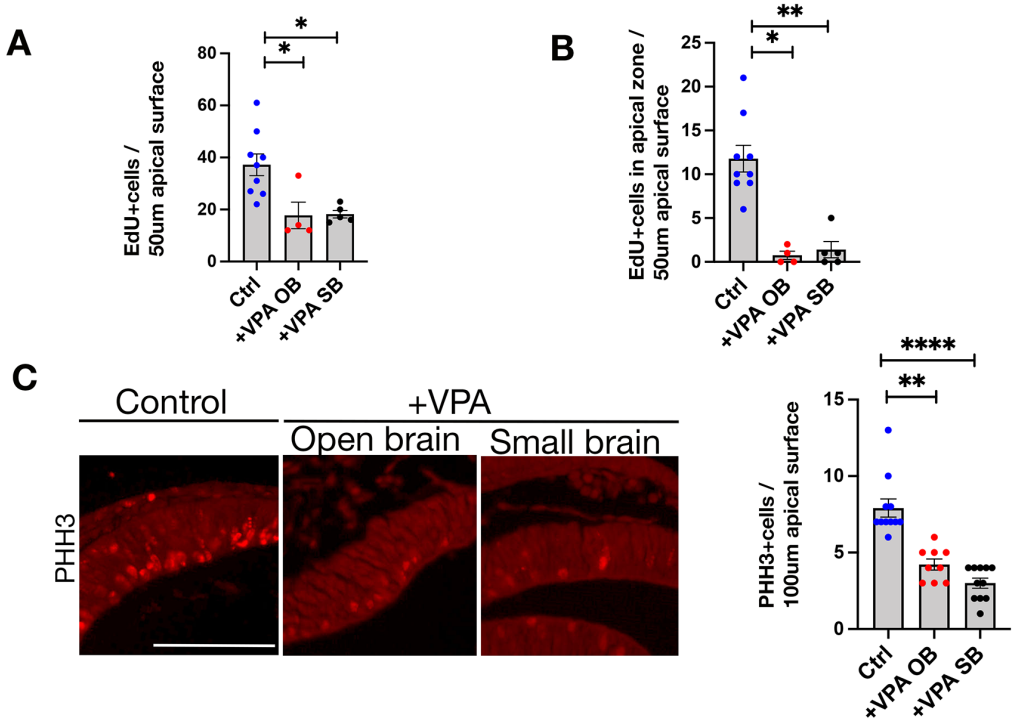

Supp. Fig. 3. VPA does not induce apoptosis in the forebrain neuroepithelium.
Control and VPA-treated embryos were stained with whole mount TUNEL assay, to assess cell death. (Left) Lateral views and frontal views of control and VPA-treated embryos dissected at E8.5. Scale bar, 500 μm. Corresponding horizontal sections at the forebrain level (3 embryos from at least 2 litters were analyzed). Scale bar, 100 μm. (Right) Lateral views and frontal views of control and VPA-treated embryos dissected at E9.5 (6 embryos from at least 5 litters were analyzed). Scale bar, 500 μm. Corresponding horizontal sections at the forebrain level. Scale bar, 100 μm. Some apoptotic cells are observed in the surface ectoderm. Positive cells are seen in the neural fold tips in all conditions (asterisk). E, embryonic day; ne, neuroepithelium; se, surface ectoderm; VPA, valproic acid.
https://doi.org/10.1371/journal.pbio.3001664.s003

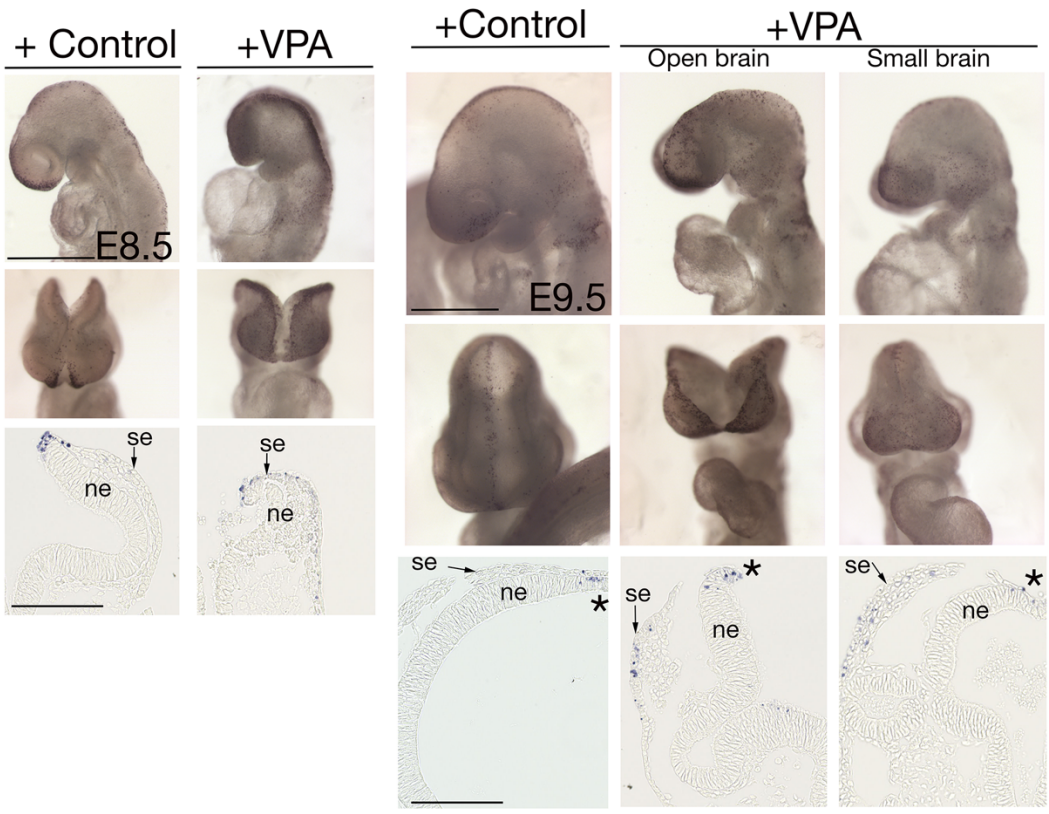

Supp. Fig. 4. Impaired neurogenesis after VPA treatment is already observed at E10.5. Cortical sections (coronal) of E10.5 embryos were immunoassayed for Pax6, Tbr2, Tuj1, and counterstained with Dapi. Scale bar, 250 μm (top row), 50 μm. Graphs show quantification of Pax6 and Tbr2 positive progenitors or the thickness of the neuronal layer in the microcephalic cortical vesicles (5 embryos from at least 4 different mothers were analyzed). Data bars represent mean ± SEM Mann–Whitney test: *$p \leq 0.05$ and **$p \leq 0.01$. The data underlying this figure can be found in S1 Data. E, embryonic day; VPA, valproic acid.
https://doi.org/10.1371/journal.pbio.3001664.s004

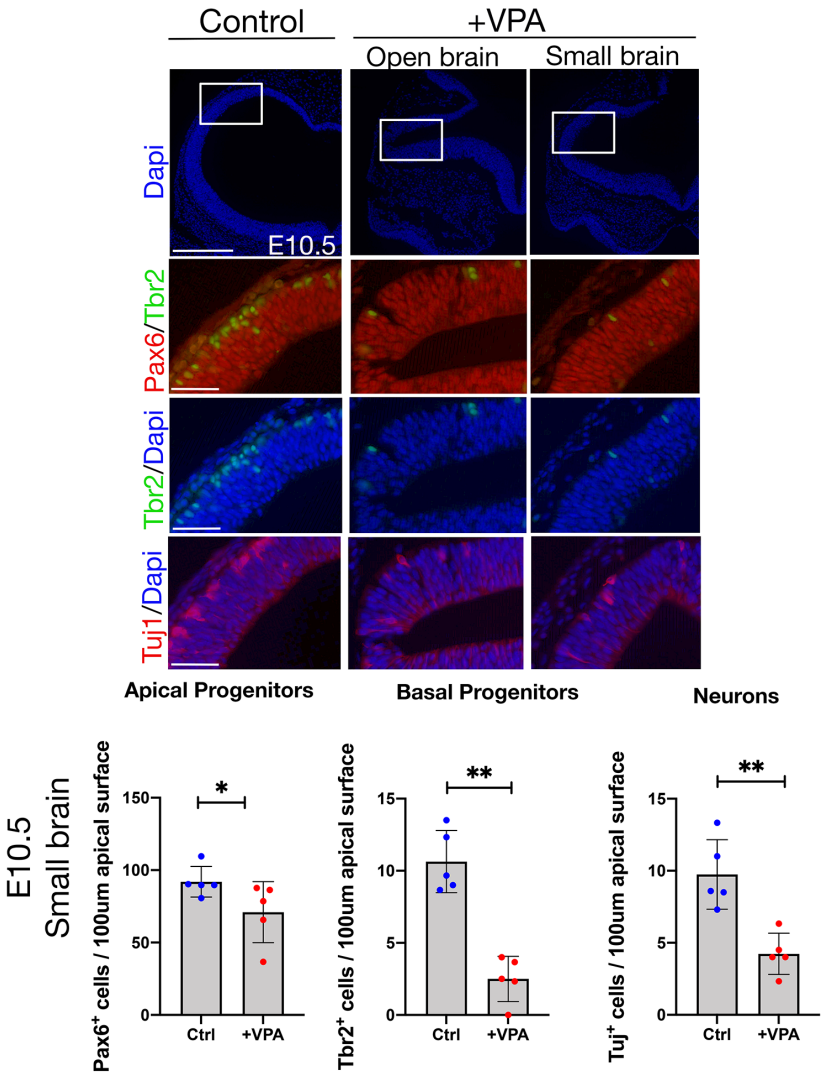

Supp. Fig. 5. Neurogenesis is impaired in human cerebral organoids treated with VPA. Sections through control and VPA-treated organoids were immunostained with Sox1(red), Tbr2 (green), and Dapi (blue) at day 42 (scale bar, 50 μm), (n = 15 (Control), 12 (1 mM VPA), 13 (2 mM VPA), 4 independent experiments). Kruskal–Wallis test: ***$p \leq 0.001$ and ****$p \leq 0.0001$. The data underlying this figure can be found in S1 Data. VPA, valproic acid.
https://doi.org/10.1371/journal.pbio.3001664.s005

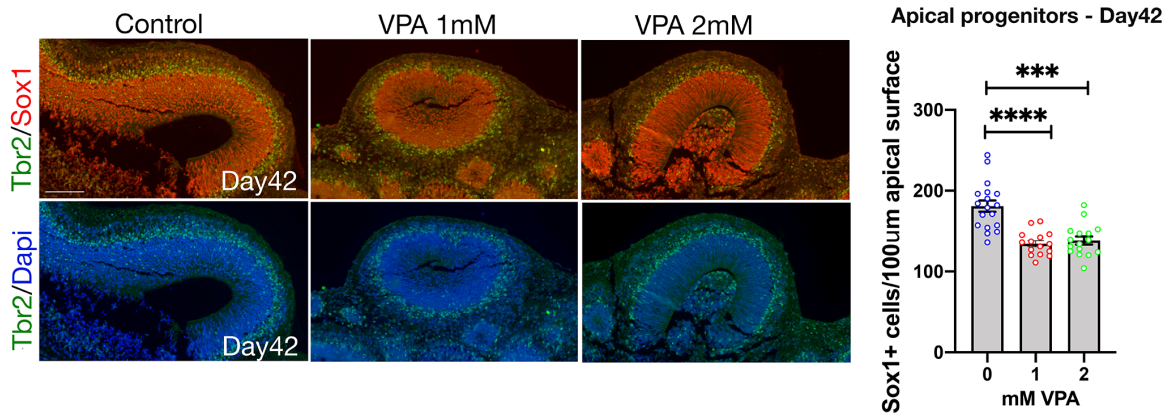

Supp. Fig. 6 Genetic deficiency of *p16^{Ink4a}* or *p21* does not rescue VPA-induced phenotypes. Lateral views of control and VPA-treated embryos deficient for *p16^{Ink4a}* or *p21* (top row). Scale bar, 500 μm. Higher magnification of the heads in lateral (middle row) and frontal views (bottom row). Scale bar, 500 μm. An open neural tube or a smaller brain, as well as a gross misalignment of the neural tube and somites are still observed after VPA treatment in the absence of *p16^{Ink4a}* or *p21*. VPA, valproic acid.
https://doi.org/10.1371/journal.pbio.3001664.s006

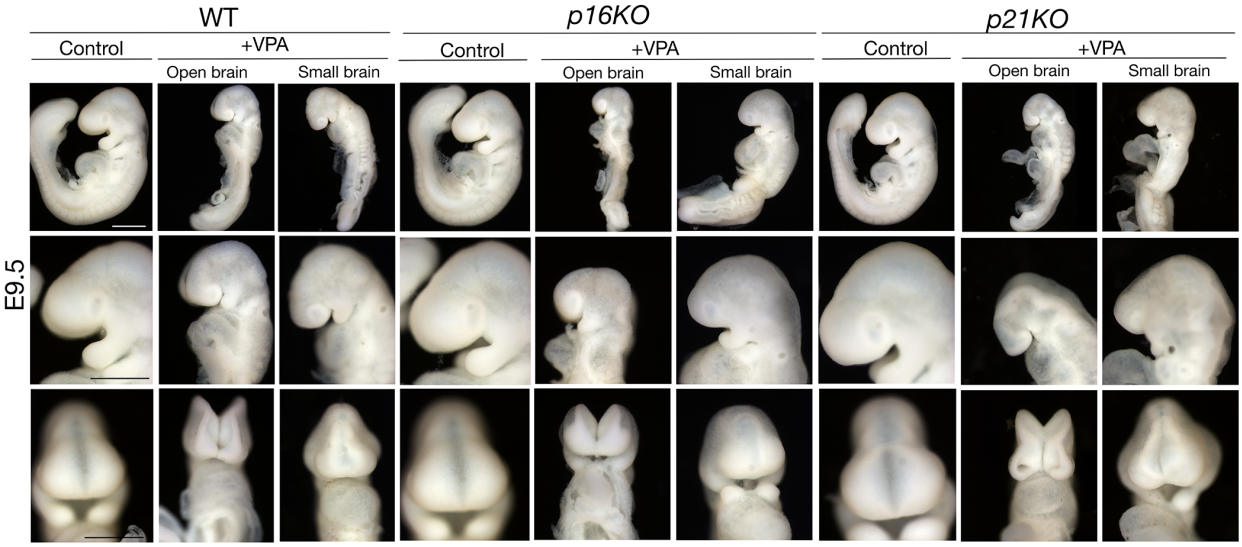

Supp. Fig. 7. The impaired somite number and reduced length is not rescued in *p19*^{Arf}-deficient mice after VPA treatment.

(A) Quantification of visibly intact somite number (WT, *n* = 8 embryos from 4 litters, WT+VPA, *n*= 30 embryos from 11 litters, p19KO, *n* = 14 embryos from 4 litters, p19KO + VPA, *n* = 17 embryos from 8 litters). Data bars represent mean ± SEM. Kruskal–Wallis test: ns, no significant, **p* ≤ 0.05 and *****p* ≤ 0.0001. **(B)** Measurements of the length of the embryo (from the otic vesicle to the tail tip (WT, *n* = 8 embryos from 4 litters, WT+VPA, *n* = 28 embryos from 11 litters, p19KO, *n* = 14 embryos from 4 litters, p19KO + VPA, *n* = 22 embryos from 8 litters). Data bars represent mean ± SEM. Kruskal–Wallis test: ns, not significant and *****p* ≤ 0.000. **(C)**Lateral views (top) and dorsal views (bottom) of control and VPA-treated embryos dissected at E9.5, illustrating the pronounced curve in the neural tube and abnormally shaped somites observed (control embryo is same as shown in S6 Fig). Scale bar, 500 μm. The data underlying this figure can be found in S1 Data. E, embryonic day; VPA, valproic acid; WT, wild-type.

https://doi.org/10.1371/journal.pbio.3001664.s007

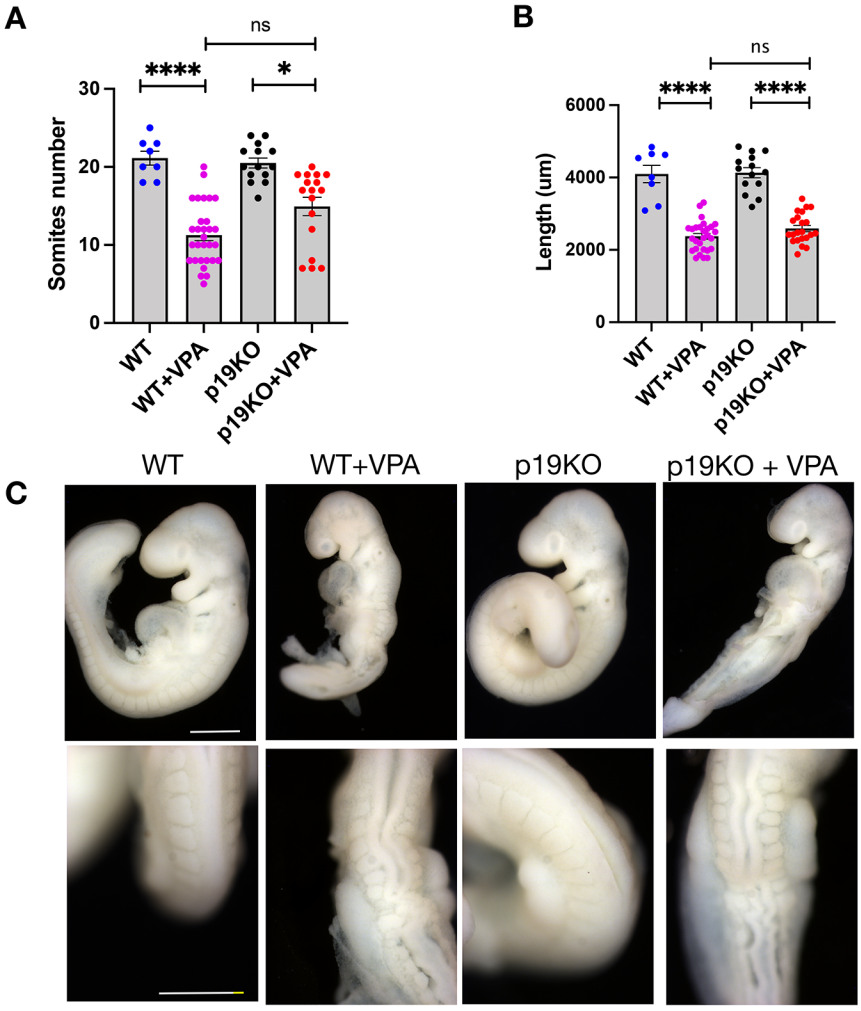

Supp. Fig. 8. Improved forebrain phenotype in *p19*^{Arf}-deficient mice after VPA treatment. Whole mount in situ hybridization for *Six3* (forebrain) and *Mox1* (somites), showing an increased size of the forebrain in *p19*^{Arf}-deficient, VPA-treated mice in comparison to the *WT*mice treated with VPA. Scale bar, 500 μm (top row) and 50 μm (bottom row). The number of embryos examined are indicated (*n* = 10 from at least 5 different litters). VPA, valproic acid; WT, wild-type.
https://doi.org/10.1371/journal.pbio.3001664.s008

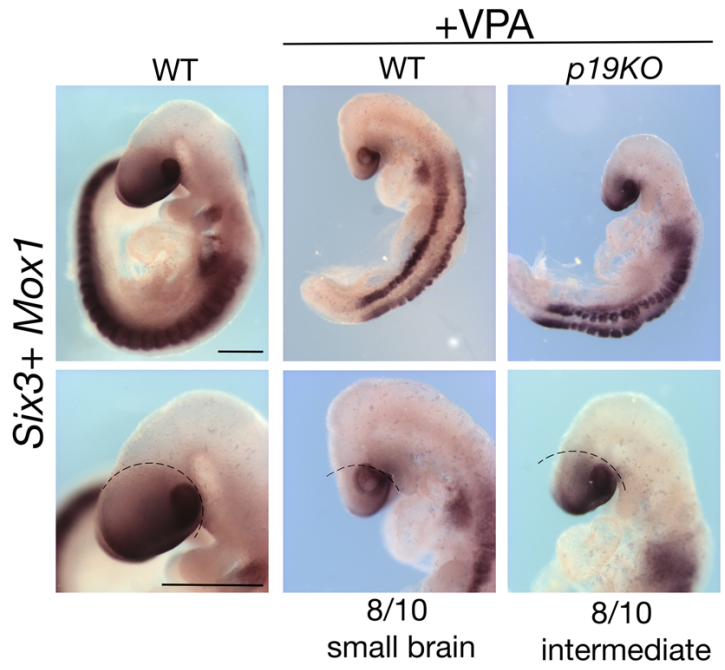

Supp. Fig. 9. Senescence is induced in the forebrain neuroepithelium in *p16*^{Ink4a}- or *p21*-deficient mice treated with VPA.
Whole mount SA-β-gal staining in control and VPA-treated embryos with small-brain phenotypes at E9.5 (WT, *n* = 9 embryos from 4 litters, WT+VPA, *n* = 10 embryos from 5 litters, p16KO, *n* = 2 embryos from 1 litter, p16KO + VPA, *n* = 10 embryos from 5 litters, p21KO, *n* = 6 embryos from 3 litters, p21KO + VPA, *n* = 5 embryos from 2 litters). Scale bar, 500 μm. Higher magnification of the heads in lateral (second row) and frontal views (third row). Scale bar, 50 μm. Bottom row, Sections through whole mount SA-β-gal stained forebrains (scale bar, 100 μm). Red asterisks highlight senescent cells. (WT, *n* = 5 embryos from 3 litters, WT+VPA, *n* = 10 embryos from 5 litters, p16KO, *n* = 2 embryos from 1 litter, p16KO + VPA, *n* = 10 embryos from 5 litters, p21KO, *n* = 6 embryos from 3 litters, p21KO + VPA, *n* = 5 embryos from 2 litters). E, embryonic day; WT, wild-type.
https://doi.org/10.1371/journal.pbio.3001664.s009

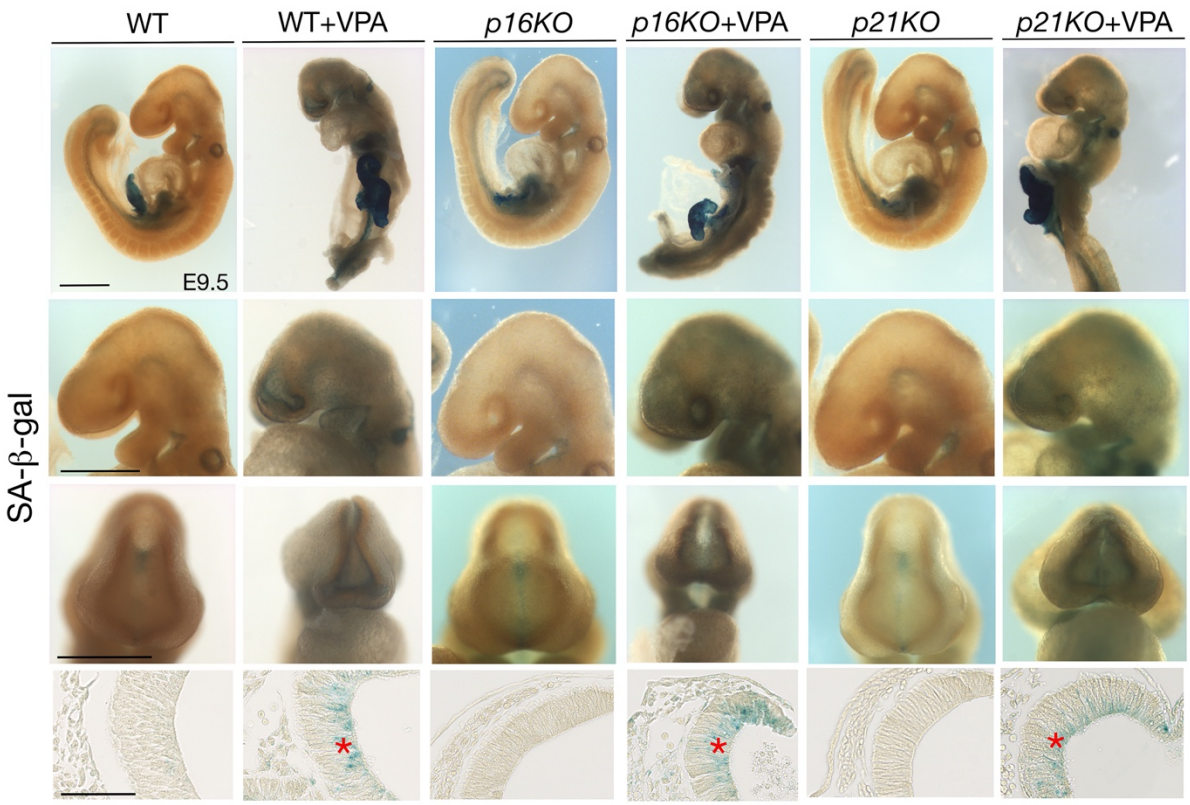

Supp. Fig. 10. Senescence and SASP genes are less induced in *p19*^{Arf}-deficient embryos with VPA treatment.
qRT-PCR analysis on E8.75 forebrain and midbrain, from control and *p19*^{Arf}-deficient mice, treated with VPA or left untreated. Graphs show fold change expression for the senescence markers (*p21* and *p16*^{Ink4a}) and for SASP genes (*IL6*, *IL1a*, *IL1b*, and *Pai1*), normalized to untreated control ($n = 12$ (Control), $n = 12$ (Control+VPA), $n = 20$ (*p19KO*), $n = 20$ (*p19KO*+VPA), from at least 3 different litters). Data bars represent mean ± SEM. Kruskal–Wallis test: ns, no significant, $^{**}p \leq 0.01$, $^{***}p \leq 0.001$ and $^{****}p \leq 0.0001$. The data underlying this figure can be found in S1 Data. E, embryonic day; qRT-PCR, quantitative real-time PCR; SASP, senescence-associated secretory phenotype; VPA, valproic acid.
https://doi.org/10.1371/journal.pbio.3001664.s010

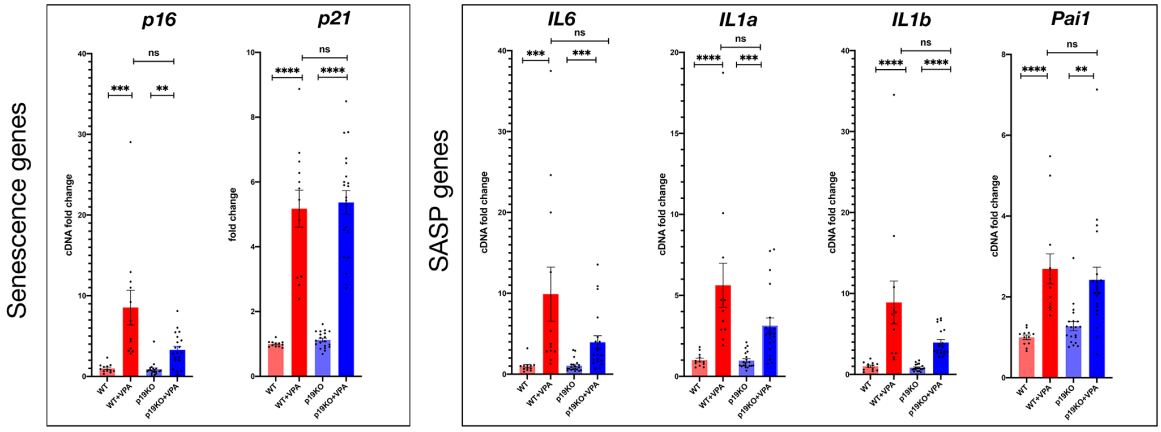

Supp. Fig. 11. Ectopic expression of *p19*^{Arf}*-GFP* in the chicken neural tube.
Sections through the neural tube of *p19*^{Arf}*-GFP* electroporated chicken embryos electroporated at stage HH12, immunostained for p19^{Arf} (red) and GFP (green), with Dapi counterstaining (blue). The green star shows the electroporated side. Scale bar, 100 μm.
https://doi.org/10.1371/journal.pbio.3001664.s011

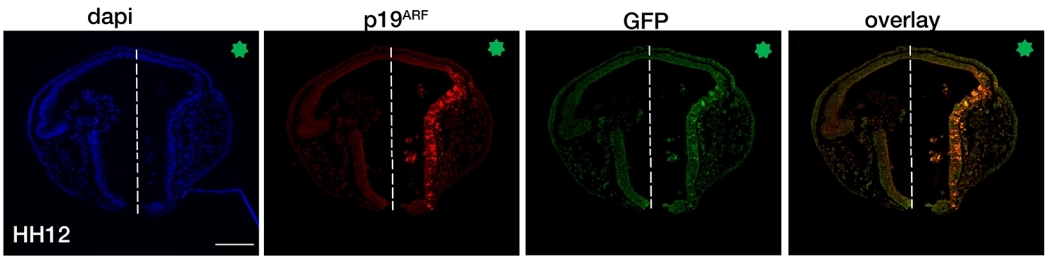

Supp. Fig. 12. RNA-seq data analysis uncovers neurodevelopmental and tRNA-related signatures as being less affected by VPA treatment in *p19*^{Arf}-deficient mice.
(A) GO Biological Processes pathway analysis on the down-regulated genes from RNA-seq of the forebrain and midbrain. Heat maps showing the relative expression of representative genes associated with **(B)** microcephaly (list generated from [35]), **(C)** autism (list generated from [35]) and **(D)** tRNA (list of genes identified in Fig 6C pathway analysis). The data underlying this figure can be found in S1 Data. RNA-seq, RNA sequencing; VPA, valproic acid.
https://doi.org/10.1371/journal.pbio.3001664.s012

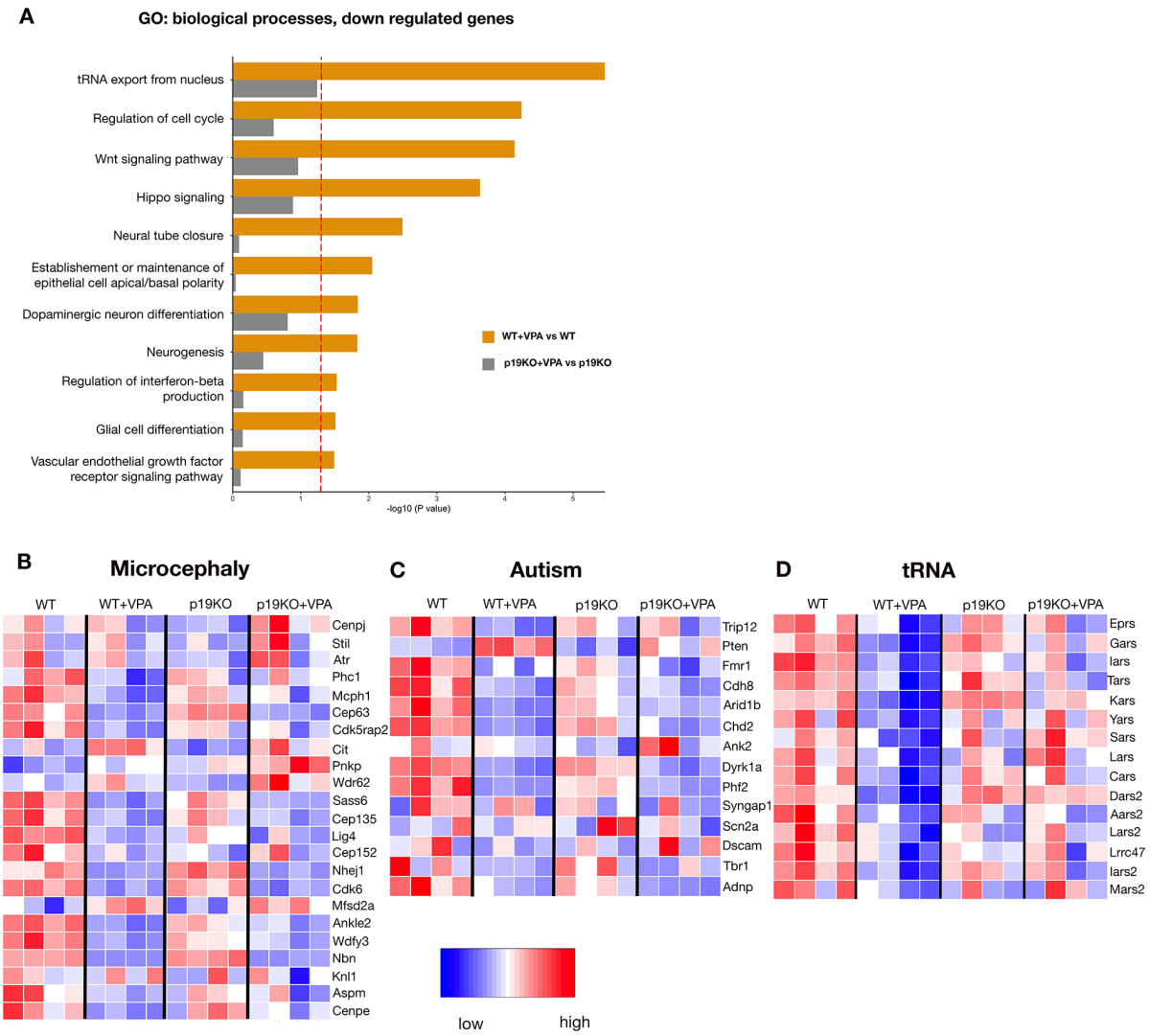

Supp. Tab. 1. Primers used for qRT-PCR in the study. qRT-PCR, quantitative real-time PCR. The table lists the primer sequences or source for both human and mouse genes used in the study.
https://doi.org/10.1371/journal.pbio.3001664.s013

Human primers	**Sequence**
GAPDH-fwd	AAGGTGAAGGTCGGAGTCAAC
GAPDH-rev	GGGGTCATTGATGGCAACAATA
$p14^{ARF}$-fwd	CTGATGCTACTGAGGAGCCA
$p14^{ARF}$-rev	TCATGACCTGGTCTTCTAGG
p16INK4A-fwd	GGTCGGAGGCCGATCCAGGTCA
p16INK4A-rev	TTCAATCGGGGATGTCTGAGG
p21-fwd	CGAAGTCAGTTCCTTGTGGAG
p21-rev	CATGGGTTCTGACGGACAT
IL1a-fwd	ACTGCCCAAGATGAAGACCAA
IL1a-rev	CCGTGAGTTTCCCAGAAGAAGA
IL1b-fwd	TTCGACACATGGGATAACGAGG
IL1b-rev	TTTTTGCTGTGAGTCCCGGAG
IL8-fwd	ACTGAGAGTGATTGAGAGTGGAC
IL8-rev	AACCCTCTGCACCCAGTTTTC
PAI1-fwd	AAGATCGAGGTGAACGAGAGTG
PAI1-rev	GACCACAAAGAGGAAGGGTCT
Mouse primers	**Sequence**
Rplp0	QT00249375(QIAGEN)
$P19^{Arf}$	QT01164891 (QIAGEN)
$p16^{Ink4a}$	QT01164898(QIAGEN)
p21	QT00137053(QIAGEN)
Il1a-fwd	GCACCTTACACCTACCAGAGT
Il1a-rev	AAACTTCTGCCTGACGAGCTT
Il1b-fwd	TTCAGGCAGGCAGTATCACTC
Il1b-rev	GAAGGTCCACGGGAAAGACAC
Il6-fwd	TAGTCCTTCCTACCCCAATTTCC
Il6-rev	TTGGTCCTTAGCCACTCCTTC
Pai1-fwd	TGGGTGGAAAGGCATACCAAA
Pai1-rev	AAGTAGAGGGCATTCACCAGC
MMP9-fwd	GCGTCATTCGCGTGGATAAG
MMP9-rev	TGGAAACTCACACGCCAGAA

Not shown*. **Supp. Data 1 (S1D) . Excel spreadsheet containing, in separate sheets, the underlying numerical data for Figs 2D, 3, 4B, 4C, 4E, 4F, 5A, 5E, 5F, 6A, 6C, S1A, S1B, S2A, S2B, S2C, S4, S5A, S7A, S7B, S10, S12A, S12B, S12C and S12D.**
https://doi.org/10.1371/journal.pbio.3001664.s014

Irene ZAPATA BODALO

Study of the role of the cyclin-dependent kinase inhibitor p21Waf1/Cip1 in cellular senescence

Résumé (français)

La sénescence cellulaire est un état d'arrêt de prolifération irréversible avec des nombreuses altérations cellulaires qui ont un impact important sur la santé. Parmi ses multiples activités, l'inhibiteur de la kinase cycline-dépendante p21 médie l'arrêt du cycle cellulaire au début de la réponse sénescent. L'objectif de ce projet est de découvrir et d'explorer des fonctions alternatives de p21 dans la sénescence. Pour ce faire, les niveaux de p21 ont été diminués dans des fibroblastes sénescentes induites par irradiation, dérivés d'un modèle murin inductible p21-knock-down. L'analyse de RNA-seq impliquais p21 dans la régulation transcriptionnelle du cycle cellulaire, des peroxysomes, de la traduction et de la sécrétion de cytokines dans la sénescence, entre autres. Certaines de ces fonctions ont été explorées par d'autres approches expérimentales. De plus, l'interactome de p21 dans les cellules sénescentes a été obtenu et identifié par co-immunoprécipitation et spectrométrie de masse.

Mots clé : sénescence, p21, Cdkn1a, RNA-seq, interactome, knock-down, peroxysome, cytokine, irradiation

Summary (english)

Cellular senescence is a state of irreversible proliferation arrest accompanied by alterations at all cellular levels that impacts many physiological and pathological processes. Among its multiple activities, the cyclin-dependent kinase inhibitor p21 is an important senescence marker which mediates the cell cycle arrest at early phases of the response. The goal of this project was to uncover and explore alternative functions of p21 in senescence. To do so, p21 levels were decreased in fully senescent cells induced by irradiation using primary fibroblasts derived from an inducible p21-knock-down mouse model. Bulk-RNA-seq analysis implicated p21 in the transcriptional regulation of the cell cycle, peroxisomes, translation or cytokine secretion in senescence, among others. Some of these functions were further explored using other experimental approaches. Additionally, the interactome of p21 in senescent cells was obtained by co-immunoprecipitation and identified by mass spectrometry.

Key words: senescence, p21, Cdkn1a, RNA-seq, interactome, knock-down, peroxisome, cytokine, irradiation